KSS-10

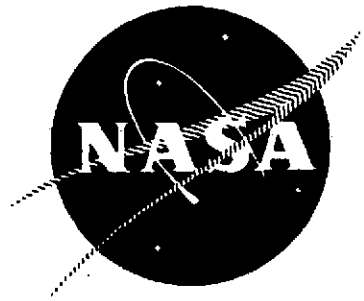

NASA CR-134510
R-9395

INVESTIGATION OF PROPELLANT FLOW CONTROL SYSTEM

By A. A. Liebman

ROCKETDYNE DIVISION
ROCKWELL INTERNATIONAL

prepared for

NATIONAL AERONAUTICS AND SPACE ADMINISTRATION

NASA-Lewis Research Center
NAS3-14390
Paul Herr, Project Manager

NOTICE

This report was prepared as an account of Government-sponsored work. Neither the United States, nor the National Aeronautics and Space Administration (NASA), nor any person acting on behalf of NASA:

A. Makes any warranty of representation, expressed or implied, with respect to the accuracy, completeness, or usefulness of the information contained in this report, or that the use of any information, apparatus, method, or process disclosed in this report may not infringe privately-owned rights; or

B. Assumes any liabilities with respect to the use of, or for damage resulting from the use of, any information, apparatus, method or process disclosed in this report.

As used above, "person acting on behalf of NASA" includes any employee or contractor of NASA, or employee of such contractor, to the extent that such employee or contractor of NASA or employee of such contractor prepares, disseminates, or provides access to any information pursuant to his employment or contract with NASA, or his employment with such contractor.

Requests for copies of this report should be referred to

National Aeronautics and Space Administration
Scientific and Technical Information Facility
P.O. Box 33
College Park, Md. 20740

1. Report No.	2. Government Accession No.	3. Recipient's Catalog No.
NASA CR-134510		

4. Title and Subtitle	5. Report Date
INVESTIGATION OF PROPELLANT FLOW CONTROL SYSTEM	November 1973
	6. Performing Organization Code

7. Author(s)	8. Performing Organization Report No.
A. A. Liebman	R-9395
	10. Work Unit No.

9. Performing Organization Name and Address	11. Contract or Grant No.
Rocketdyne Division, Rockwell International Canoga Park, California 91304	NAS3-14390
	13. Type of Report and Period Covered
12. Sponsoring Agency Name and Address	Contractor Report
National Aeronautics and Space Administration Washington, D.C. 20546	14. Sponsoring Agency Code

15. Supplementary Notes

Project Manager, Paul Herr, NASA-Lewis Research Center, Cleveland, Ohio

16. Abstract

Mechanical, electromechanical, and fluidic concepts were studied as propellant flow control systems for oxygen/hydrogen attitude control thrusters. A mechanical flow controller was designed, fabricated, and tested with hydrogen, oxygen, and nitrogen over a range of inlet pressures and temperatures. Results of these tests are presented along with a discussion of a flight-weight design. Also presented are recommendations for further design and development. A detailed coverage of the fluidics investigation is included.

17. Key Words (Suggested by Author(s))	18. Distribution Statement
Mass Flow Control Gas Flow Control Flow Regulation	

19. Security Classif. (of this report)	20. Security Classif. (of this page)	21. No. of Pages	22. Price*
Unclassified	Unclassified		

* For sale by the National Technical Information Service, Springfield, Virginia 22151

CONTENTS

Page intentionally left blank

ILLUSTRATIONS

SUMMARY

The objective of this program was to develop a gaseous hydrogen and oxygen flow controller to be used with the SS/APS thrusters. The flow controller was to maintain thrust and mixture ratio within ±3 percent over a wide range of propellant inlet pressures and temperatures.

The program included the investigation of mechanical, electromechanical, and fluidic related control concepts.* This included system analysis, computer modeling, and some testing of certain fluidic elements. A hybrid fluidic concept which exhibited early promise was later eliminated because fluidic compoments did not meet required performance. A mechanical concept was then selected for design and test.

The design of the mechanical flow controller included a unique arrangement of a temperature-sensitive linear pressure divider circuit which was pneumatically linked to a pressure spring balanced metering poppet. Testing of the device demonstrated its operation with hydrogen, oxygen, and nitrogen. Results indicated good control at ambient temperatures (±5 percent, GH_2). Control accuracy diminished at the lower temperatures due to adjustment limitations and the need for fine tunning of the temperature sensitive device. However control within ±10 percent was achieved over a good part of the pressure temperature envelope (194 to 294 K (350 to 530 R) and 3.45×10^6 N/m^2 to 5.17×10^6 N/m^2 (500 to 750 psia). Pneumatic response was about 50 milliseconds and thermal response about 300 milliseconds. Stability was controllable with the dashpot design.

It is suggested that further development be accomplished to better tune the controller to improve its control accuracy. Consideration should be given to incorporating sonic flow in the outlet venturi to provide independence of operation from the downstream installation. In addition it is recommended that the integration of a shutoff feature be explored to obtain a combination shutoff valve and flow controller.

*A separate report covering fluidic related work is contained in Appendix A.

INTRODUCTION

With the consideration of gaseous oxygen and hydrogen propellants for space shuttle auxiliary propulsion came the need to study some means of controlling flowrates to the attitude control thrusters. Control requirements were established to provide for constant thrust and mixture ratio with appropriate response to produce predictable and repeatable impulse for attitude control.

The objective of the program was to devise a flow control system which would maintain thrust and mixture ratio within ±3 percent over a wide range of propellant inlet pressures and temperatures as indicated in Table 1 . The flow control system is located just upstream of the thruster propellant valves as shown in Fig. 1 . The accumulators as shown are charged by a propellant conditioning system. Their output is regulated by central regulators upstream of propellant distribution lines. Variations in temperature and pressure of gaseous propellants trapped between closed thruster propellant valves and a locked up pressure regulator can result from thermal and flow perturbations witihin the overall system. To obtain accurate and responsive thrust and mixture ratio, control must be exercised at the thrust chamber valve assembly inlets. The effects of the lack of control can be seen in Fig. 2 and 3 which depict thrust and mixture ratio sensitivity to propellant inlet pressure and temperature variations. The impact of mixture ratio variation on combustion temperature is shown in Fig. 4 . An approximate ±140 K (±250 F) variation in combustion temperature for a ±10 percent change in mixture ratio is indicated.

TABLE 1. PERFORMANCE REQUIREMENTS

Propellants	GO_2, GH_2
Mass Flowrates	GO_2 1.25 Kg/sec (2.76 lb/sec)
	GH_2 0.31 Kg/sec (0.69 lb/sec)
Operating Temperature Range	139 to 306 K (250 to 550 R)
Accuracy	Thrust and Mixture Ratio ±3 percent
Response	50 msec
Pressure Drop	Minimium
Envelope and Weight	Minimum
Failure Criteria	Fail Safe Open
Maintenance	No Maintenance
External Leakage	1×10^{-6} scc/sec GHe

Analysis of the thrust chamber assembly has indicated that there is a unique inlet pressure for a given inlet temperature which produces the nominal flowrate as shown in Fig. 5 . In effect, these data indicate that a device which can regulate inlet pressure to the thrust chamber assembly as some function of temperature will deliver a constant flowrate.

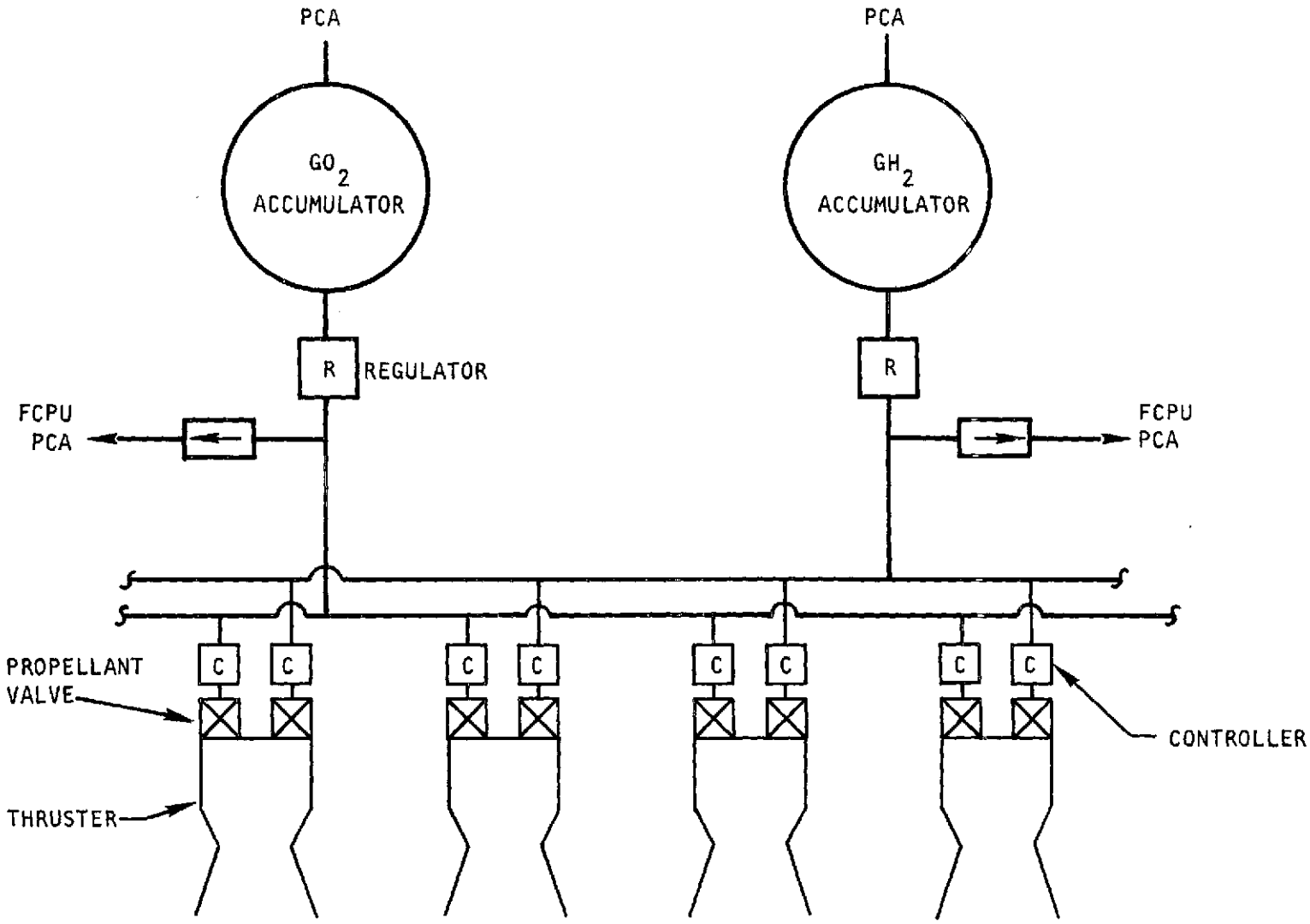

Figure 1. System Application

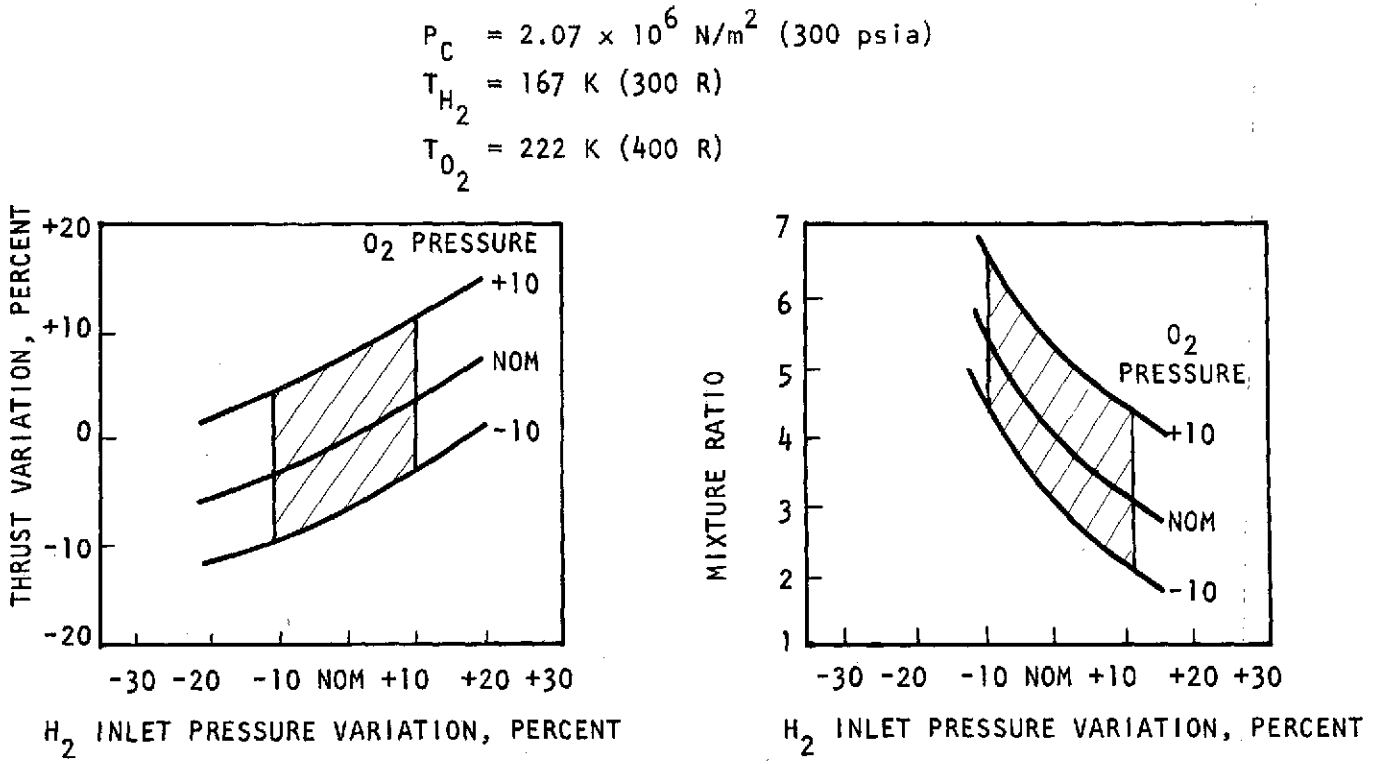

Figure 2. Sensitivity to Thruster Inlet Pressure

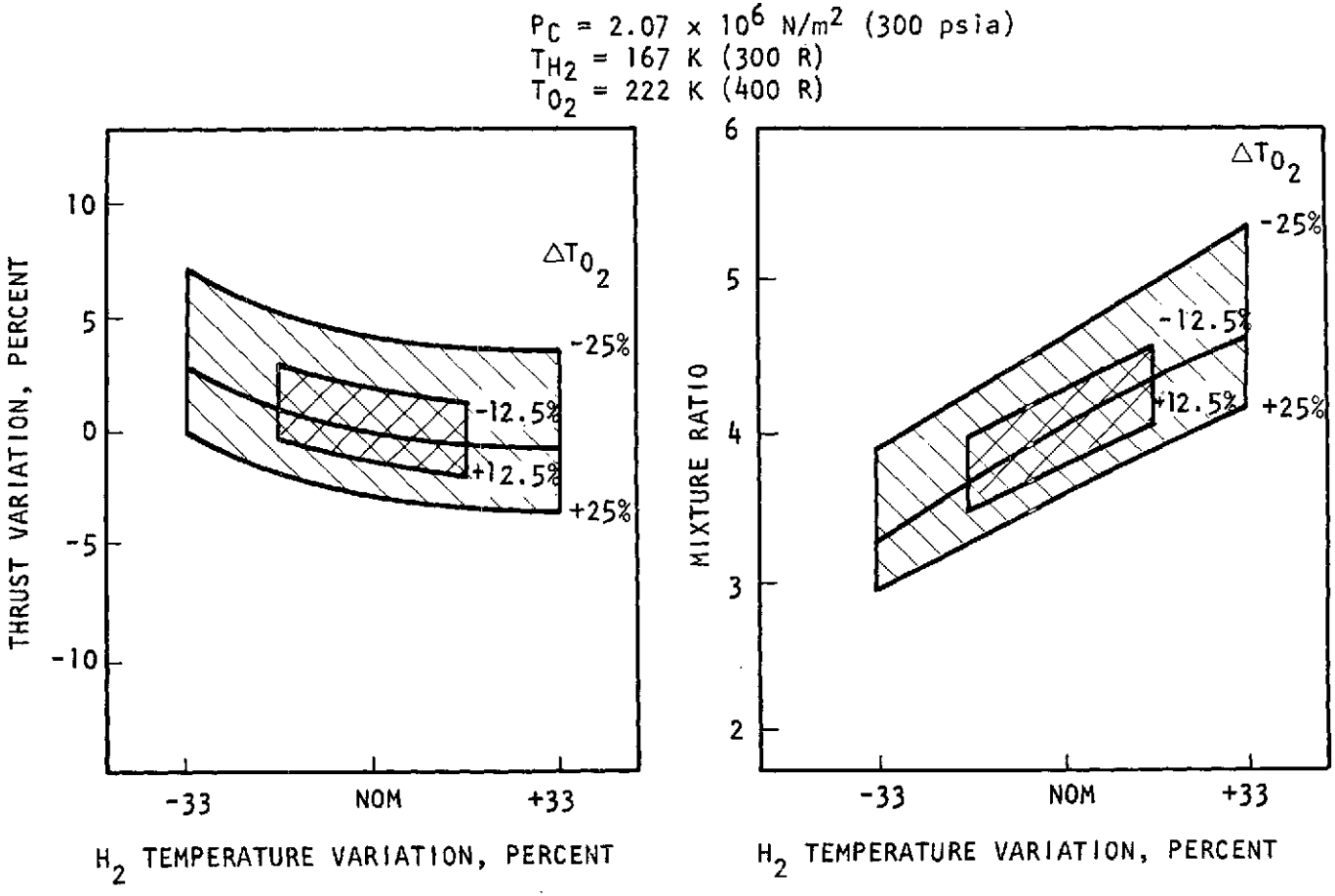

Figure 3. Sensitivity to Thruster Inlet Temperature

The technical effort was divided into four major tasks: Task I - Propellant Control Analysis and Conceptual Design, Task II - Propellant Control Fabrication, Task III - Evaluation Testing, and Task IV - Final Design. An additional task (V) was provided for reporting. Concepts were developed and evaluated that can be categorized as: mechanical, electromechanical, and hybrid fluidic. Rocketdyne Division of Rockwell International was responsible for the study of mechanical and electromechanical devices while Bendix Research Laboratories of Southfield, Michigan, a subcontractor, investigated fluidic related devices. The report of their work is presented in Appendix A.

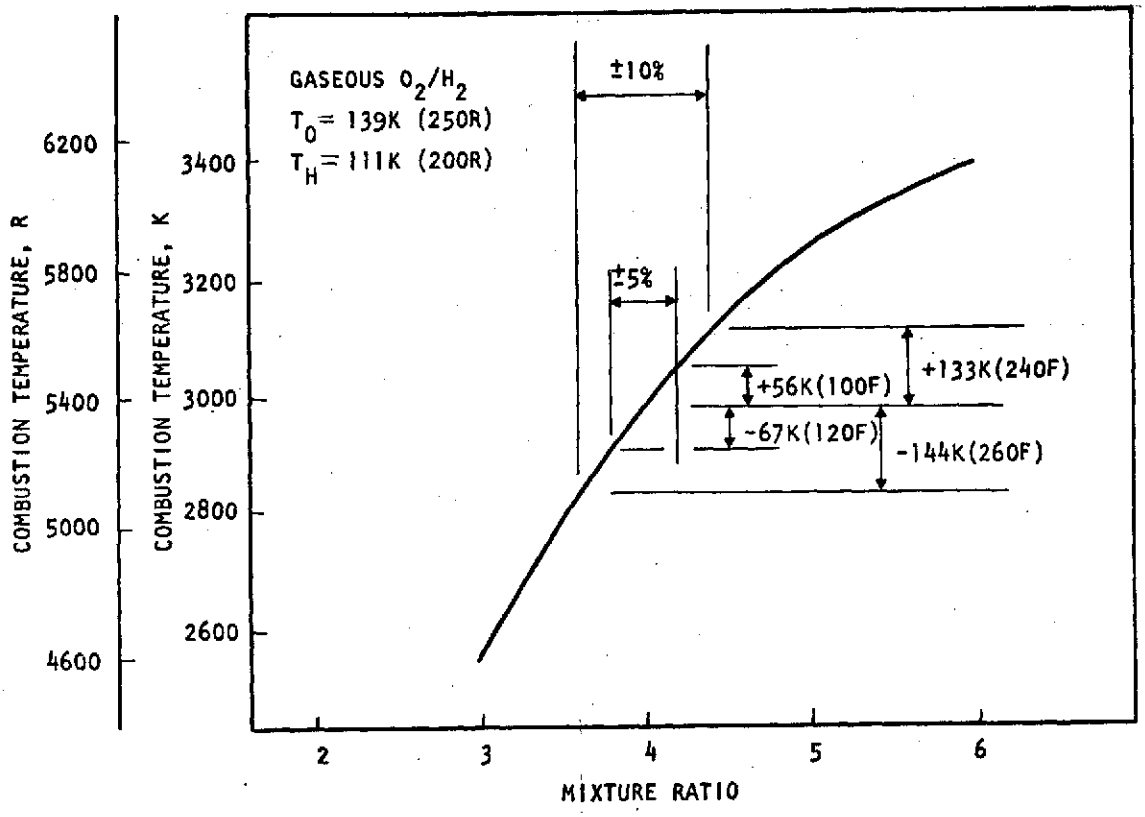

Figure 4. Effect of Mixture Ratio Variation on Combustion Temperature

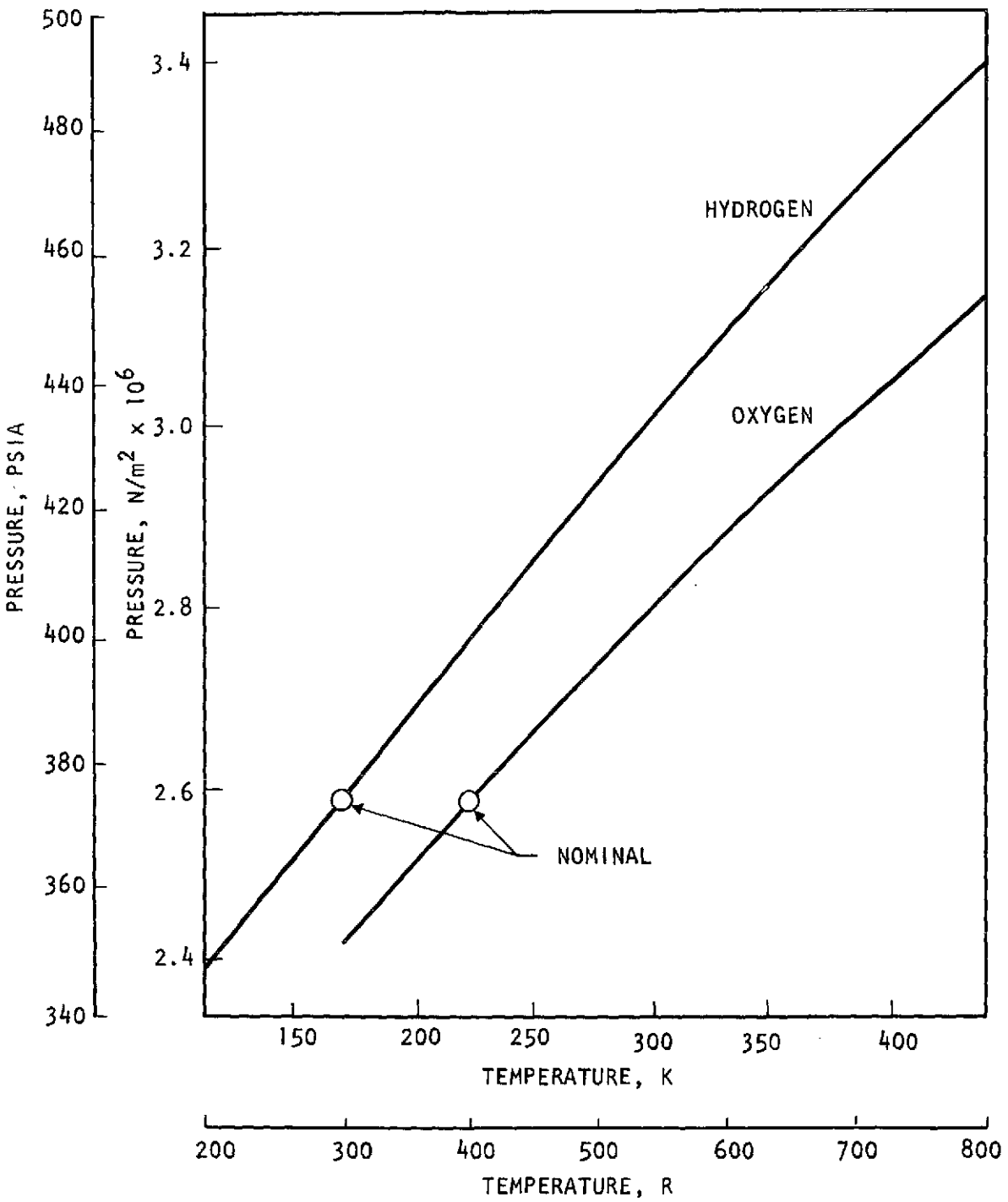

Figure 5. Inlet Pressures Required to Give Constant Flowrates for Varying Inlet Temperatures for Real Gas Propellants

FLOW CONTROL PROGRAM

ANALYSIS AND CONCEPTUAL DESIGN

During the early portion of the program, several concepts were developed which were thought to have potential for this application. These included two mechanical, one electromechanical, and four hybrid fluidic concepts.

The evaluation process which began with concept synthesis and was completed with concept selection is described by block diagram in Fig. 6 . The breadboard testing was performed for certain critical fluidic elements whose operating characteristics did not lend themselves to description by analysis.

Concept Descriptions

Block diagram descriptions of candidate controller concepts are presented in Fig. 7 and 8 . Mechanical concepts are operated from a pressure balanced metering device with some means of adjustment for temperature effects. The electromechanical system utilizes an electronic computer to drive positioning servos which control the position of throttling sonic venturis. The hybrid fluidic concepts combine certain fluidic elements with some type of pressure actuated mechanical metering element.

All controller concepts with the exception of the electromechanical are individual controllers in that they control oxygen and hydrogen flows individually and separately and are linked only by the pressure feedback from the thrust chamber. The electromechanical concept is a system approach which considers the temperature and pressure effects of both propellants in the control of the flow of each propellant. In that sense, its control is coupled.

Mechanical Flow Controller. The mechanical flow controller as depicted in Fig. 7 consists of a pressure balanced mechanical metering assembly and a temperature sensitive reference pressure circuit. The pressure balanced metering assembly illustrated in Fig. 9 shows the offsetting effects of the supply pressure, P_s, and bellows pressure, P_b, so that metering element position is primarily dependent on the regulated pressure, P_r, and spring force. As the regulated pressure drops, the metering element tends to open, allowing more flow, which in turn brings up the regulated pressure. The reverse is also true.

The unique feature of this device is the linear relationship between the supply pressure and bellows pressure. This is obtained from the circuit shown in Fig. 10 which consists of a temperature sensitive subsonic orifice in series with a sonic venturi. The pressure at a point between the two orifices turns out to be proportional to the supply or inlet pressure. Thus, by nearly balancing the bellows pressure force, P_bA_b, against the supply pressure force, P_sA_p, the effects of supply pressure variation are all but removed.

As the propellant inlet temperature varies, the pintle length changes so that the ratio of P_b/P_s varies as shown in Fig. 11. In effect, as propellant temperature increases, the bellows pressure for a given inlet pressure increases

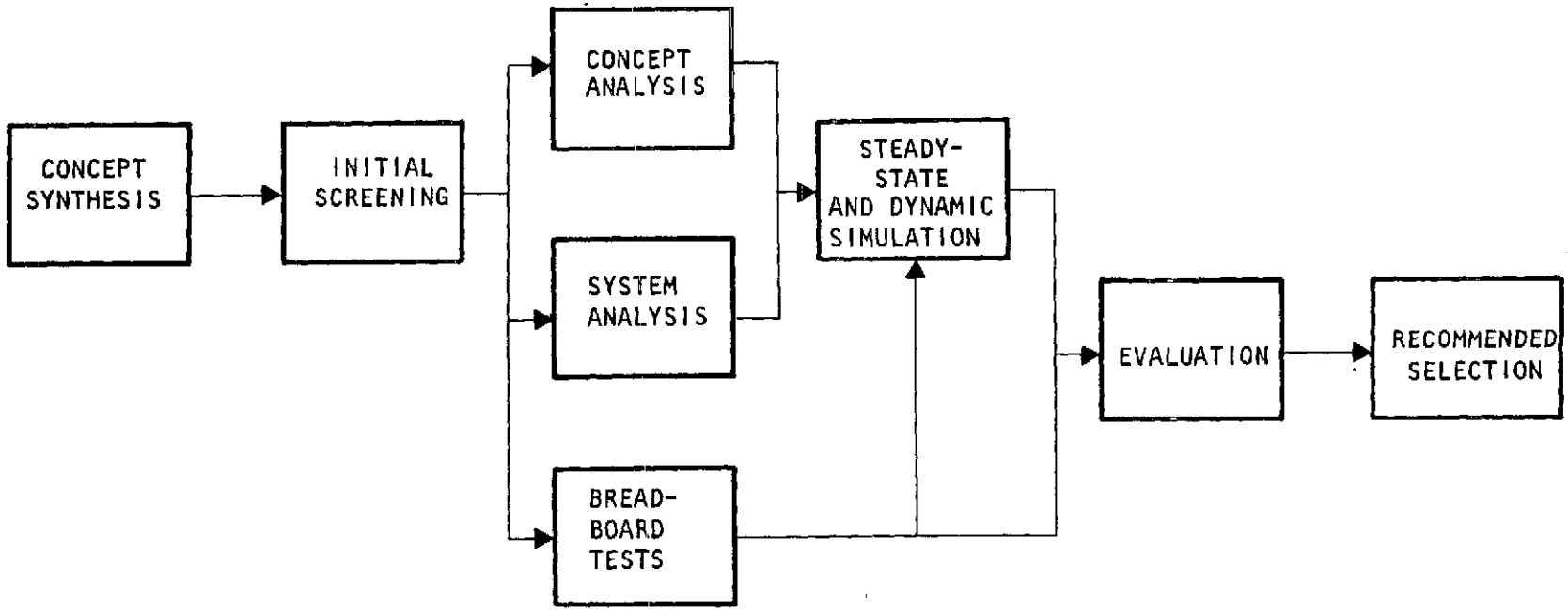

Figure 6. Concept Evaluation Process

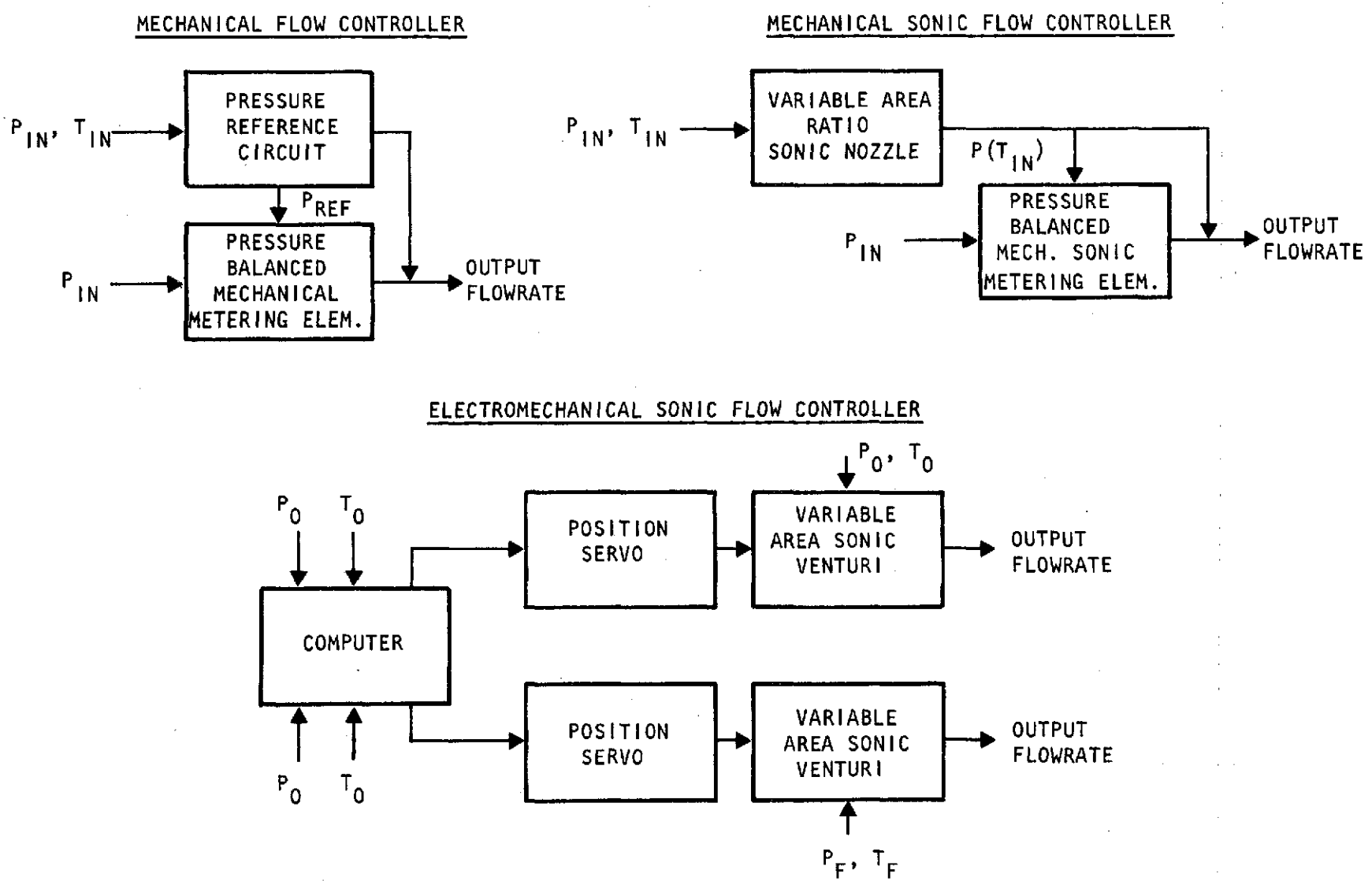

Figure 7. Mechanical and Electromechanical Conceptual Block Diagram

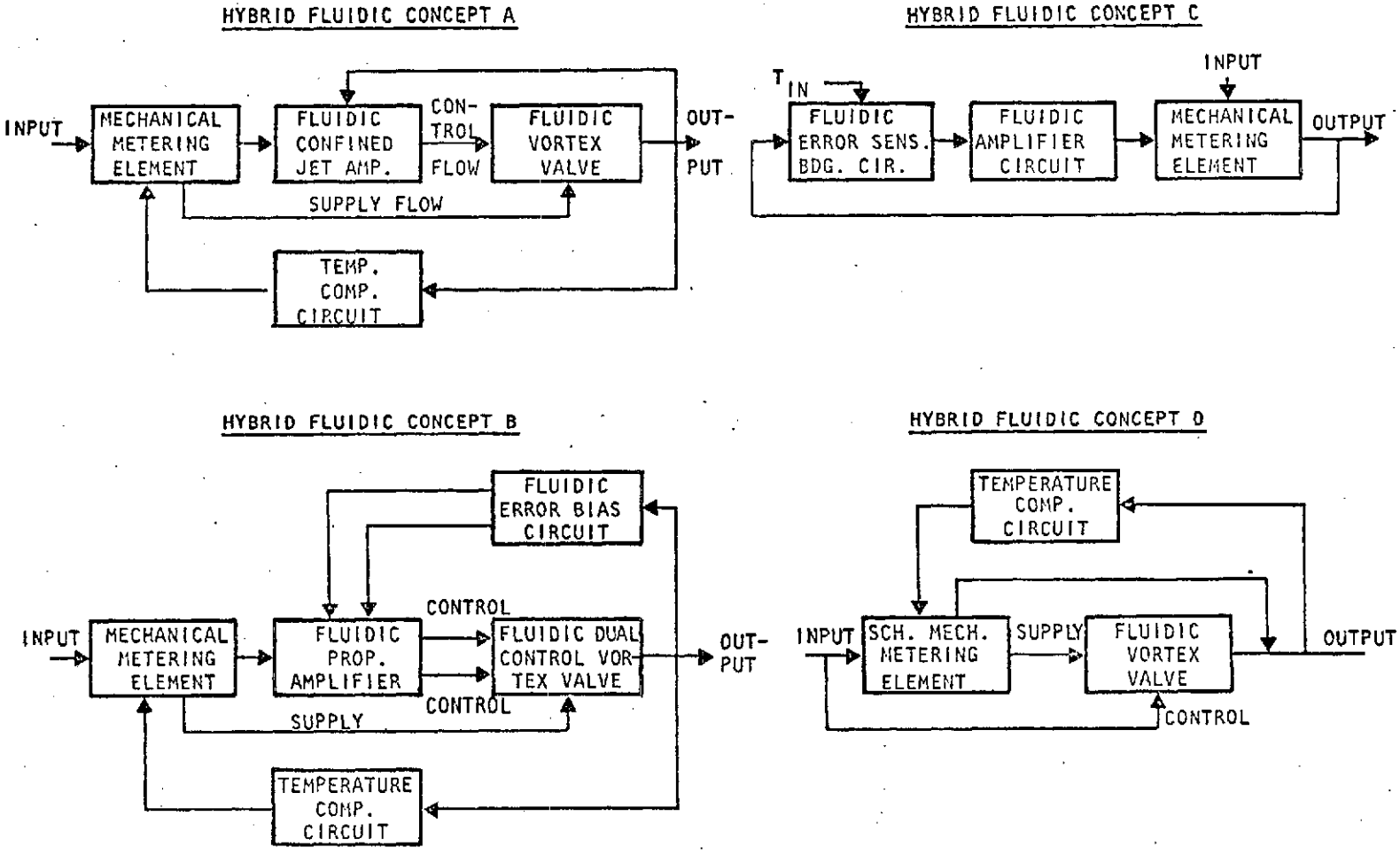

Figure 8. Hybrid Fluidic Conceptual Block Diagrams

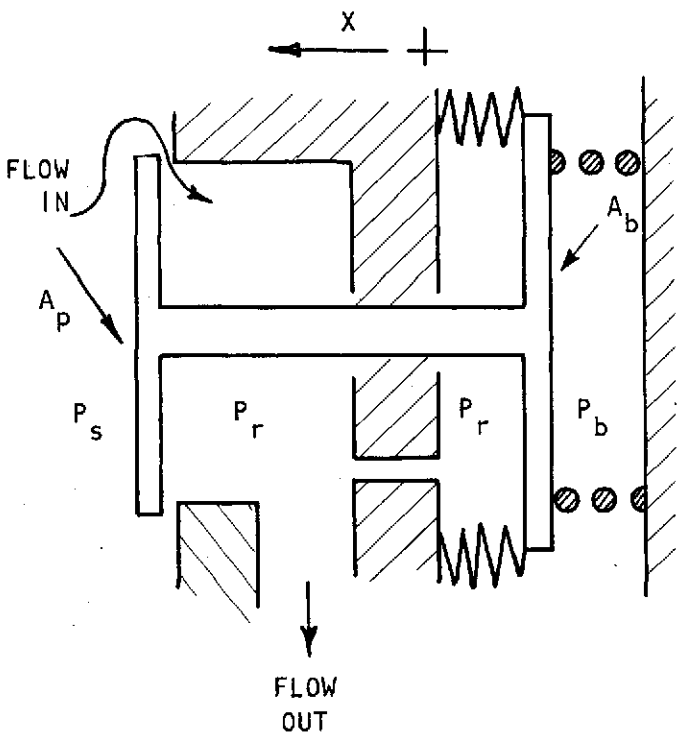

FORCE BALANCE

$$-P_s A_p + P_b A_b + P_r (A_p - A_b) = Kx - F_o$$

for $P_b = P_s (A_p/A_b)$

$$P_r = \frac{Kx - F_o}{A_p - A_b} \quad \text{OR} \quad \Delta P_r = \Delta x \frac{K}{A_p - A_b}$$

POSITION ERROR

TO OFFSET POSITION ERROR, LET $P_b = C P_s$

$$P_r = \frac{Kx - F_o + P_s (A_p - CA_b)}{A_p - A_d}$$

OR

INLET PRESSURE ERROR

$$\Delta P_r = \Delta x \frac{K}{A_p - A_b} + \Delta P_s \frac{A_p - CA_b}{A_p - A_b}$$

POSITION ERROR

Figure 9. Pressure Balanced Metering Assembly of the Mechanical Flow Controller

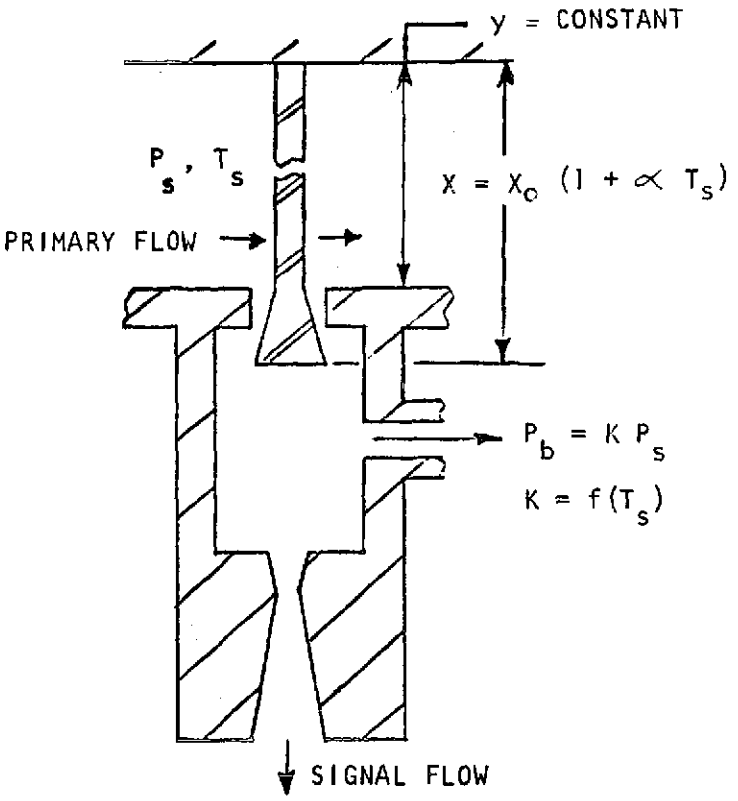

Figure 10. Reference Pressure Circuit of the Mechanical Flow Controller

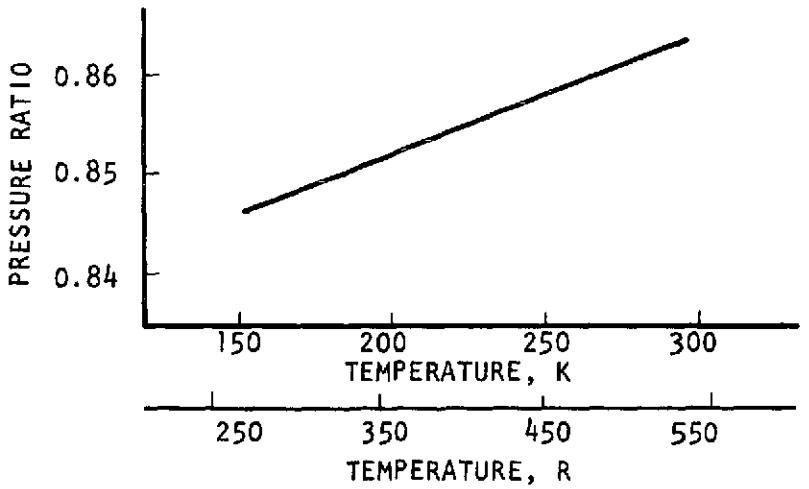

Figure 11. Reference Pressure Circuit Output Pressure Ratio as a Function of Temperature of the Mechanical Flow Controller

allowing more flow area for the less dense gas thus maintaining near constant flow. Combining this reference pressure circuit with the metering assembly schematic results in the controller schematic in Fig. 12 .

Mechanical Sonic Flow Controller. The mechanical sonic flow controller also consists of a pressure reference circuit and a pressure balanced metering element as shown in Fig. 7 . However, in this case the metering element flows sonic so that downstream conditions do not impact its operation. The controler schematic in Fig. 13 shows a shaped movable pintle within a high recovery sonic venturi. The pintle is pressure actuated by supply (inlet) pressure, pressure forces on the pintle, and a reference pressure generated by flow around a linked sonic pintle.

This reference pressure varies with pintle position to balance force changes on the metering pintle. This reference pressure is further varied by changes in the inlet pressure to the linked pintle as a result of temperature effects on the position of the temperature compensating pintle.

Electromechanical Sonic Flow Controller. This controller consists of temperature and pressure transducers, a special purpose electronic computer circuit, positioning servos, and throttling sonic venturis as shown in the schematic in Fig. 14. The system computes an appropriate throttle position based on temperature and pressure measurements of incoming propellants and then drives the venturi throttling pintles to the related positions. The system is open loop with respect to thrust and mixture ratio. Because of sonic flow through the venturis, the controller is decoupled from downstream effects.

The computation process depicted in Fig. 15 takes into account real gas properties as well as temperature effects on combustion. The system drives both controls simultaneously and is unique in this respect when compared with other candidate systems.

Hybrid Fluidic Flow Controller - A. This controller, shown schematically in Fig. 16, utilizes fluidic elements to sense output pressure and generate appropiate pressures to drive a pressure-activated mechanical metering element. The controller is made up of a vortex amplifier, confined jet amplifier, mechanical metering element, and subsonic orifices.

In operation, if the output pressure, P_r, should exceed the set point, feedback to the confined jet amplifier causes increased tangential flow to the vortex amplifier which impedes primary flow through it and increases back pressure, P_s', to the mechanical metering element. This increase in pressure tends to decrease mechanical metering area cutting back on controller flowrate which will result in output pressure moving back towards its set point. Orifices provide a reference back pressure to the metering element which is temperature dependent to compensate for varying propellant inlet temperature. Should output pressure drop below the set point, the system reacts in a similar but opposite manner.

Hybrid Fluidic Flow Controller - B. This approach is similar to that discussed in the previous section except that implementation of the fluidic element is

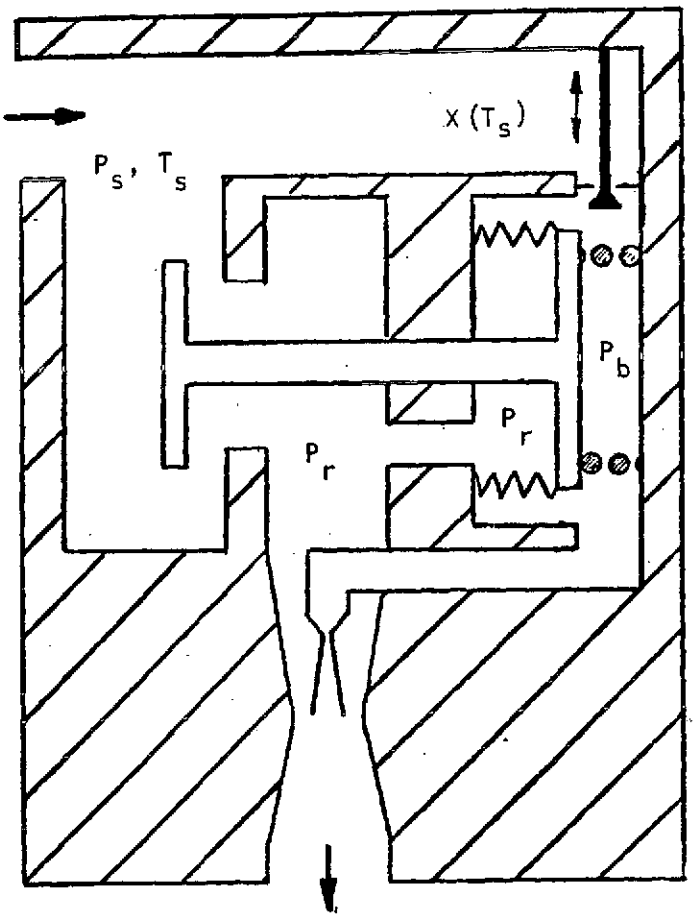

Figure 12. Mechanical Flow Controller

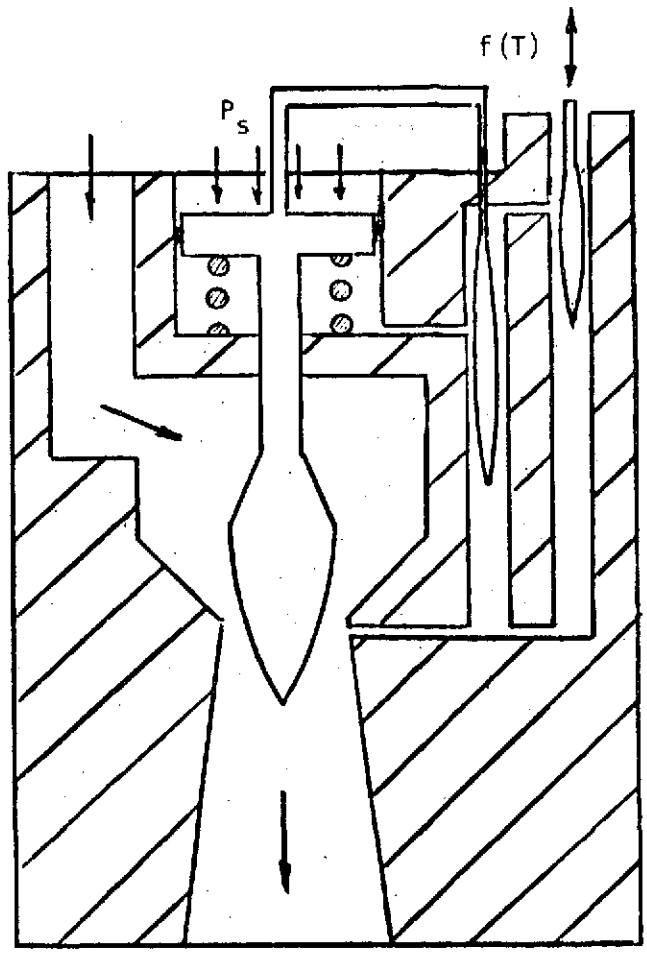

Figure 13. Mechanical Sonic Flow Controller

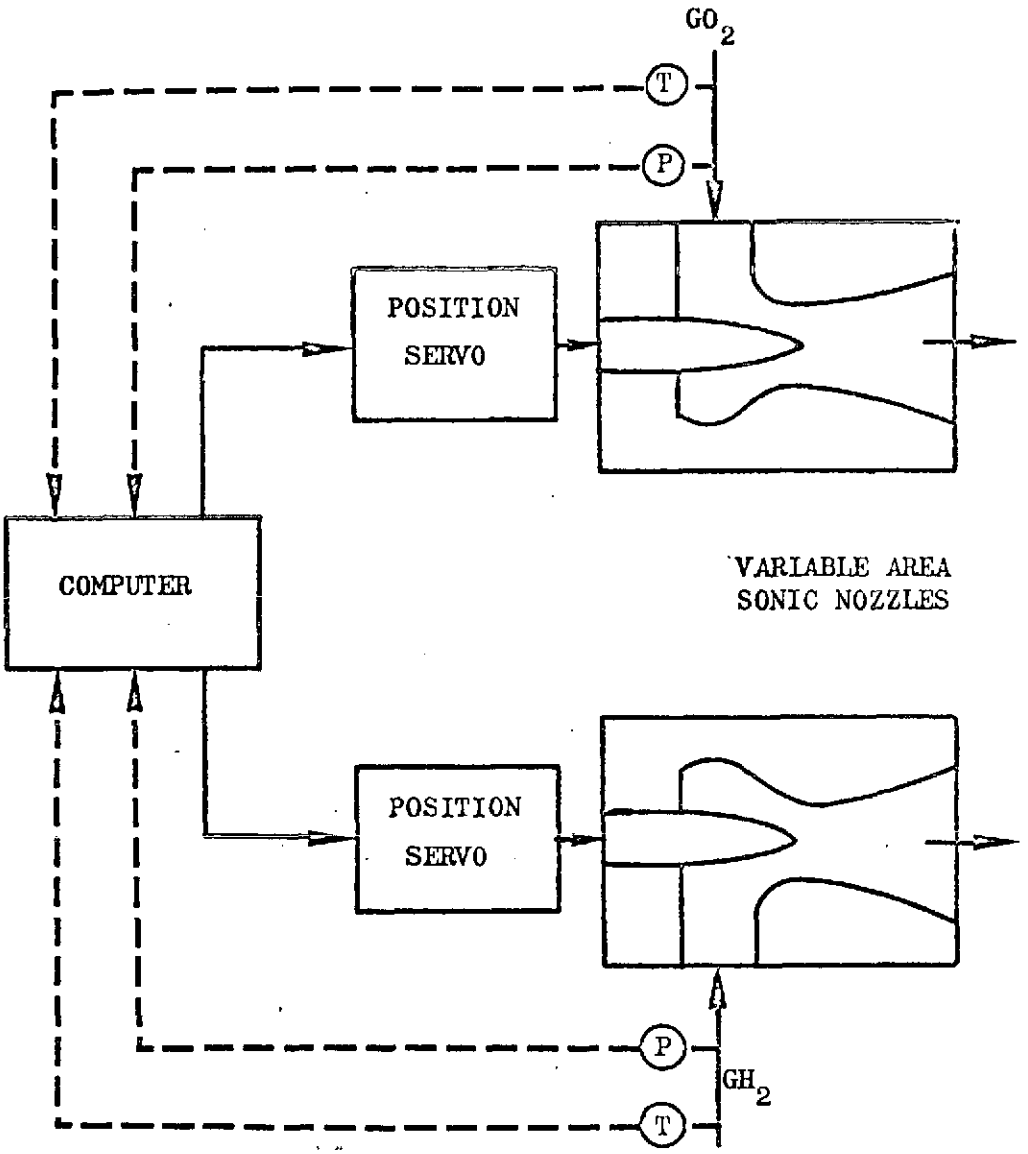

Figure 14. Electromechanical Sonic Flow Controller

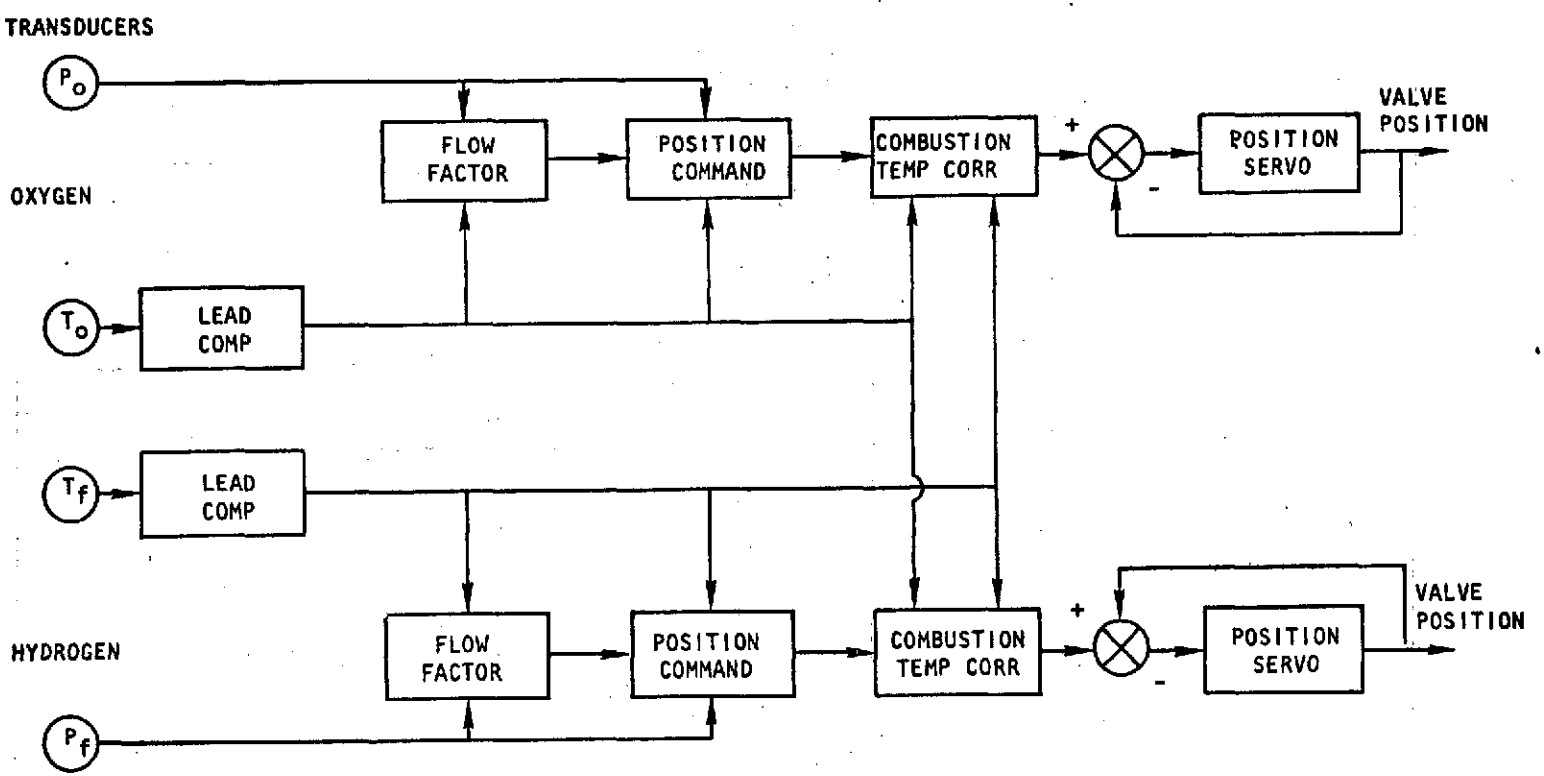

Figure 15. Computer and Control Logic

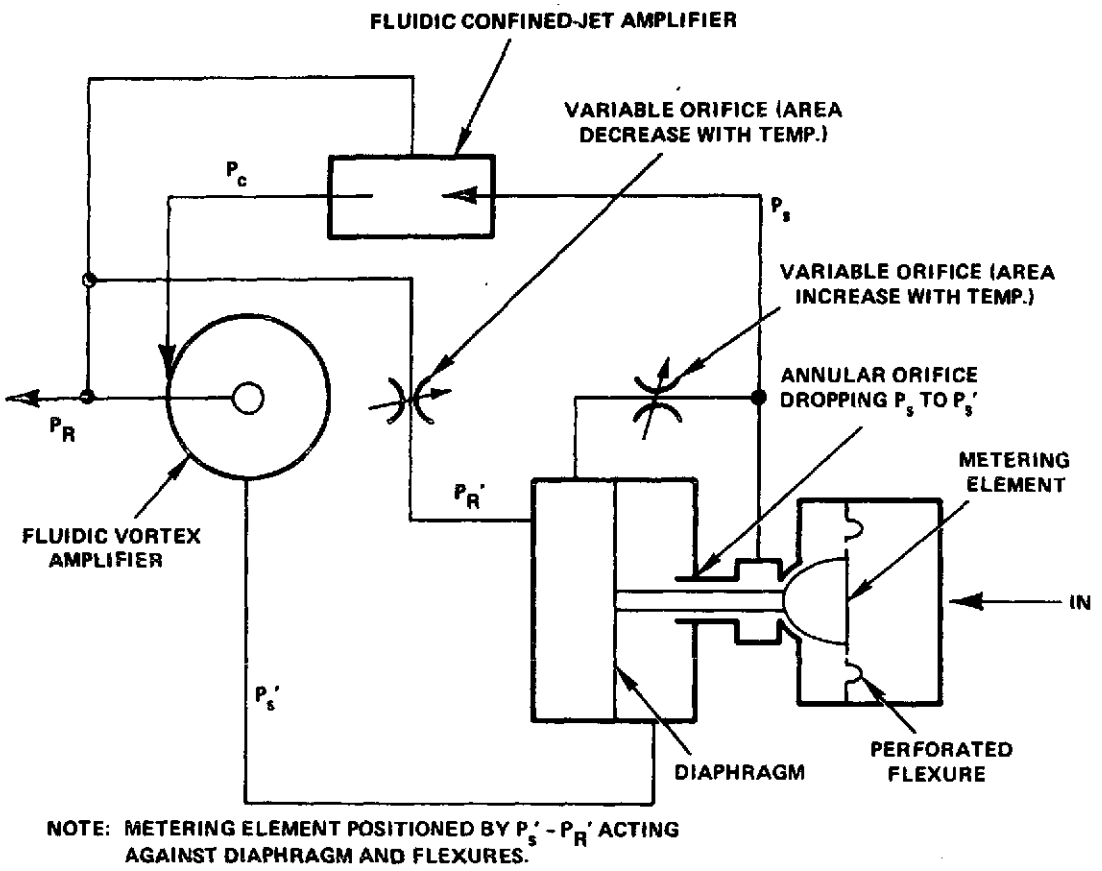

Figure 16. Hybrid Fluidic Flow Controller-A

quite different. The schematic is shown in Fig. 17 . The vortex valve in this case has two opposing control pressures, and a third control is brought in to obtain some initial swirl. The initial swirl places the steady-state operating point down on the throttling curve. Any change in the output pressure (P_r) feeds back through both laminar and turbulent orifices to obtain an error signal. If P_r is at the proper setting, ΔP_a would be set to zero and the output of the amplifier (ΔP_c) would also be zero. The vortex would thus remain balanced by P_{c_1} and P_{c_2}. If P_r increased by some error, a ΔP_a would exist so as to create an output difference between P_{c_1} and P_{c_2}. This difference (ΔP_c) would act to increase the swirl in the vortex, thereby causing P_s to rise and throttle the flow back at the metering element. If P_r tended to drop, the reverse action would take place.

It should be pointed out that in this configuration flow is drawn into the proportional amplifier from the output regulated flow by an internal venturi-type effect which would be designed to create a lower vent pressure than P_r.

Hybrid Fluidic Flow Controller - C. This approach is shown in Fig. 18 . It combines a simple throttling diaphragm-type pressure regulator with the fluidics controlling the diaphragm to achieve the necessary accuracy. The effective areas and the valve unbalanced area are matched and, when flow is developed, the fluidic sensing and amplifying circuits apply a bias pressure difference to the diaphragm to trim the flow as required.

The large propellant flows in relation to the small flows needed for sensing and amplification permit the use of a venturi to develop a pressure difference for these functions. In the right-hand circuit, an upstream laminar flow orifice develops a pressure drop very nearly linear with temperature. In the left-hand circuit, an upstream turbulent orifice develops a pressure drop proportional to input pressure in a ratio determined by the ratio of its area to the area of a variable downstream orifice. The sensor amplifier nulls these two pressure drops by using the diaphragm to bias the pressure regulator setting as necessary. The output of the R3 restrictor is temperature dependent to compensate for changes in propellant temperature.

Later in the program an additional amplifier stage was added between the bridge circuit and output amplifier as shown in Fig. 6 of Appendix A.

Hydraulic Fluidic Flow Controller - D. A fourth type of hydrid regulator is shown in Fig. 19. The inlet supply pressure is used directly to schedule the poppet area between P_c to P_o. P_o is the radial component of flow in the vortex chamber. The inlet pressure acts directly as a control source to obtain swirl and thereby throttle the flow. P_r is shown fed back as a reference to the back side of the diaphragm. Temperature compensation is achieved by the use of a venturi and a set of temperature-compensating orifices. The reference flow to the venturi throat is a small percentage of total flow.

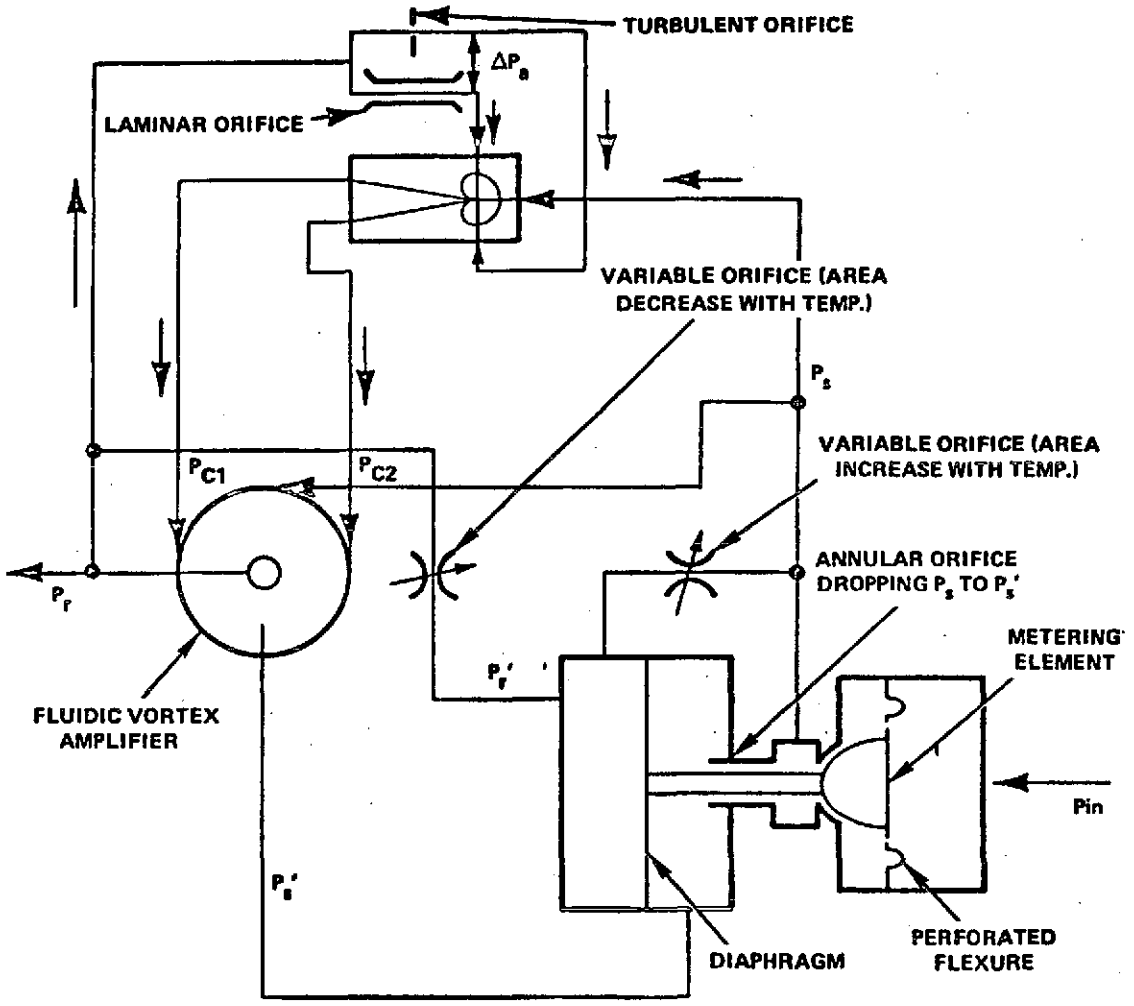

Figure 17. Hybrid Fluidic Flow Controller-B

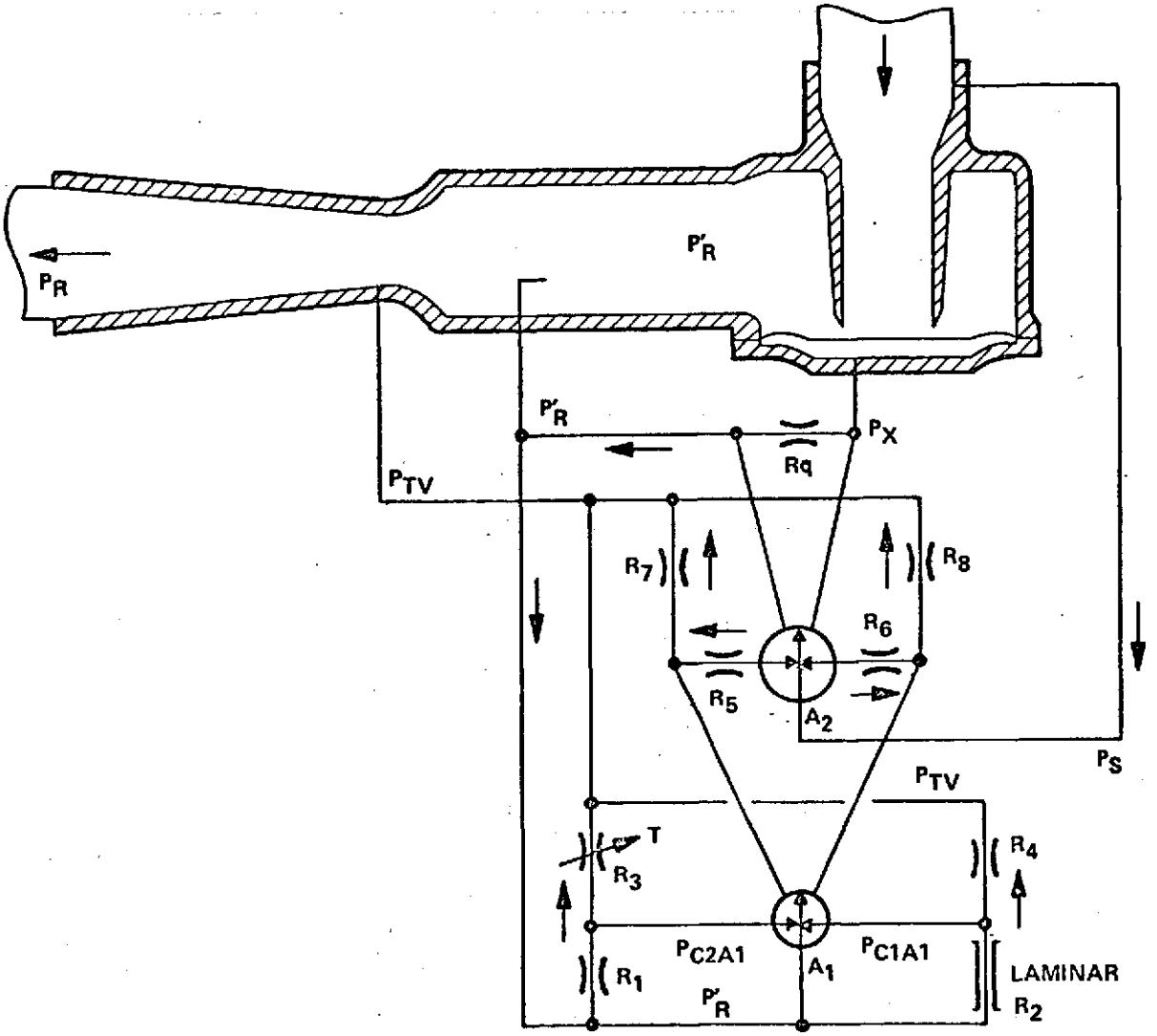

Figure 18. Hybrid Fluidic Flow Controller-C

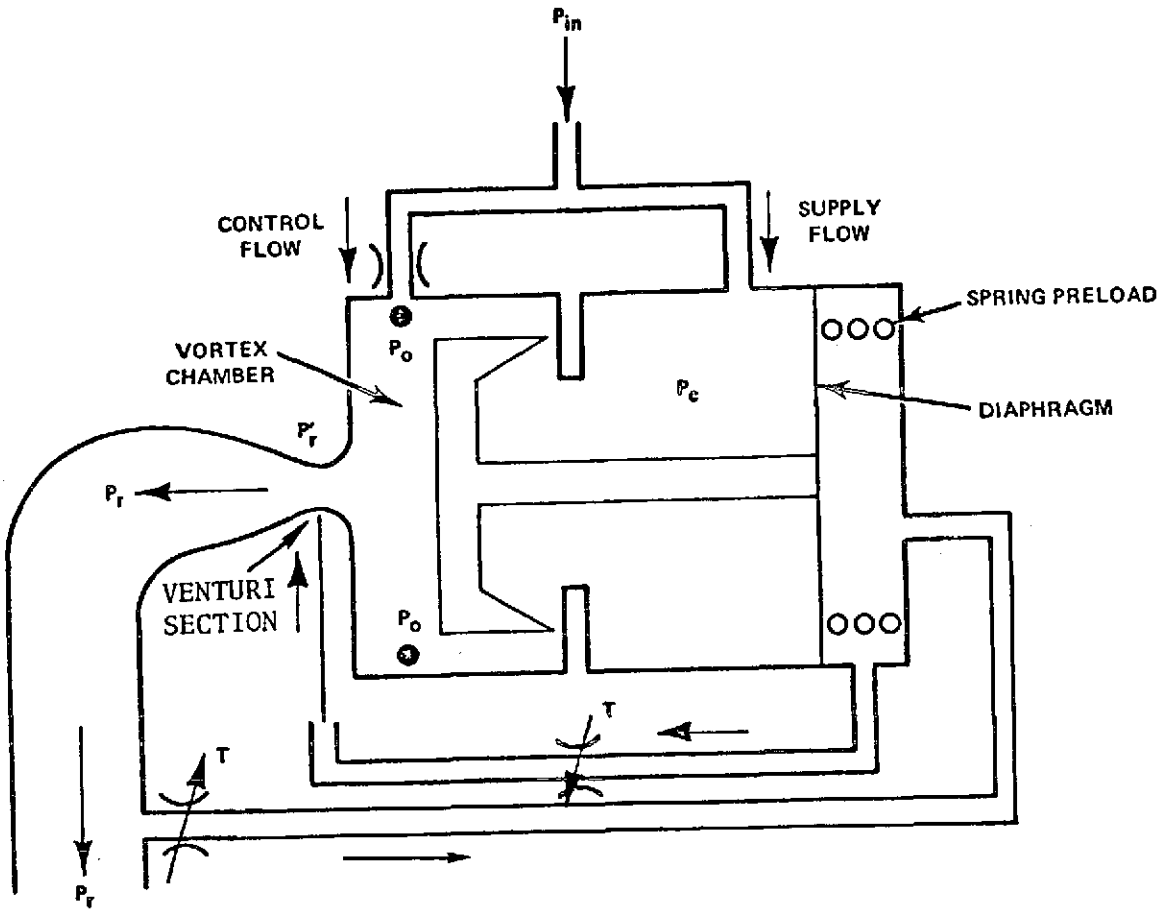

Figure 19. Hybrid Fluidic Flow Controller-D

Concept Evaluation and Selection

Analyses were performed to determine the steady-state operating characteristics of the mechanical and electromechanical concepts. Testing of certain critical fluidic components was done to characterize operation under the conditions of this application. In addition, computer dynamic simulations of the mechanical, electromechanical, and hybrid fluidic-C configurations were run. The evaluation process occurred in several phases as indicated in Fig. 20. As a result of analyses and testing, the mechanical sonic flow controller and the hybrid fluidic controllers were found to be inadequate in meeting the basic control requirements as specified in Table 1.

At the first concept evaluation review at NASA-Lewis Research Center on 26 January 1972, the hybrid fluidic controller-C looked promising. However, questions were raised relative to its dynamic stability as well as the operation of its fluidic amplifier circuit and laminar restrictor. Further testing and analysis were performed. At a subsequent review at NASA-Lewis Research Center, 13 October 1972, it was concluded that the hybrid fluidic controller-C could

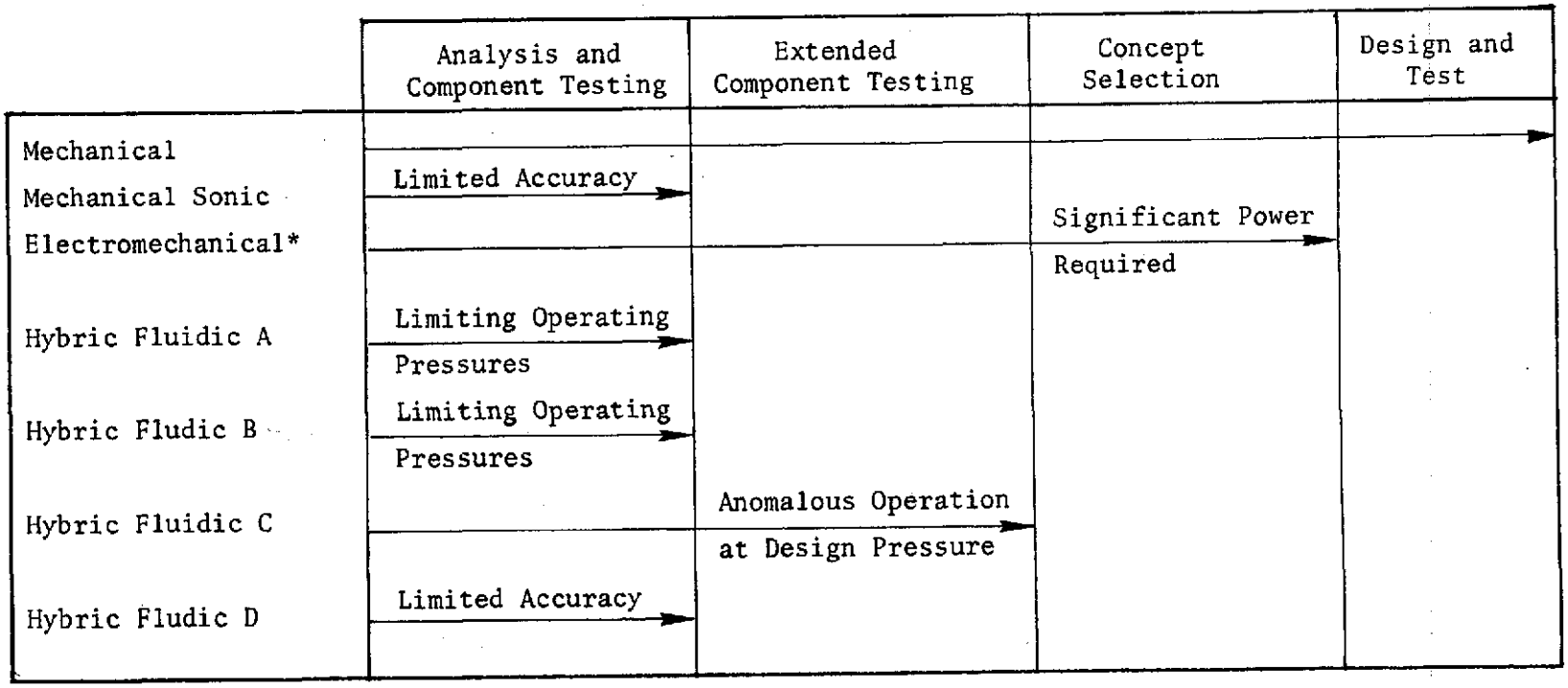

*The electromechanical concept was carried as a back up candidate because of its indicated feasibility. However, because of its complexity and power consumption was eliminated when the feasibility of the mechanical candidate concept was evaluated.

Figure 20. Concept Elimination Summary

not be developed within the resources of the current program to meet the required control operation. A decision was made at that time to proceed with the development of the mechanical flow controller. The electromechanical concept while considered feasible from an operating standpoint was eliminated because of its significant power requirement and system complexity.

Mechanical Flow Controller. Analysis of the mechanical controller configuration indicated a flow control accuracy of ±3 percent over a major portion of the pressure-temperature envelope. However at lower inlet pressures an estimated ±5 percent as shown in Fig. 21 was indicated. The estimated steady-state control performance is indicated in Fig. 22. The dynamic response depicted in Fig. 23 shows flowrate to be within ±10 percent of nominal in less than 50 msec from start of propellant valve motion and is based on a propellant valve travel time of 20 miliseconds.

Because of the indicated inaccuracy at the lower inlet pressures, this concept was not initially selected. However, after considerable work was completed on the hybrid fluidic controller-C, the mechanical concept was selected for design and test.

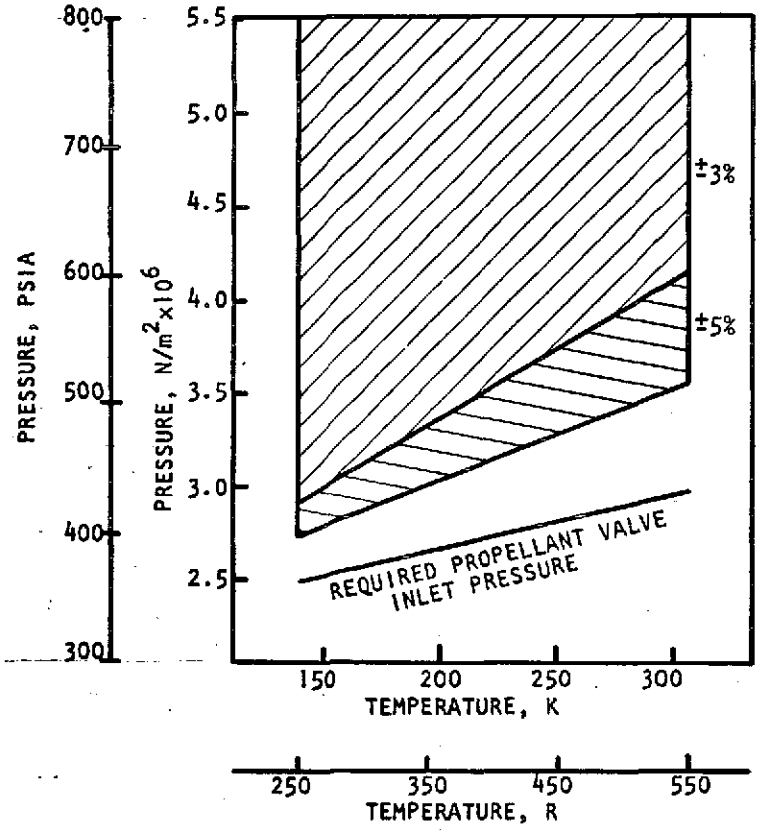

Figure 21. Estimated Theoretical Accuracy of Mechanical Flow Controller as a Function of Inlet Temperature and Pressure

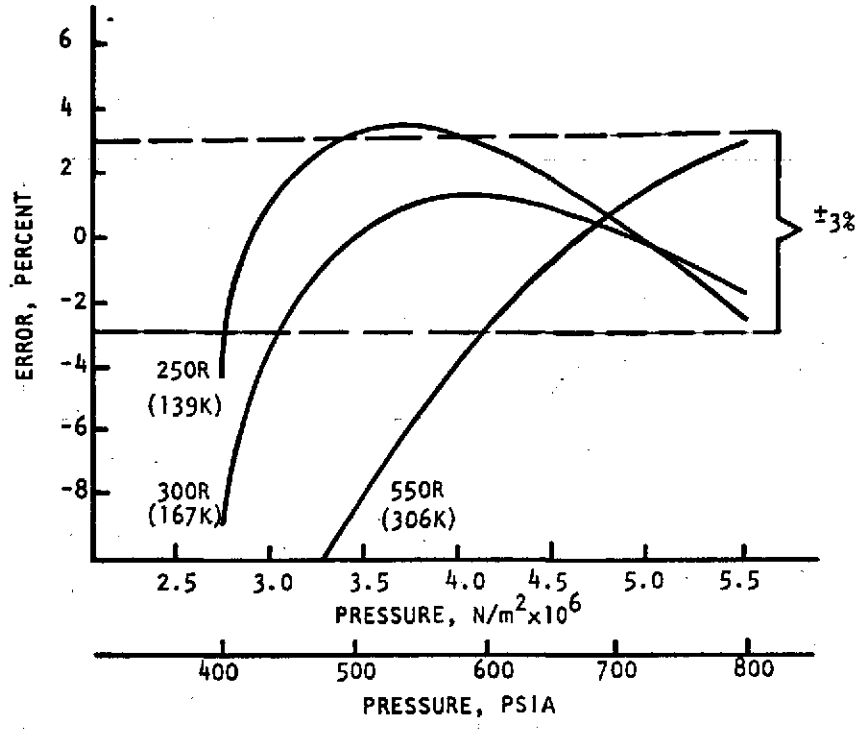

Figure 22. Controller Flowrate Error as a Function of Inlet Pressure at Various Propellant Temperatures

Mechanical Sonic Flow Controller. Early analysis of the sonic flow controller indicated an accuracy over the temperature/pressure range very close to ±3 percent. To increase confidence in these results, a closer look was taken at the force balance across the pintle as a function of position to determine its impact on control. Initially, the unbalance area was assumed to be that at the nozzle throat. During this period, a computer program was constructed to integrate pressure forces along the entire surface of the pintle as a function of position and the force-position characteristic was integrated into the mathematical model of the controller. The pintle forces were found to be sufficient to significantly upset the steady-state accuracy.

A modification of an earlier concept was then synthesized as shown in Fig. 13, which utilized a mechanically linked, variable-position sonic pintle to provide pressure correction for the pintle unbalance and a thermomechanically actuated, variable-position sonic pintle for temperature adjustment. An analysis was made that defined the contour of the position pintle. Then, at given propellant temperatures, the appropriate piston balance pressures were determined as a function of inlet pressure. The ratio of this pressure to that required for the same inlet pressure at the nominal temperature defines a temperature adjustment ratio to be built into the temperature pintle. It was desired that this ratio be the same for all inlet pressures at a given inlet temperature because, at a given temperature, there can be but one adjustment regardless of pressure.

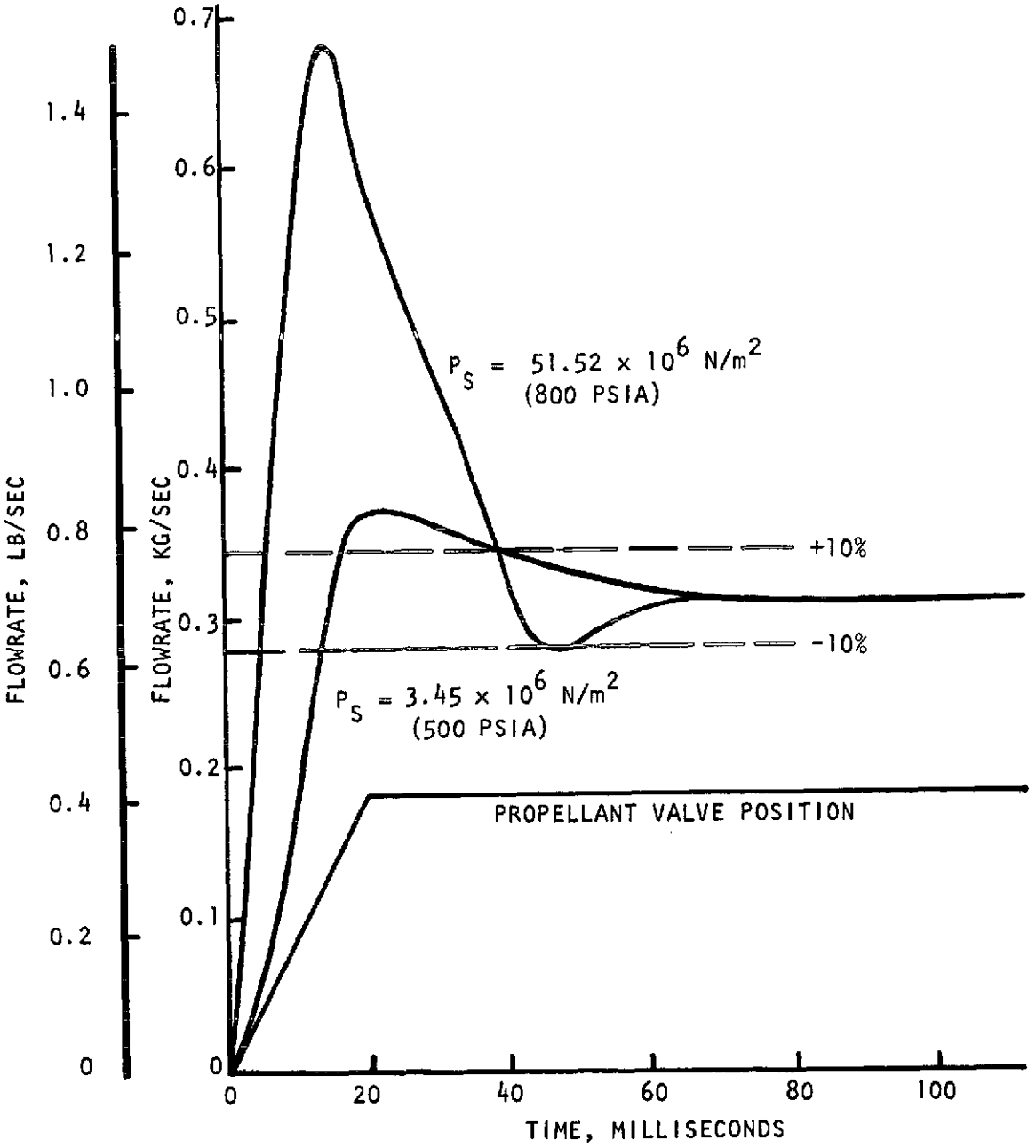

Figure 23. Mechanical Controller Dynamic Response

The results of the analysis yielded adjustment ratios with some variation as a function of inlet pressure. The resulting flowrates shown in Fig. 24 varied too widely at maximum temperature (+10, -20 percent), eliminating this concept from further consideration.

Electromechanical Sonic Flow Controller. Analyses were performed to demonstrate both the steady state and dynamic operation of the electromechanical controller. Both accuracy and response were analytically demonstrated. However this was the only concept under evaluation that required power for operation. The level of power estimated was about 50 watts per controller operating and 10 watts holding. In addition, the number of components and overall complexity exceeded that of all other concepts. Because of the substantial power requirement and system complexity, this concept was eliminated from further consideration.

Hybrid Fluidic Controller A. The confined jet amplifier was considered the critical component in the circuit for operation with low pressure drop. To examine this element, a variable-model confined-jet amplifier was built and tested. Test results presented in Fig.25, revealed that a minimum input pressure of about 5.45×10^6 N/m^2 (775 psia) would be necessary for proper operation with the confined-jet amplifier as a control element. This was excessive for this application.

An option to the confined jet that had potential was a proportional amplifier used in line with error-sensing orifices. A closed-vent proportional amplifier was built and tested for its potential in the circuit shown in Fig. 26. Results of the tests at low pressure ratios showed that gain was too low for feedback control. In addition, high-pressure drop (1.33 N/m^2 (200 psi)) and fluid noise were problems. It might have been possible to improve the noise conditions in the design of the amplifier, but the other factors of low gain and high pressure drop led to the elimination of this concept.

Hybrid Fluidic Controller B. An important element in this design is the proportional amplifier. Tests were conducted to consider proportional amplifier operation in this type of circuit. As noted above the results shown in Fig. 26 indicate that low gain, large pressure drop, and fluid noise made this concept unattractive. In addition, the multiple-input type of vortex would require its own development because most prior work on vortex devices has been for a single signal input. This concept was therefore eliminated from any further consideration.

Hybrid Fluidic Controller C. In the earlier part of the program, this concept appeared to be the most promising based on limited breadboard testing and some analytical modeling.

Testing was conducted on the fluidic portion of one controller. Tests were initially conducted at a low pressure, i.e., 0.34×10^6 N/M^2 (50 psia), since several properly sized fluidic elements were available in this range. Tests on the fluidic elements and the fluidic circuit indicated highly promising steady-state performance as part of a flow controller.

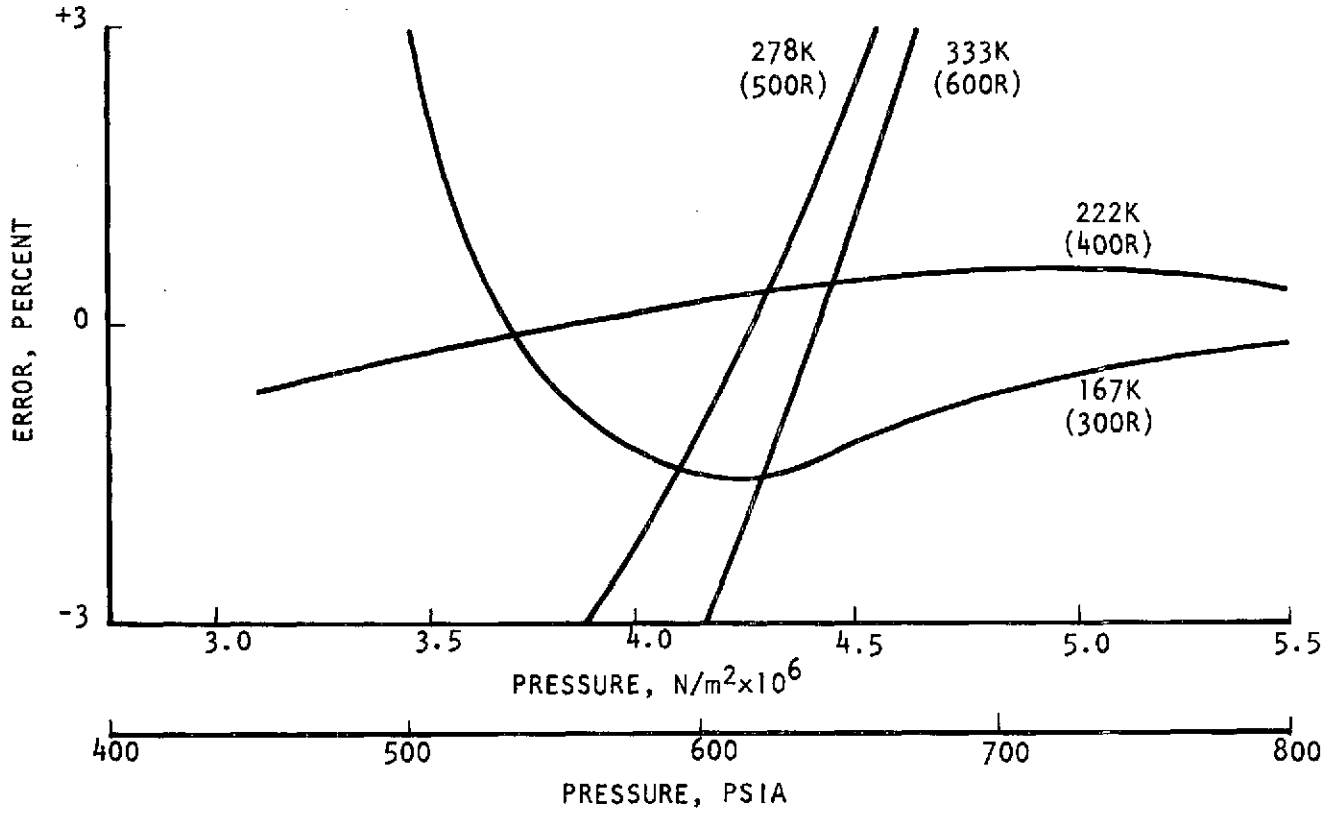

Figure 24. Mechanical Sonic Controller Control Accuracy Prediction

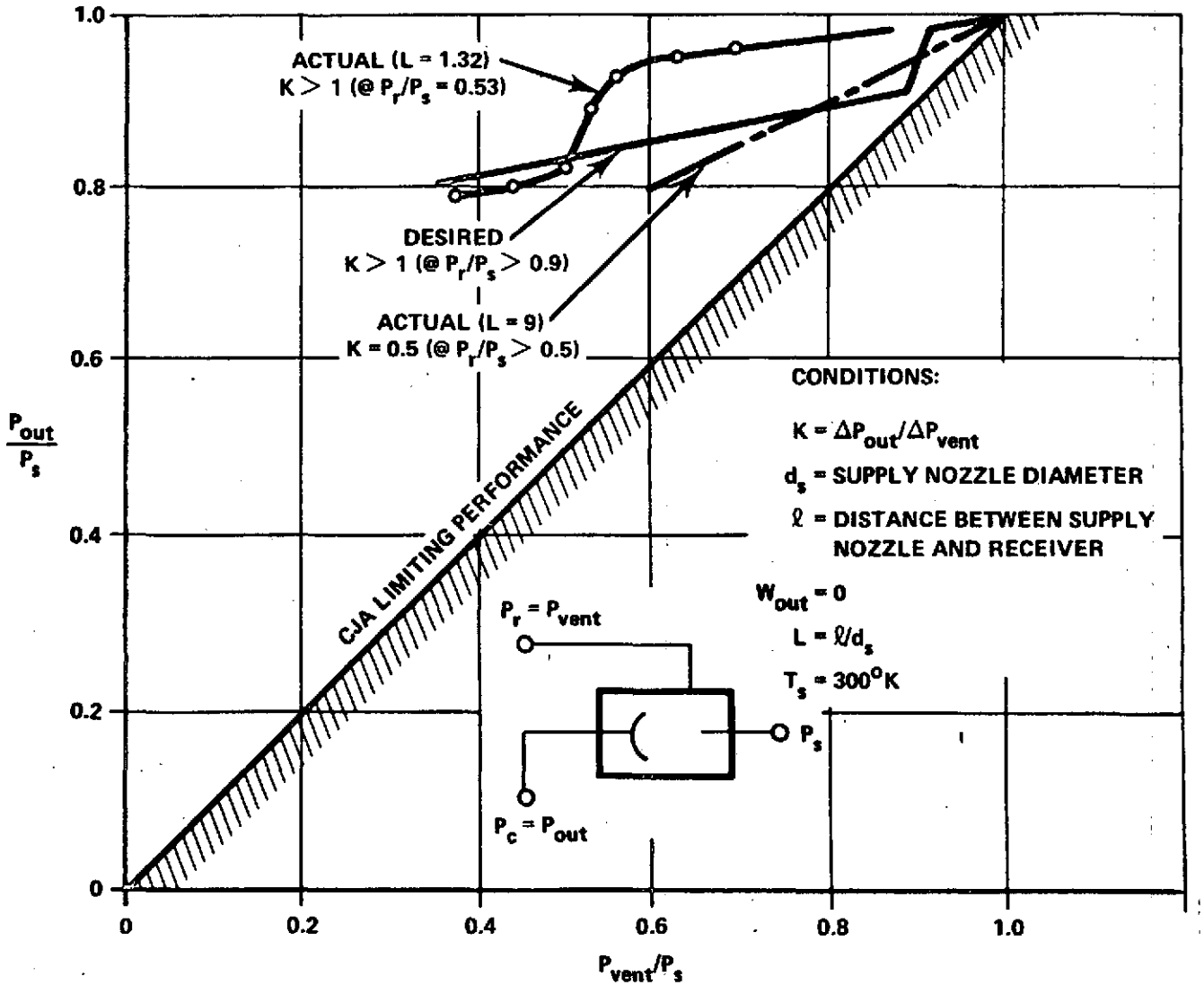

Figure 25. Confined Jet Amplifier Performance

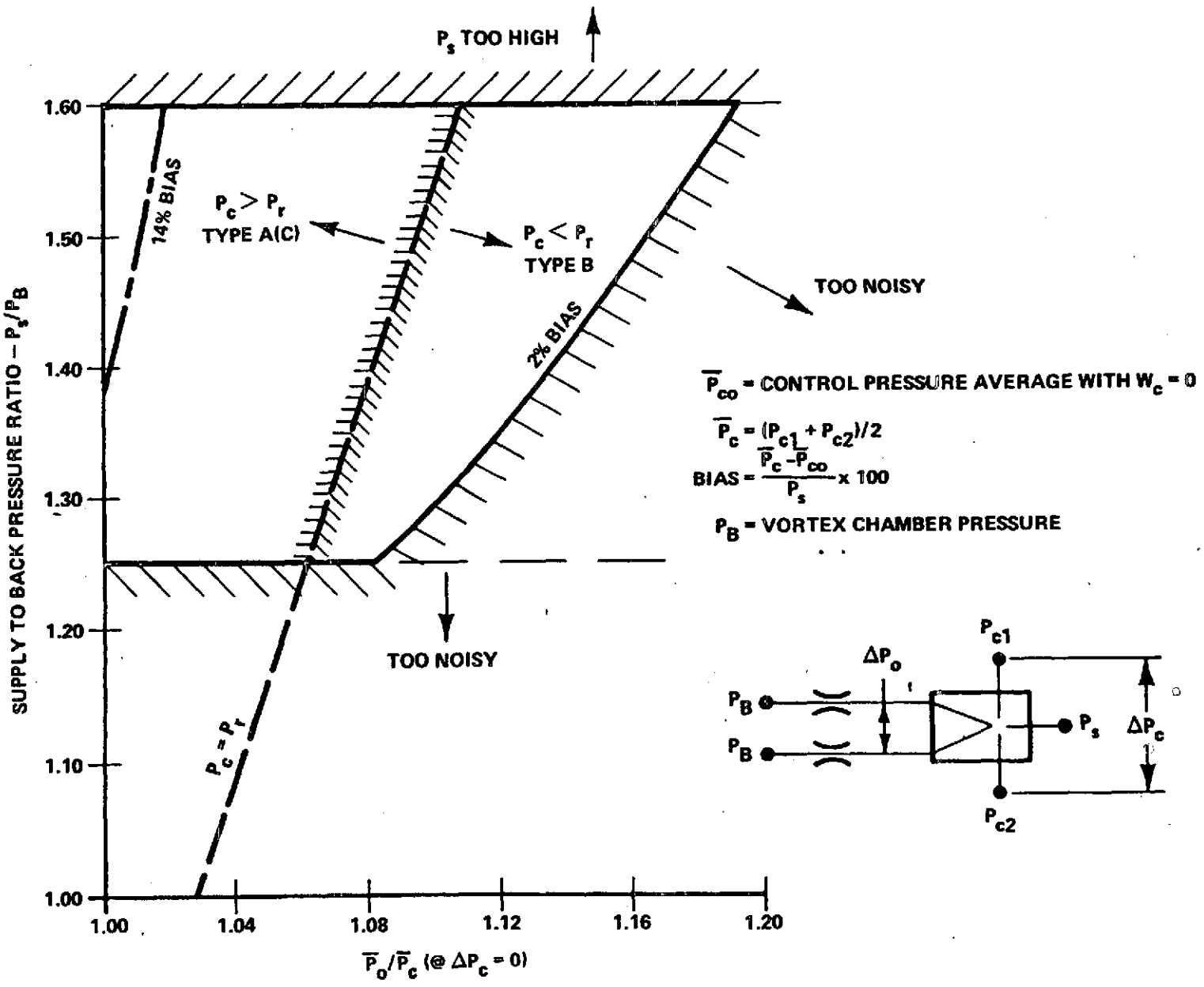

Figure 26. Proportional Amplifier Performance

A computer study of the controller dynamics was conducted. Performance at the lower supply pressures, 317 x 10^6 N/m^2 (460 psia), was indicated to be stable and responsive within 50 msec. Performance at the high end of supply pressures, 5.51 x 10^6 N/m^2 (800 psia), indicated a possible stability problem.

As a result of a technical review meeting with NASA, it was decided that two areas needed further investigation before full development might begin on this concept. One area dealt with the accuracy of the fluidic circuitry over full ranges of absolute pressure, temperature, and flow rate. The other concern was with the dynamic stability and response over the operating range.

To examine these areas, testing and/or analysis were conducted on the key fluidic elements in the circuit for a range of the required operating conditions. Results showed that some of the fluidic elements had significant nonlinearities in performance over the range of required absolute pressures. While these nonlinearities were repeatable they did add to further inaccuracies in the control circuit. It appeared that amplifier performance at lower fluidic operating pressures did not lend itself to scaling up to high pressures. As a net result it was concluded that this fluidic concept would have required further development to improve accuracy and that the required development exceeded the resources of this program. This concept was therefore eliminated from further consideration at that time.

A detailed report of this and other fluidic investigations performed is described in Appendix A.

Hybrid Fluidic Flow Controller-D. The metering element and the vortex valve were built separately for testing. The prime items that were investigated by the tests were (1) vortex characteristics with subsonic exit flow, (2) minimum pressure drop for operation, (3) sensitivity to spring force, and (4) other potential anomalies. Test results indicated sufficient vortex strength at subsonic flow conditions, sensitivity to spring force setting, and a larger minimum pressure drop than needed in the type C controller.

Although this design has few moving parts and potentially good response, it requires a nonlinear spring force and high pressure drop. It is also sensitive to downstream oscillations and results in a large package volume. Control accuracy is estimated as no better than ±15 percent. Based on these considerations, the concept was eliminated.

PRELIMINARY DESIGN OF THE MECHANICAL CONTROLLER

The preliminary design was fabricated as a test prototype of a flight type design to demonstrate the functional concepts of its operation. The major difference from a flight type version is in the design of the main body which was simply machined with more regard to low cost than to the minimum weight. The internal configuration and components would be virtually the same as the flight weight design.

Configuration

The configuration depicted in Fig. 27 consists of two major subassemblies: a temperature sensitive pressure divider circuit and a pressure-spring balanced metering poppet. The pressure divider circuit is comprised of an invar hollow cylinder with a sonic nozzle at the downstream end. Inside the housing is a variable area pintle which is supported by a thin aluminum tube, fixed at the upper end to the invar outer cylinder. The cylinder has large ports which allow gas flow through and around the aluminum tube as well as through the flutes in the pintle and out through the sonic nozzle. A pressure port is provided upstream of the sonic nozzle which is pneumatically linked to the bellows. A detail of the pintle is presented in Fig. 28.

The metering poppet assembly contains a movable poppet mechanically linked to a bellows/spring combination. A dashpot has been incorporated with the downstream side of the poppet. A pressure sensing tube is linked to the dashpot through an orifice and also feeds back pressure to one side of the bellows.

The main housing contains a subsonic nozzle into which the sonic venturi of the pressure divider circuit flows. Sensing ports are provided in various parts of the assembly for the measurement of pressure and temperature.

Operation

As propellant enters the controller, it passes around and through the pressure divider circuit. The flow thermally conditions the aluminum tube resulting in a given displacement for a specific inlet gas temperature. This displacement results in a certain ratio of pintle flow area to sonic venturi flow area and fixes the ratio of the pressure in the region upstream of the sonic venturi as some proportion of inlet pressure. This pressure is fed to the outside of the bellows through internal passages. The action of this pressure on the bellows drives the metering poppet in the direction of the open position.

The bulk of the incoming gas flows around the pressure divider assembly into the region of the poppet. Here some of the flow stagnates against the upstream side of the poppet thereby applying a pressure force which drives the poppet towards the closed position.

As flow passes through the poppet opening, the downstream pressure is picked up by the pressure sensing tube which feeds it back to the back side of the poppet and the inside of the bellows. The effective area of the bellows being larger than that of the poppet results in a net force in the closed direction. The flow downstream of the pressure sensing tube passes through a subsonic venturi which maintains a static pressure at the exit plane of the smaller sonic venturi that is low enough under all required conditions to maintain choked flow through the sonic venturi.

The position of the metering poppet which determines propellant flow area is determined by the balance of the just mentioned pressure forces and bellows/spring forces. Increasing inlet pressures tend to close the poppet as does

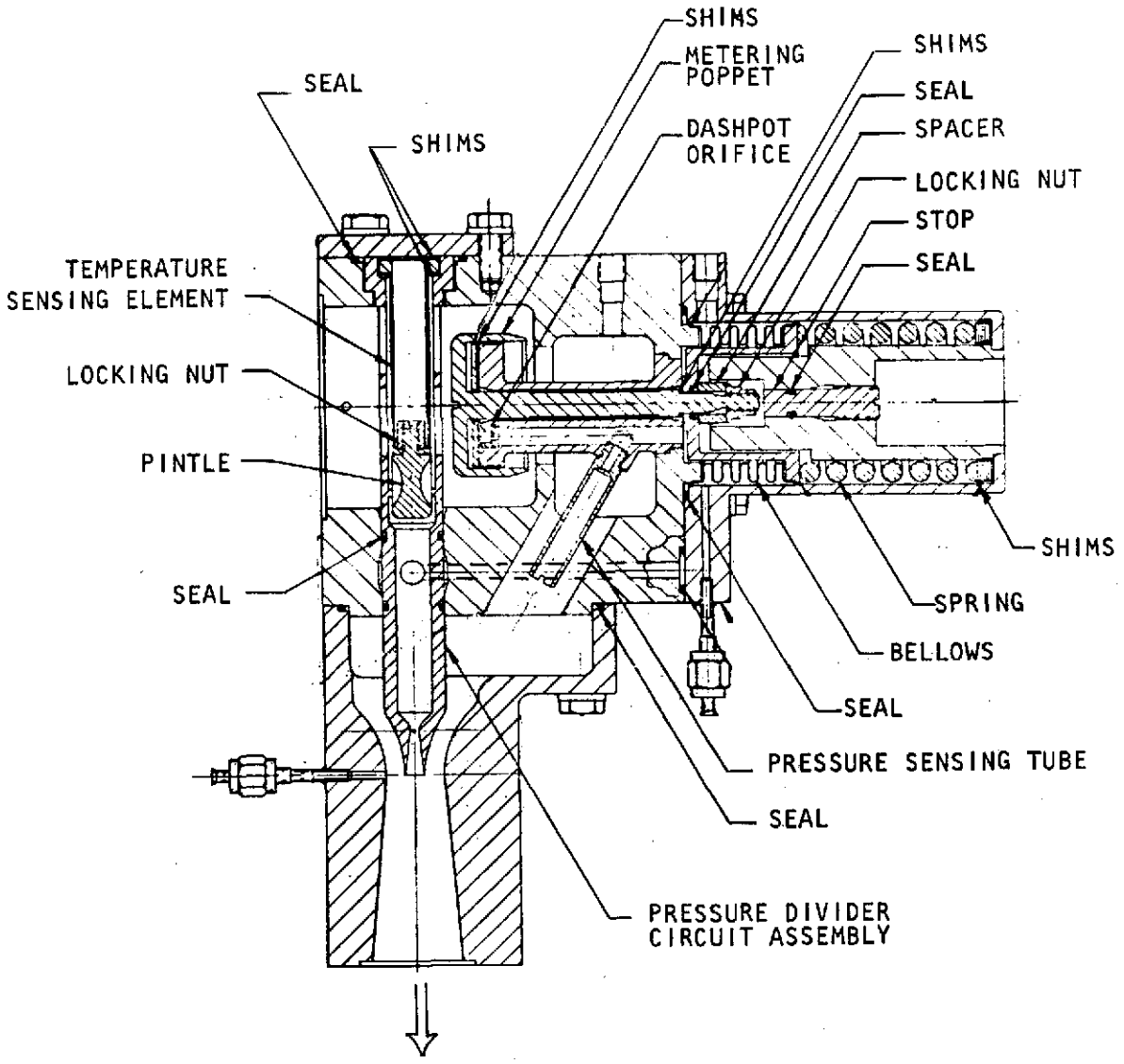

Figure 27. Preliminary Design Configuration

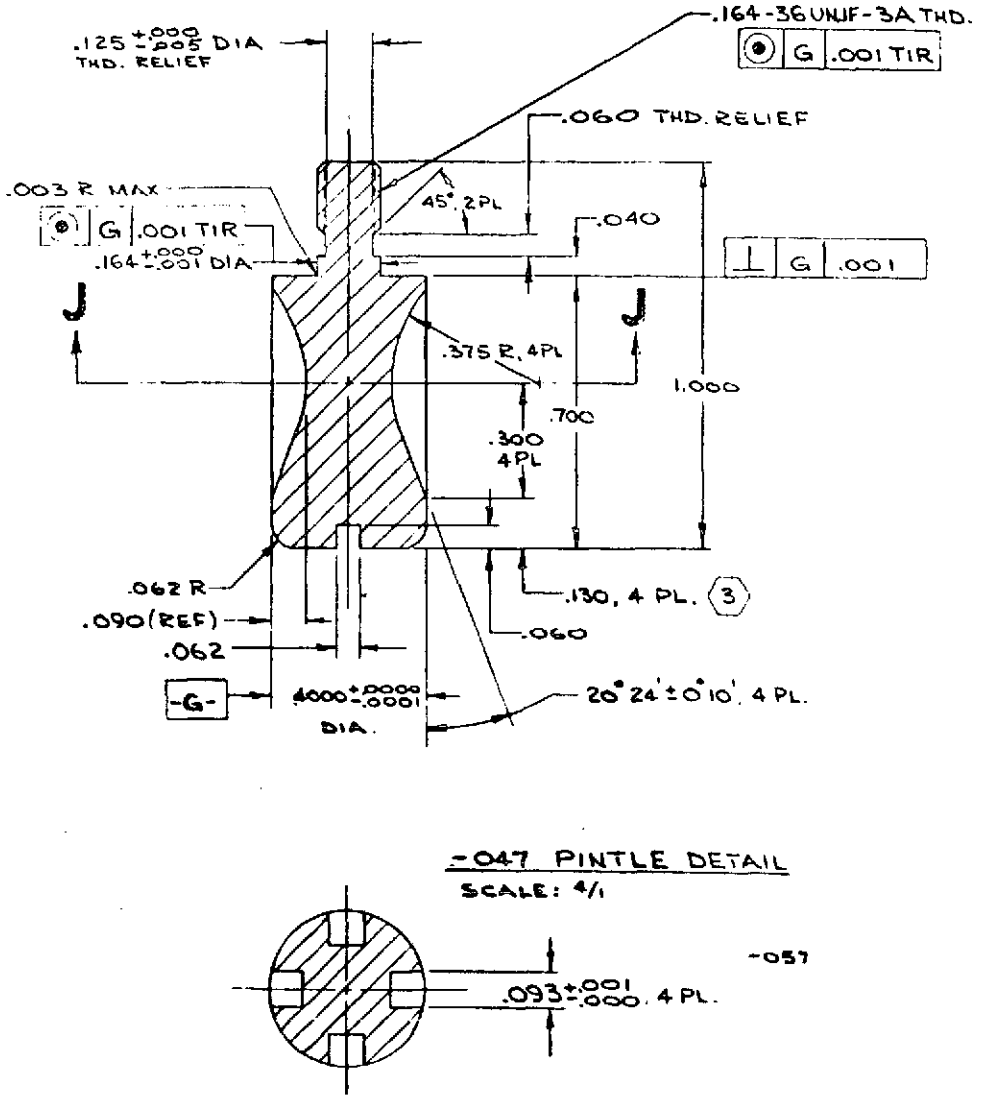

Figure 28. Temperature Sensor Pintle

increased regulated or downstream pressure. As the temperature increases, pintle flow area increases which causes the ratio of bellows pressure to inlet pressure to increase. The result is a shift of the poppet towards the open position. As the temperature of incoming gas decreases, the reverse is true.

Design Features

Certain features of the design are peculiar to the functioning of this controller over the range of temperature and pressure conditions. The features relate to material selection, dynamic stability, and adjustment of various parts of the controller.

Material Selection. Because of the requirement to control over a wide temperature range, a material which had little or no dimensional change with temperature was desired. Invar, an iron-nickel alloy, was selected as the basic material. The coefficient of expansion is approximately one twelfth that of aluminum and one tenth that of stainless steel. Parts not constructed of invar include the temperature sensitive aluminum tube in the pressure divider circuit, the Inconel (718) bellows, the Ni-span C spring, the Teflon sleeve on the poppet shaft, the Teflon lip seals, steel tubing and fittings for sensing lines, and steel connecting hardware. The Ni-span C material has a near constant modulus of elasticity with varying temperature.

Dynamic Stability. Experience has indicated that pressure feedback sensing in pressure regulators should be located in a region of well behaved uniform flow. Sensing in turbulent regions can result in instability. For this reason, a sensing tube was designed to project into a stream of uniform cross section.

Dynamic modeling indicated marginal stability at higher inlet pressures. To control oscillation, a separate dashpot was designed into the poppet assembly. The two features of the dashpot design was the minimization of dashpot volume to achieve maximum effectiveness and the ability to vary the damping orifice size.

Adjustment Capability. To facilitate adjustment of the controller to deliver the appropriate flowrate, provisions were made to adjust several parts of the controller. Shims have been provided for varying spring preload, poppet position, pintle position, and dashpot volume. Various length sensing tubes were also fabricated; and as previously mentioned, the size of the dashpot orifice can easily be varied by replacement of an Allen head socket nut with a drilled hole.

FABRICATION

Fabrication was primarily by machining with some electron beam welding. No problems were encountered with either the machining or welding of the invar material. The steps followed are outlined below.

1. Rough machine body and poppet guide
2. Electron-beam weld guide into housing
3. Heat shrink Teflon on guide OD and poppet shaft OD
4. Finish machine
5. Install poppet
6. Heat assembly to 480 K (400 F)
7. Assemble and weld bellows
8. Assemble spring and cover
9. Adjust maximum and minimum poppet stops
10. Assemble temperature sensor assembly

A photograph of the component parts after step 7 is presented in Fig. 29.

EVALUATION TESTING

Tests were performed with gaseous hydrogen, oxygen, and nitrogen over a pressure range of 2.76×10^6 Kg/m (400 psia) to 5.52×10^6 Kg/m (800 psia) and a temperature range of 139 K (250 R) to 306 K (550 R). Both steady state and dynamic characteristics were demonstrated.

Test Facility

Testing was performed at the Thermodynamics Laboratory of the B1 Division of Rockwell International. The test facility is depicted schematically in Fig. 30 and a photograph of the facility is presented in Fig. 31. Controller inlet pressure is controlled by the facility regulator upstream of the heat exchanger. The inlet temperature is controlled by soaking the 900 Kg (2000 lb) heat exchanger mass of steel balls with liquid nitrogen. By adjusting the mixing valve, a combination of ambient and cooled propellant can be obtained to cover the range of inlet temperatures. The J-2 valve downstream of the controller is the actuating device for initiating and curtailing flow through the controller. An orifice downstream of the J-2 valve simulates the fluid resistance of the thrustor injector and an adjustable back pressure valve provides a simulation of chamber pressure. Flowrate is determined by pressure and temperature measurements upstream of a calibrated sonic venturi which vents to the atmosphere.

Operation of the facility is remote and executed using the control panel shown in Fig. 32.

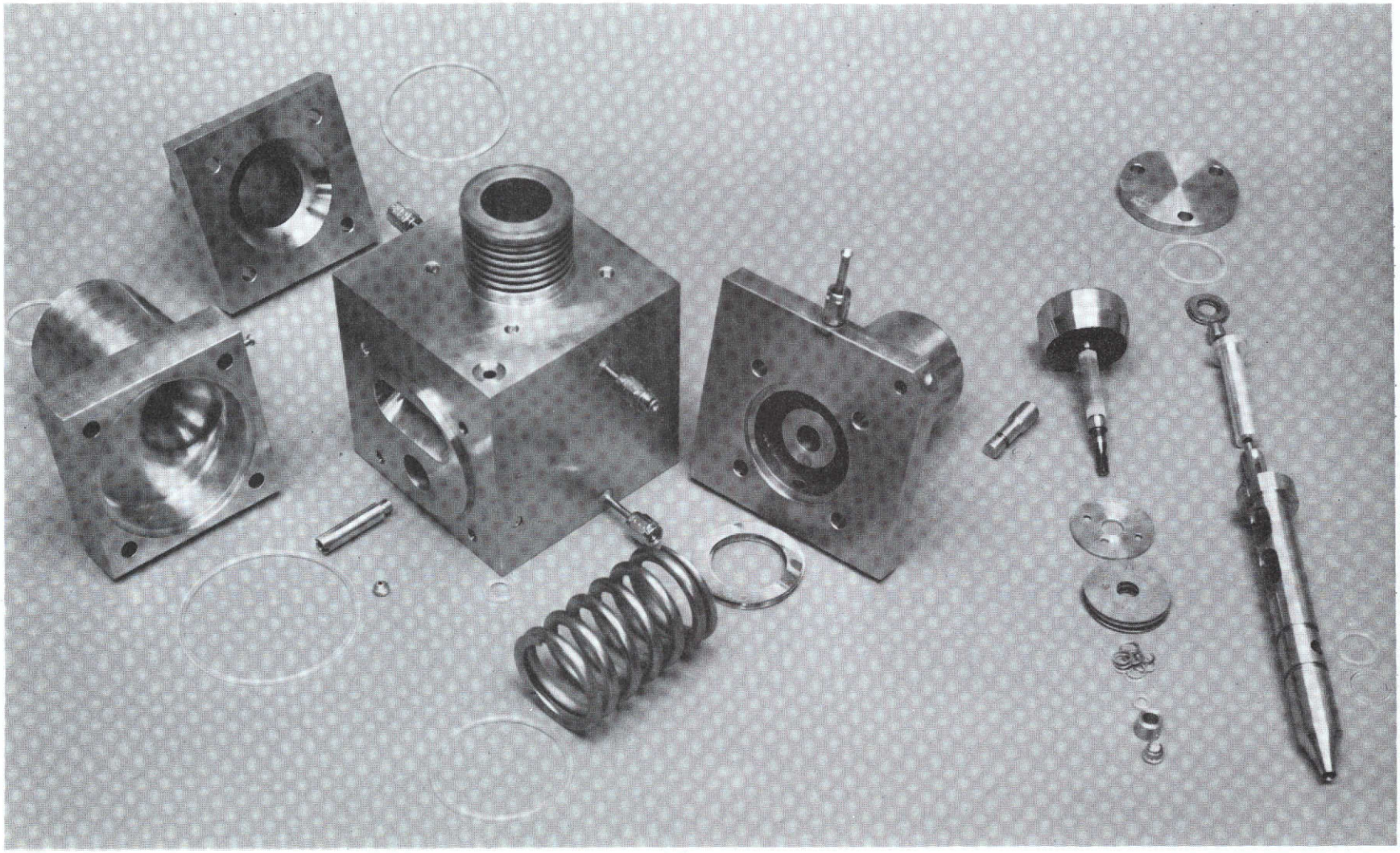

1XZ61-6/22/73-C1A*

Figure 29. Mechanical Flow Controller Component Parts

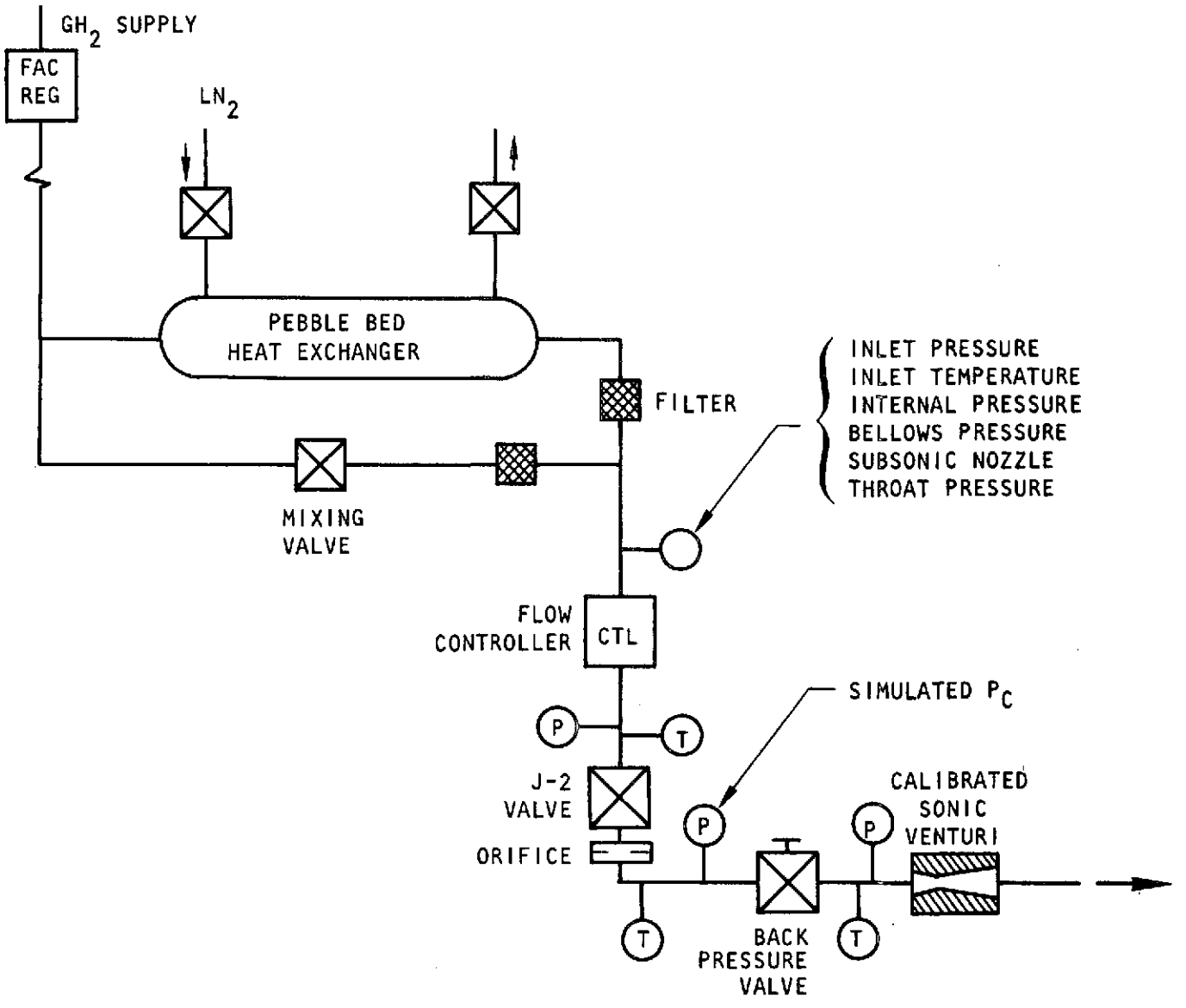

Figure 30. Flow Controller Test Facility Schematic

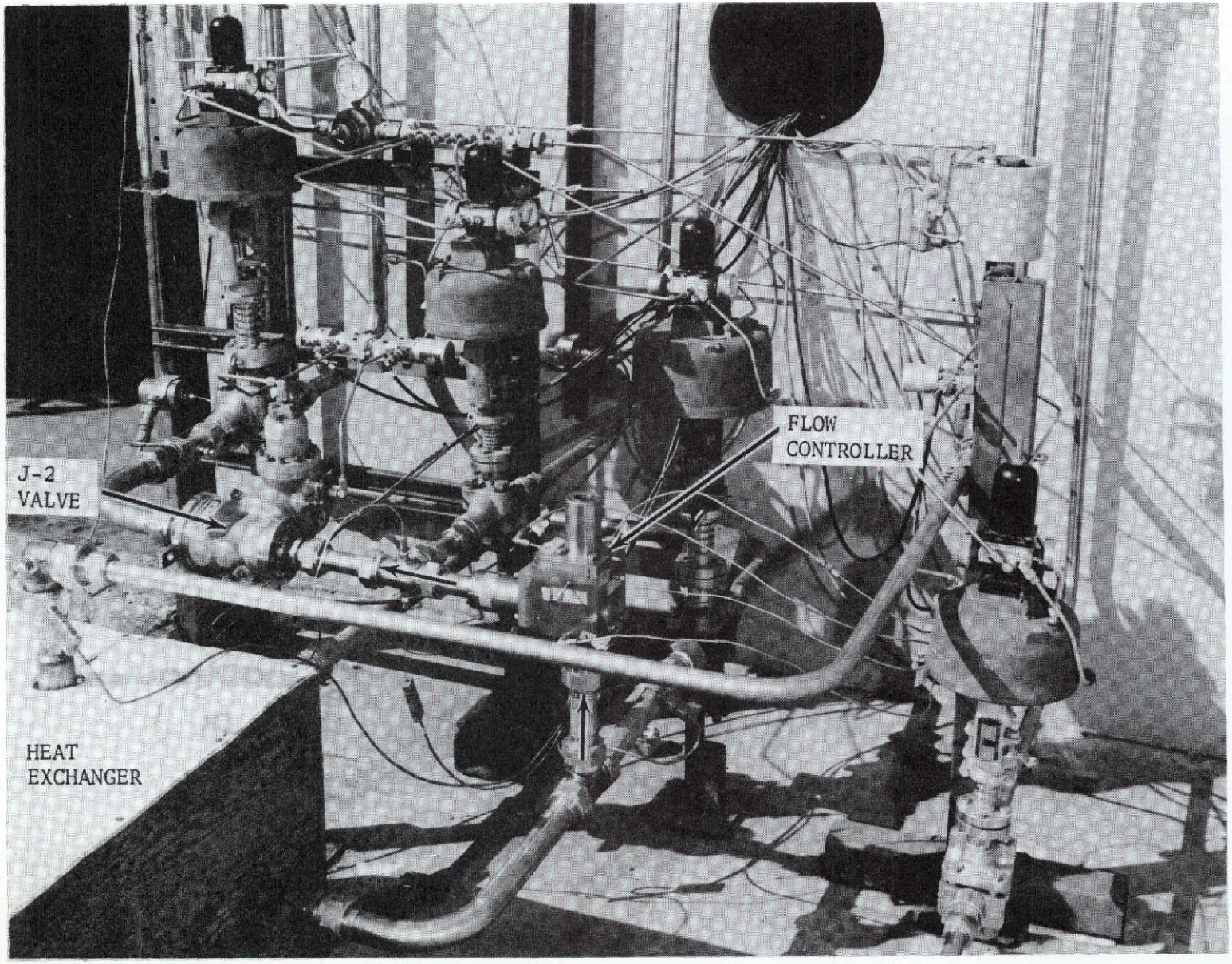

10-19-73, 7862-95-2A

Figure 31. Flow Controller Test Facility

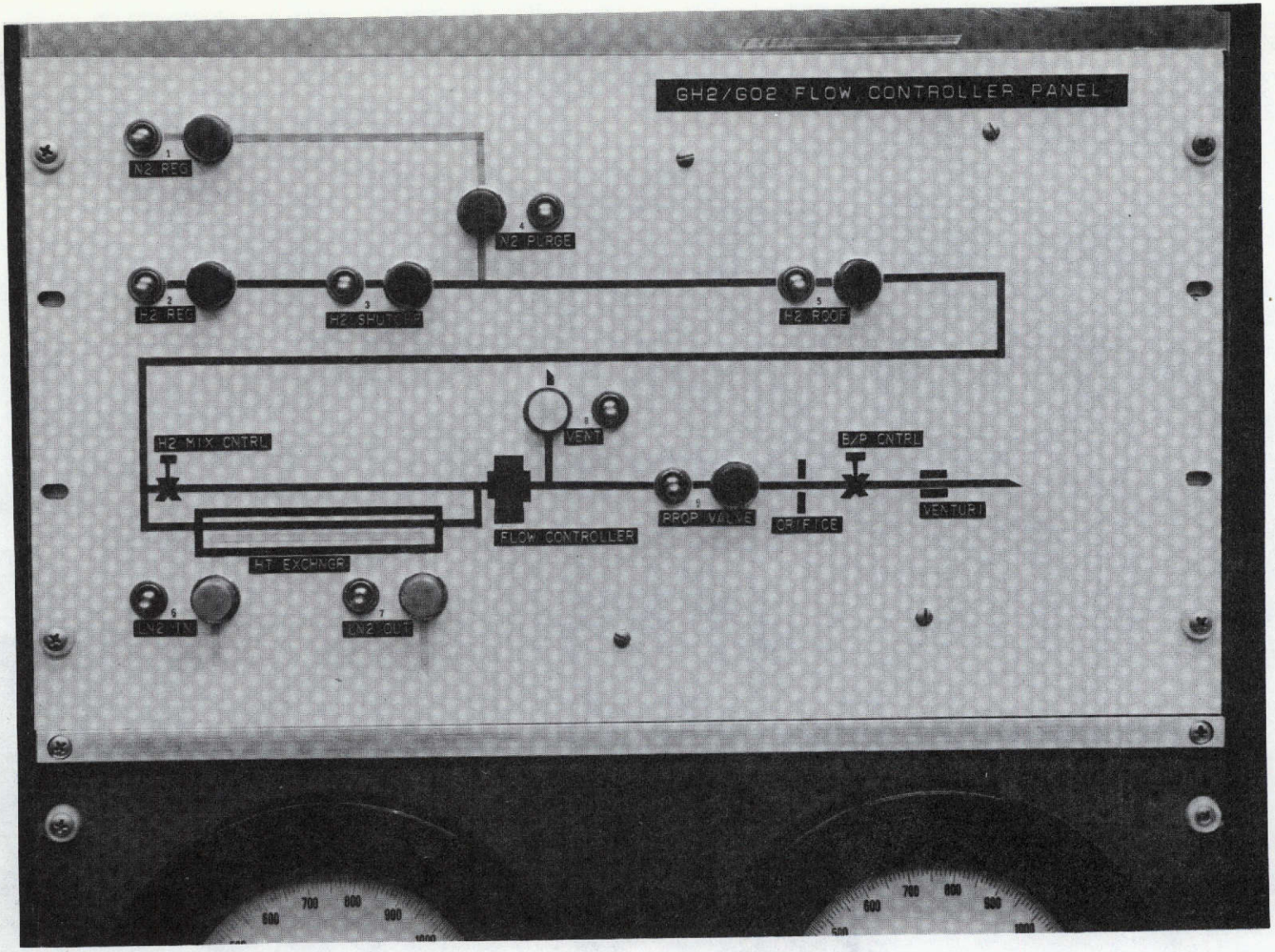

10-19-73 7862-95-2D

Figure 32. Test Facility Control Panel

Instrumentation and Recording

The location and types of measurements are indicated on the facility schematic in Fig. 30 and in the controller assembly drawing in Fig. 33. The pressure transducers were the strain gage type with a precision of 1 percent and a transient response of 1 millisecond. Although sensing ports were provided for high frequency pressure measurements, their use was not required. The temperature transducers were copper-constantan thermocouples with a precision of 1 percent.

Data was recorded on Brush analog recorders and on the digital Astro Data System. Test results were initially monitored using the Brush output. The digital data was used to evaluate steady state performance. Also available for higher frequency data (>60 Hz) was an oscillograph. It was found that when oscillations did occur that the Brush recorder was adequate in displaying the data. Thus the oscillograph did not find extensive use.

Ambient Temperature Testing - Hydrogen

After considerable adjustment of spring preload and pressure divider pintle position, a series of tests were run at ambient temperature over a pressure range of about 3.31 Kg/m^2 (480 psia) to 5.62 Kg/m^2 (815 psia). Control accuracy and dynamic response were characterized as was the performance of the pressure divider circuit.

Control Accuracy. Two type of tests were performed: (1) flow was pulsed for several seconds at a given inlet pressure, (2) flow was initiated at the low end of the inlet pressure range and continued as inlet pressure was varied up to about 5.79×10^6 kg/m^2 (840 psia) and down to 3.28×10^6 Kg/m (475 psia)

The results of the first type of tests are presented in Fig. 34. The variation in flowrate over the range covered was ±3.3 percent about the mean value for a given run. Run to run variation is suspected to be due to friction in moving parts. Some difficulty was encountered with mechanical fits.

A continuous run of inlet pressure variation up and down the range indicated approximately the same control accuracy as in the individual pulse tests. These results, shown in Fig. 35, indicate slight hysteresis.

Flowrate was somewhat below nominal (0.31 Kg/sec, 0.69 lb/sec) in these tests. It was decided to proceed with testing at this condition rather than expend effort in further tuning of the device.

Response and Stability. Output pressure of the controller and simulated chamber pressure are depicted as a function of time in Fig. 36, a Brush recording of a flow start transient. Note that controller output pressure responds in less than 50 milliseconds. Simulated chamber pressure is somewhat slower but overshoots and decays to within 10 percent of steady state in about 50 milliseconds. Estimated opening time of the J-2 value is 20 to 30 milliseconds.

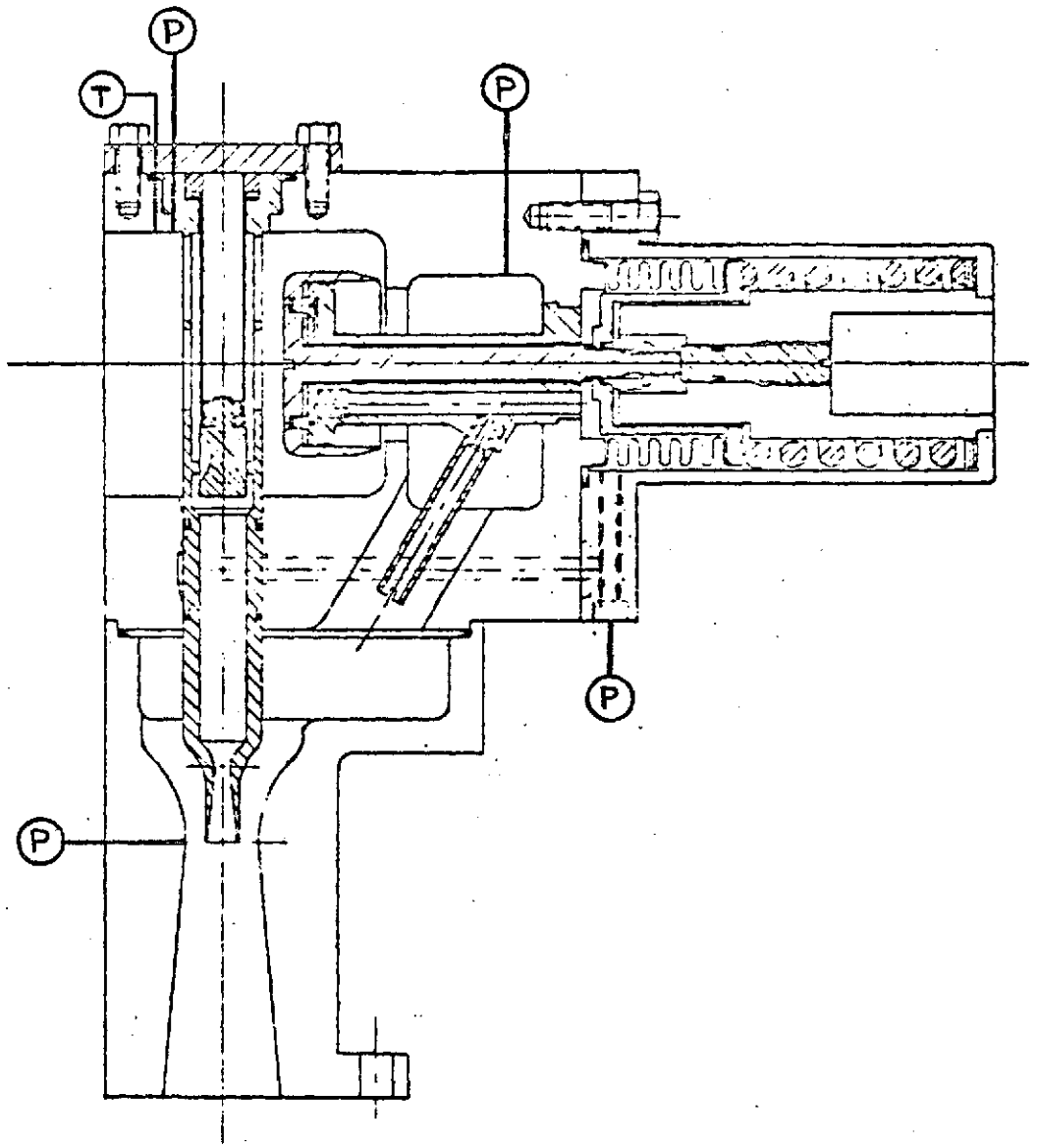

Figure 33. Flow Controller Instrument Location

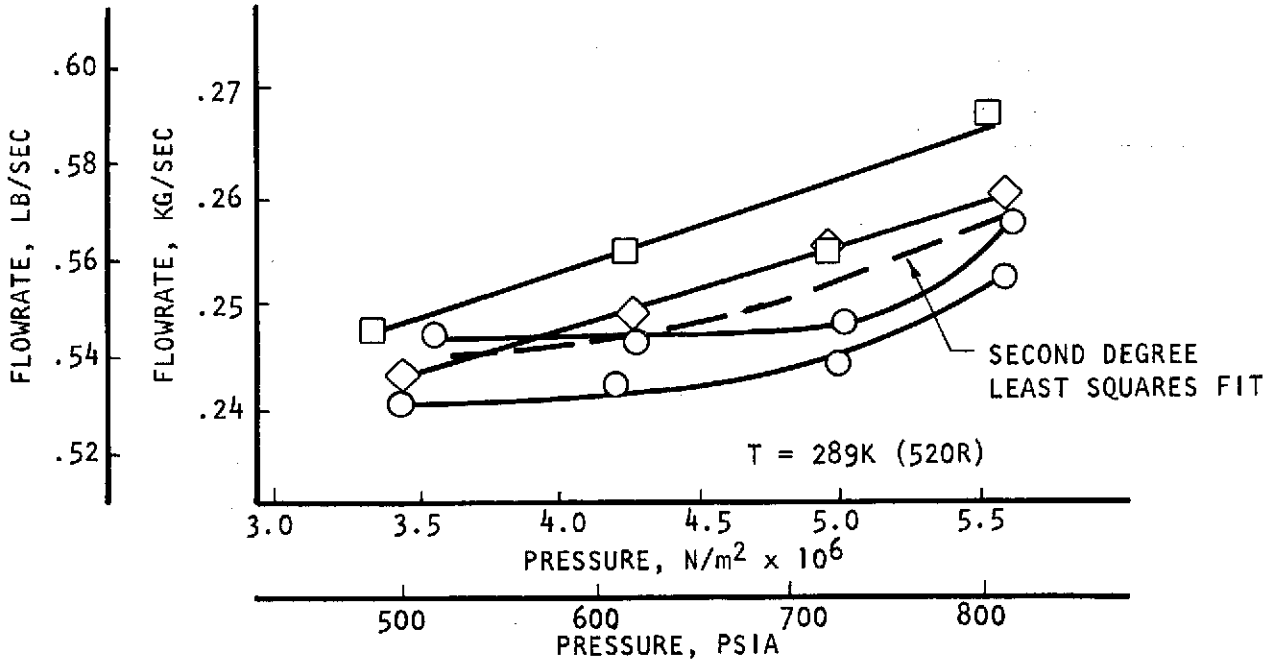

Figure 34. GH_2 Flowrate vs Inlet Pressure--Pulsed Flow

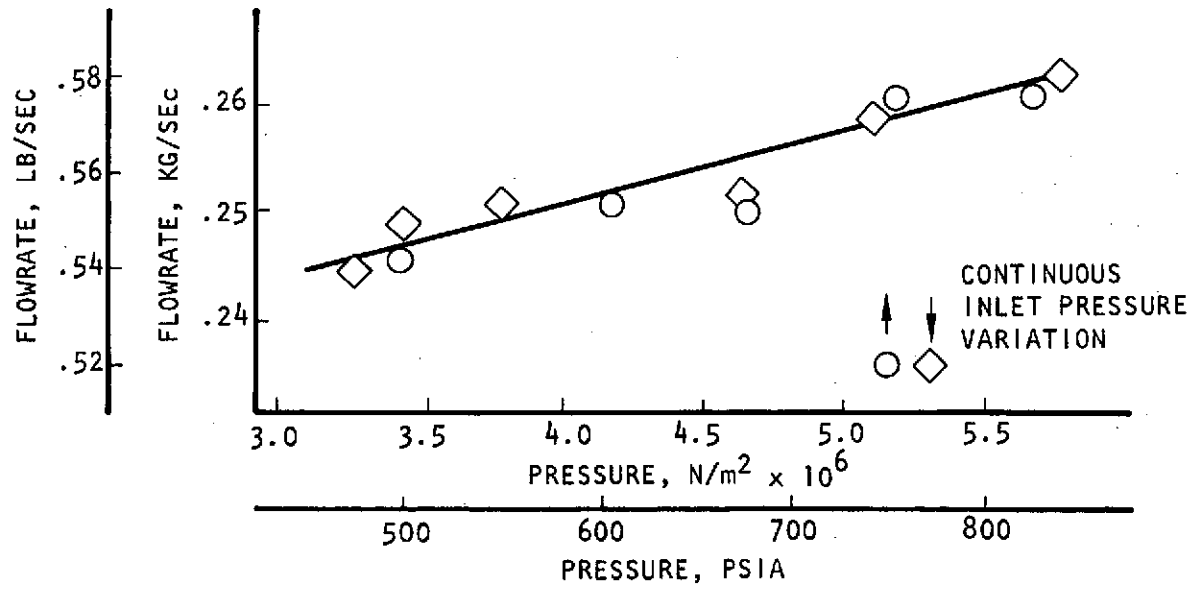

Figure 35. GH_2 Flowrate vs Inlet Pressure--Continuous Flow

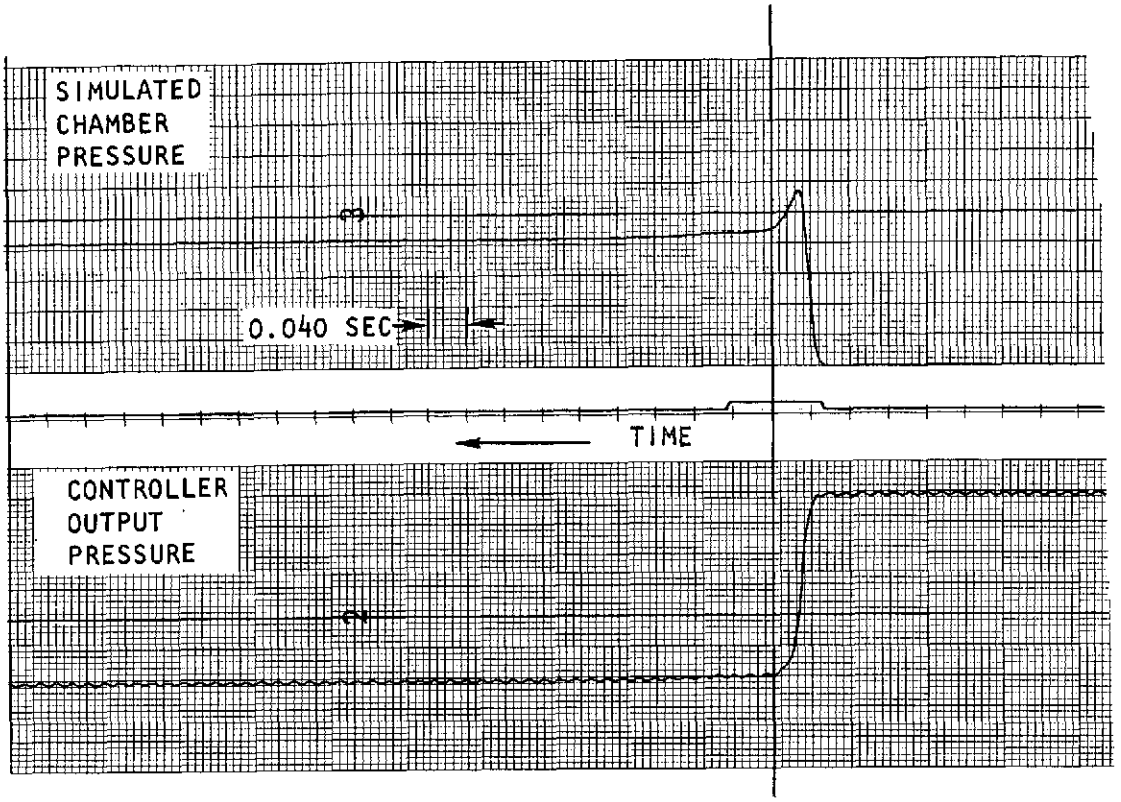

Figure 36. Dynamic Response

This response was accomplished with a damping orifice of 0.0015 m (0.06 inch). The transient appears to be well behaved in that it settles quickly with virtually no subsequent oscillation. In the course of making adjustments, some of the shims were removed from behind the poppet, increasing the volume of the dashpot. The following traces in Fig. 37 indicate the resulting oscillatory behavior showing the sensitivity of the dashpot performance to its volume. This confirms earlier analytical work which indicated the need for effective damping.

Pressure Divider Circuit. At a given temperature the pressure divider circuit is supposed to produce an output pressure which has a constant ratio to the inlet pressure.

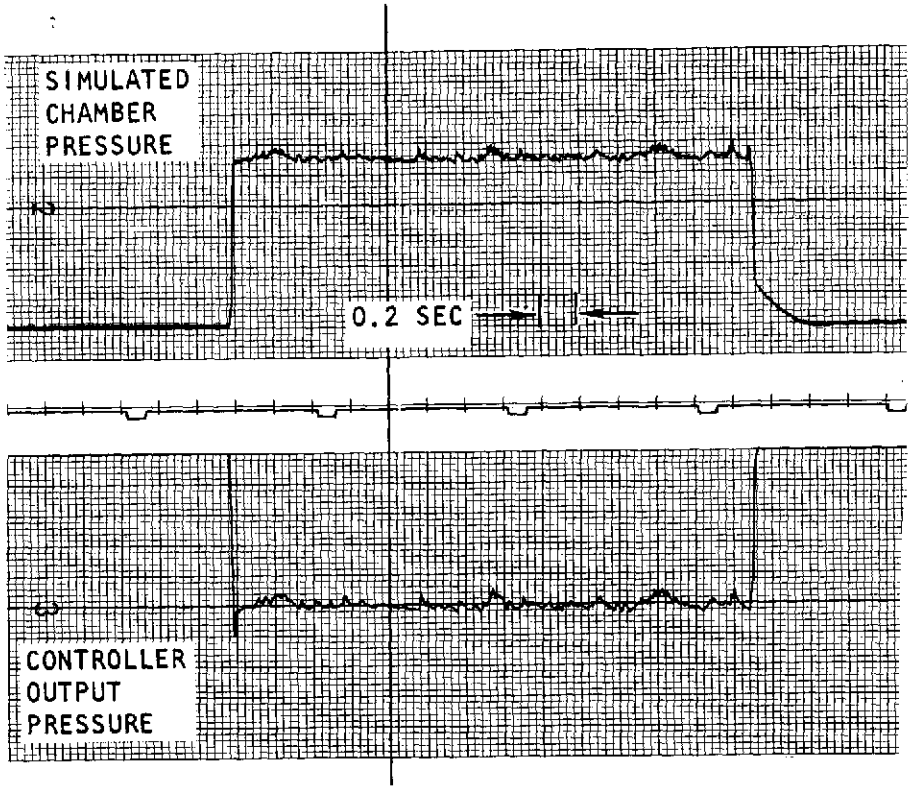

Figure 37. Pressure Oscillations

Data presented in Fig. 38, depicts this relationship. As the pintle is shifted (adjusted) in the direction away from the sonic nozzle, the pintle flow area is diminished, causing the output pressure to decrease. This relationship is characterized by the data in Fig. 39.

Low Temperature Testing-Hydrogen

Tests were conducted with gaseous hydrogen with inlet temperatures ranging from 111 K (200 R) to about 294 K (530 R) over a pressure range of 3.28×10^6 Kg/m^2 (475 psia) to 5.52×10^6 Kg/m^2 (800 psia)

Control Accuracy. Results of these tests are depicted in Fig. 40 and 41 which show flowrate as a function of inlet pressure and temperature. The calculated effective displacement (with C_d) is shown in Fig. 42 as a function of inlet pressure and temperature.

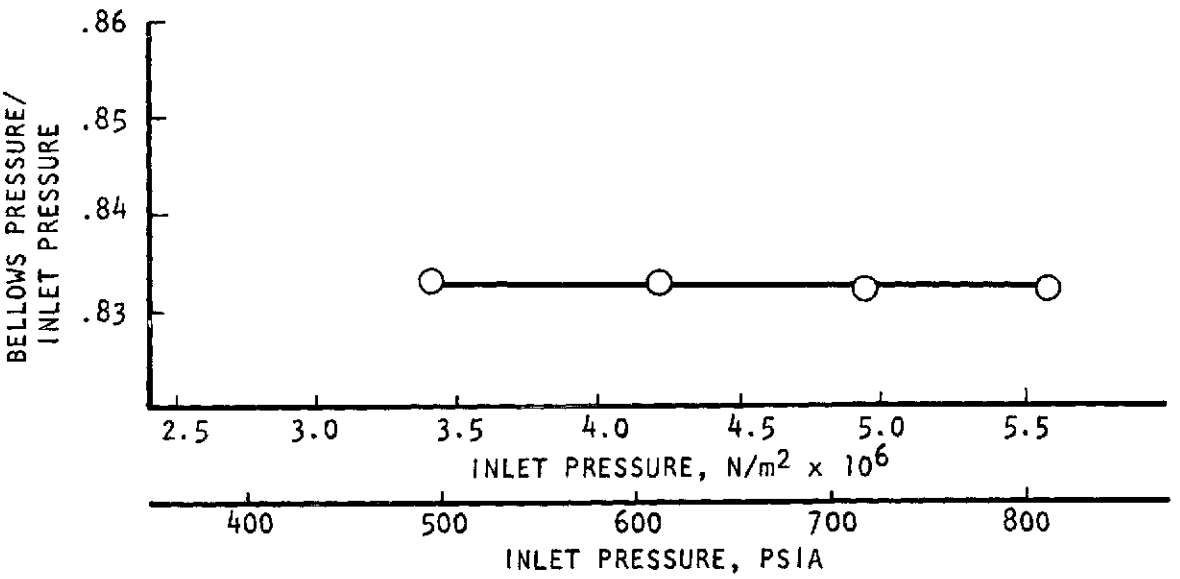

Figure 38. Ratio of Bellows Pressure to Inlet Pressure as a Function of Inlet Pressure

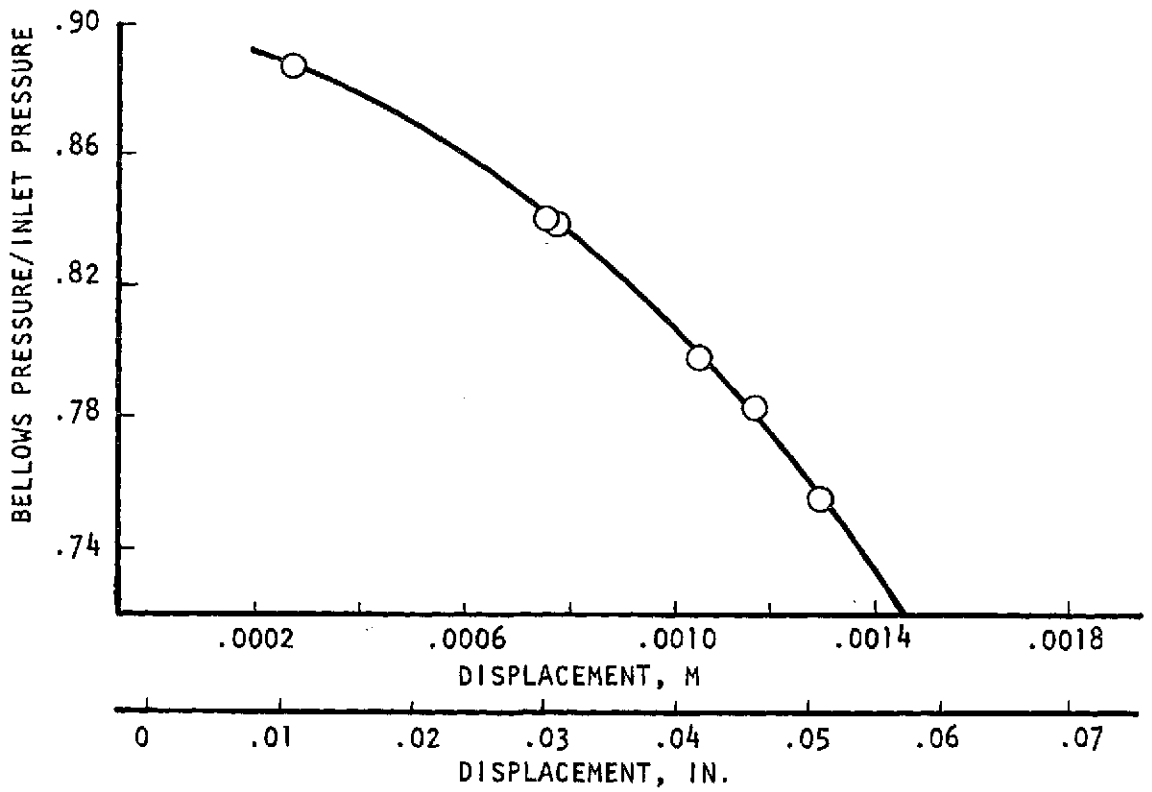

Figure 39. Ratio of Bellows Pressure to Inlet Pressure as a Function of Pintle Displacement

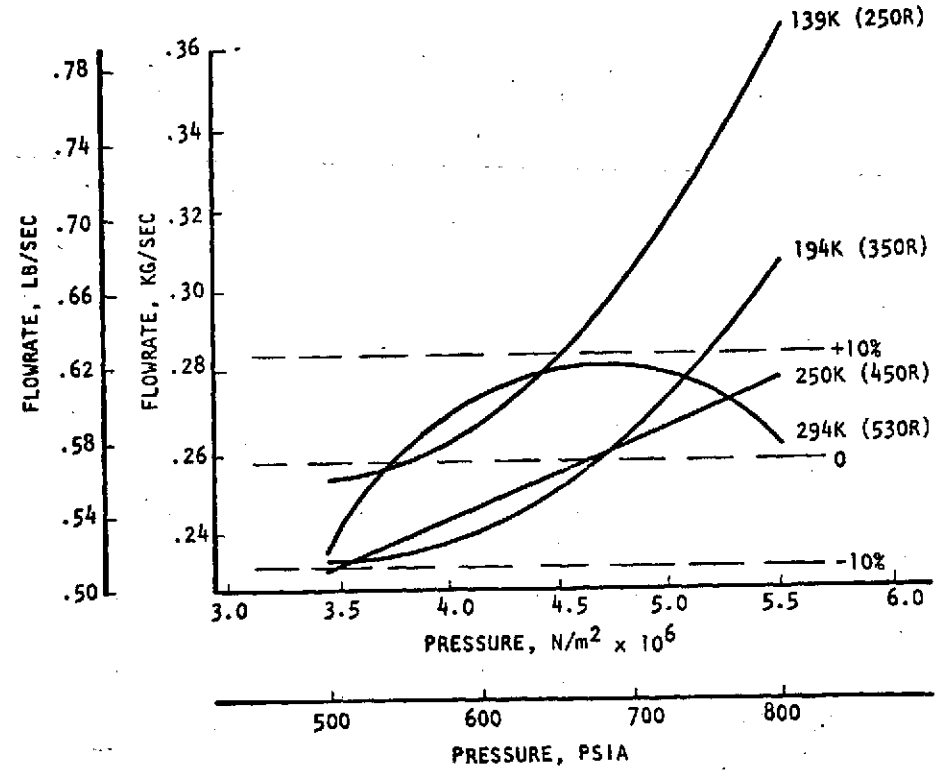

Figure 40. Flowrate as a Function of Inlet Pressure and Temperature

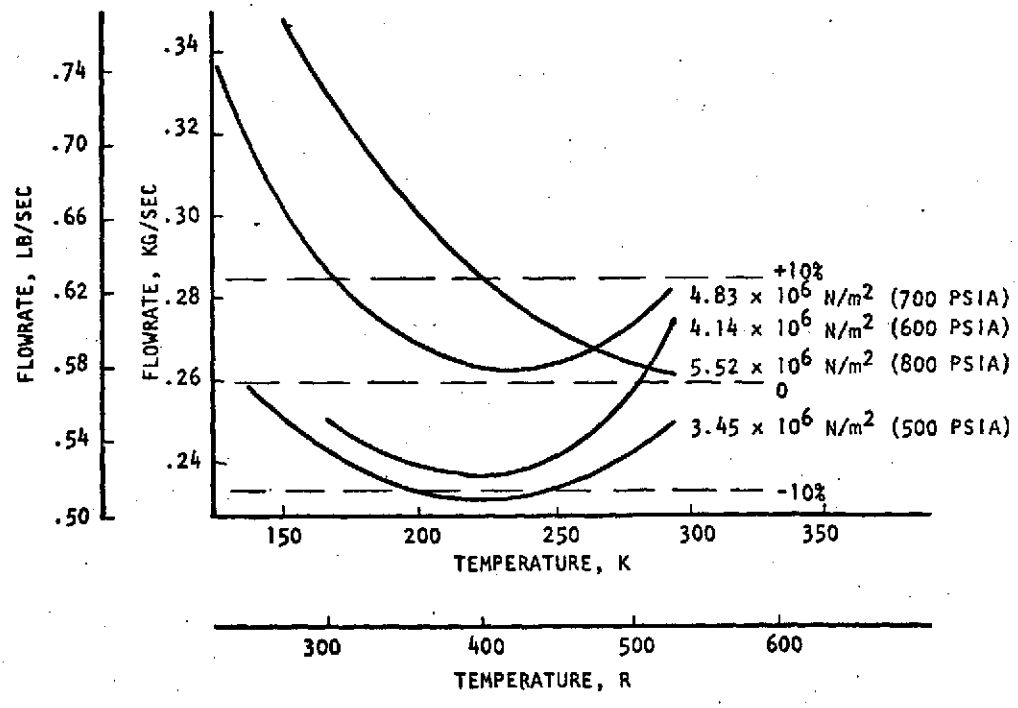

Figure 41. Flowrate as a Function of Inlet Temperature and Pressure

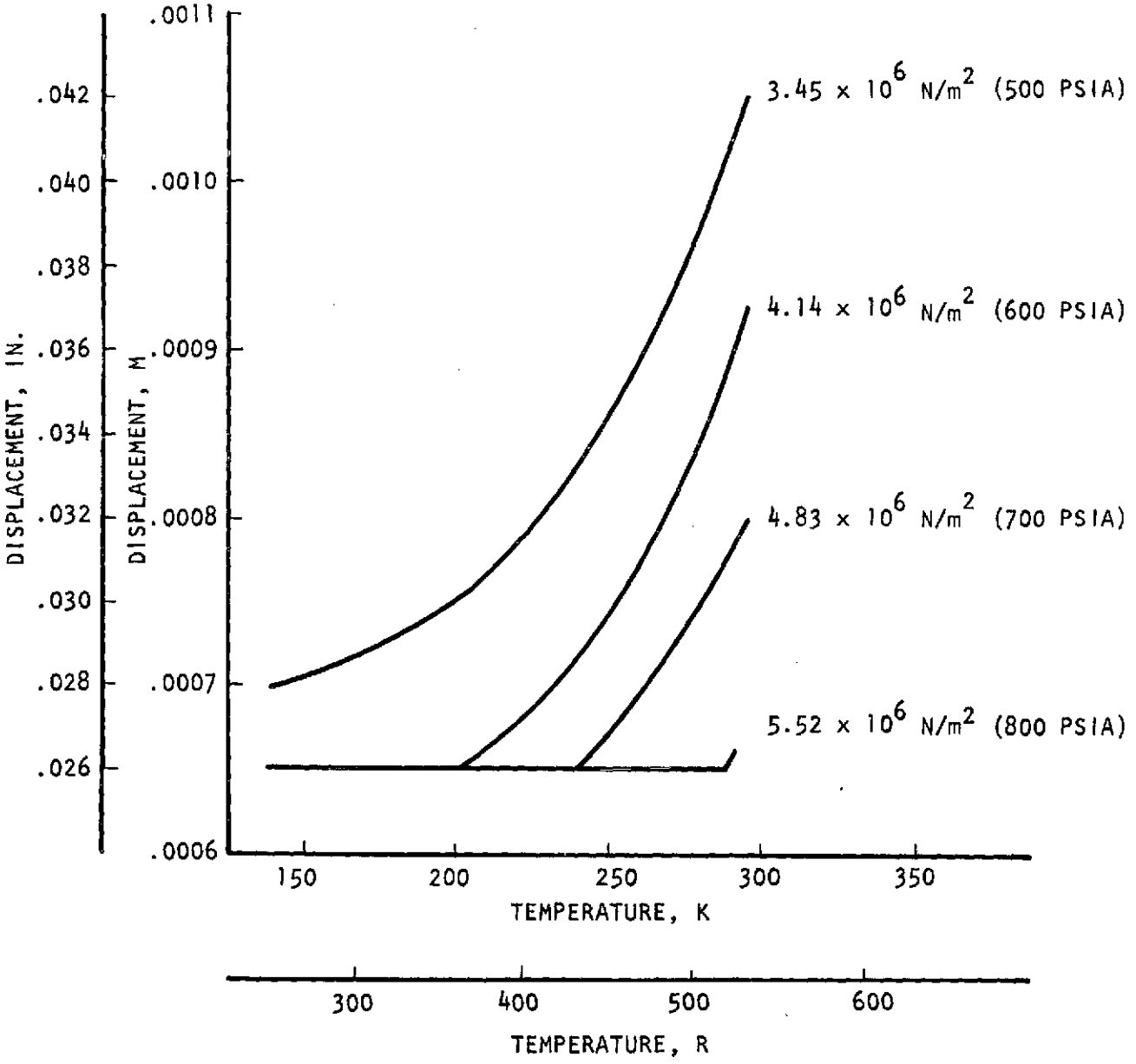

Figure 42. Calculated Effective Poppet Displacement as a Function of Test Inlet Temperature and Pressure

During early low temperature testing, a mechanical interference was found in the temperature adjustment pintle assembly. In addition, the aluminum sensitive element was damaged from bombardment of a contaminant particle. Reworking of the pintle and replacement of the aluminum element resulted in somewhat different performance. The ratio bellows pressure to inlet pressure for best control shifted from about 0.845 to 0.78 at ambient temperature.

The reason for this shift was not apparent. The accuracy at ambient temperature was less than that previously obtained, however testing at lower temperatures proceeded. At ambient temperature, the flowrate varied from 0.24 Kg/sec (0.52 lb/sec) to 0.28 Kg/sec (0.62 lb/sec) over the pressure range. Taking 0.26 Kg/sec (0.57 lb/sec) as a reference mean, ±10 percent variation is indicated in Fig. 40 and 41 as a guide, and covers the temperature pressure envelope of 194 to 294 K (350 to 530 R) and 3.45×10^6 N/m^2 to 5.17×10^6 N/m^2 (500 to 750 psia).

The effective displacement of the poppet as indicated in Fig. 43 shows the effect of temperature compensation or adjustment. Note that movement of the poppet is unimpaired by mechanical limits at the lowest pressure. However as inlet pressures increase, the poppet appears to bottom out in an effort to decrease flow area with decreasing temperature. Note that even with the limitation in poppet movement, the controller flow is within ±10 percent in the major portion of the data.

Pressure Divider Circuit. The function of the pressure divider circuit is twofold: (1) at a given temperature, to produce a bellows pressure which is proportional to inlet pressure, and (2) as temperature varies, to change the proportionality relationship in a direct relation. As the inlet temperature rises, the bellows pressure should increase causing the poppet to displace toward the open position. This compensates for the increased specific volume of the propellant and allows for the maintenance of near constant flow.

Test data were fit to a linear relationship with the resulting function depicted in Fig. 44. Note that the variation in pressure ratio is only about ±1.6 percent. Looking back at poppet displacement in Fig. 42 it is apparent that the operation of the controller is quite sensitive to this ratio of bellows pressure to inlet pressure. At 3.45×10^6 Kg/m^2 (500 psia) the poppet travelled 0.000356 m (0.014 inch) due to this effect.

Thermal Response. The thermal dynamic response of the controller is characterized by the ratio of bellows pressure to inlet pressure as a function of time for a given step change in the temperature of incoming propellant. This

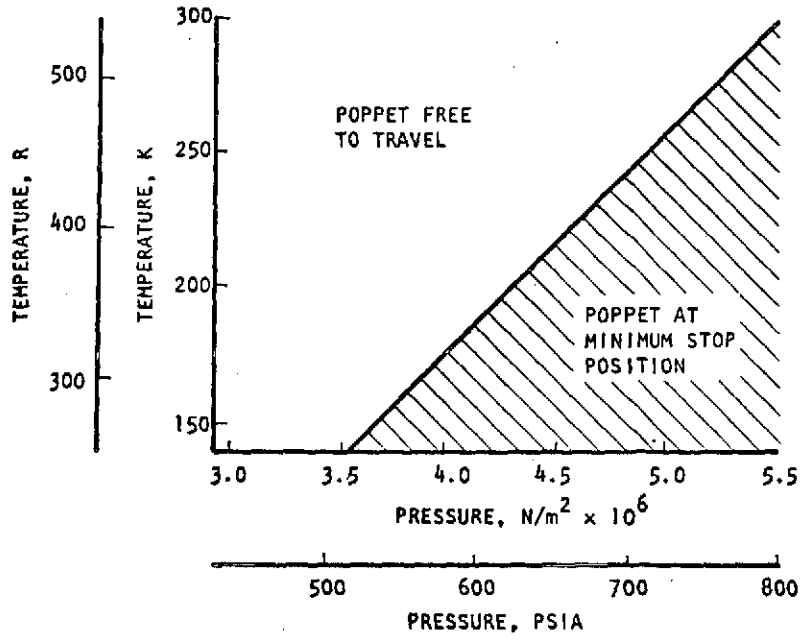

Figure 43. Poppet Operating Regions as a Function of Inlet Pressure and Temperature

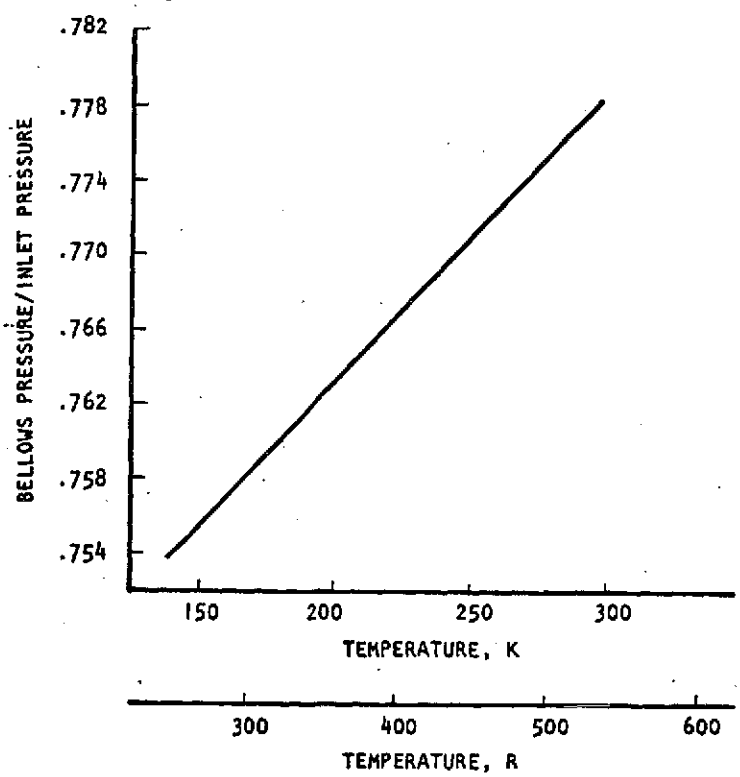

Figure 44. Ratio of Bellows Pressure to Inlet Pressure as a Function of Inlet Temperature

response characteristic is depicted in Fig. 45 which shows the pressure ratio as a function of time leveling off at around 300 millisecond. If we take this as a linear response, the time constant is then about 100 milliseconds.

Stability. It was observed that at propellant temperatures below 170 K (300 R) the behavior of the controller became more oscillatory. A 0.000762 m (0.03 inch) diameter dashpot orifice was used in place of the 0.00152 m (0.06 inch) diameter orifice. No intermediate sizes were tried. The effect on pneumatic response was an increase of 10 to 20 milliseconds.

Ambient Temperature Testing-Oxygen

The controller was tested with ambient gaseous oxygen over a pressure range of 3.1×10^6 Kg/m^2 (450 psia) to 5.52×10^6 Kg/m^2 (800 psia). No adjustments were made to the controller from the previous hydrogen testing. The flowrates as depicted in Fig. 46 varied from 1.02 Kg/sec (2.24 lb/sec) to 1.26 Kg/sec (2.77 lb/sec). The variation about the mean flowrate is ±10.5 percent. If the 3.45×10^6 Kg/m^2 (500 psia) to 5.52×10^6 Kg/m^2 (800 psia) range is considered, this variation becomes 1.1 Kg/sec (2.42 lb/sec) to 1.26 Kg/sec (2.77 lb/sec). The variation about this mean is ±6.8 percent.

Low temperature testing with oxygen was not performed due to the lack of a LOX-clean condition of the facility. Instead, testing at low temperature was performed with gaseous nitrogen. A comparison of ambient temperature performance over the pressure range is also shown in Fig. 46. Note that the nitrogen flowrate is slightly less due to its lower molecular weight. Nitrogen flow varied from 0.98 Kg/sec (2.2 lb/sec) to 1.13 Kg/sec (2.5 lb/sec) resulting in a variation about the mean of ±6.4 percent, slightly less than with oxygen.

Low Temperature Testing-Nitrogen

Tests were conducted with ambient and low temperature nitrogen with inlet temperatures ranging from about 139 K (250 R) to 283 K (510 R) over a pressure range of 3.28×10^6 Kg/m^2 (475 psia) to 5.52×10^6 Kg/m^2 (800 psia). The results of these tests are presented in Figs. 47 and 48 which show flowrate as a function of inlet pressure and temperature.

As with the hydrogen testing, at the lower inlet temperatures, around 167 K (300 R), and higher inlet pressures, around 5.58×10^6 N/m^2 (810 psia), the controller did not effectively function due to the poppet travel being limited at its minimum position by the mechanical stop adjustment. Note that the shape of the flowrate curves of the nitrogen was quite similar to that of the hydrogen.

FINAL DESIGN

The basic internal design of the flow controller was found to function as conceived. The poppet position was sensitive to inlet pressure due to the balance of pressure, spring, and bellows forces. The poppet position was also sensitive to inlet temperature through effect of the pressure divider circuit on bellows pressure. The temperature sensitive element also functioned as

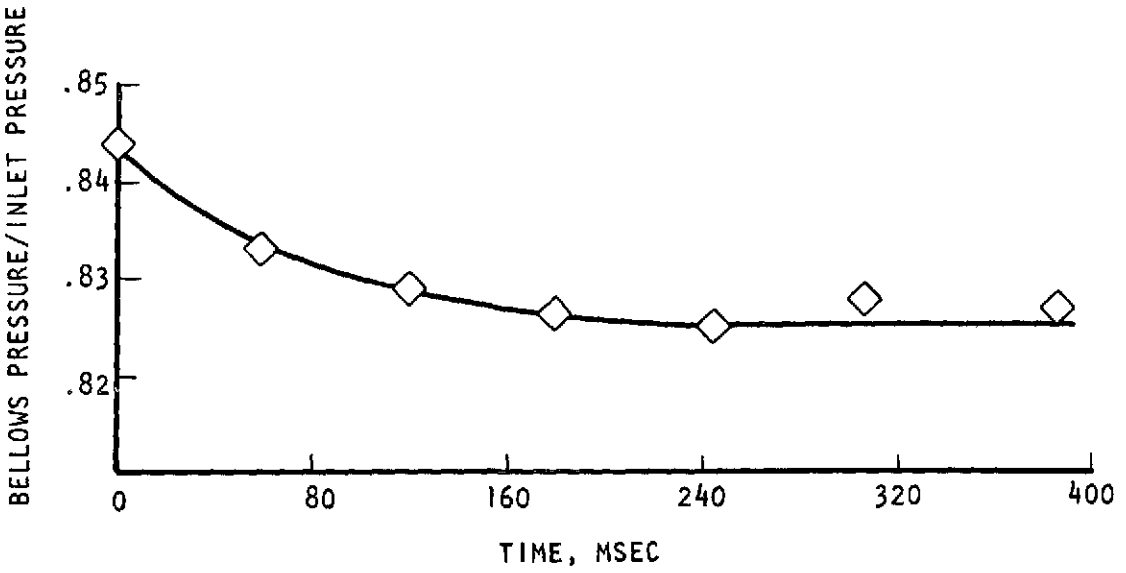

Figure 45. Thermal Response of Pressure Divider Circuit

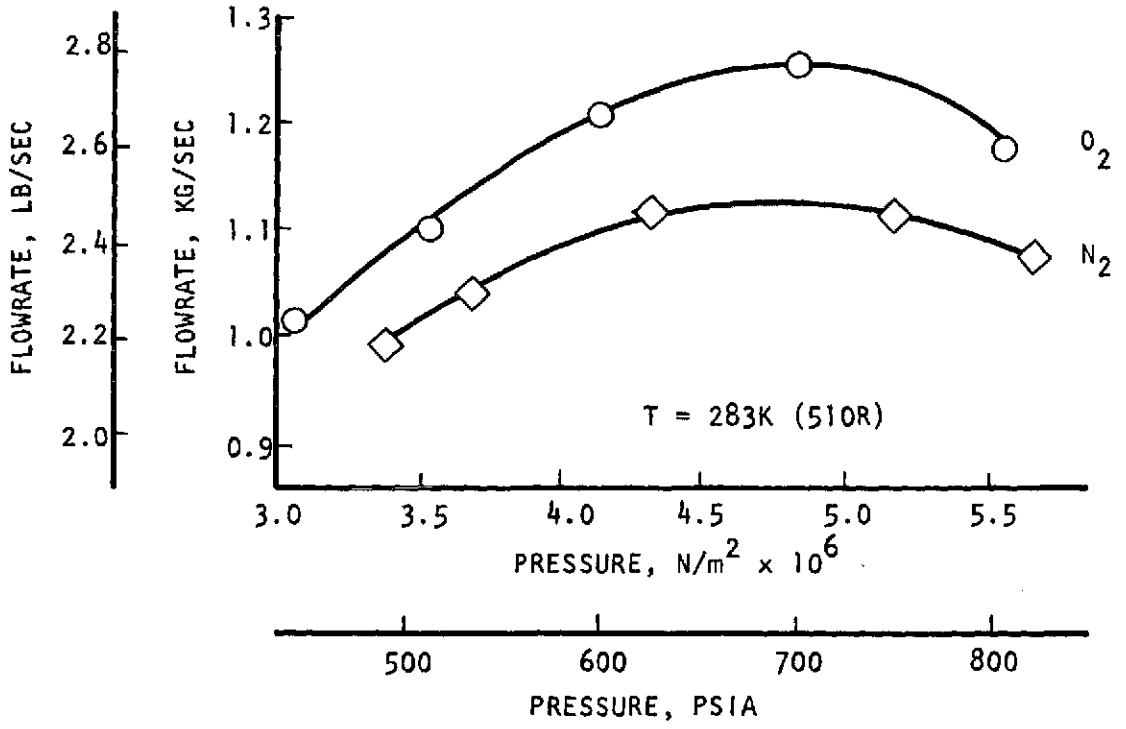

Figure 46. GO_2 and GH_2 Flowrate as a Function of Inlet Pressure

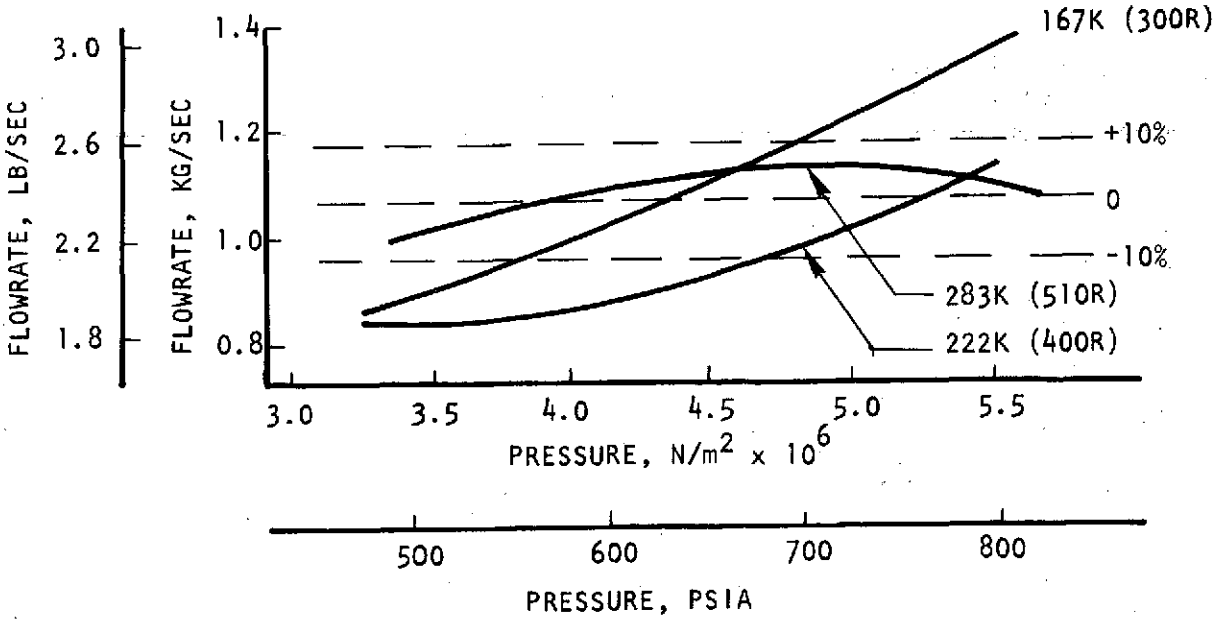

Figure 47. GN_2 Flowrate as a Function of Inlet Pressure and Temperature

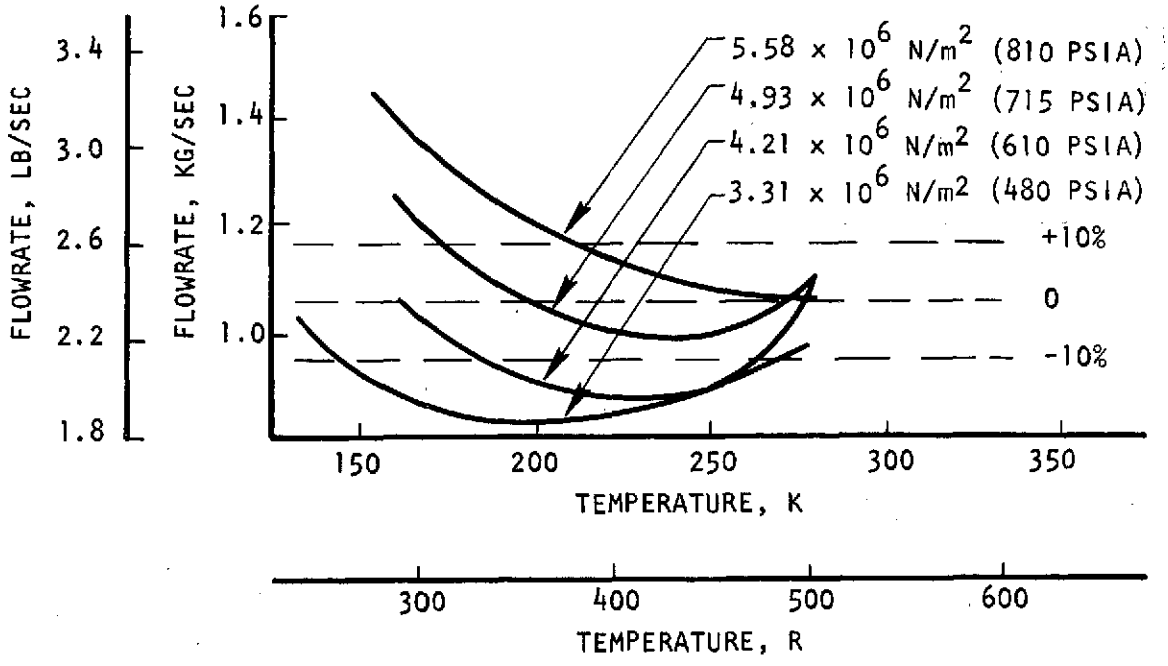

Figure 48. GN_2 Flowrate as a Functional Inlet Temperature and Pressure

designed. The subsonic nozzle maintains a choked condition for the smaller sonic venturi. The dashpot design proved to be effective as did the pressure sensing tube design.

The flexibility of adjustment also proved to be useful. It was found that the screw adjustment in the spring housing was not needed and that the minimum position stop could be better handled by the dashpot shims. Some difficulty was encountered in centering the shims of the temperature sensitive element in the pressure divider circuit and in removal of the pressure divider circuit housing.

The addition of a spacer between the cover plate and shims with appropriate deepening of the shoulder to accommodate the spacer thickness is suggested. In addition, some type of lip should be extended from the shoulder of the pressure divider housing to facilitate its removal from the main assembly.

The primary area of change for a flight-weight design would, of course, be in the main body design. The excess material would be removed where structural considerations permit. Fabrication would probably be by casting with finish machining of appropriate surfaces. Where appropriate, seams would be welded for permanent sealing.

DISCUSSION OF RESULTS

The basic questions to be answered by the evaluation testing are: (1) did the controller function as conceptually designed; (2) how accurately was flow controlled over the inlet pressure/temperature envelope; and (3) was the dynamic response timely and stable. The controller did function as conceived. Flow control accuracy was good in some regions of inlet pressure and temperature but limited in others due to lack of adjustment of metering-poppet travel range, some required fine tuning of the temperature compensating pintle contour, and facility limitations. Pneumatic and thermal response were as predicted by analysis, and stability was adequate and controllable.

CONTROL ACCURACY

In evaluating the flowrate control accuracy, two aspects should be considered: (1) absolute level of flowrate, and (2) the variation of flowrate with inlet pressure and temperature. In the tests performed, emphasis was placed on the control of flow variation rather than absolute level.

To adjust for control of variation, the major impact is from the positioning of the pressure divider circuit pintle which determines the ratio of bellows pressure to inlet pressure. The adjustment of spring preload is next in importance. These adjustments are interrelated to some extent and a certain amount of cut and try is required. The level of flow is controlled primarily with the shifting of poppet shaft length. To increase flow, the poppet shaft length is increased by the addition of shims. There is, however, an effect on other parameters such that this relationship is not a simple one. During the course of testing, it was decided that it was more important, within the limitations of the test facility and time, to concentrate on control of flow variation rather than absolute level.

Flow variation at ambient conditions was near to that predicted by earlier analytical work. However, it appeared that the discharge coefficient of the metering poppet varied over the range of travel of the poppet. This proved to be limiting when propellant inlet temperatures were diminished and the controller could not adjust to maintain constant flow. Discharge coefficients were estimated to vary from about 0.6 at the maximum poppet opening to 0.8 at the minimum opening.

A factor which affected control accuracy during propellant inlet temperature variation was the limited ability of the facility to maintain a near constant simulated chamber pressure. In an actual thrustor system, the chamber pressure is almost insensitive to propellant temperatures. Therefore at constant propellant flow, the chamber pressure may vary only a couple of percent over the temperature range. In the test facility the pressure drop across the valve used to simulate chamber pressure varied substantially over the temperature range. It was necessary therefore to adjust this valve manually to maintain near constant back pressure during the tests. This was done to some extent but did contribute to control error.

This problem would be avoided if the controller were a sonic flow device. An additional pressure loss would result but would certainly aid in the development of an accurate control. This could be easily accomplished in this configuration by merely designing the larger subsonic venturi to flow sonic.

RESPONSE AND STABILITY

The pneumatic response varied from 50 to 70 milliseconds for the dashpot orifice diameters used. Orifice diameters were 0.00152 m (0.06 inch) and 0.000762 m (0.03 inch). The larger orifice resulted in the more rapid response. At lower temperatures, the system was more oscillatory thus necessitating the smaller orifice. Thermal response was approximately 300 milliseconds.

The controller stability was found to be very dependent on dashpot volume. When volume was increased, the controller became considerably more oscillatory. The adjustment in poppet shaft length must be accompanied by adjustment of dashpot volume. This feature was provided for in the design.

PROPELLANT EFFECTS

The results indicate that the control trends as functions of inlet pressure and temperature were similar for hydrogen, oxygen, and nitrogen. This indicates the feasibility of the design for both hydrogen and oxygen as well as other gases.

COMPARISON WITH ANALYSIS

The characteristics of control accuracy and dynamic response compare closely to the early computer modeling results. Ambient temperature accuracy predictions were fairly close as were dynamic response times. Low temperature accuracy data (below 170 K (300 R)) did not compare as well due to the limitation in actual performance at those conditions.

CONCLUSIONS

This program has resulted in the design and testing of a gaseous propellant flow controller which maintains a near constant flowrate over a range of propellant inlet pressures and temperatures. The feasibility of the design concept which utilizes mechanical, pneumatic, and thermomechanical components was demonstrated with hydrogen, oxygen, and nitrogen. The control accuracy was less than the design objective but indicated a potential for improvement to an applicable accuracy. The pneumatic dynamic response was within the design goal and the thermal response was close to that predicted. Further development is required to more comprehensively characterize the operation of the flow controller and the interaction of the various adjustments. Test results compared closely with earlier analytical work.

It is recommended that the subsonic venturi be modified to produce sonic flow in order to allow realistic testing to be performed as well as to isolate controller operation from downstream (back pressure) effects. The additional pressure drop is estimated at 0.41 N/m^2 (60 psia). It is also suggested that the design be expanded to include a shutoff capability thus precluding the need of separate thrustor valves. The shutoff capability could be provided by modification of the poppet design to include a closure capability and by the addition of a three way pilot valve between the pressure divider circuit and bellows. The three way valve would either connect bellows and divider circuit for "on" operation or vent bellows pressure for "off" operation.

APPENDIX A

FLUIDIC PROPELLANT FLOW CONTROL SYSTEM

The investigation of fluidic mass flow control concepts was conducted by the Bendix Research Laboratories. Findings of this investigation are referred to or summarized in the main body of this document. The complete report is presented in this appendix.

The
Bendix
Corporation

Bendix
Research
Laboratories

Southfield, Michigan

Final Report

Fluidic Propellant Flow Control System

March 1973

Prime Contract
No. NAS 3-14390

BRL Project 2882

Prepared by:

L. E. Slimak

Prepared for:

Rocketdyne
Division of
Rockwell International
Canoga Park, California

Report No. 6508
Copy No.

This report was prepared by the Bendix Research Laboratories of The Bendix Corporation for the Rocketdyne Division of Rockwell International, Canoga Park, California.

CONTENTS

LIST OF ILLUSTRATIONS

LIST OF TABLES

SUMMARY

The objective of this program was to conceive, analyze, design and test a reliable propellant mass flow control system to meet the requirements of the Space Shuttle Attitude Control Propulsion System. The mass flow control system is required to maintain accurately propellant flow rates for constant thrust and mixture ratio in the presence of significant variations in propellant gas source temperature and pressure.

Mechanical, electromechanical and fluidic concepts were considered and compared. Rocketdyne Division of Rockwell International investigated mechanical and electromechanical approaches; fluidic approaches were investigated by Bendix Research Laboratories of The Bendix Corporation.

The general control approach adopted combined pressure regulation with temperature scheduling to achieve constant mass flow. Fluidic systems considered included both "flueric" (no moving parts) and hybrid types. The approach ultimately selected as most promising was a hybrid configuration using flueric elements for reference, sensing and amplification and a pneumomechanical diaphragm valve for throttling of the main flow. One configuration would be used for oxygen flow while an almost identical configuration would be used to control hydrogen flow.

During the first months of the program, several fluidic concepts were investigated in parallel. A combination of some testing and some analysis was used to evaluate the concepts that appeared to have good potential. The hybrid approach, which was eventually shown to have the most potential, was evaluated in further detail. Major aspects of the selected concept are summarized briefly in the following items:

- The concept employs separate control on gaseous hydrogen and on gaseous oxygen.
- In each gas line, flow is controlled by regulating the pressure at the inlet of the thrust chamber assembly.
- The required pressure is scheduled with the upstream gas temperature to provide the constant flow rate.
- There is only one moving part (non-frictional) in each controller.
- A mechanical metering element passes the primary flow in each controller.
- A network comprised of fluidic elements is used for pressure error sensing, control of the mechanical metering element, and temperature sensing and scheduling of the regulated pressure.

The selected hybrid fluidic approach was first evaluated through a combination of some analysis and some breadboard testing. The testing was conducted on the fluidic portion of one controller. Tests were initially conducted at low

pressures (i.e., 0.34×10^6 N/m^2 (50 psia)) since several properly sized fluidic elements were available in this range. Tests on the fluidic elements and the fluidic circuit indicated highly promising steady-state performance as part of a flow controller.*

A computer study of the controller dynamics was conducted. Performance at the lower supply pressures (i.e., 317×10^6 N/m^2 (460 psia)) was very good. Performance at the high end of supply pressures (i.e., 5.51×10^6 N/m^2 (800 psia)) indicated a possible stability problem. It was felt, however, that a stability problem could be solved by proper adjustment of gain and/or damping within the control circuitry.

As a result of a technical review meeting with NASA, it was decided that two areas needed further investigation before full development might begin on this concept. One area dealt with the accuracy of the fluidic circuitry over full ranges of absolute pressure, temperature and flow rate. The other concern was with the dynamic stability and response over the operating range and conditions.

To examine these areas, testing and/or analysis were conducted on the key fluidic elements in the circuit for a range of the required operating conditions. Results showed that some of the fluidic elements had significant nonlinearities in performance over the range of required absolute pressures. While these nonlinearities were repeatable they did add to further inaccuracies in the control circuit. As a net result it was felt that the fluidic concept would have required further development to improve accuracy. However, at a subsequent technical review meeting NASA decided to develop the mechanical controller concept designed by Rocketdyne.

The status of the most promising fluidic flow controller can be summarized in the following items:

- Accuracy theoretically obtainable is excellent.
- The concept represents an advancement in the state of the art.
- Pressure and temperature nonlinearities have been shown to exist in the fluidic amplifiers which places some question as to the obtainable accuracy.
- Pressure and temperature response are theoretically adequate.
- The concept would be a reliable design once developed.
- The functionality has yet to be demonstrated for a complete controller under the required pressure and temperature conditions.
- The work, to date, shows that more development is necessary to demonstrate the concept.

---

*It is in this lower pressure range that much prior experience with the fluidic elements exists.

- Narrowing the operating temperature range would improve the potential of this concept.

- Narrowing the pressure range by some coarse pressure regulation would help improve the potential of this concept.

Should additional funds become available, two areas of the selected hybrid fluidic concept recommended for further investigation would be:

- Elimination of anomalies in the fluidic amplifiers at system pressures and temperatures by studying influence on performance of the interaction region of the basic amplifier profile.

- Breadboard one complete controller with existing fluidic amplifiers and optimize accuracy and stability factors.

These two recommendations tend to be divergent in that the first would attempt to obtain more uniform operation within the basic amplifier before building the complete controller while the second recommendation would attempt to consider the potential operation of the system using the fluidic amplifiers as they are. Following the first recommendation would be the better approach in attempting to arrive at a highly accurate flow controller. However, it would require more development than the second. Pursuit of the second recommendation would arrive at a controller in less time and cost but would probably result in less accuracy.

INTRODUCTION

The objective of this program has been to conceive, analyze, design and test a reliable propellant flow control system that will meet the requirements of the Space Shuttle Attitude Control Propulsion System. The flow control system has the requirement of controlling engine thrust and mixture ratio for a range of gaseous hydrogen and oxygen inlet temperatures and pressures. The system application schematic is shown in Figure 1 and the performance requirements are listed in Table I.

The initial effort of the project was devoted toward evaluating various mechanical, electromechanical and fluidic concepts for the flow control system. Rocketdyne has investigated the mechanical and the electromechanical approaches. The Bendix Research Laboratories of The Bendix Corporation has been evaluating the fluidic concepts. Fluidic approaches have been investigated because fluidics has the potential of being highly reliable and accurate once developed.

Before considering the approaches in detail, consider first what a mass flow controller must do. As depicted in Figure 2(a), the output mass flow is the desired controlled parameter with the variables of pressure and temperature serving as the input variables. One controller on each gas would be required for control of mixture ratio into the thrust chamber.

One way of achieving mass flow control would be as depicted for one of the gases in Figure 2(b). In this manner the output pressure is regulated but the regulated value is scheduled with temperature. The required values of regulated pressure versus temperature have been calculated by Rocketdyne and are shown in Figure 3.

In further defining the control system, the key elements of control for the hybrid fluidic systems investigated by Bendix are shown in Figure 4 for one of the gases. Two of these controllers would be required (i.e., one for oxygen and one for hydrogen).

Thus, the general approach that is described in the following pages is to maintain a scheduled regulated pressure for each controller (i.e., one controller for hydrogen and one for oxygen). The output pressure is held constant for variations in input pressure but is scheduled to increase or decrease with temperature in order to maintain constant mass flow and thereby constant mixture ratio.

The performance requirements listed in Table I have some immediate implications on fluidic elements. One such requirement is that any overboard dumping of gas could result in a hazardous condition. Therefore, any venting that is required for any of the fluidic elements must be contained within the controller system. The vent of any fluidic element would have to be closed off internal to the element or connected to some lower reference pressure such as the regulated pressure (P_R). Internal venting of fluidic elements has generally led to noisy performance. The other means of venting would produce uncontrolled inaccuracies in the very pressure (P_R) that the control circuit attempts to regulate.

Table I - Performance Requirements

Parameter	Requirement
Propellants	GO_2/GH_2
Mass flow rates	GO_2 - 2.76 lb/s (1.25 kg/s) GH_2 - 0.69 lb/s (0.31 kg/s)
Operating pressure range	400 to 800 psia (2.76 to 5.52 N/m^2)
Propellant inlet temperatures	GO_2 - 300 to 800R (167 to 444K) GH_2 - 200 to 800R (111 to 444K)
Accuracy	Thrust and mixture ratio ± 3 percent
Response	50 milliseconds
Pressure drop	Minimum
Envelope and weight	Minimum
Failure criterion	Fail-safe open
Maintenance	No maintenance
External leakage	61×10^{-9} in^3/s GHe (1×10^{-6} scm^3/s)

P-85-242-3

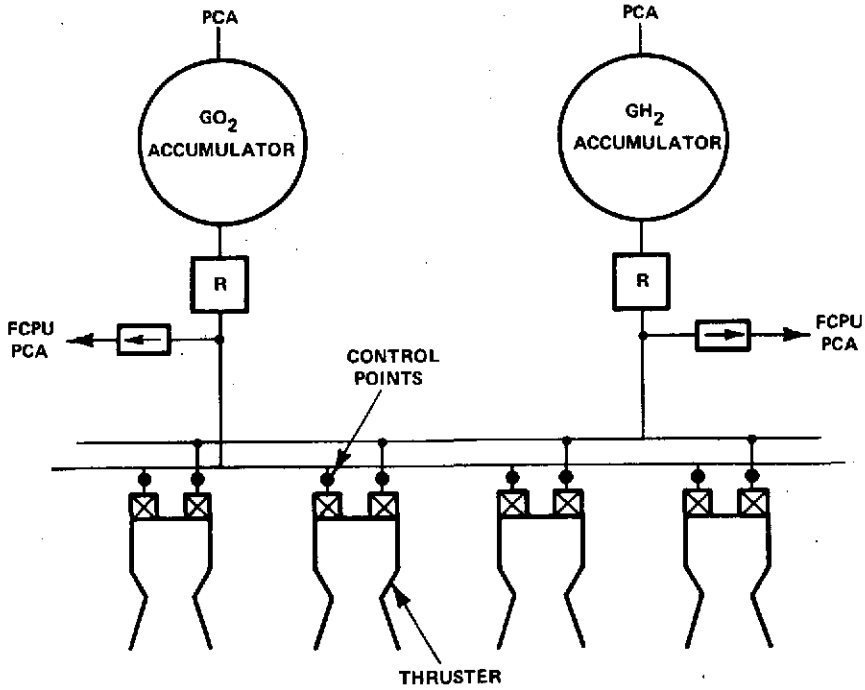

Figure 1 - Schematic of Flow Control System Application

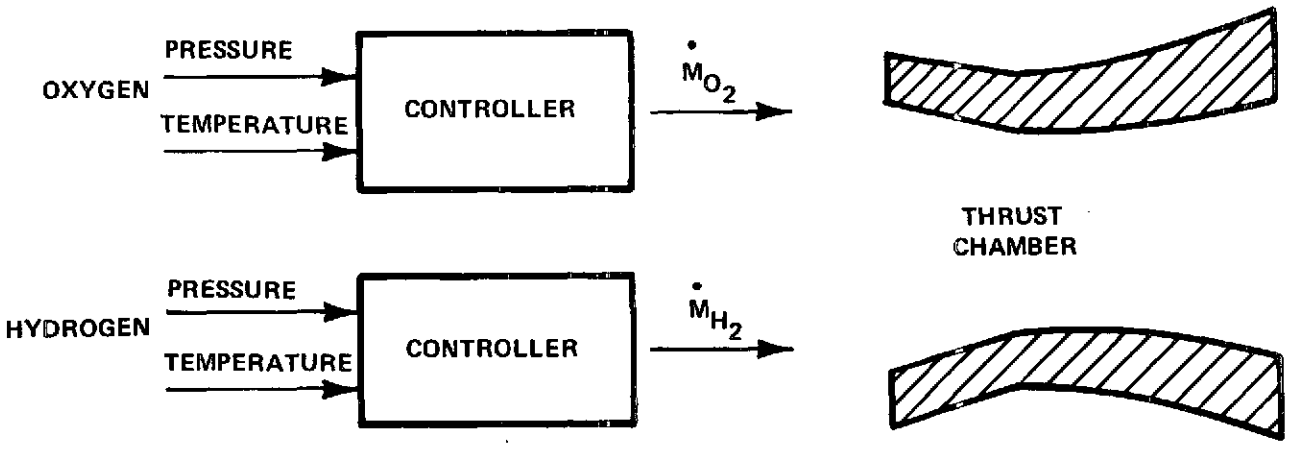

(a) GENERAL MASS FLOW CONTROL

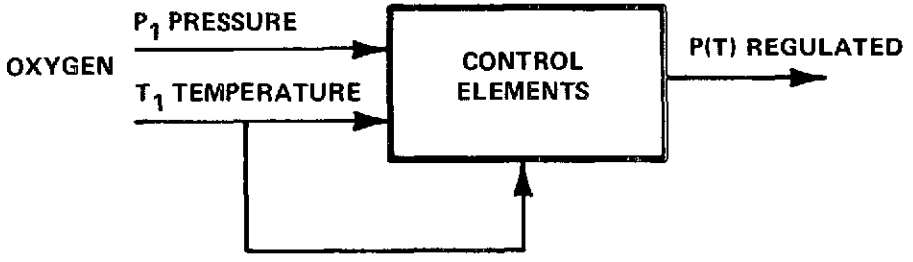

(b) REGULATED PRESSURE AS A FUNCTION OF TEMPERATURE

Figure 2 - Mass Flow Control

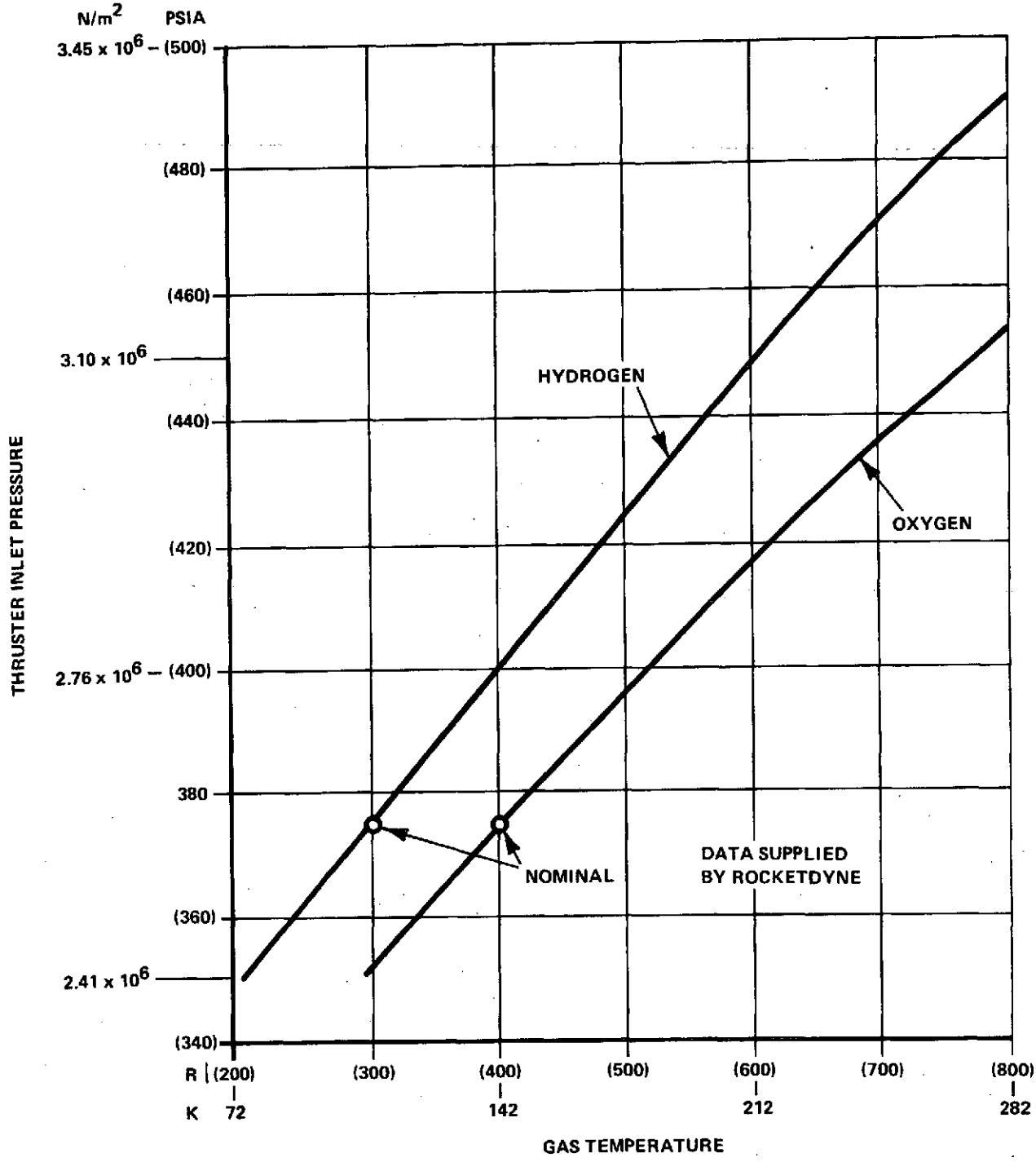

Figure 3 - Thruster Inlet Pressures Required to Give Constant Flow Rates for Varying Inlet Temperatures for Real Gas Propellants (Rocketdyne Data)

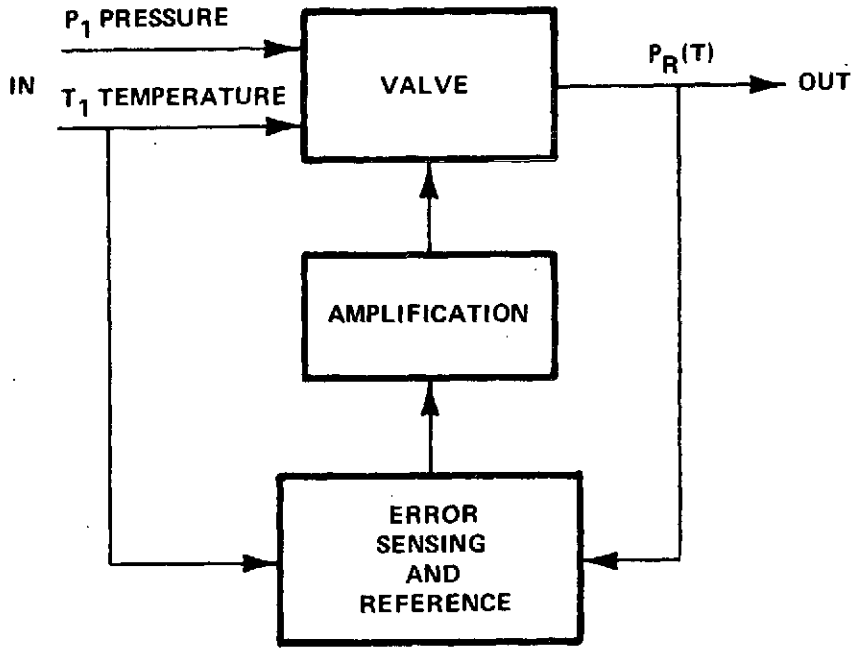

Figure 4 - Major Elements of Control

Another important factor to fluidic element operation is the range of pressure ratios across the element. Most fluidic elements operate best with gas when the pressure ratio across them is better than 2 to 1. As an example of what the given requirements mean in terms of pressure ratio, assume that the gas temperature is 222 K (400 R). Then the required regulated pressure for oxygen from Figure 3 would be 2.59×10^6 N/m^2 (375 psia). Assume also that the vent of the fluidic element is connected to the required regulated pressure. Then with the supply pressure to the fluidic element varying from 2.76×10^6 N/m^2 (400 psia) to 5.52×10^6 N/m^2 (800 psia), the pressure ratio across the element varies from

$$\frac{2.76}{2.59} = 1.1$$

to

$$\frac{5.52}{2.59} = 2.1$$

In general the fluidic element would be required to operate with a pressure ratio that is below 2 and that can also be varying.

The above items have been discussed to point out that the effort discussed in detail on the following pages is aimed at an advancement in the state of the art. Such was the need for some detailed testing of fluidic elements.

Although the development effort for such a fluidic control problem is longer than more conventional control methods, the reliability and accuracy would be well established for production controllers once a prototype controller was developed.

In attempting to arrive at a selected concept, Bendix concentrated primarily on the oxygen controller since preliminary evaluation testing could be done with gaseous nitrogen which is safer and has properties quite similar to those of oxygen.

The program started with primary investigations directed toward several flueric approaches and toward one hybrid fluidic concept. The flueric approaches were given a cursory investigation which resulted in only one feasible concept for the required system. This was a controller which had a single-source, fluidic, vortex valve controlled by a fluidic amplification circuit. However, the total number of fluidic elements that were involved to make one controller presented serious questions about its potential. This was because of potential interactions between the elements at these pressures. Most of the prior work with the fluidic elements had been at considerably lower absolute pressures. Therefore, this concept was eliminated as considered in its flueric configuration.

The hybrid fluidic concept was initially investigated since the pressure regulation portion of the concept had been previously developed on a contract for the U.S. Navy, although that development was for a blowdown system which had almost no temperature effects. As the initial investigation proceeded, a second hybrid concept evolved from the one mentioned above. Both concepts were later eliminated from further development because of the large pressure drop needed to make either of the concepts operable. This conclusion came about as a result of testing some critical components on gaseous nitrogen.

A third hybrid fluidic concept was conceived part way through the concept evaluation phase. The critical elements in this concept were investigated. The results of testing and analysis showed that this concept could be rated as no better than a coarse controller for this application. Subsequently, this concept was eliminated from further development.

A fourth hybrid fluidic concept evolved from a flueric version by replacement of some of the questionable fluidic elements with state-of-the-art pneumomechanical parts. This concept eventually turned out to be the most promising fluidic concept for this particular system application. In the initial portion of the evaluation, various performance aspects of this last concept were investigated under low pressure, constant-temperature conditions. Although absolute pressure was low, the fluidic elements and subcircuits were tested at pressure ratios that they would experience under actual conditions. These initial tests showed quite favorable results for the concept. As a result of a concept review meeting at NASA-Lewis, this concept was selected as the most potential fluidic approach. It was concluded that further testing should be conducted before a concept selection could be made for the overall program. The testing was to be conducted on the critical elements under actual pressures and temperatures. Test results showed wide variations in the gain characteristics of the fluidic

amplifiers, primarily due to pressure effects. The spread in gain characteristics did not appear during the earlier tests at lower pressure. After much investigation it was concluded that the gain anomalies in the amplifier could not be easily disposed of by design in the amplifier; although gain variations in the feedback loop of the concept could be reduced by proper circuit connections. Some gain variation can be tolerated in the feedback loop since errors due to the gain variation are reduced roughly by the steady-state magnitude of the overall gain. The detailed discussion of this concept and its evaluation are covered in the main body of this report.

At a technical review at NASA-Lewis, a decision was made to develop further a mechanical controller approach which Rocketdyne had been pursuing. Although the selected hybrid fluidic concept of Bendix was still considered a second approach, the additional time and cost needed to develop the fluidic concept, as opposed to the mechanical one, was of prime importance in the decision. At this point, however, the hybrid fluidic concept C must still be considered a good potential concept for this application and it may have strong potential in the considerations of other flow control or pressure regulation applications.

A list of flueric approaches is presented in Table II and the hybrid fluidic approaches are listed in Table III, along with a summary of the basic control elements.

HYBRID FLUIDIC CONTROLLER - C

CONCEPT DESCRIPTION

One of the most promising fluidic concepts, to date, has been a hybrid-type fluidic controller. The simplified block diagram for the concept is shown in Figure 5 and a detailed schematic is shown in Figure 6.* The major control items are:

- valve
- diaphragm
- venturi
- temperature compensator
- laminar restrictor
- amplifier cascade
- orifices

This concept is comprised of a simple throttling diaphragm-type pressure regulator with the fluidics controlling the diaphragm to achieve the necessary accuracy. Diaphragm position is governed by the A3 amplifier outlet pressure,

*Since there were other hybrid fluidic approaches, this concept is referred to as concept C in this report, as it was during the course of the program.

Table II - Flueric Approaches

Concept	Discussion
Diverter System	Appendix B
Single-Source Vortex Valve	Appendix B
Dual-Source Vortex Valve	Appendix B

P-85-242-3

Table III - Control Elements for Fluidic Concepts

Hybrid Concept	Primary Flow Area Modulation	Pressure Error Sensing	Amplification	P(T) Reference	Discussion
A	Mechanical Metering Element	Confined-Jet Amplifier	Vortex Amplifier	Temperature-Sensitive Orifices With Bypass Flow	Appendix C
B	Mechanical Metering Element	Orifice-Amplifier Bridge	Vortex Amplifier	Temperature-Sensitive Orifices With Feedback Flow	Appendix C
C	Mechanical Metering Element	Orifice-Laminar Restrictor Bridge	Fluidic Proportional Amplifiers	Temperature-Sensitive Orifice With Feedback Flow	Main Text
D	Mechanical Metering Element	Vortex Amplifier	Vortex Amplifier	Temperature-Sensitive Orifices With Feedback Flow	Appendix C

P-85-242-3

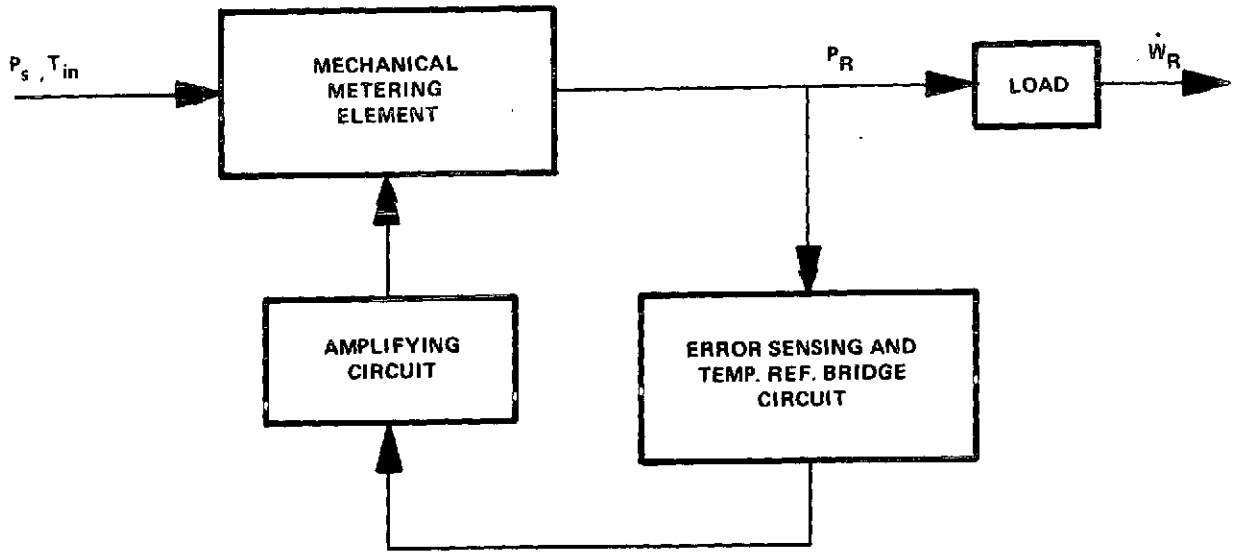

Figure 5 - Simplified Block Diagram of Type C Hybrid Fluidic Controller

P_X, acting on the diaphragm against the pressures P_S and P_R' on the other side. When flow is developed, the fluidic sensing and amplifying circuits apply a bias pressure difference to the diaphragm to trim the flow as required.

Since the flow through the valve accounts for about 98 percent of the total flow, W_R, a venturi can be used to develop a pressure, P_{TV}, lower than P_R'. This is accomplished when the downstream side of the sensing bridge is connected to the throat of the venturi. The pressure difference ($P_R' - P_{TV}$) is used to produce flow through the sensing bridge and, therefore, a means of error sensing.

In the left-hand portion of the sensing bridge, a downstream laminar flow element, R_3, develops a pressure drop very nearly linear with temperature.

The temperature compensating orifice, R_2, is then used in conjunction with the laminar restrictor, R_3, to program the desired regulated pressure for each temperature.

As an example of the operation, consider the system to be regulating at some nominal value of pressure, say 2.59×10^6 N/m^2 (375 psia). For such a value, P_R' would be about 2.76×10^6 N/m^2 (400 psia) and P_{TV} at the venturi throat would be about 2.24×10^6 N/m^2 (325 psia). These pressures serve as the input (P_R') to the bridge network and as a downstream sink (P_{TV}). Under nominal conditions the bridge is set to balance at $P_{c1} = P_{c2}$. If P_R' tends to increase, P_{c1}, in the bridge network, increases more than P_{c2} and an error signal ($P_{c1} - P_{c2}$) is applied to sensing amplifier A_1. The output of this amplifier is amplified further by amplifiers A_2 and A_3. The output flow of A_3 acts on the diaphragm to increase P_X which acts to throttle down the incoming flow, thereby forcing P_R' to return to the nominal regulating point.

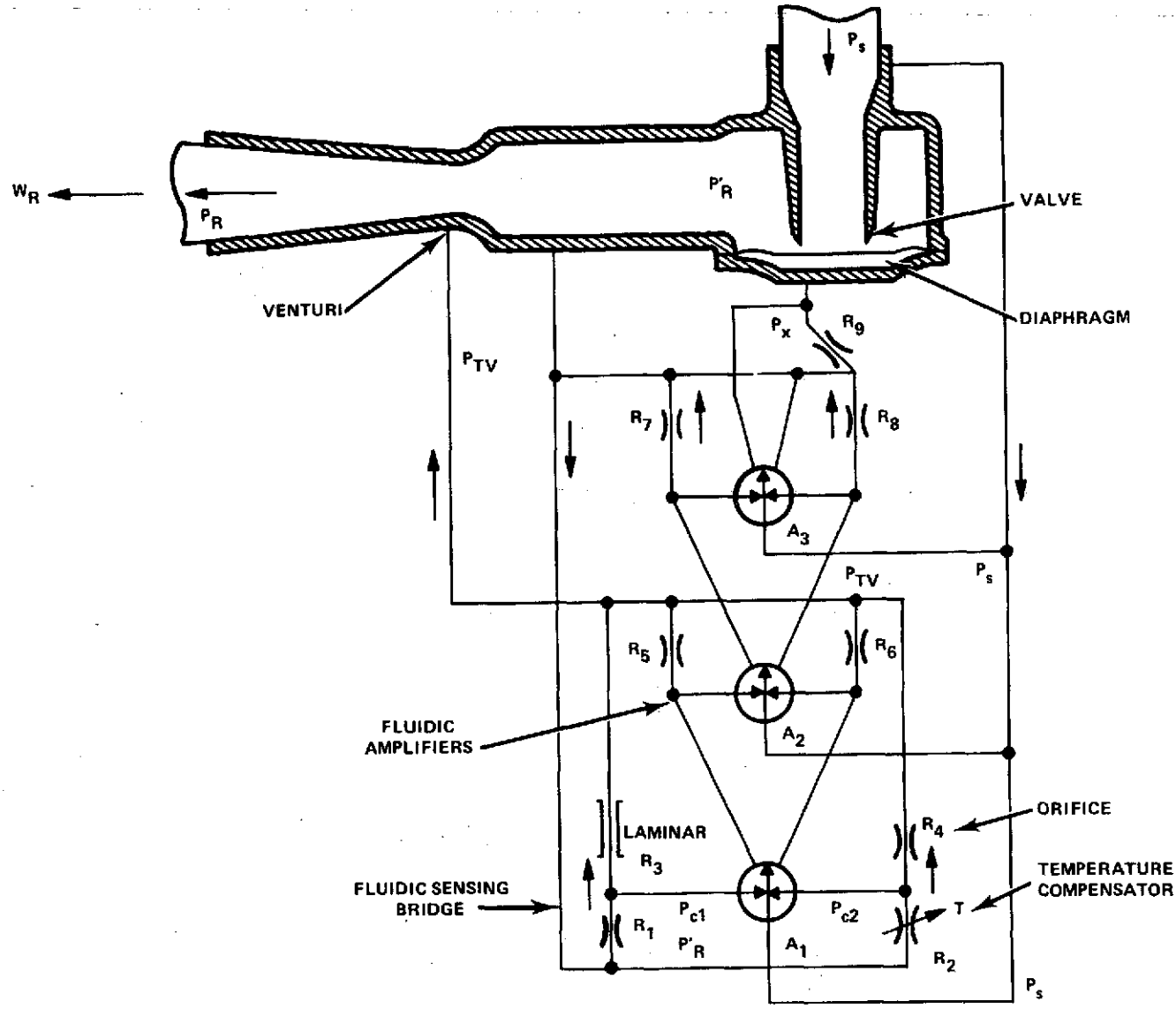

Figure 6 - Schematic Diagram of Hybrid Fluidic Flow Controller - Type C

To consider temperature effects, let the incoming propellant temperature be increasing. The flow through the bridge network senses the change in temperature from its nominal setting and a pressure difference across amplifier A_1 is produced which will result in a lower value of P_X which, in turn, will cause an adjusted increase in P_R' and P_R. Any pressure error signals would then be operated on by the bridge network about the new setting of P_R'.

The concept described above is the most promising fluidic one that has been evaluated. As a result of the evaluation, there are various factors influencing accuracy and response that has led to several alternatives in the implementation of this basic approach. These alternatives in implementation are discussed in a later section. The next few sections consider the evaluation of this concept by both test and analysis.

CONCEPT EVALUATION

The hybrid fluidic concept C was an outgrowth of a flueric concept that was eliminated from further consideration for this application. During the first months of the program, multiple concepts were being investigated in parallel. Due to the highly nonlinear characteristics of fluidics, completely analytical approaches to evaluate the concepts were not feasible. Therefore, a combination of some testing and some analysis was used to evaluate the concepts that appeared to have good potential. Limited testing was conducted toward each potential concept to help arrive at a single selection. Testing that is involved with the other concepts (i.e., the ones eventually eliminated from further development) is discussed in Appendix C along with the description of that concept. For the hybrid fluidic concept C, some limited testing at low absolute pressures (although at proper pressure ratios) and some analysis were initially conducted to show the feasibility of the concept. Further detailed testing was conducted after selection of this concept as the best potential fluidic approach. The initial screening of the concept is discussed below and the detailed testing and evaluation is discussed starting on page 27.

Preliminary Evaluation Operation over Pressure Range

To evaluate the operation and design values needed in the fluidic portion of the network, several breadboard tests were conducted. In the schematic of the concept, which was shown in Figure 6, there were several conditions of performance regarding the proportional amplifiers that were in question. These questions are briefly outlined for each amplifier:

Pilot Amplifier, A_1

- Matching characteristics with sensing bridge
- Closed-vent performance
- Gain characteristics over the required pressure ratio range

Second Amplifier, A_2

- Matching characteristics with amplifiers A_1 and A_3
- Closed-vent performance
- Gain characteristics for six parallel stages which made up amplifier A_2
- Gain characteristics over the required pressure ratio range

Power Amplifier, A_3

- Matching characteristics with amplifier A_2 and the diaphragm
- Closed-vent performance
- Gain characteristics for ten parallel stages which made up amplifier A_3
- Gain characteristics over the required pressure ratio range

The basic amplifier considered for use in this circuit is a high-impedance amplifier (i.e., could be actuated by pressure signal and little or no flow). The critical area profile of this amplifier is shown in Figure 7. For adequate matching characteristics between the bridge and the diaphragm, three amplifiers were shown to be needed. The first amplifier (A_1) was a single stage with a supply power nozzle 0.0059 cm by 0.0063 cm (2.32×10^{-3} in. by 2.48×10^{-3} in.). The second amplifier (A_2) was a bonded stack of six stages in parallel, each with a supply power nozzle 0.0059 cm by 0.0063 cm (2.32×10^{-3} in. by 2.48×10^{-3} in.). The last amplifier (A_3), which is the power amplifier, was made up of a bonded stack of ten parallel stages with a 0.0165 cm by 0.0117 cm (6.50×10^{-3} in. by 4.61×10^{-3} in.) supply power nozzle on each stage.

To evaluate the operation and design values needed in the fluidic portion of the network, several breadboard tests were conducted. Component amplifiers were built and tested for gain characteristics at the proper pressure ratios and over the pressure range, although at reduced absolute pressures. The use of low absolute pressures allowed the use of an available laminar restrictor to study the open-loop characteristics of the fluidic network. Representative curves for the A_2 amplifier performance are shown in Figure 8. Performance for the A_3 amplifier was not as good as expected although the circuit was still functional with the amplifier.

After component tests were conducted on the fluidic proportional amplifiers, the bridge sensing network was assembled and tested. The bridge network was shown to operate as expected for pressure sensing, as shown in Figure 9. Temperature effects were not tested by this network. The steady-state temperature effects on the bridge are predictable, however, based on calculations and prior experience.

The next step in testing was to combine both the bridge and amplifier cascade to study the open-loop performance of the fluidic network. The test schematic is shown in Figure 10 and representative results of testing are indicated in

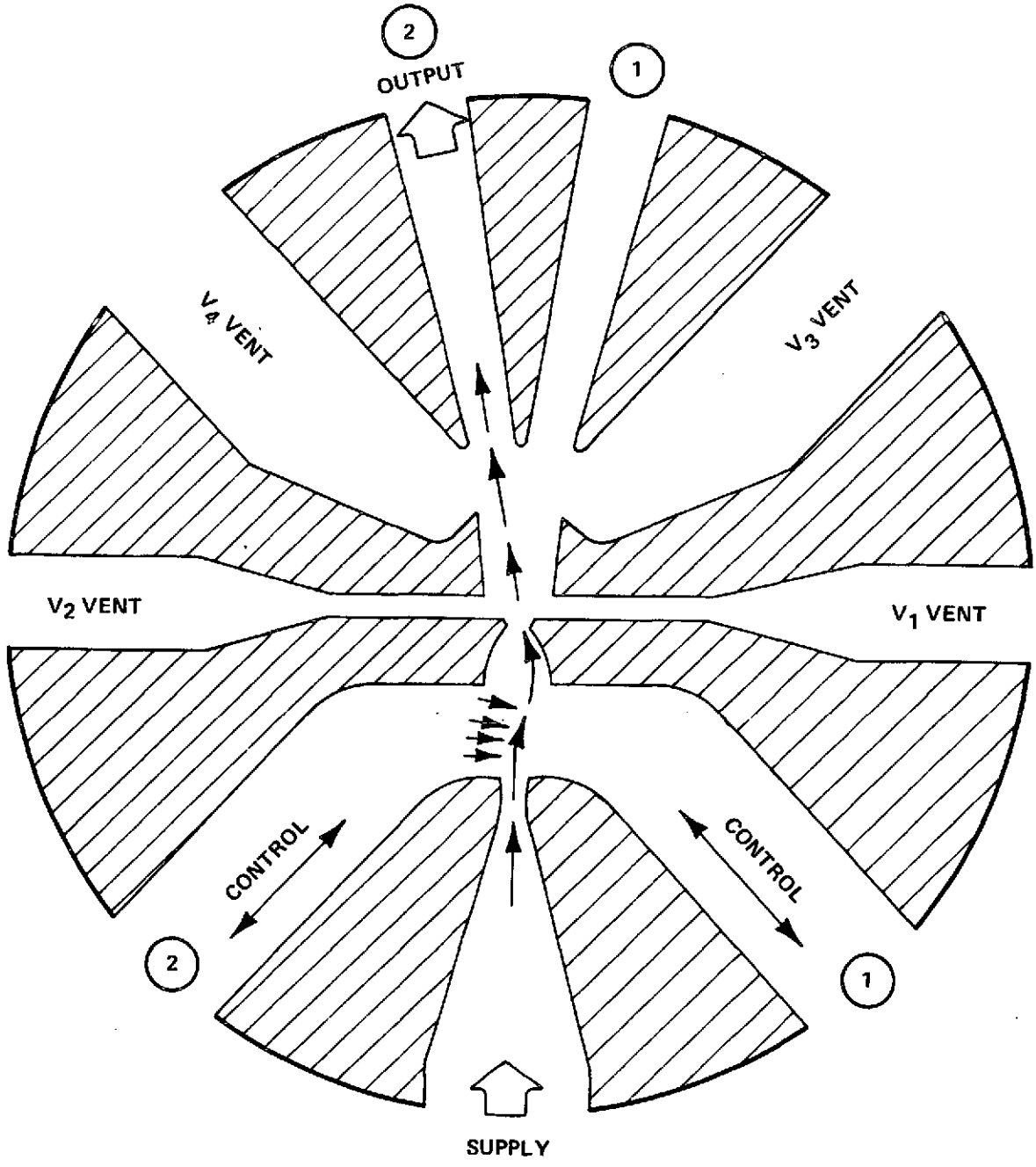

Figure 7 - AM31 Amplifier Profile

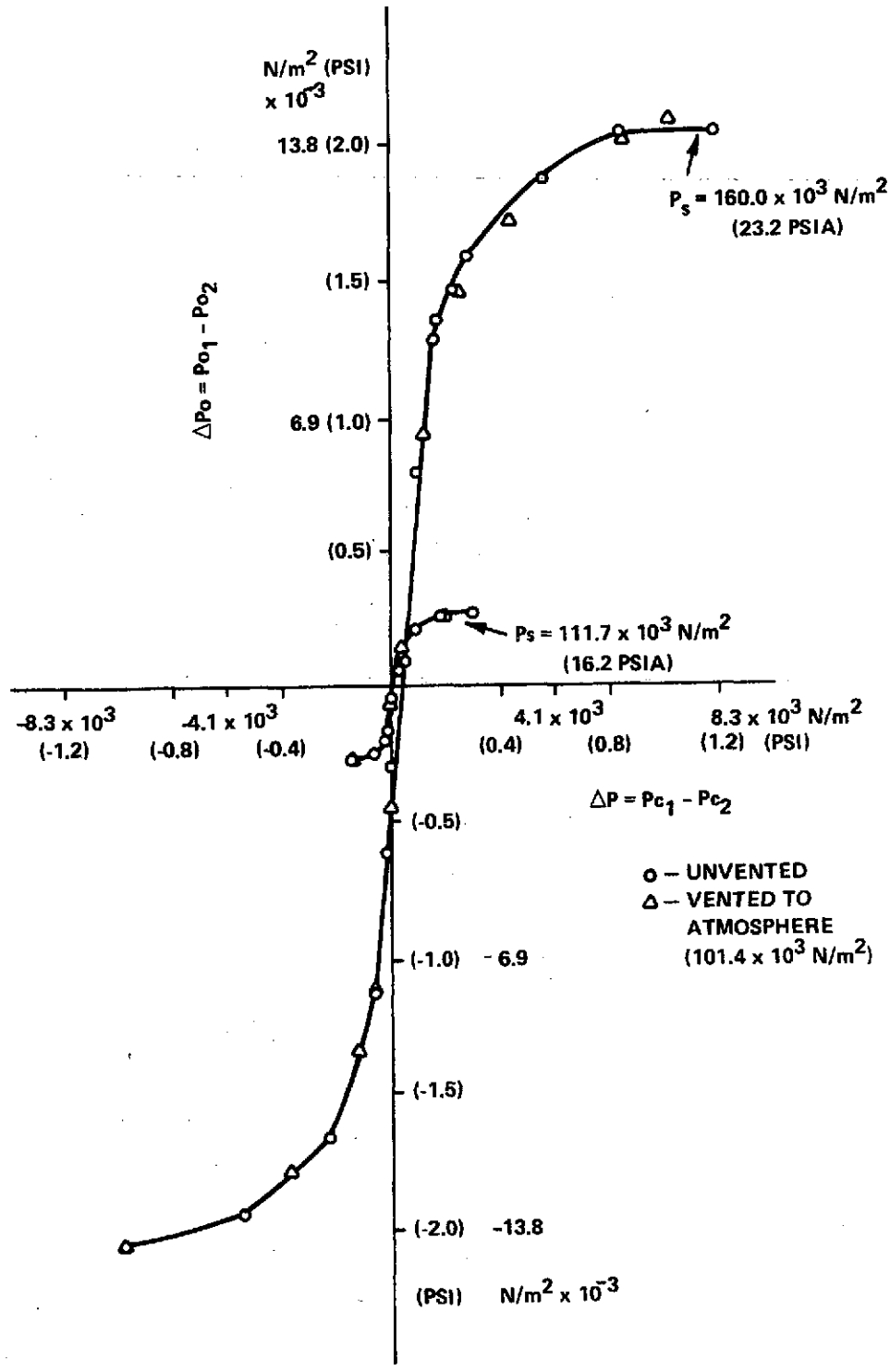

Figure 8 - Typical Operating Characteristics of AM31 Fluidic Amplifier

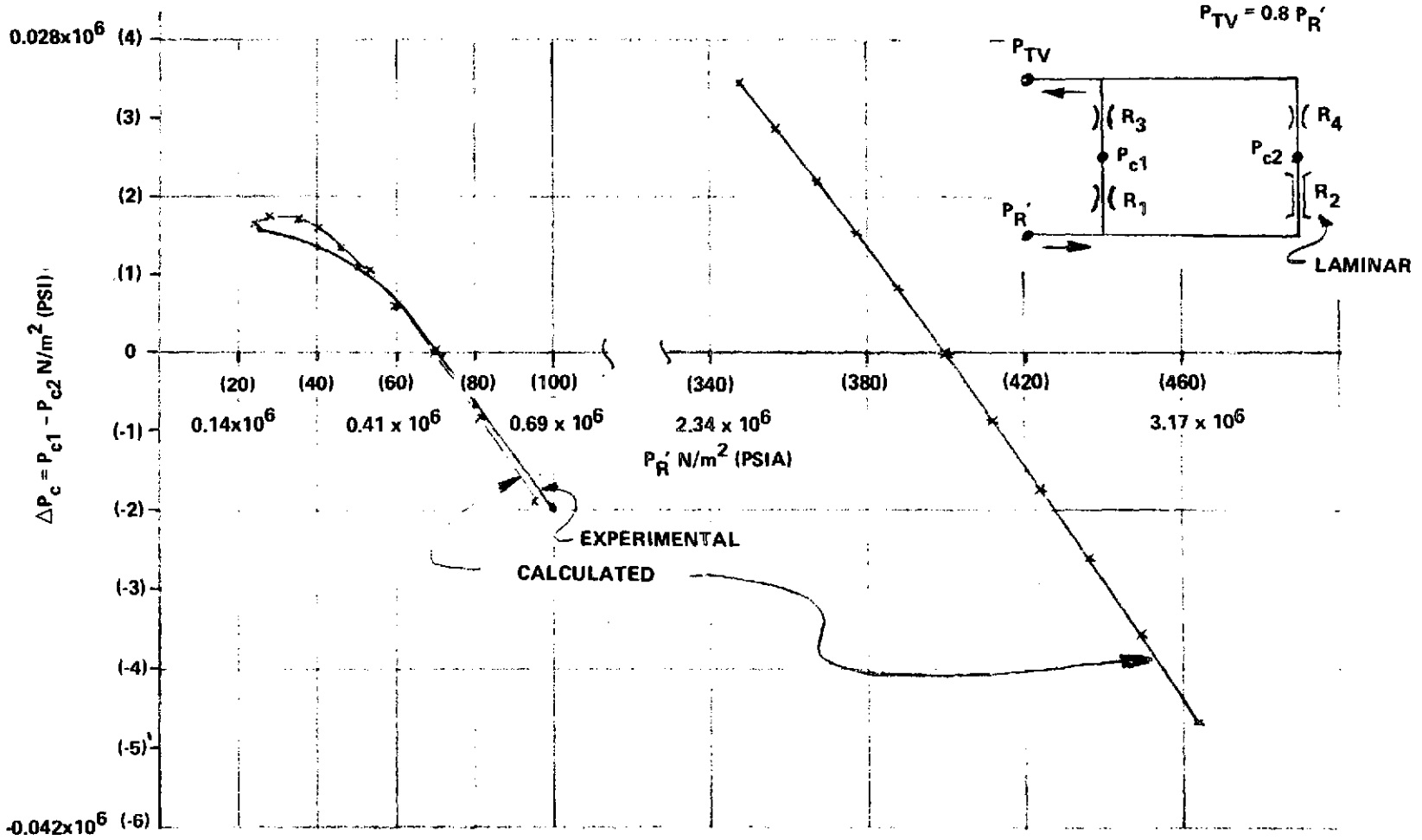

Figure 9 - Bridge Circuit Performance

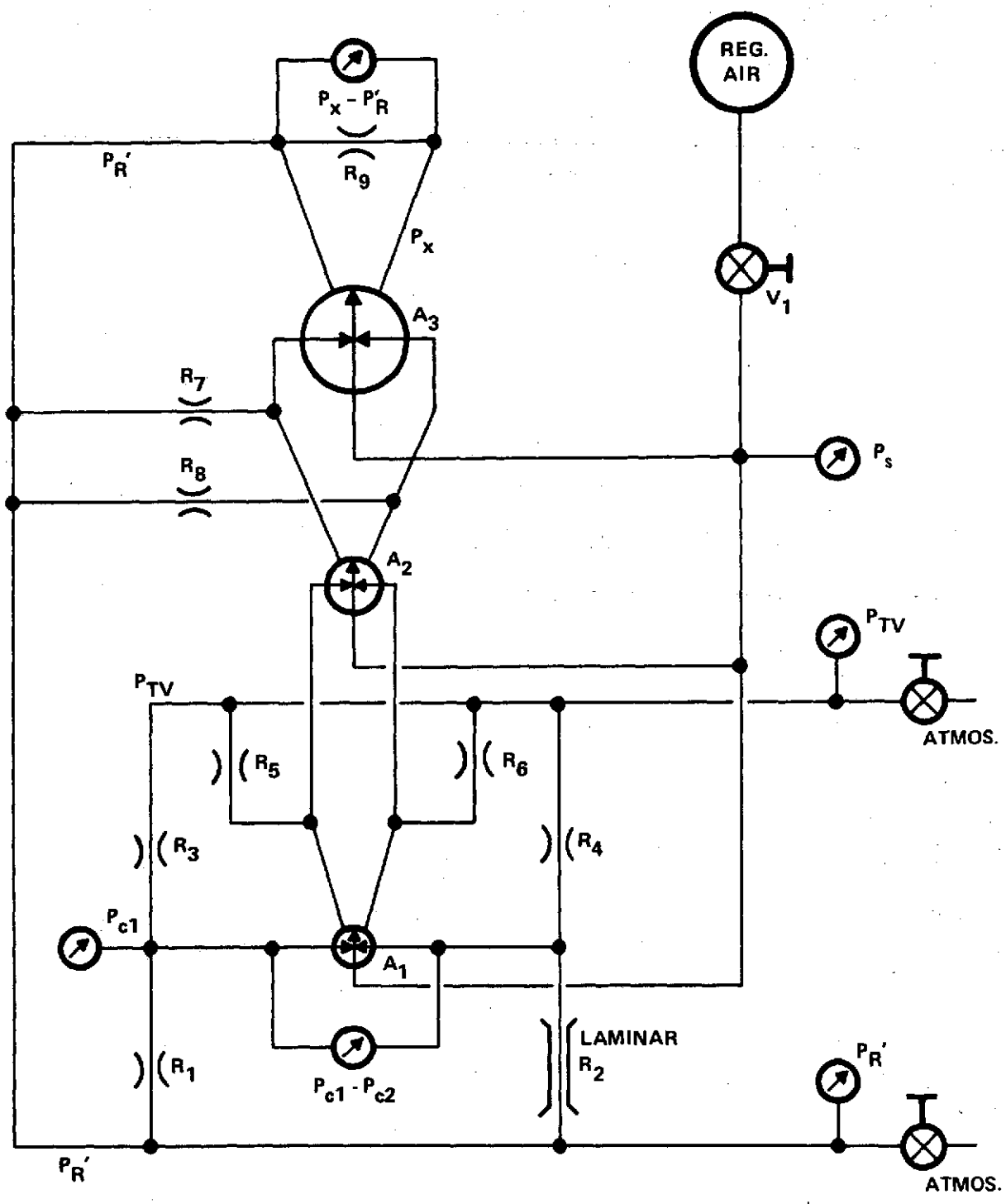

Figure 10 - Open-Loop Test Schematic for Concept C

Figures 11 and 12. It is desirable to have the high-gain region of the curves coincident for all pressure ratios. The tests were run to study effects of gain, null balance, pressure recovery, pressure ratio and range, absolute pressure, and potential setting of the diaphragm pressure P_X.

Discussing briefly the test results shown in Figure 11, the open-loop performance indicates potential operation within a well-controlled band (as indicated by the high-gain region) over the pressure ratio range for a regulated value, P_R', of 0.34×10^6 N/m^2 (50 psia). The curves run at the higher P_R' value of 1.03×10^6 N/m^2 (150 psia) do not fall within a controlled band like the curves at the lower P_R' value. The curves indicate a shifting is caused by increasing P_S/P_R' ratio.

The Y-axis indicates the possible design points for diaphragm equilibrium which would be selected in the high-gain region of the curve. The higher the ratio of $(P_X-P_R')/(P_S-P_R')$ that can be selected for equilibrium, the smaller the diaphragm size.

At a higher regulated value, P_R', of about 1.03×10^6 N/m^2 (150 psia), the potential pressure regulation of P_R' would be worse. A test to correct this was run by unbalancing the restrictors R_5 and R_6. The results are shown in Figure 12. The lower regulated pressure at 0.34×10^6 N/m^2 (50 psia) fell within a narrow band of accuracy over the pressure ratio range. The higher regulated pressure of 1.03×10^6 N/m^2 (150 psia) is also within a narrow band with pressure ratio.

These results indicated that the fluidic network (shown in Figure 6) could be made to control diaphragm position, and therefore P_R and W_R, over the input pressure range with a minimum input pressure of about 3.17×10^6 N/m^2 (460 psia) for a regulated value of $P_R = 2.59 \times 10^6$ N/m^2 (375 psia). These two values define a minimum operating pressure ratio of about 1.2.

Temperature Compensation. To obtain the desired regulated pressure with temperature, the bridge circuit must be programmed. The laminar element senses the temperature of the fluid and changes its operation with the fluid viscosity. The changes in the laminar restrictor alone are not sufficient to program the desired regulated pressure. The temperature compensating orifice must therefore change its characteristics by the proper amount with temperature. The required change in orifice area with temperature was calculated for the temperature compensating orifice. Based on isentropic relationships, the required scheduled area is shown in Figure 13 for oxygen. This would have to be modified somewhat for the actual system to include real gas effects. Other potential temperature anomalies within the circuit could also be offset by the temperature compensator design. This curve could be followed quite readily by an orifice area controlled by differential expansion between dissimilar materials due to temperature.

Dynamic Response. To study the effects of the system start-up operation, the system was modeled on the digital computer at Rocketdyne. Preliminary results of the computer analysis indicated regulated pressure within ± 3 percent at about 30 milliseconds after start for the minimum input pressure 3.17×10^6 N/m^2 (460 psia). This is shown in Figure 14. When the model was run with the highest input pressure of 5.52×10^6 N/m^2 (800 psia), the model showed large instability as depicted by Figure 15. A computer run, with decreased volumes in

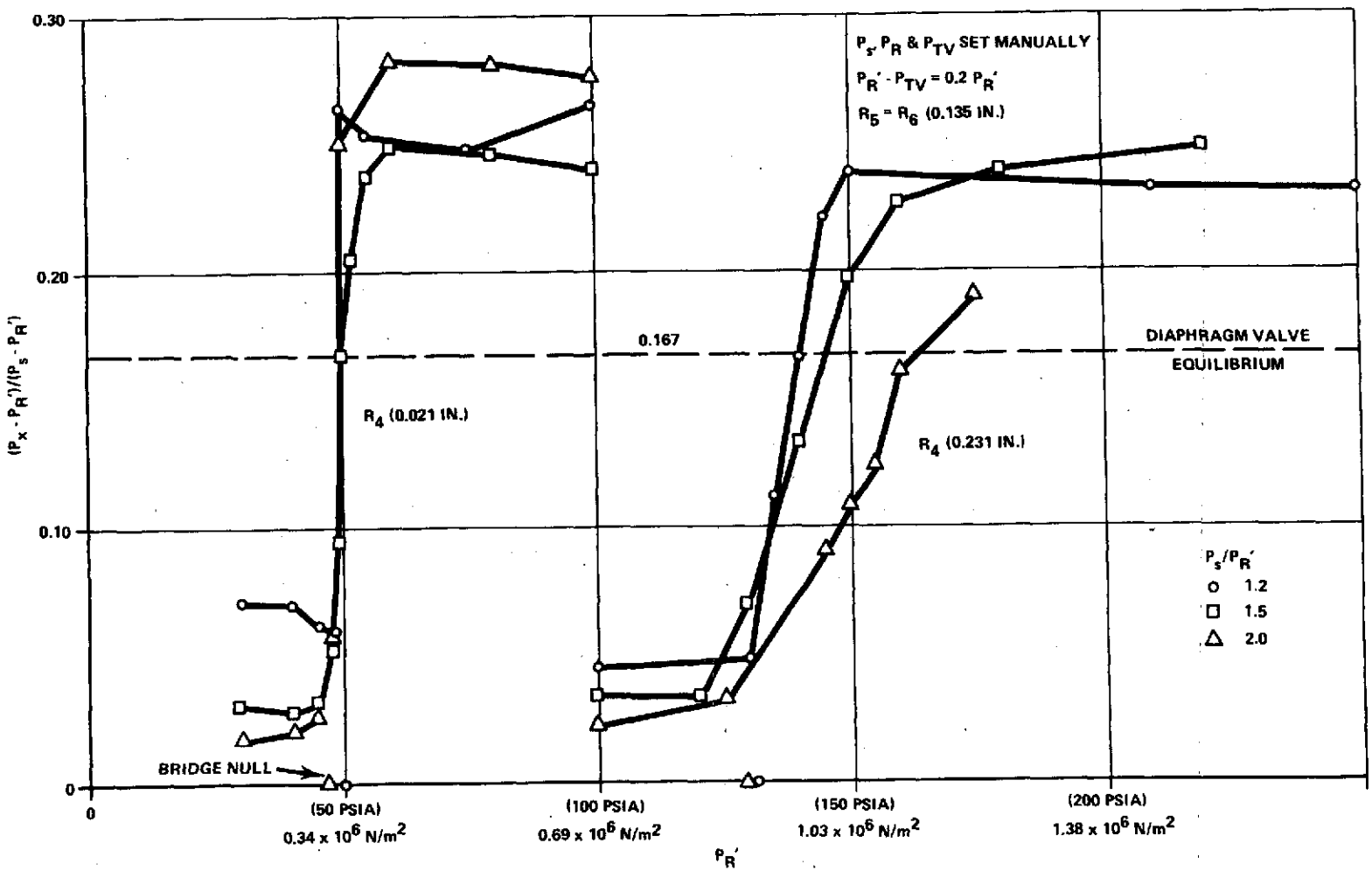

Figure 11 - Open-Loop Test Schematic for Bridge Circuit and Amplifier Cascade

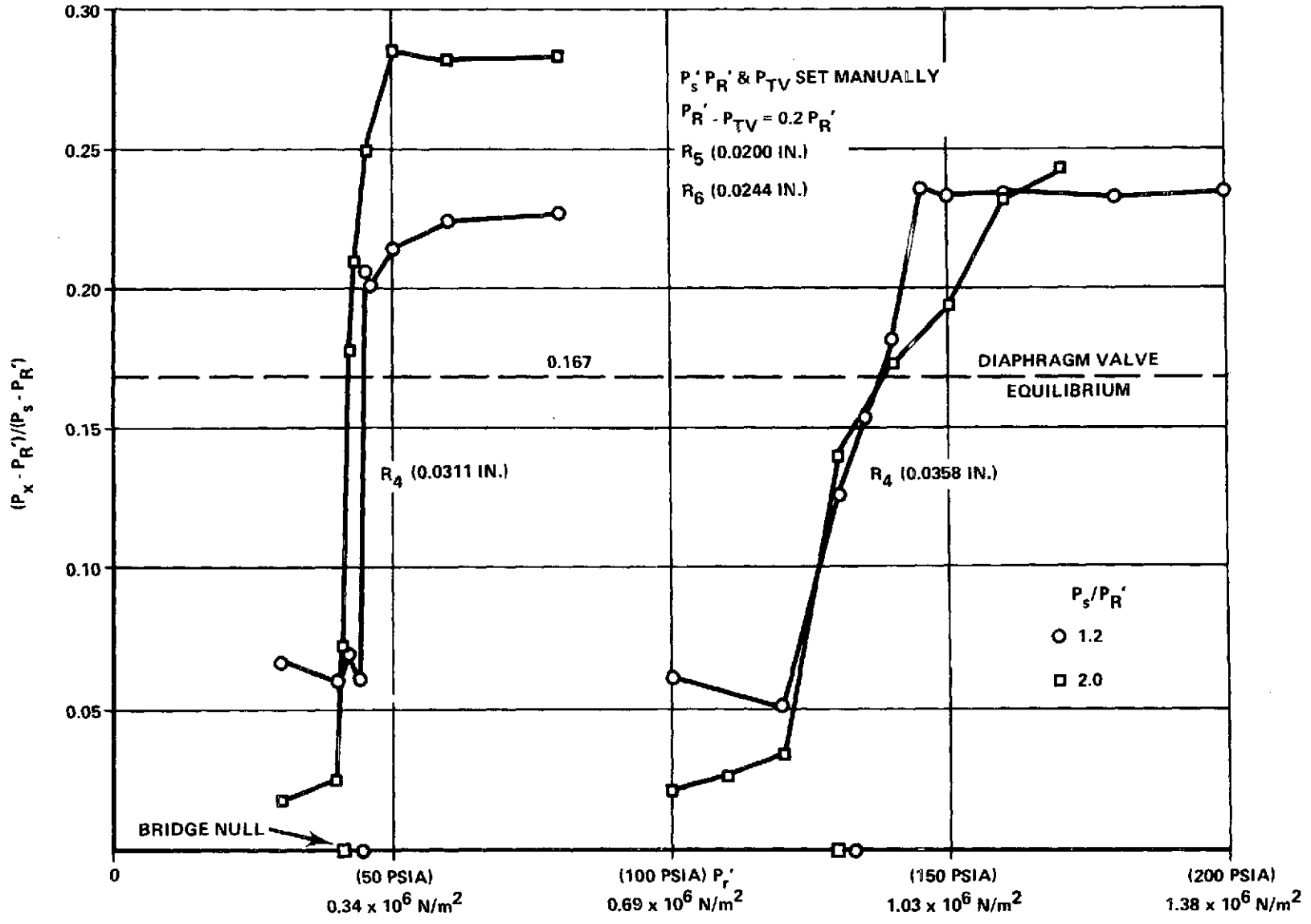

Figure 12 - Open-Loop Test with R5 ≠ R6

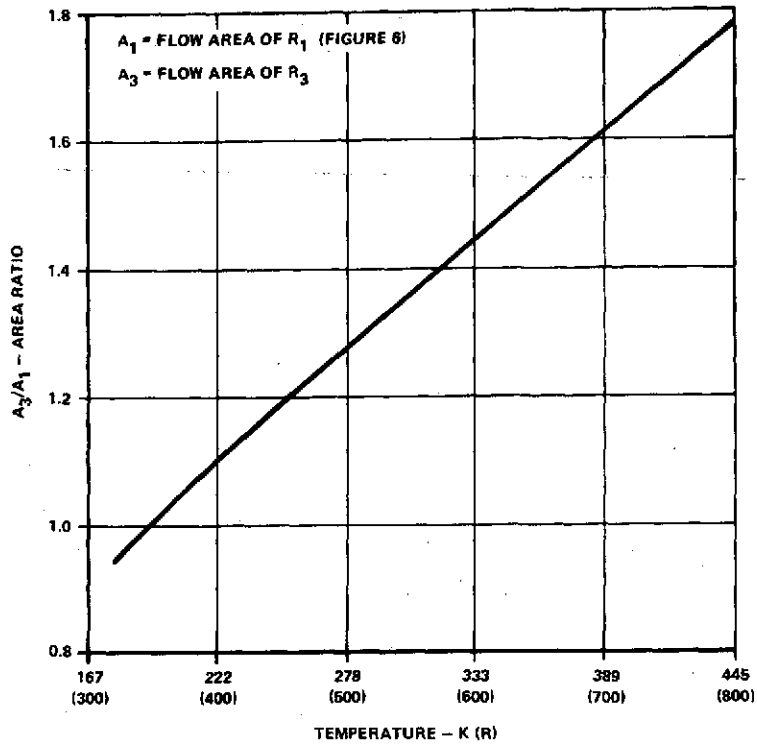

Figure 13 - Required Scheduled Area for Oxygen (Calculated)

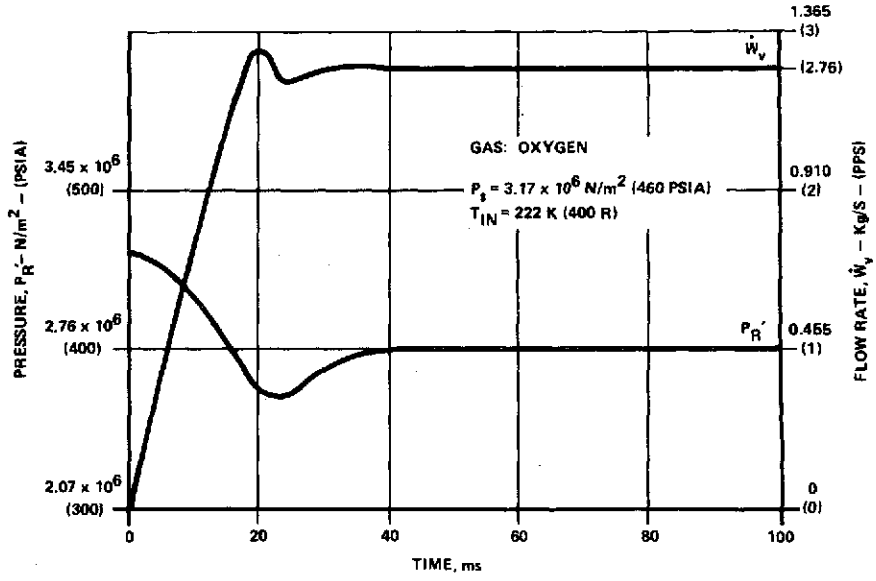

Figure 14 - Dynamic Operating Characteristics at P_{in} = 3.2 x 10^6 N/m^2 (460 psia)

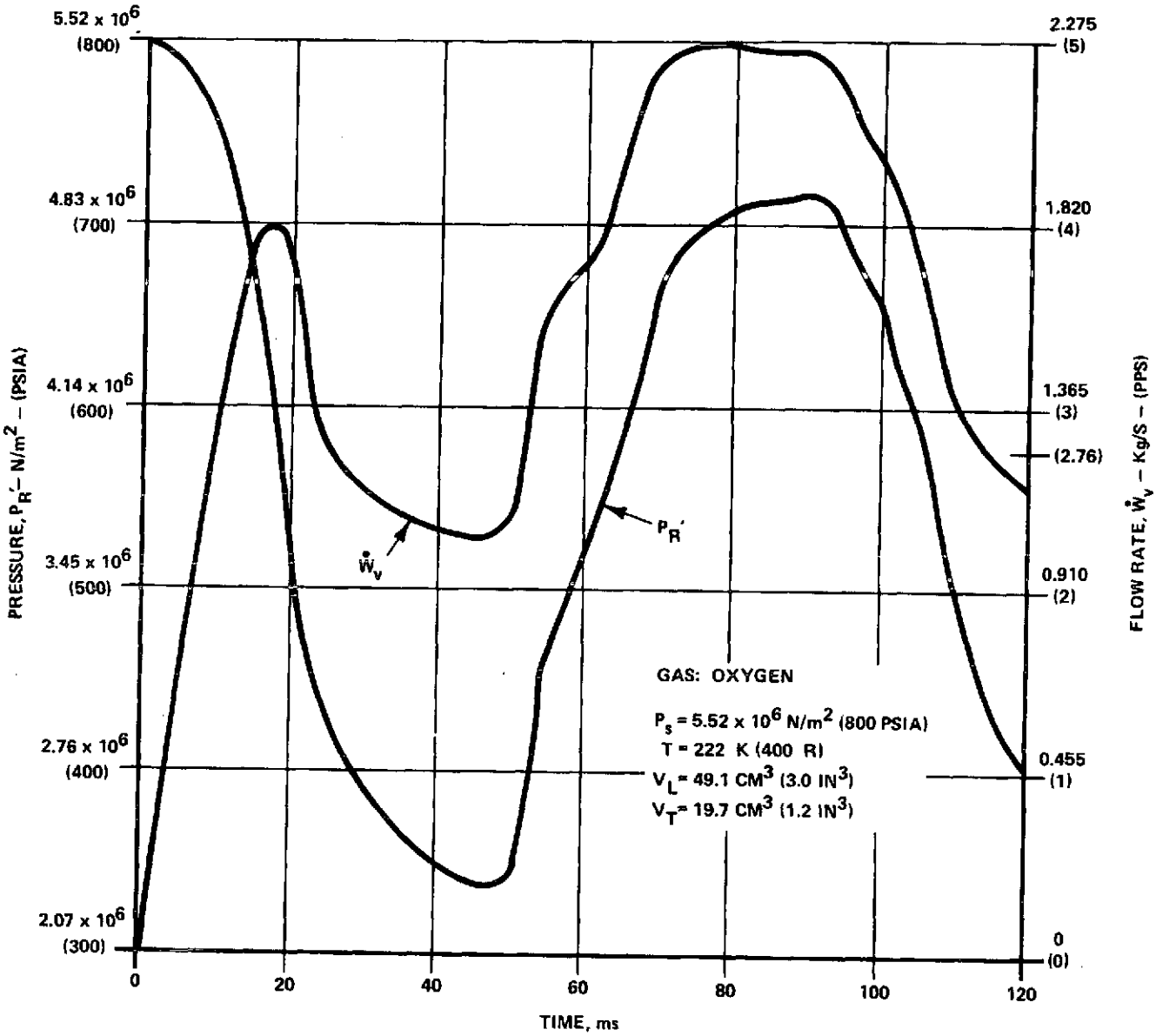

Figure 15 - Dynamic Operating Characteristics at P_{in} = 5.5 x 10^6 N/m^2 (800 psia)

the bridge circuit, resulted in considerable improvement as shown in Figure 16. The oscillations, however, still depict an under-damped system. A further run (Figure 17) had the main flow volume downstream of the diaphragm increased by a factor of three. The results showed more improvement in reducing oscillations, while sacrificing on response time.

The computer program was run with the laminar restrictor both upstream in the bridge and downstream. Stability improved when the laminar restrictor was placed downstream in the place of R_4.

At this point it was concluded that the model indicated* a stability problem at higher input pressures. Further investigation with the computer model could help identify the critical parameters and ways to stabilize the dynamics while optimizing the response time.

The temperature dynamics were not included, but the desired pressure regulation at each steady-state temperature was quite accurate, as predicted. The temperature response of the controller could be designed to be as fast as is mechanically possible by bathing the temperature-sensitive elements in the main flow stream to obtain best heat-exchange effects.

Preliminary Technical Review at NASA-Lewis. Based on the preceding discussion, a review meeting was held at NASA-Lewis to select a concept for further development. The merits of the hybrid fluidic concept C were listed along with those of the electromechanical and mechanical approaches of Rocketdyne. The merits of the hybrid fluidic concept C listed were:

- only one moving part
- potential high accuracy
- potential good response
- low pressure drop
- applicability to other gases
- applicability to other systems

The basic potential for pressure regulation of this concept was shown. However, before a full development of the concept could produce a successful flow control system, the effects of the following items had to be considered before NASA could make a concept selection:

- fluidic circuitry accuracies over full ranges of absolute pressure, temperature, and flow rate
- dynamic stability and response over operating range and conditions

*The term "indicated" is used since the model was a very simplified version of the actual, highly nonlinear, circuitry.

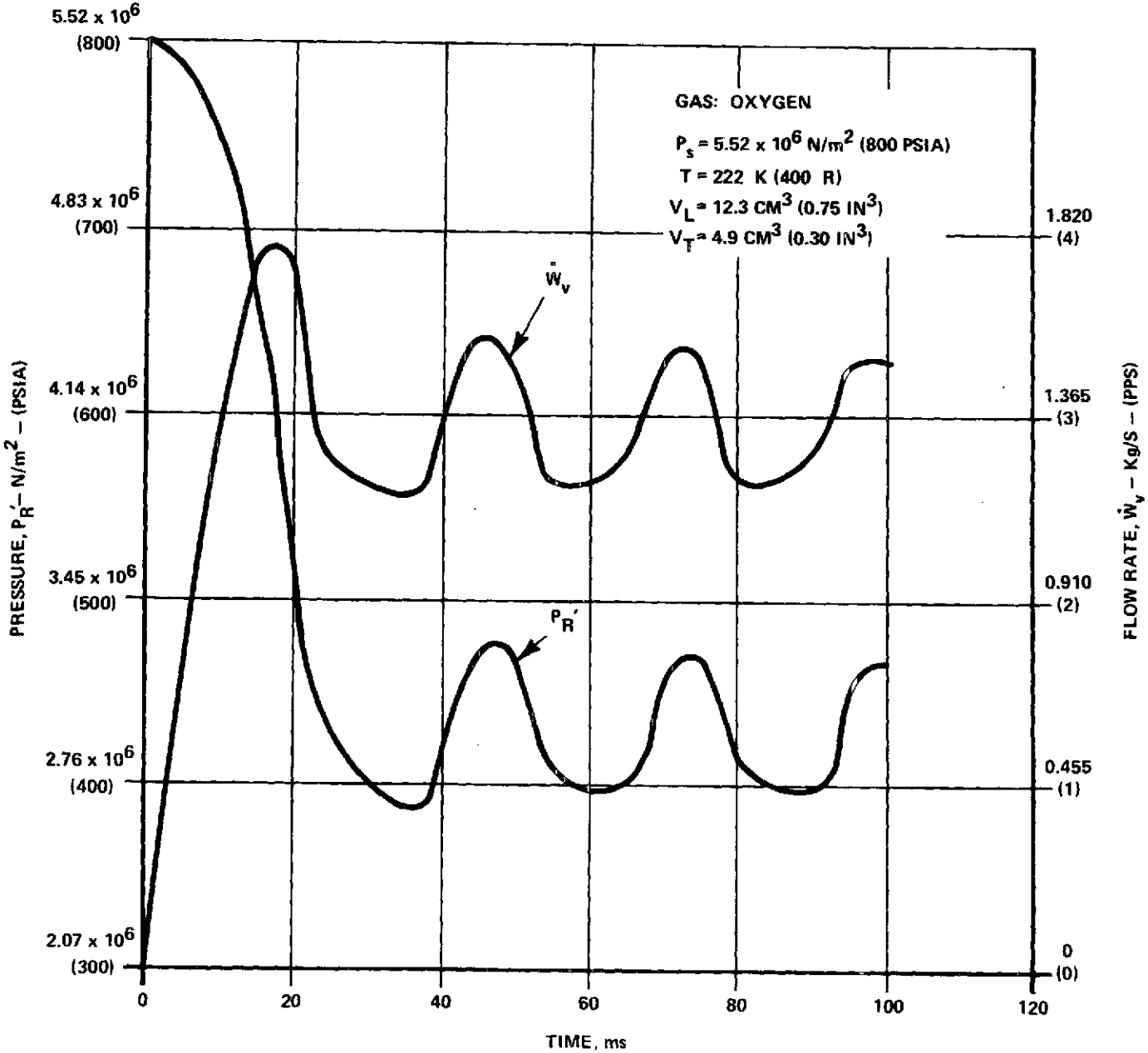

Figure 16 - Dynamic Operating Characteristics with Decreased Volumes in Bridge Circuit

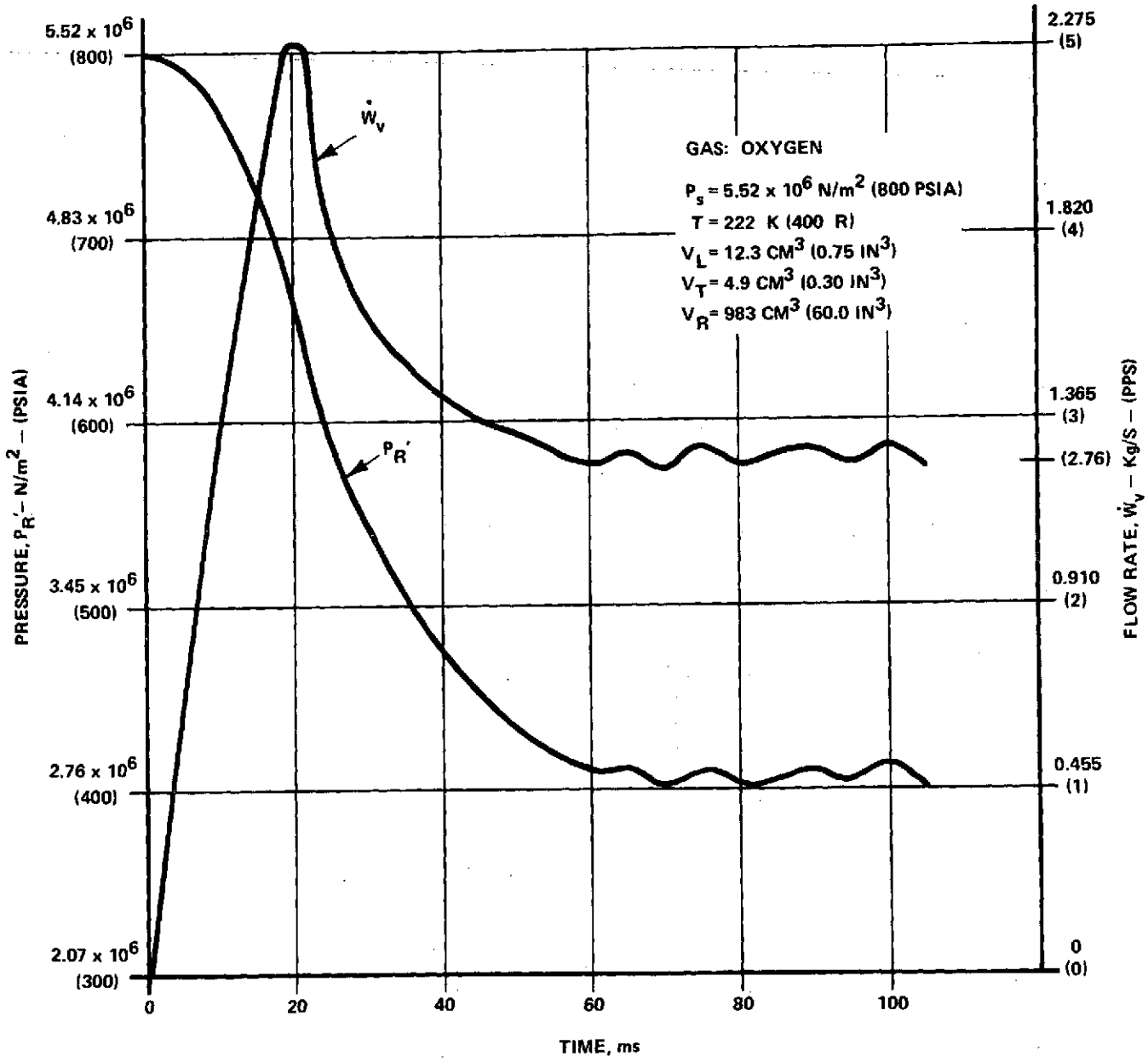

Figure 17 - Dynamic Operating Characteristics Showing Reduced Oscillations

- temperature response
- downstream oscillations
- development time and cost

As a result of the meeting at NASA, it was decided to investigate further the performance of two critical elements in the fluidic circuit: the proportional amplifier and the laminar restrictor. The follow-on evaluation of these elements is discussed in the next section.

Detailed Evaluation

In order to provide more technical information that would assist NASA in making a concept selection, it was decided to investigate the performance of two critical elements in the hybrid fluidic concept C. These elements were the proportional amplifier and the laminar restrictor.

To assist in a concept selection, the primary objectives that were sought for each element were:

Proportional Amplifiers

(1) To evaluate operation over required temperature and pressure range

(2) To achieve an operable closed-vent configuration

(3) To insure structural integrity

(4) To define transient response

Laminar Restrictor

(1) To evaluate operation over required temperature and pressure range

(2) To achieve minimum time response to temperature

(3) To insure structural integrity

(4) To define transient response

Proportional Amplifier Evaluation. In attempting to achieve the various objectives for the proportional amplifier, fabrication and testing of several proportional amplifier designs with closed vents were conducted. The basic amplifier tested for the control circuit was shown in Figure 6 as the A_1 amplifier. The circuit pressure P_R' and P_{TV} required at each temperature are a function of P_R and are shown in Figure 18.

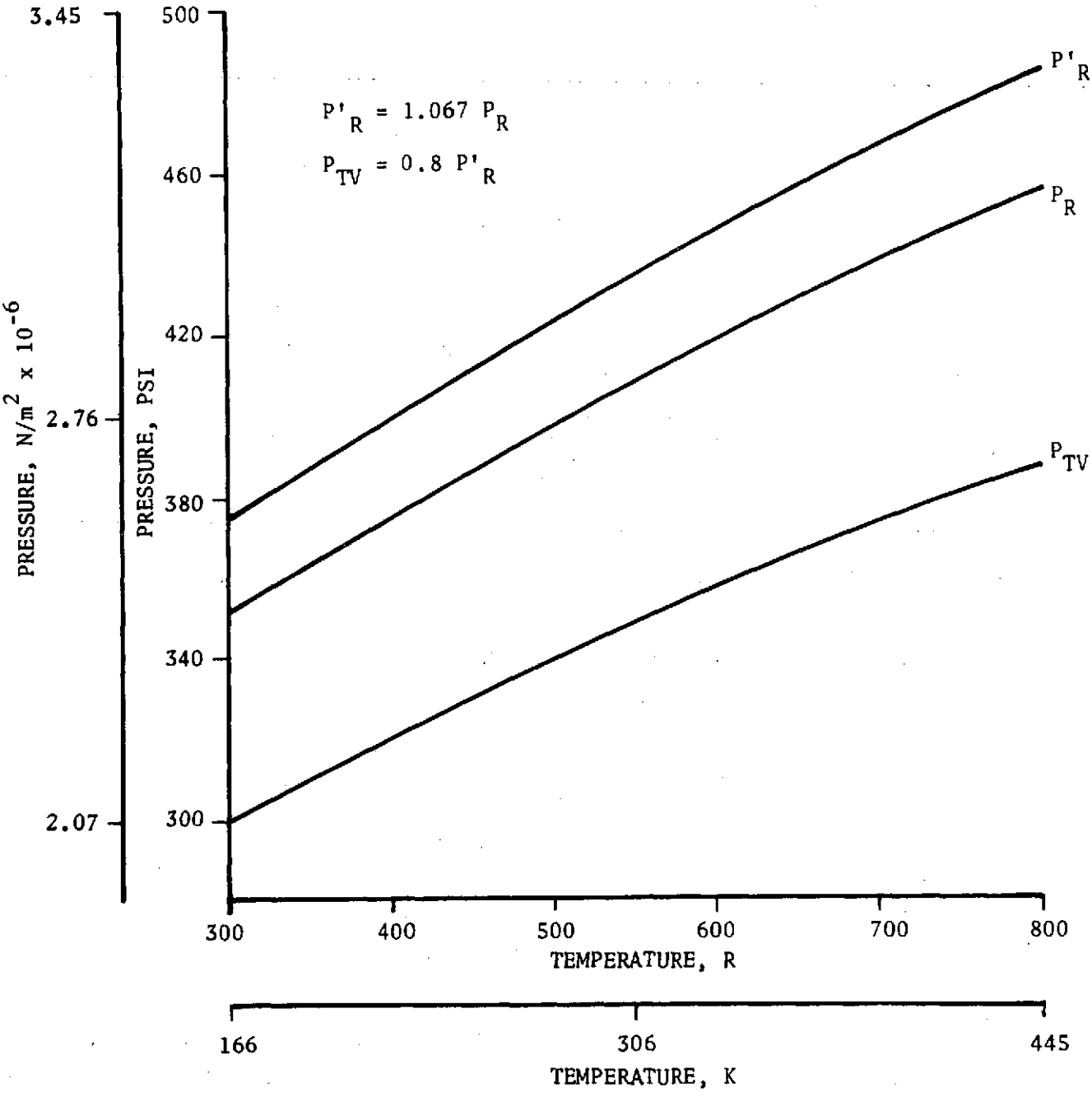

Figure 18 - Pressure versus Temperature for Basic A_1 Amplifier

The primary design considered in this circuit is of the AM31 profile design shown in Figure 7. This has been considered as the primary type of amplifier profile because of its known high-impedance characteristics. Such an amplifier would thus require little or no control flow. However, a momentum amplifier could possibly be used as the A_1 amplifier if the control ports of the amplifier were used as the R_3 and R_4 orifices of the sensing bridge. A Bendix momentum amplifier which has multiple control ports, as depicted in Figure 19, was tested. Generally, the lower control ports serve as the gain-producing ports while the upper control ports could be used to enhance gain, to obtain or offset null conditions, or to employ dynamic compensation for system response and/or stability.

Testing for both types of amplifiers was conducted with GN_2 over the pressure range of 2.76×10^6 N/m^2 (400 psia) to 5.52×10^6 N/m^2 (800 psia) at temperatures of 290 K (520 R) to 425 K (760 R).

The ideal performance characteristics desired are shown in Figure 20. Idealized gain curves in part (a) of the figure show a linear region of constant slope (gain) between input (ΔP_C) and output signals (ΔP_O) for various supply pressures. Part (b) of the figure shows, in another way, the desire to have gain constant with pressure ratio. Parts (c) and (d) show that a gain characteristic that is fairly independent of bias and temperature is desired. Although these are idealized trends based on a single amplifier, it is probable that circuit stability could require slightly different characteristics, such as decreasing gain with increasing P_S/P_{TV} ratio (Part (b)) or with increasing temperature (Part (d)).

Although all of the details of the results are not presented here, some of the trends of the AM31-profile-type amplifier performance are shown in Figures 21 through 26.* In general, the data show that AM31-profile amplifier pressure gain is variable with supply pressure, control bias level, temperature, load, and vent configuration. The net effect of these gain variations is important only insofar as the net gain might vary in the overall amplifier cascade. It would be acceptable to have one amplifier increase in gain while another decreases as, say, P_S increases so long as the net gain variation in the amplifier cascade is minimal. This point is further discussed after considering the performance of the PA25-profile amplifier.

The PA25-profile amplifier was investigated, since the AM31-profile-type amplifier markedly decreased in gain with increasing absolute pressure level. This allowed the PA25-profile-type amplifier to be competitive in pressure gain. The results of this gain change are depicted in Figure 27.

The trends of the PA25-profile momentum amplifier are shown in Figures 28 through 31. The amplifier has, in general, lower pressure gain than the AM31-profile amplifier but has better gain linearity and lower noise.

---

*The data points for these figures are derived by taking the gain from the original data of P_C versus P_O and plotting gain against some pressure factor. A list of nomenclature is shown in Appendix A to assist in understanding the data.

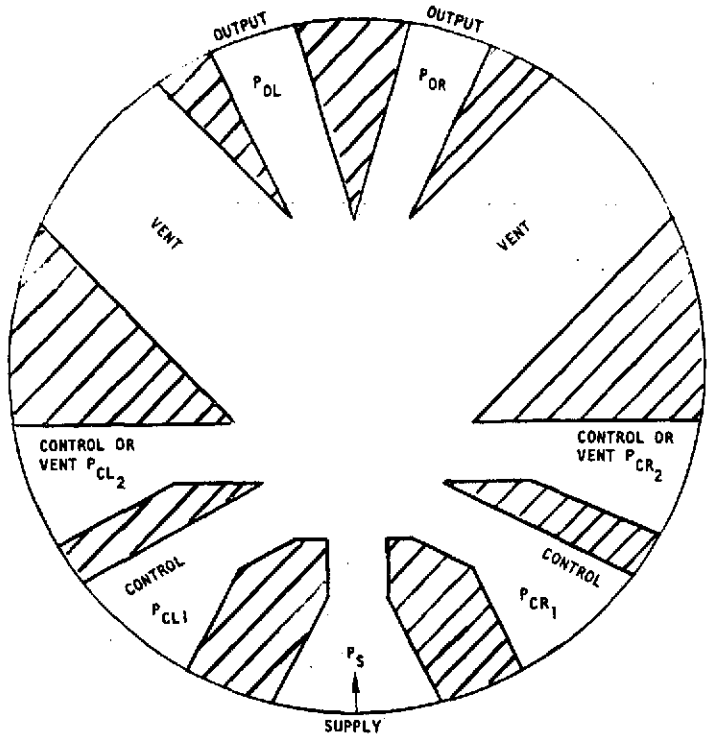

Figure 19 - PA25 Amplifier Profile

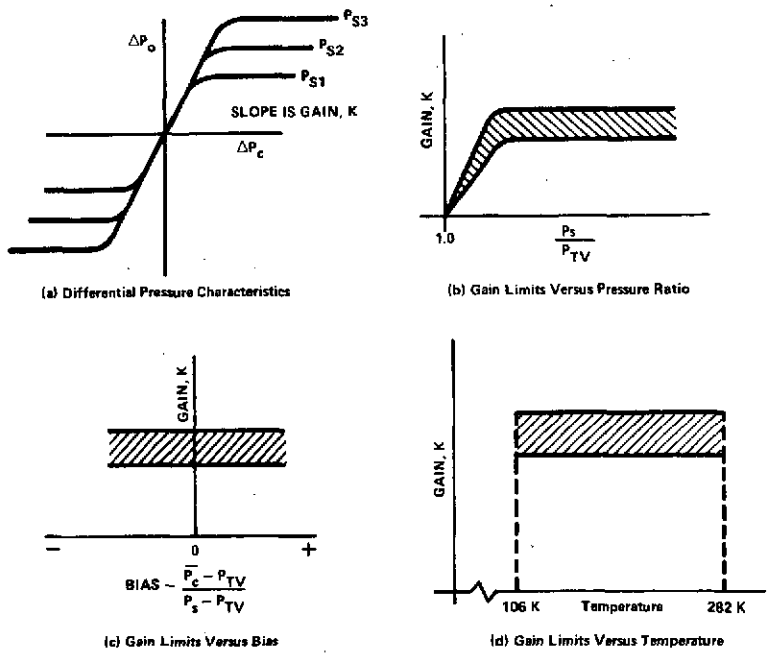

Figure 20 - Desired Proportional Fluidic Amplifier Performance

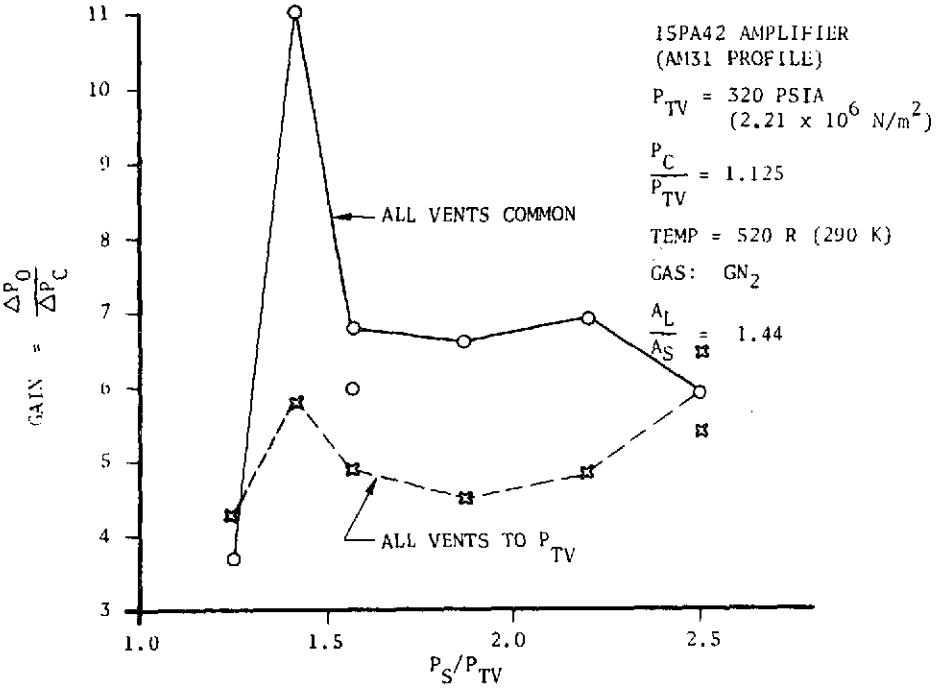

Figure 21 - AM31 Amplifier Gain versus Pressure Ratio

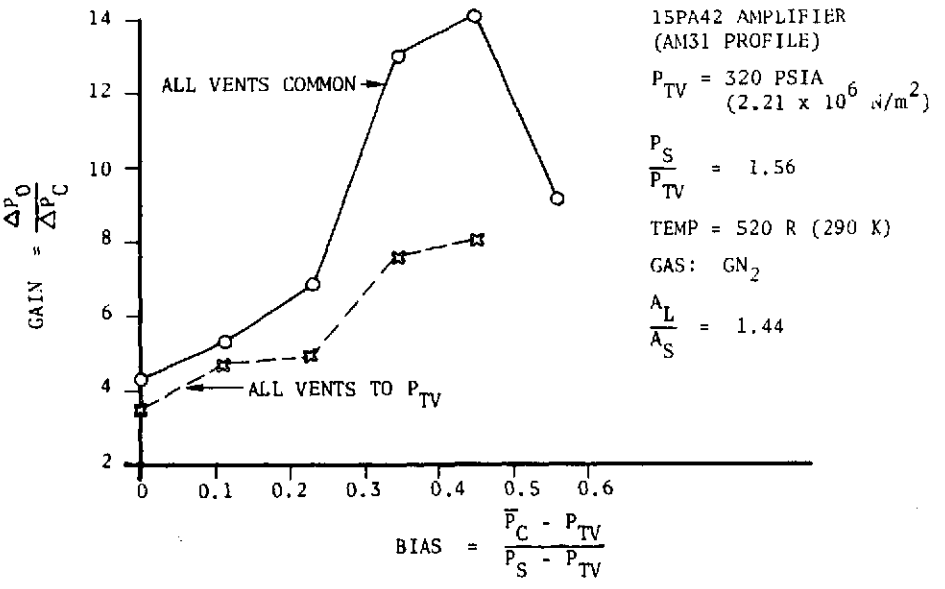

Figure 22 - AM31 Amplifier Gain versus Bias for P_s/P_{TV} = 1.56

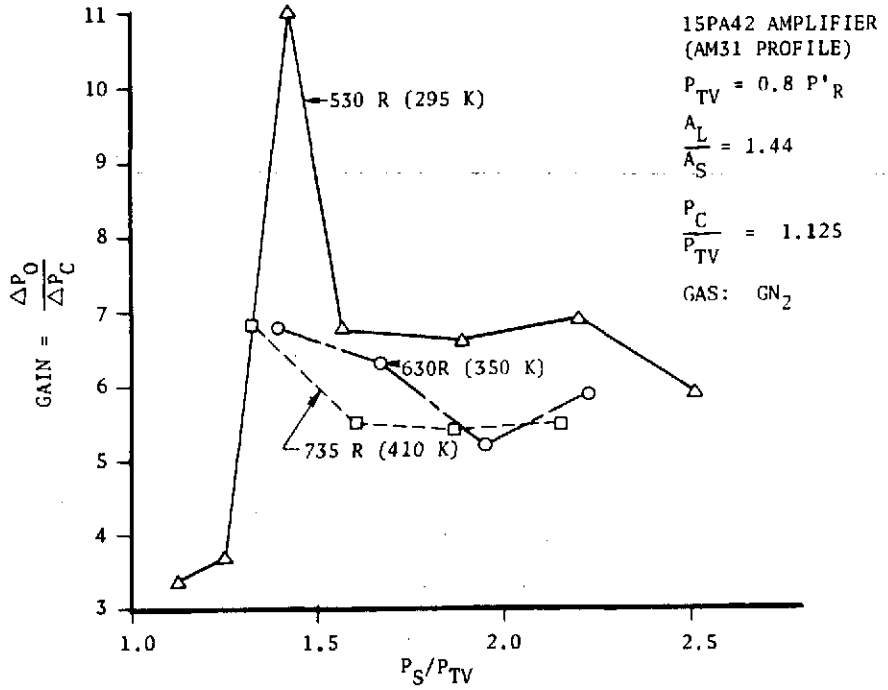

Figure 7. AM31 Amplifier Performance

Figure 23 - AM31 Amplifier Gain versus Pressure Ratio for Various Temperatures

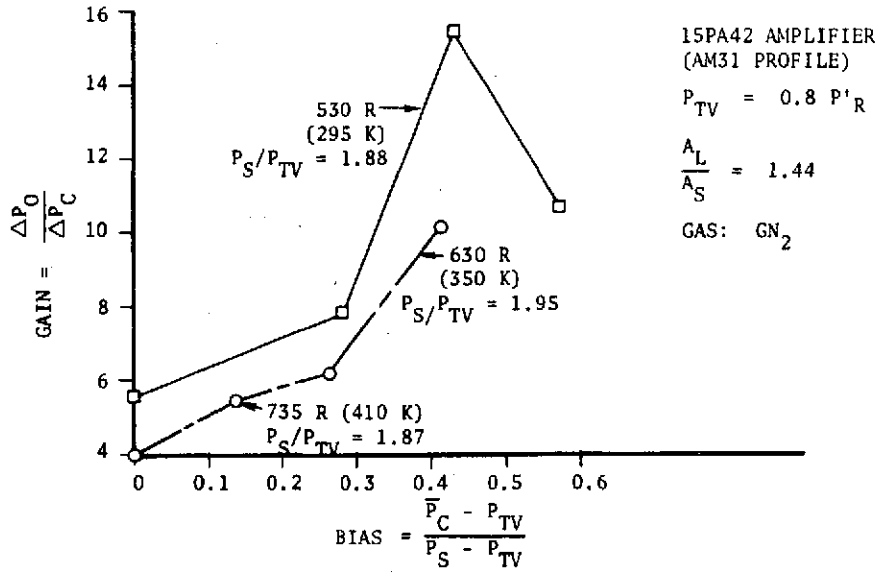

Figure 24 - AM31 Amplifier Gain versus Bias for Various Temperatures

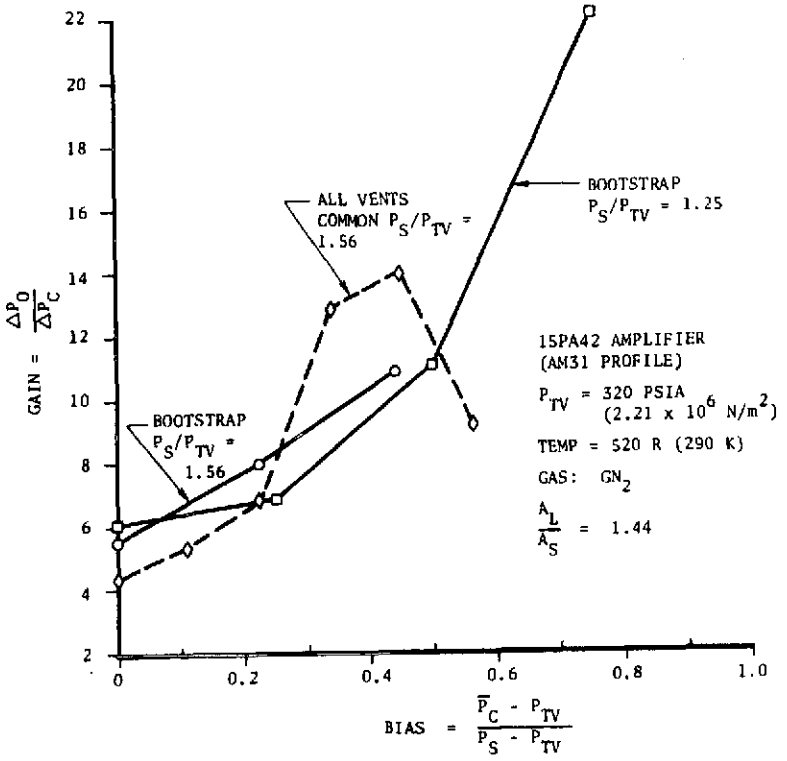

Figure 25 - AM31 Amplifier Gain versus Bias for Various Connections

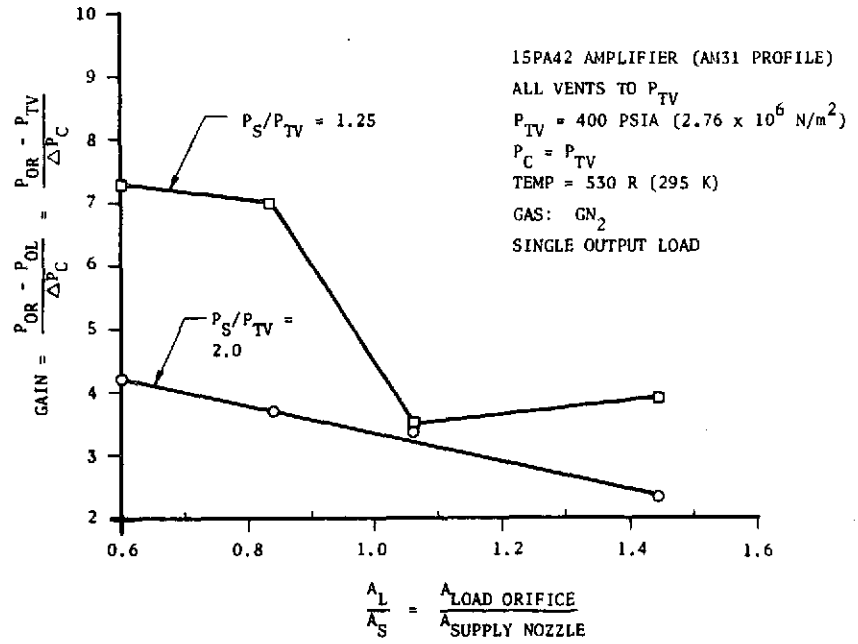

Figure 26 - AM31 Amplifier Gain versus Load Ratio

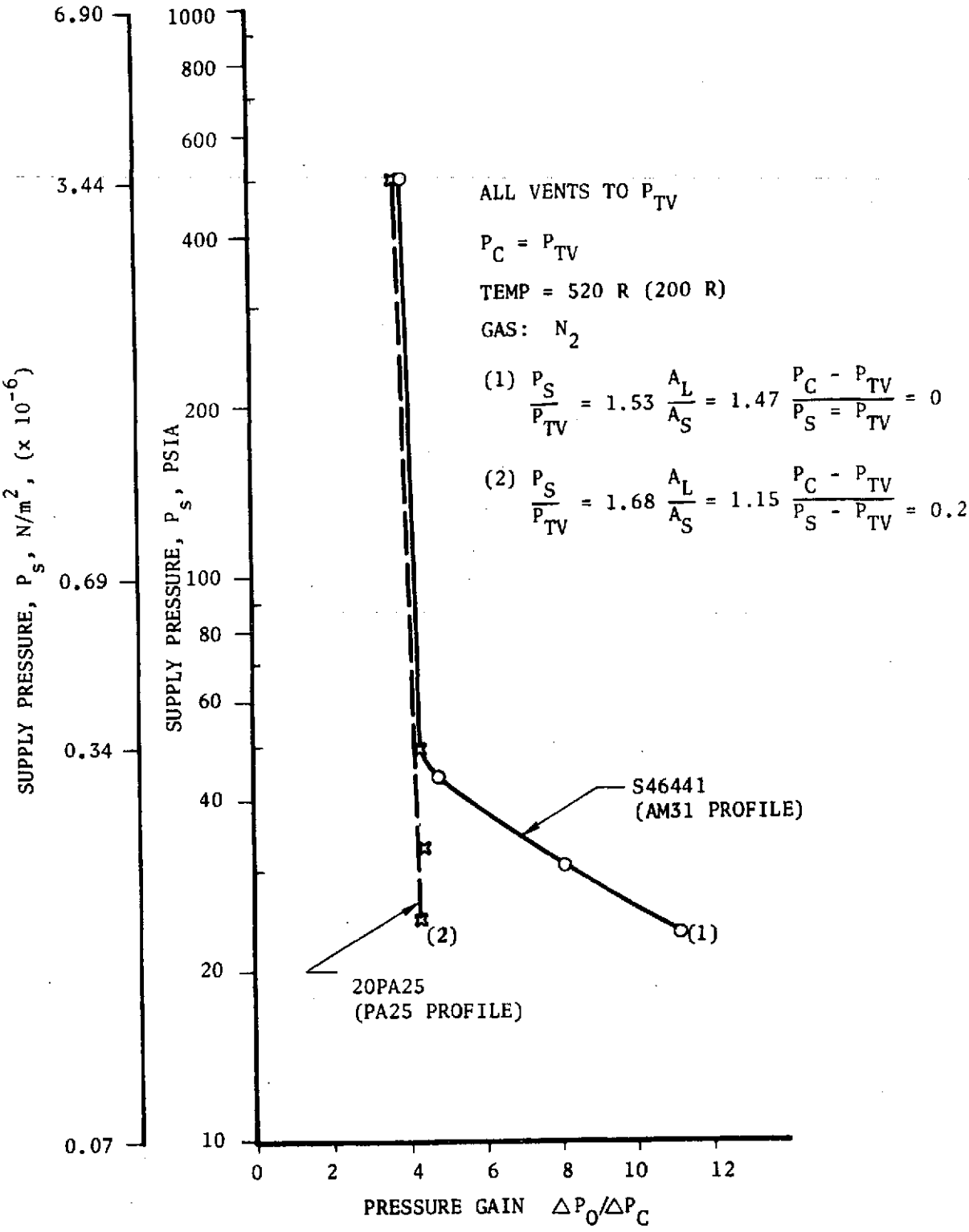

Figure 27 - Effect of Pressure Level on Gain

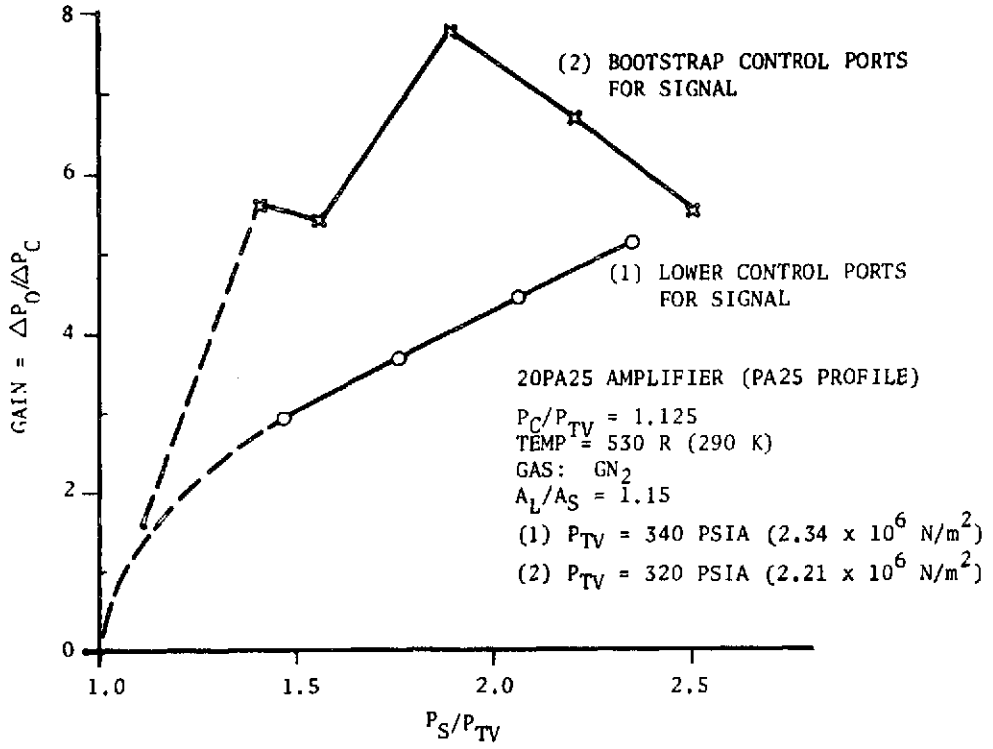

Figure 28 - PA25 Amplifier Gain versus Pressure Ratio

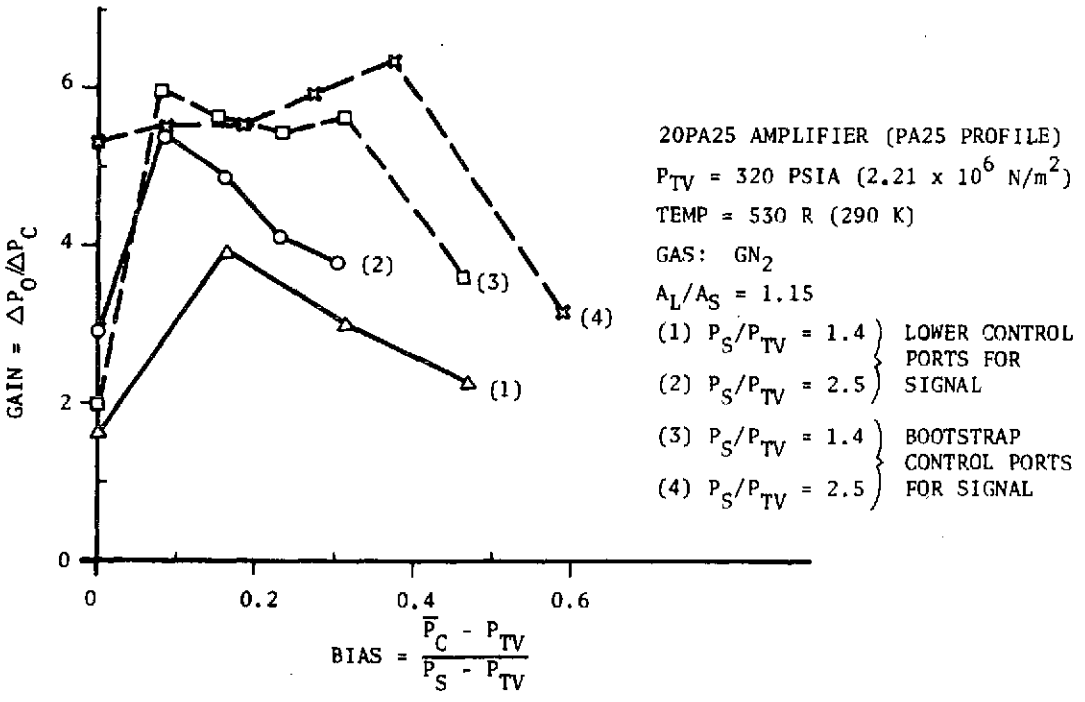

Figure 29 - PA25 Amplifier Gain versus Bias for Various Connections

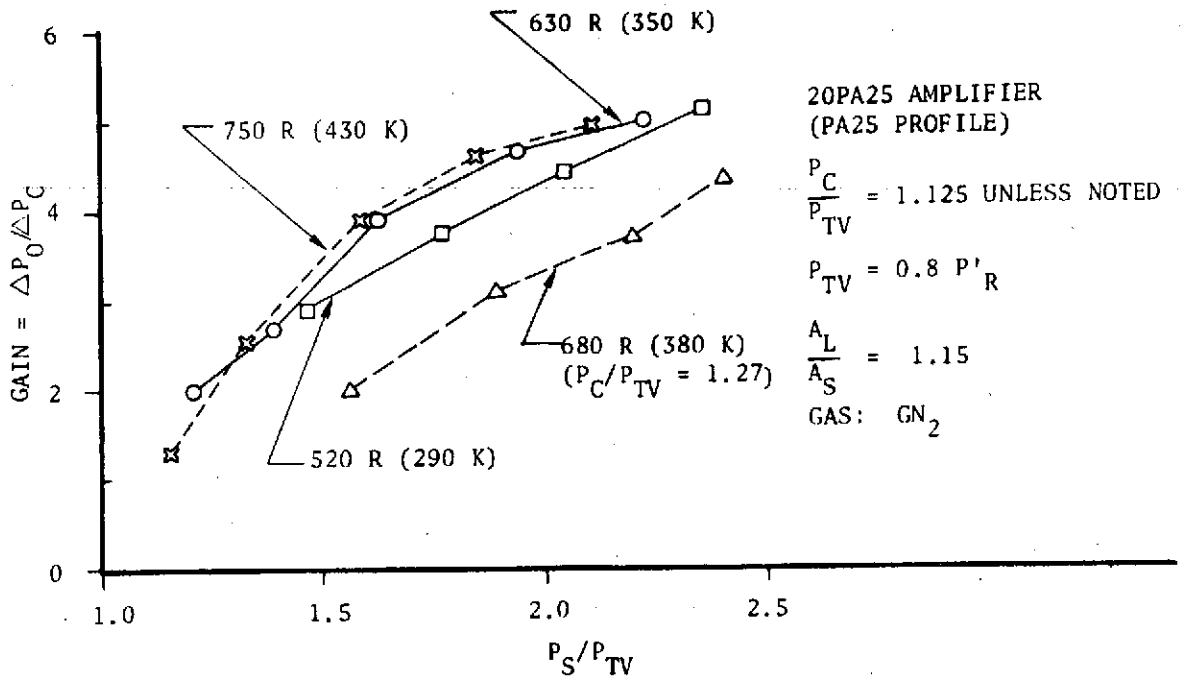

Figure 30 - PA25 Amplifier Gain versus Pressure Ratio for Various Temperatures

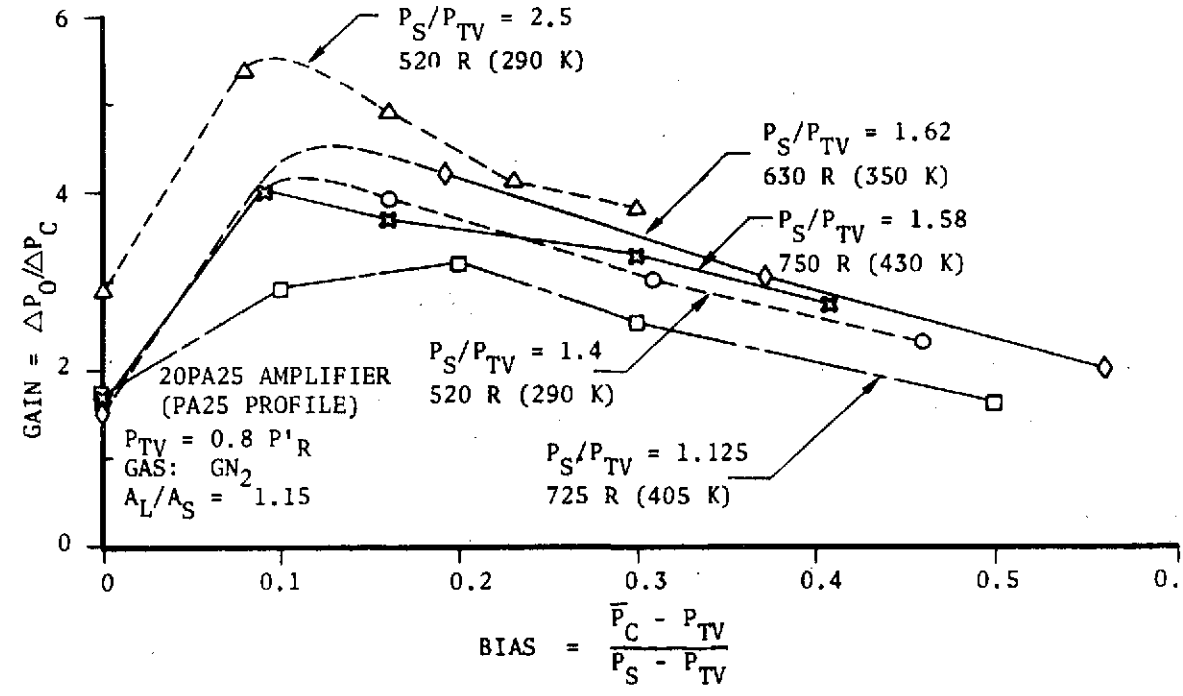

Figure 31 - PA25 Amplifier Gain versus Bias for Various Temperatures

The impact of these variations on the circuit is important in that a net gain variation be minimized to maintain closed-loop control as the supply pressure changes from, say, 3.10×10^6 N/m^2 (450 psia) to 5.52×10^6 N/m^2 (800 psia). Staging the amplifier cascade together analytically has shown several possible cascades which could minmize gain changes for a given temperature and control pressure. However, because of the number of variables involved, the amplifier cascade would have to be built and tested to insure accurate and reliable operation for use in the circuit.

In order to summarize the findings of the various tests, Table IV presents the results relevant to the high-impedance amplifier which must be used as the A_2 and A_3 amplifiers in the circuit. The reason that the A_2 and A_3 amplifiers must be high impedance is because of the increasing power required for each successive amplifier. The first amplifier, or pilot amplifier, must be sensitive enough to detect the changes in the bridge circuit and would, therefore, be a low-power element. On the other hand, the last amplifier must have sufficient power capability to drive the diaphragm to a desired position with sufficient response. The last amplifier is then a high-power element. Use of a high-impedance amplifier is required since in the amplifier cascade, a lower-power amplifier must drive a higher-power one. This can be done by using a high-impedance amplifier, but not with a momentum type.

TABLE IV - PROPORTIONAL-AMPLIFIER EVALUATION

Desired*	Test Results
Structural Integrity	No apparent problems at these pressures
Relatively constant pressure gain with	Gain varies
	Moderately / Significantly
• Supply pressure	High P_s/P_R / Low P_s/P_R
• Control pressure	Low P_c/P_R / High P_c/P_R
• Temperature	275-425 K (495-765 R)
	Variations are caused by closed vent conditions and possibly absolute pressure level
Low noise level	Moderately low noise
Input/Output linearity	Generally good linearity about null
Good saturation	Good saturation

*This is actual near normal atmospheric conditions where vents are connected to the ambient.

The A_1 amplifier in the circuit, as previously mentioned, could possibly be either the AM31-profile high-impedance type or the PA25-profile momentum type.

The general findings on the PA25-profile-type amplifier are quite similar to those on the AM31-profile type although absolute values of gain may differ.

The influence of these variations on the overall system are summarized after the discussion of the laminar restrictor.

Laminar Restrictor. The laminar restrictor was also considered to be an important element in the circuit. The thermal response of the hybrid fluidic concept is much dependent on the response of the laminar restrictor. In order to obtain maximum possible response from the laminar restrictor, it was envisioned that it would actually be placed in the main gas flow as a heat exchanger such as depicted in Figure 32. The main gas flow would thus heat or cool the small flow going through the restrictor. An example of the restrictor cross section is shown in Figure 33.

Although the laminar restrictor was not built, a detailed layout of an annular version was conducted. The unit was never built because of more complex problems that arose with the proportional amplifiers. However, a transient heat-transfer analysis was performed to determine the thermal time response of the preliminary design. The results depicted in Figure 34 indicate a time constant of about 60 milliseconds for a stainless steel restrictor in response to a temperature step input. Analysis revealed that the material thermal conductivity was not a significant parameter relative to response but that the time constant was primarily proportional to the product of density and specific heat. For steel, copper, and aluminum, this product is 3.62, 3.45 and 2.41 J/cm^3-K (31.23×10^{-3}, 29.77×10^{-3} and 20.79×10^{-3} Btu/in^3-R), respectively. This indicates a lower time constant for aluminum. However, because of Bendix' experience with diffusion bonding of steel, it was anticipated that the restrictor would have been constructed of steel.

The computer analysis discussed previously pointed out some concern about the dynamic pressure response of the laminar restrictor since it was a part of the sensing bridge. It was intended that this would have been checked out during a test of the laminar restrictor.

The following summarizes the work on the laminar restrictor:

- analysis of temperature response shows adequacy
- designed in detail
- not built and, therefore, no test results

Multiple Orifices in the Bridge. In place of the laminar restrictor, another possibility to help establish a pressure difference in the sensing bridge would be a number of series orifices. They could make for a smaller package size and weight if they did not appreciably affect the configuration of the temperature compensating orifice in the bridge. The sensitivity of the bridge would be less but the pressure and temperature dynamics might be improved. This approach

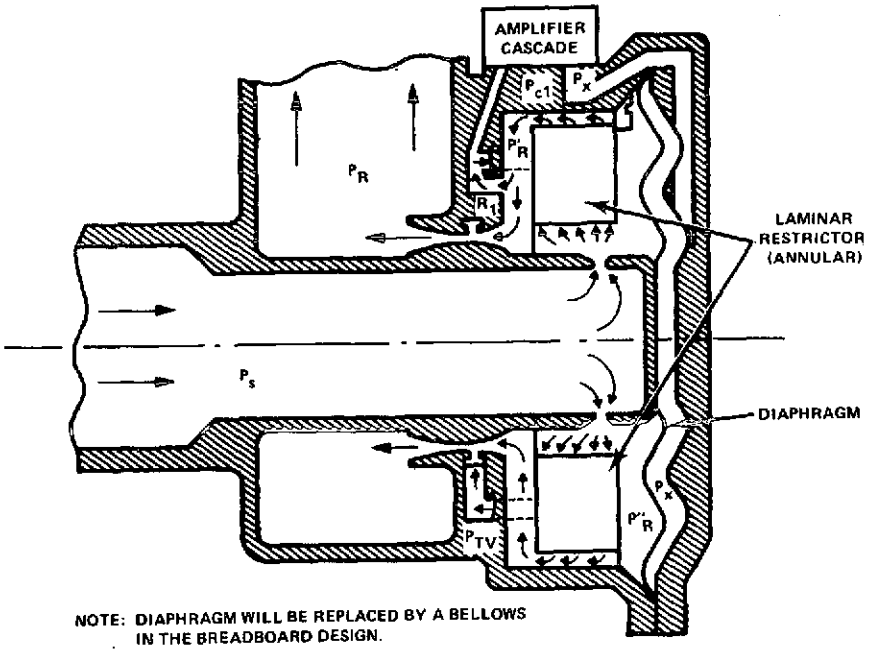

Figure 32 - Partial Schematic of Flow Controller

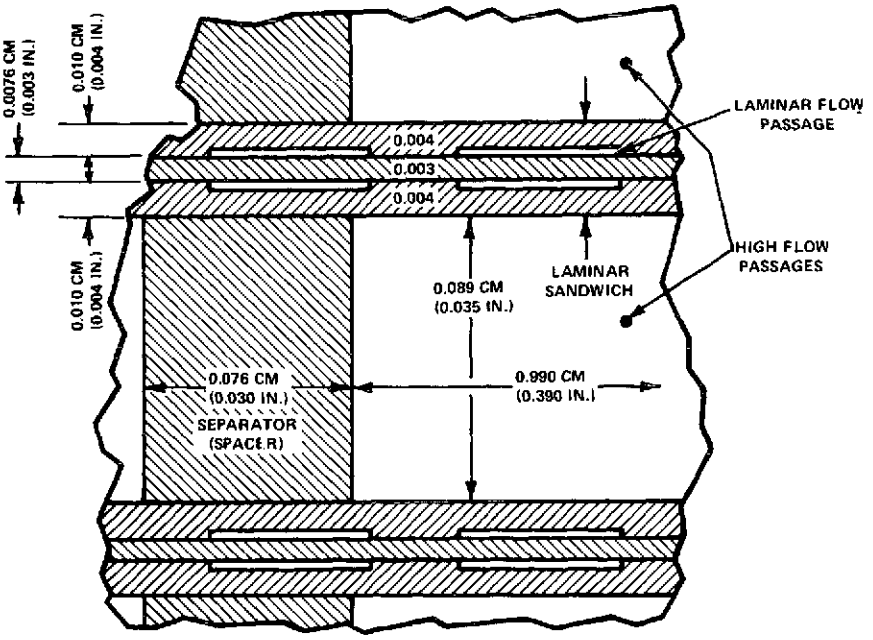

Figure 33 - Example of Laminar Restrictor Cross Section

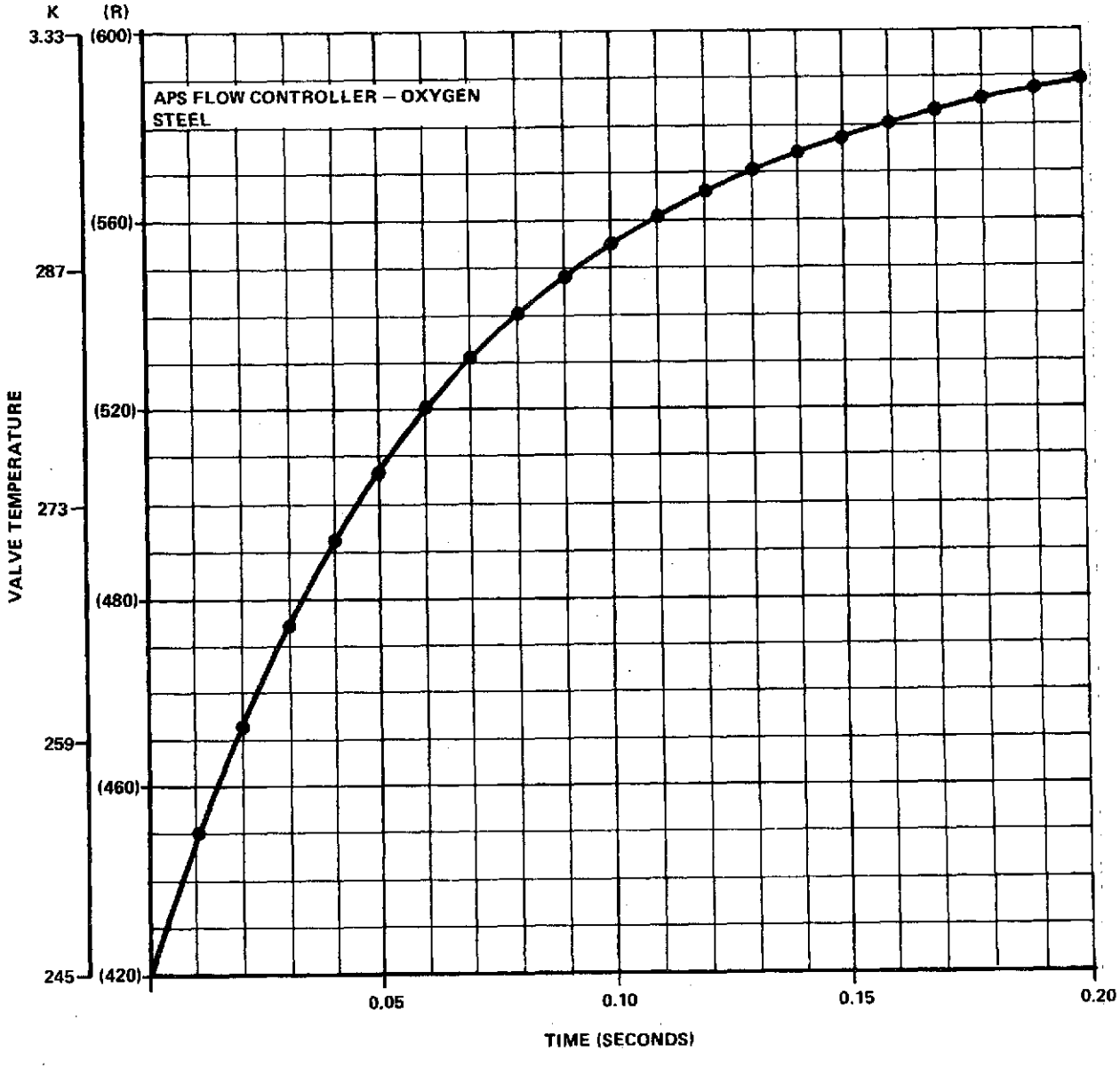

Figure 34 - Thermal Response of Laminar Restrictor

has been explored successfully in the past by Bendix for some applications. However, for the current application, no detailed analysis has been conducted since it was felt that the higher sensitivity in the bridge with the use of the laminar restrictor was more warranted.

Effects of Test Results. The foregoing test results and analyses have the following implications on the hybrid fluidic circuit operation:

(1) Gain variations in the amplifier cascade with supply pressure level, temperature, and control pressure level points to a tradeoff between instability (i.e., high gain) and dynamic accuracy (i.e., low gain).

(2) The number of variables and anomalies point out a higher development cost and risk for the development of this concept.

(3) Since actual pressure or temperature testing has been conducted only on components, the potential accuracy of the system has yet to be demonstrated.

Modifications to the Basic Configuration. The previous paragraphs have discussed the hybrid fluidic concept C in its original configuration. The fact that anomalies in amplifier performance began appearing under actual required pressures and temperatures led to the evolution of several modified arrangements of the basic concept to pursue alternate ways of circuit implementation in order to deal with gain variations while maintaining accuracy.

Numerous variations in circuitry hook-up are made possible by the use of a double-bellows arrangement of the valve to meter the main flow. A schematic of one such arrangement is shown in Figure 35. The double-bellows configuration would make the mechanical elements slightly more complicated. However, the use of a double bellows allows for both legs of the power amplifier (A3) to be used in a push-pull manner. Also, the bellows areas can be unbalanced by design, as shown in Figure 36, so that the upstream pressure will act as a coarse measure to move the valve opening in the proper direction with changing values in supply pressure. This movement is a coarse adjustment to hold constant flow rate. The fluidics then serve to trim on the difference needed to hold the flow rate constant. This would result in a smaller third-stage amplifier since not as much power would be needed in the fluidic part of the control loop to control valve opening. In addition, the dynamics at start-up could be improved over the single-diaphragm valve arrangement since the upstream supply pressure would help as a coarse position control on the valve as shown in Figure 37. The nonlinear curves are the required functions for constant flow for 222 K (400 R) and 445 K (800 R). Each linear curve is that portion of the required function that would be coarsely controlled by the supply pressure acting on the bellows. The curves are drawn for the equilibrium cases where $P_{x1} - P_{x2} = 0$ across the bellows and the downstream regulated pressures are assumed at their nominal values (i.e., $P_R' = 2.76 \times 10^6$ N/m^2 (400 psia) for T = 222 K (400 R) and $P_R' = 3.34 \times 10^6$ N/m^2 (484 psia) for T = 445 K (800 R)). The fluidic circuit is used to establish the reference value of regulated pressure for a given temperature and provide the trim control to maintain the desired area flow curve for the valve.

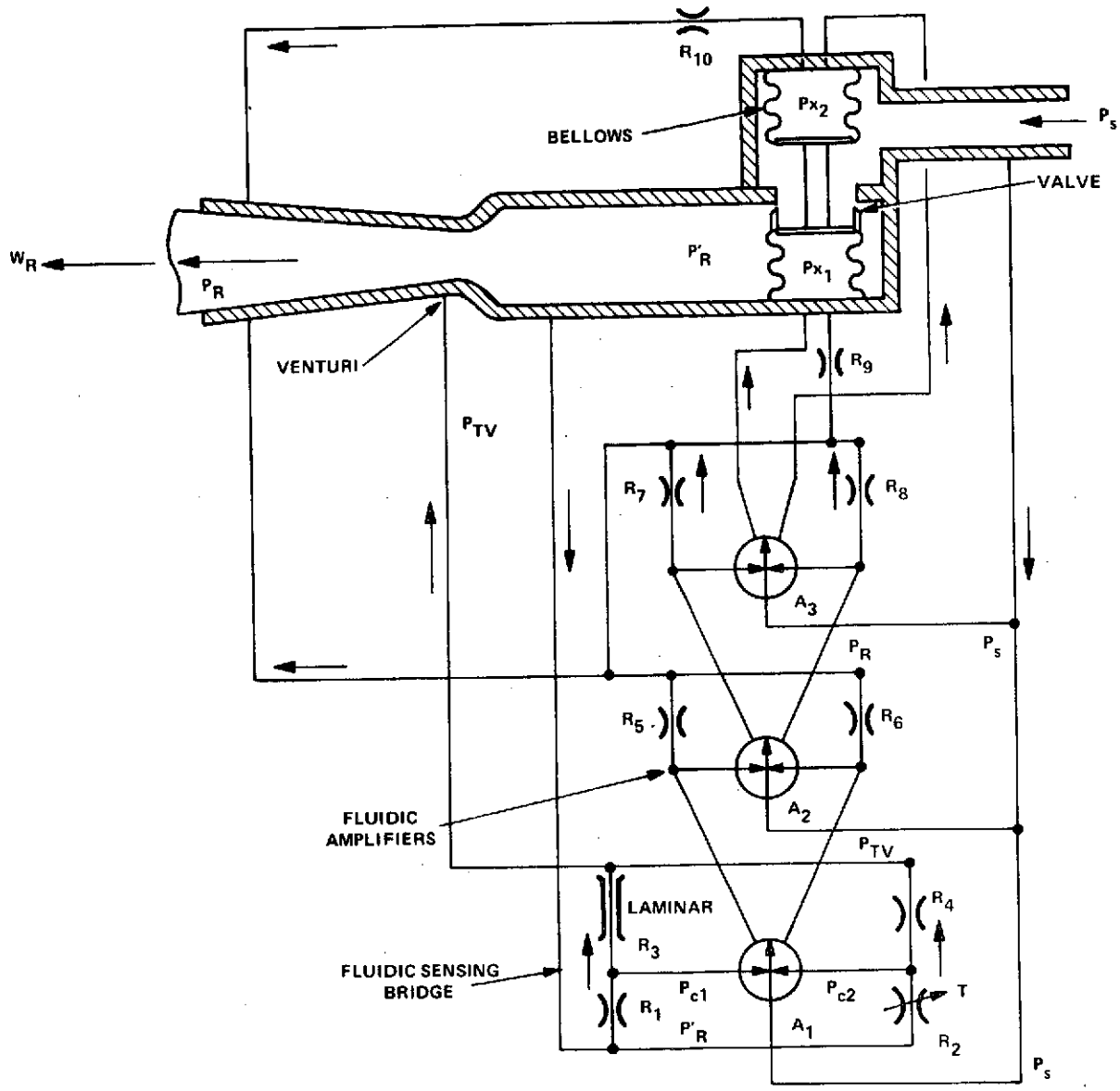

Figure 35 - Schematic Diagram of Hybrid Fluidic Flow Controller

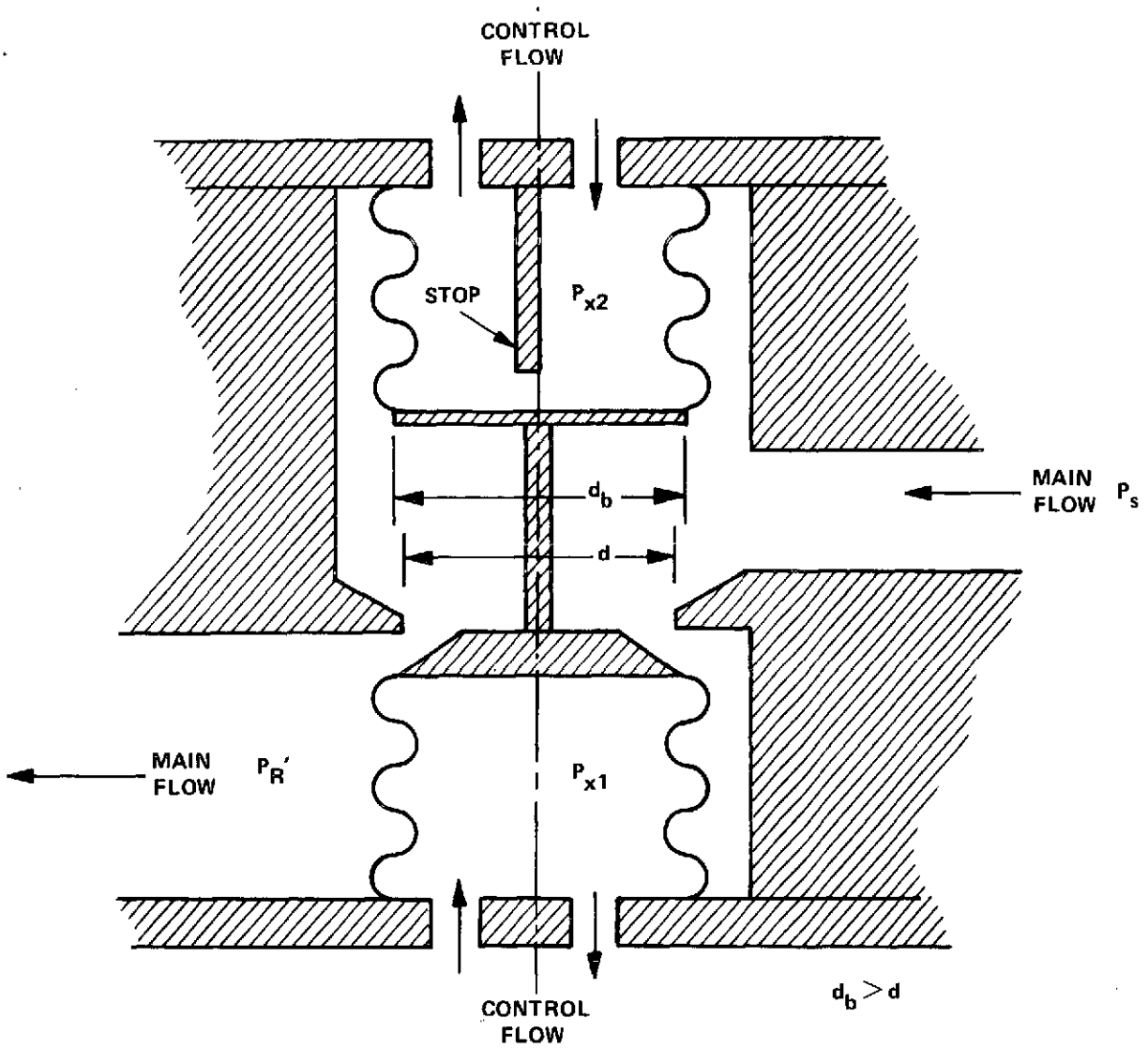

Figure 36 - Double-Bellows Arrangement for Metering Main Flow

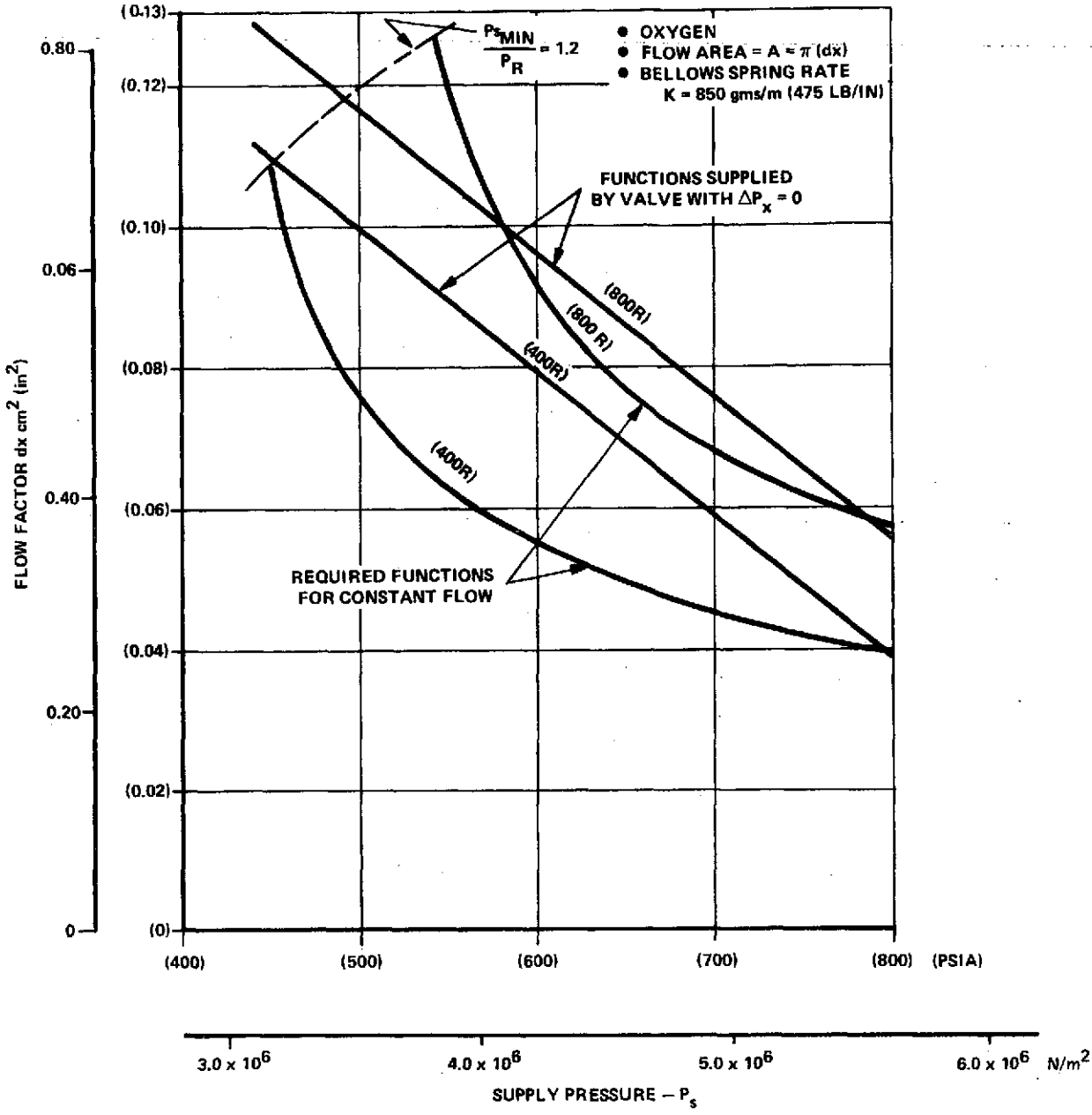

Figure 37 - Flow Factor as a Function of Supply Pressure

Other possibilities that could be considered to help improve accuracy of the system are various combinations of how the amplifiers are connected into the system. Some possible combinations of circuits are shown in Table V.

TABLE V - SOME POSSIBLE CIRCUIT COMBINATIONS

Case	Regulator to Main Valve	Regulator to Amplifier	A_1 to P_R	A_1 to P'_R	A_2 to P_R	A_2 to P'_R	A_3 to P_R	A_3 to P'_R
1			X		X		X	
2		X	X		X		X	
3			X			X		X
4		X	X			X		X
5			X		X			X
6		X	X		X			X
7				X		X		X
8		X		X		X		X
9	X		X			X		X

Also shown in this table are circuit combinations using coarse pressure regulators. One would regulate supply pressure to the amplifiers only and would require little power (Cases 2, 4, 6, and 8). The other would regulate pressure to the main metering valve (Case 9). These two possible coarse regulator combinations are depicted in Figures 38 and 39.

The tradeoffs between these various circuit combinations all deal with optimizing accuracy. Slight accuracy is sacrificed by bypassing any flow downstream of the regulated pressure, P'_R. However, some bypass flow must be sacrificed to keep the gain in the amplifier cascade within controlled bounds which also is a measure of accuracy.

The section on concept status (page 49) summarizes all of these circuit possibilities and the test results of this phase.

Effects of Specifications. The specified values over which constant flow control is desired are shown in Figure 40. Also shown are curves of the required regulated pressure, P_R, at the inlet of the thrust chamber to maintain flow rate at 1.25 kg/sec (2.76 lb/sec) and curves of the required minimum supply pressure for the hybrid fluidic concept C.

Some possible alternatives can be considered that would make the concept more feasible. If the specifications for temperature range were narrowed to the

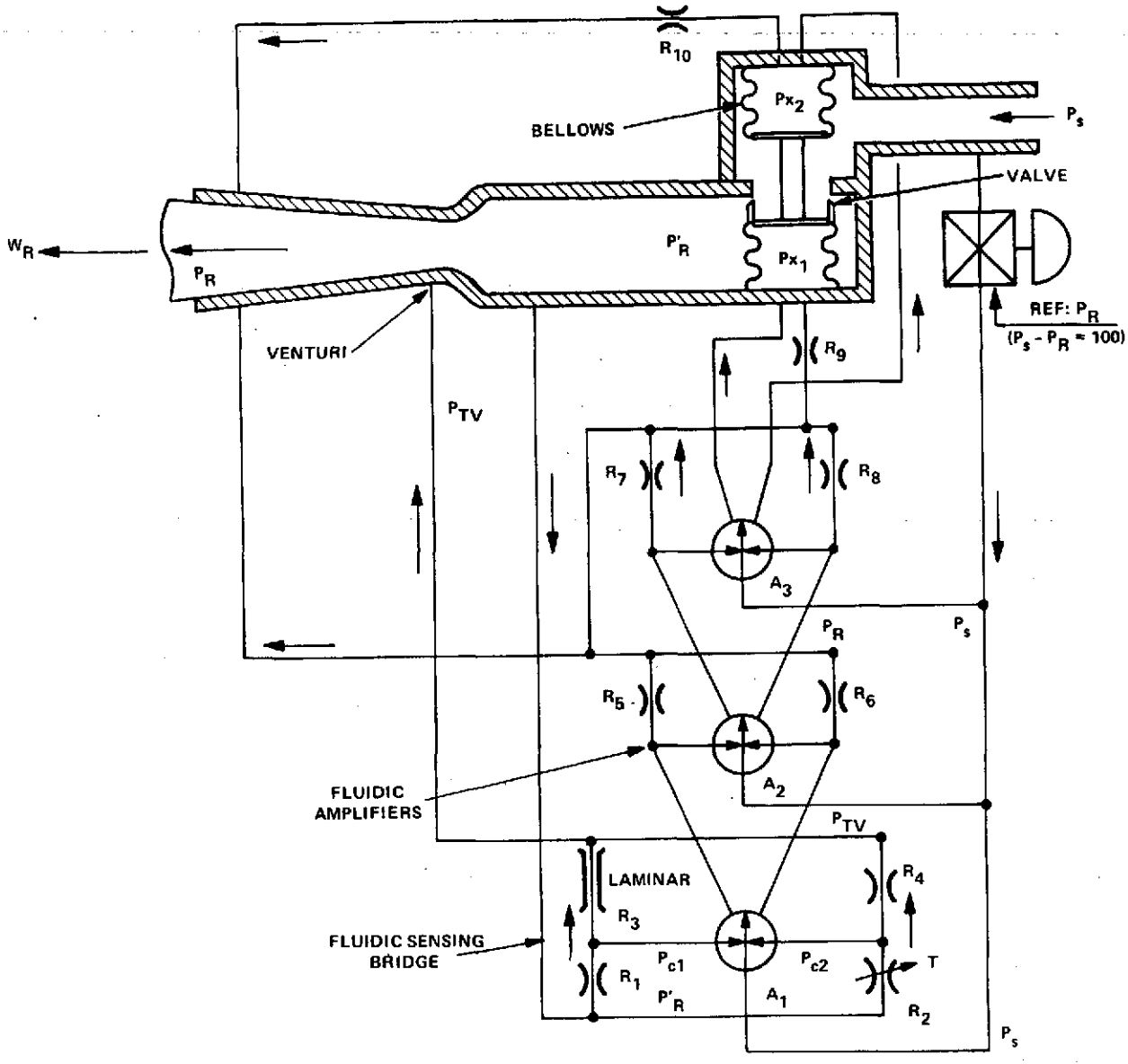

Figure 38 - Schematic Diagram of Hybrid Fluidic Flow Controller - Regulated Supply Pressure to Amplifiers

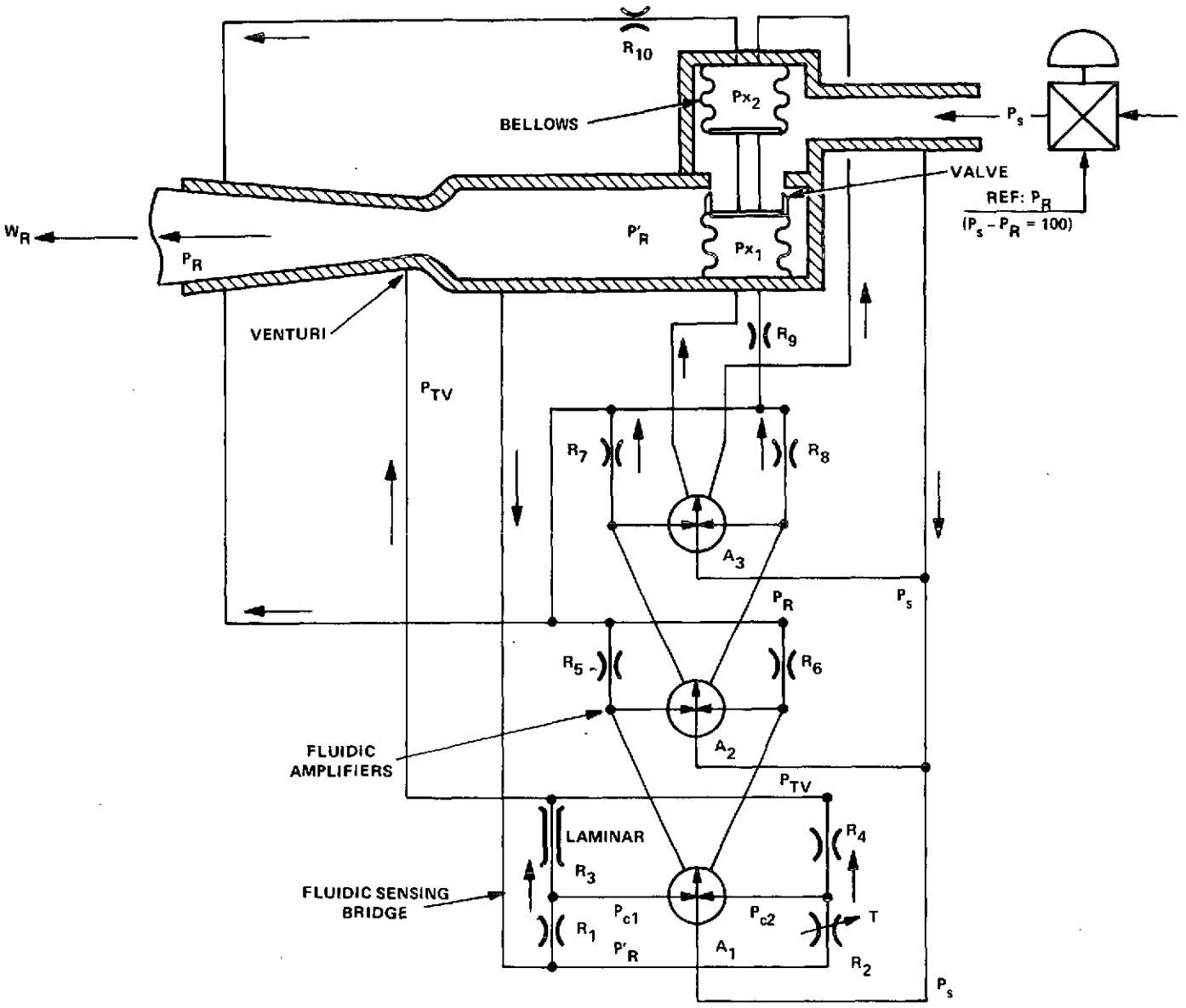

Figure 39 - Schematic Diagram of Hybrid Fluidic Flow Controller - Regulated Supply Pressure to Main Metering Valve

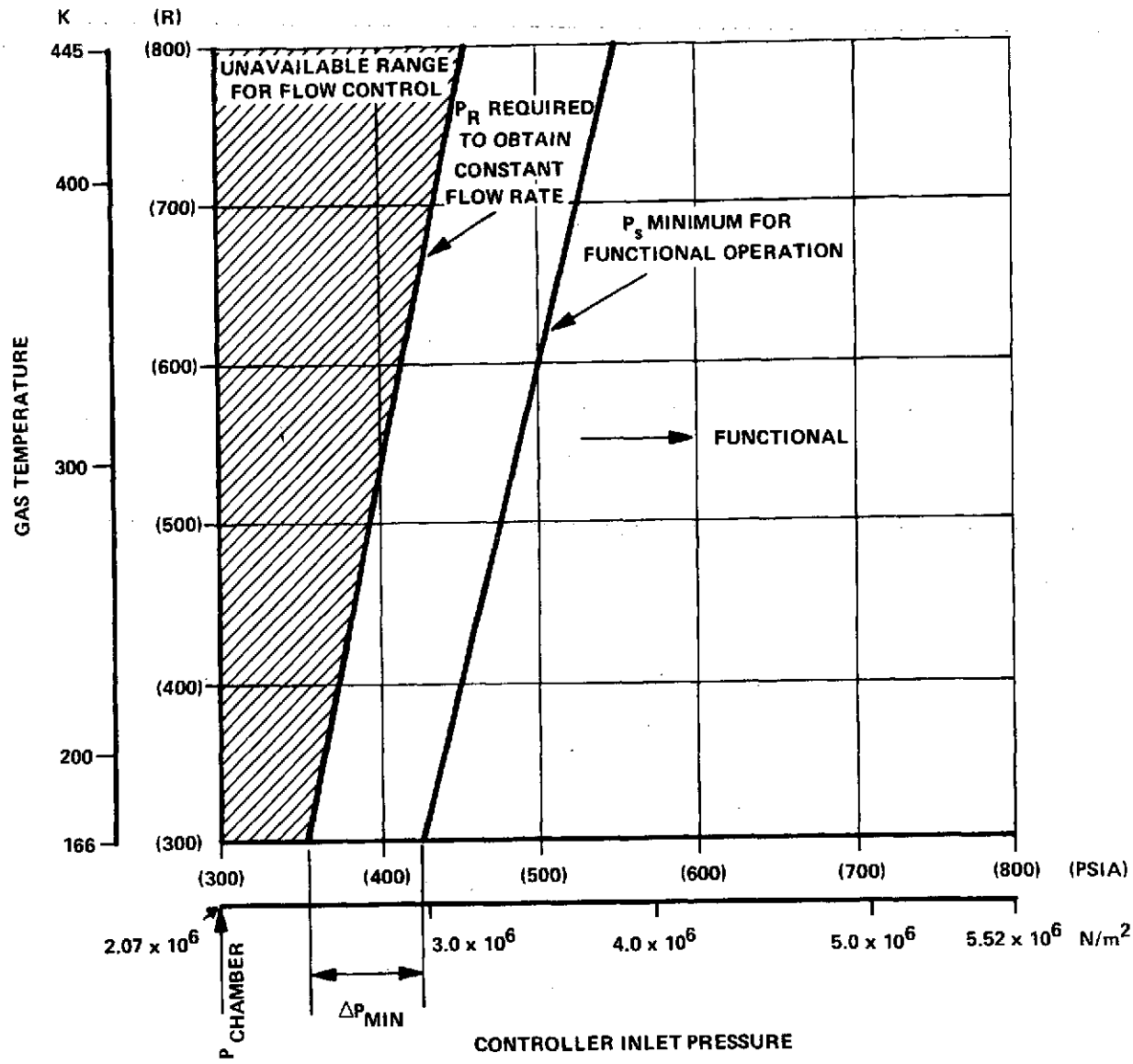

Figure 40 - Specification Map for Oxygen

more probable values to be encountered in operation, the specification map might look like that shown in Figure 41. The temperature is seen to range from about 228 K (410 R) to 367 K (660 R). With the temperature range narrowed, the variable effects of temperature would be greatly reduced. The addition of a follower regulator as was suggested by Figures 39 or 40 could also enhance operation and accuracy. The follower regulation is depicted in Figure 42 by the line "P_S-P_R regulated."

Another possibility with this reduced temperature range would be to employ a sonic venturi in the circuit. This would help improve operation and accuracy by negating the possible effects of downstream oscillations on the controller. The required values of inlet pressure to make it possible to use a sonic venturi are shown in Figure 43.

An absolute regulator might also be used to coarsely control the supply pressure above minimum conditions required for a sonic venturi. This is shown by the "P_S regulated" line in Figure 43.

Although the above variations in specifications show that the concept accuracy could be generally improved, it is difficult to estimate which set of conditions would provide for the most accurate control system. The best way to obtain an estimate would be to build and test the circuit under the varied conditions to find the optimum way or ways of obtaining accurate flow control.

Although the foregoing has dealt with the oxygen controller only, most of the parts would be identical for the hydrogen side. Also, the trends in performance discussed for the oxygen side would apply to the hydrogen controller.

CONCEPT STATUS

Based on the foregoing detailed discussion of the critical elements for the hybrid fluidic concept, consideration of the possible modifications in the configuration and consideration of the effects of the specifications, the status of the concept can be summarized briefly as follows:

- The concept employs separate control on GH_2 and GO_2.
- There is only one moving part (non-frictional) in each controller.
- The concept represents an advancement in the state of the art.
- Accuracy theoretically obtainable is excellent.
- Pressure anomalies are known to exist in the amplifiers although the unwanted effects on the controlling of accuracy can be minimized by proper circuit hook-up or by having coarse pressure regulation to the amplifiers (low power) or by having coarse pressure regulation to the main flow.
- Temperature anomalies are known to exist in the amplifiers but are not well understood.

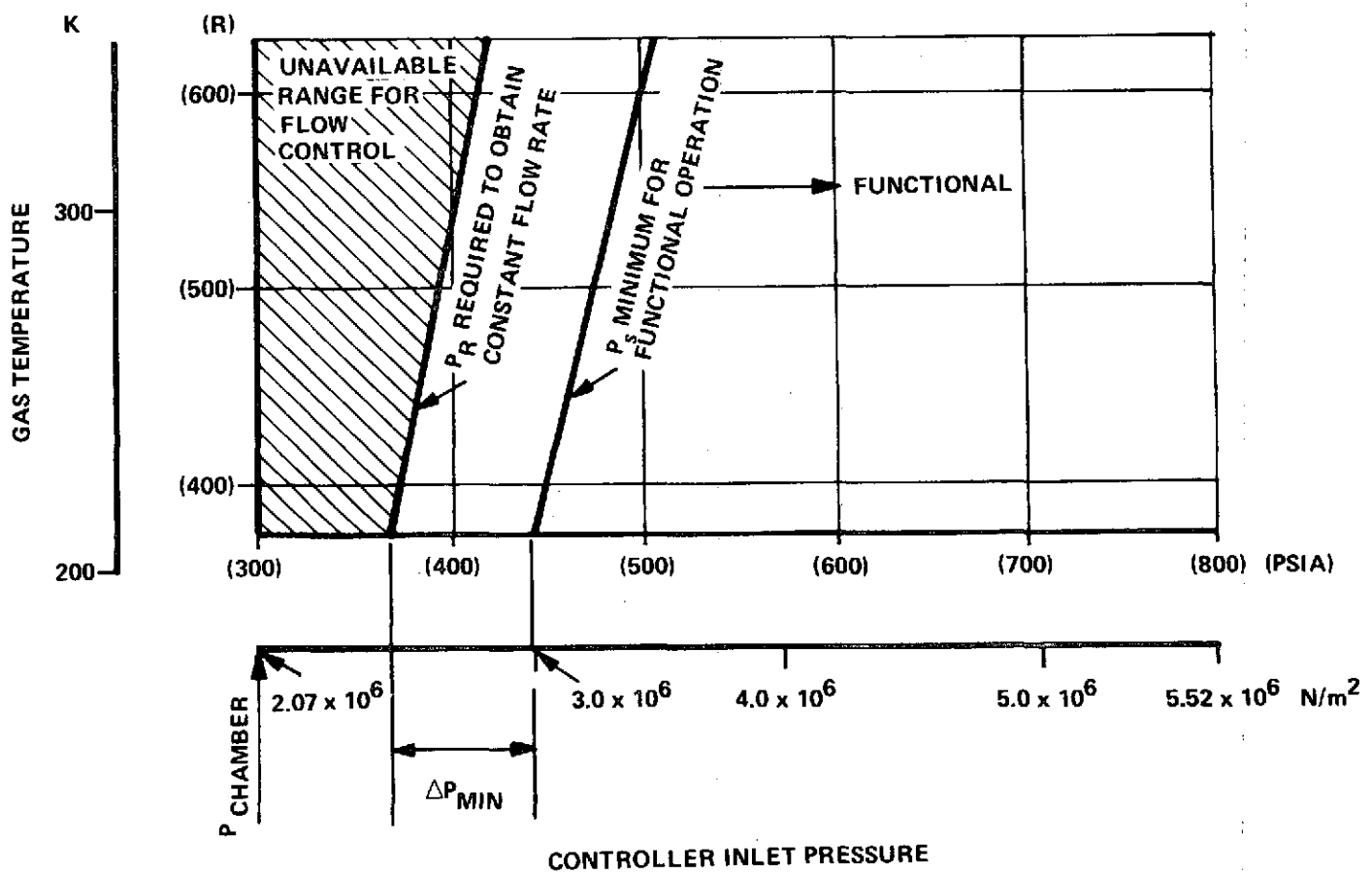

Figure 41 - Alternate Specification Map for Oxygen

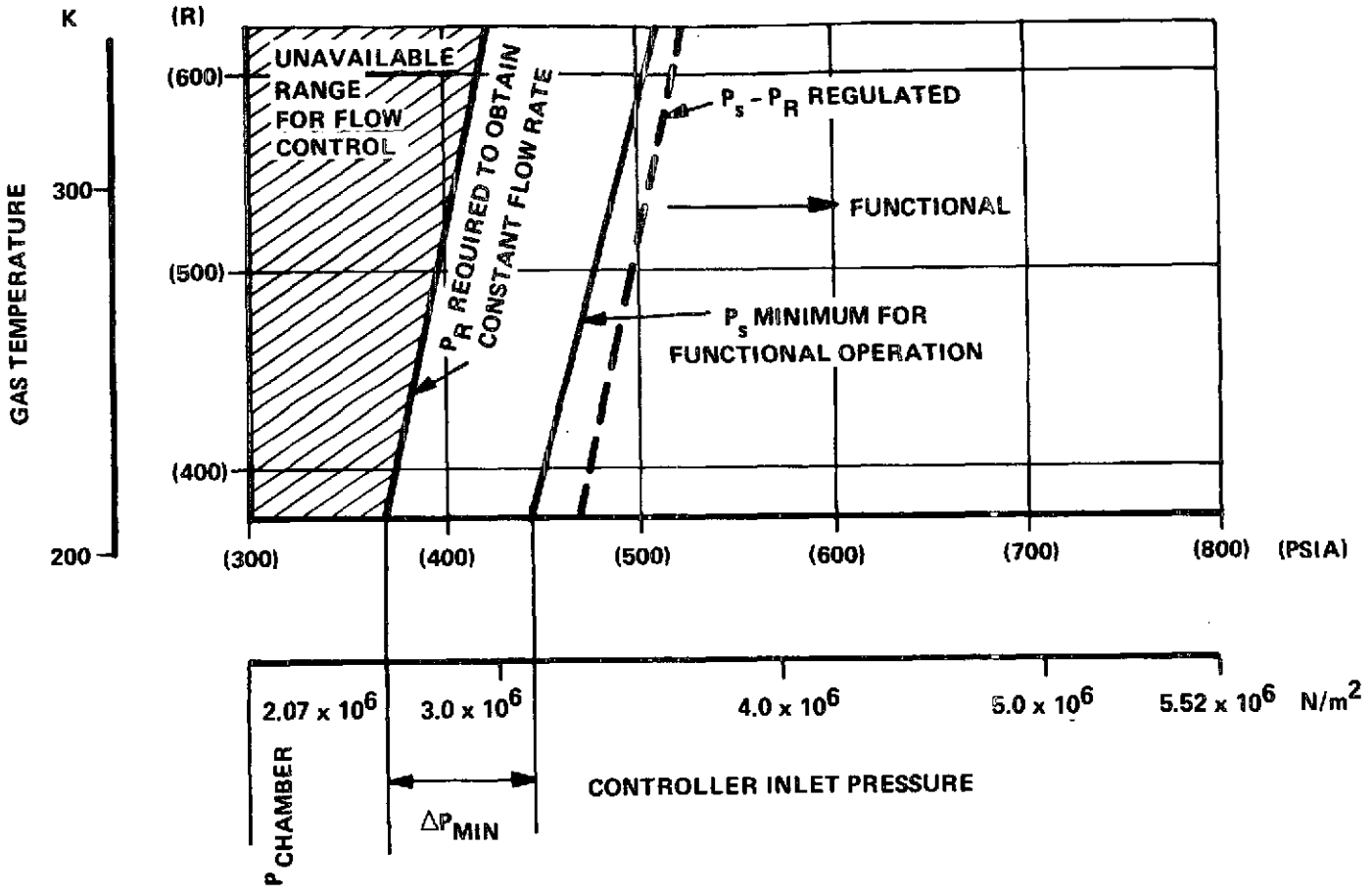

Figure 42 - Alternate Specification Map for Oxygen Showing $P_S - P_R$ Regulated

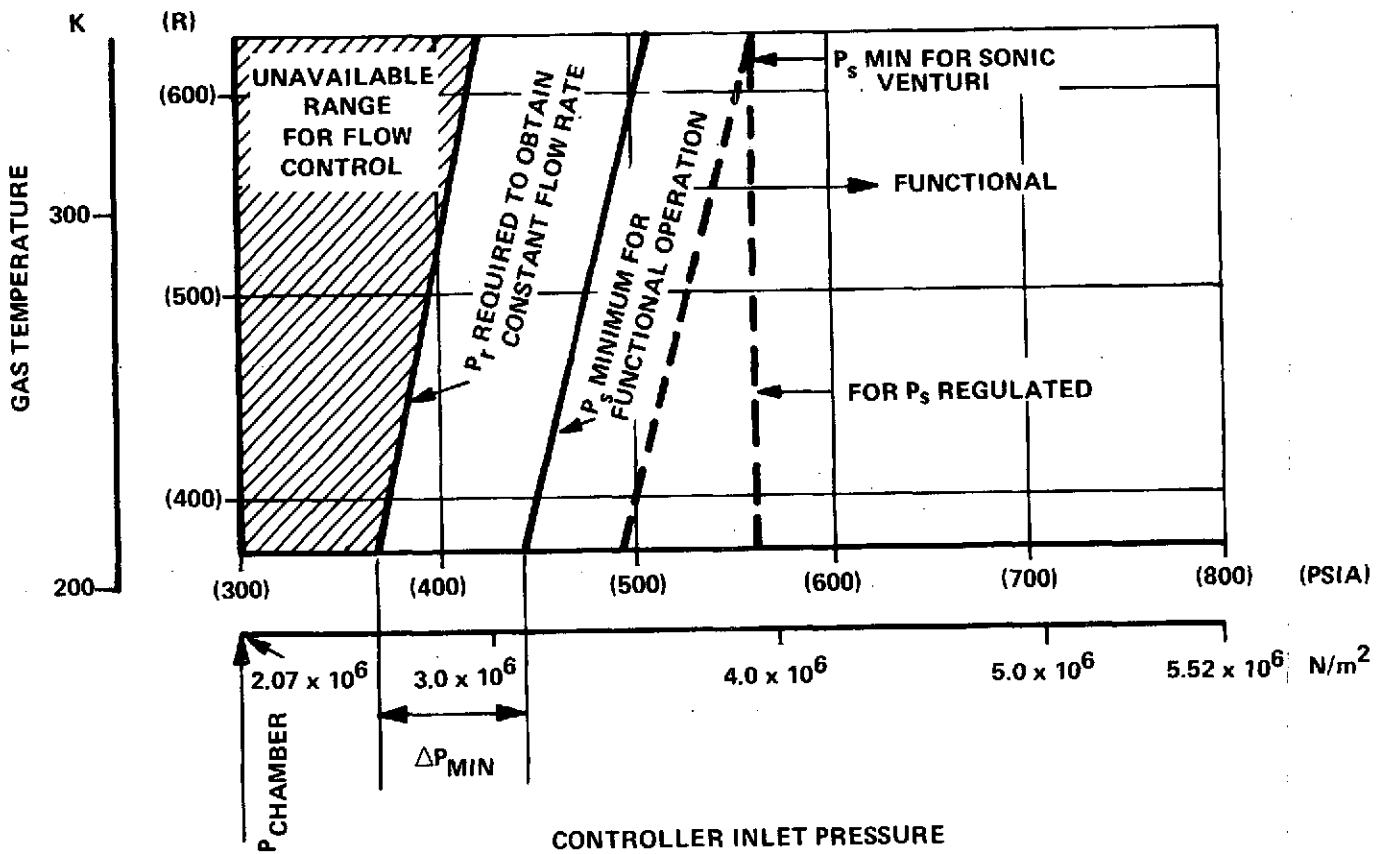

Figure 43 - Alternate Specification Map for Oxygen Showing Minimum P_s and Absolute Regulation for a Sonic Venturi

- Pressure and temperature response are theoretically adequate but not yet demonstrated.

- Changes in specifications as discussed previously would improve the potential of this concept.

- Possible oscillations at the high input pressures may have to be damped out at the expense of accuracy or response to maintain stability.

- The laminar restrictor has been designed but not yet built. The nature of the metal etching and diffusion bonding process used for fabrication of an annular restrictor design for this concept suggests that stainless steel should be selected as the material of construction. This selection would minimize possible fabrication problems.

- The work to date shows that more development is necessary for the first controller.

- The concept would be a reliable design once developed.

- The functionality has yet to be demonstrated for a complete controller under the required pressure and temperature conditions.

RECOMMENDATIONS

Although the decision has been made to proceed with development of the Rocketdyne mechanical flow controller, it would do well to consider several recommendations with regard to the effort to employ fluidic principles in a flow control concept. The first two recommendations are the most important steps that could be further pursued for this controller concept. These first two recommendations are opposite in direction in that the first would attempt to obtain more uniform operation within the basic amplifier before building a complete controller while the second recommendation would attempt to consider the potential operation of the system using the amplifiers as they are. Following the first recommendation would be the better approach in attempting to arrive at a highly accurate flow controller. However, it would require more development time and cost than would following the second recommendation directly. Pursuit of the second recommendation would arrive at a controller in less time and cost but controller accuracy would probably be less than the first approach.

The majority of the following, then, are recommendations to improve the potential of this concept as an accurate flow controller:

- Investigate elimination of anomalies in the amplifiers, at these pressures and temperatures, by studying influence on performance of basic amplifier profile in the interaction region.

- Breadboard one complete controller and test out factors influencing accuracy and stability. Check under different circuit hook-ups for the amplifiers and consider if coarse P_s regulation could help. Coarse regulation could be tried for pilot flow to the amplifiers and/or to the main metering valve.

- If the P_s value would be high enough, consider the use of a sonic venturi in breadboard testing to make the concept insensitive to downstream oscillations.

- Consider in detail the tradeoffs between a laminar restrictor and series orifices in the sensing bridge to establish the optimal means of sensing pressure error.

- Investigate a more narrow band of operation with temperature and/or pressure.

- Consider the hybrid fluidic concept C for use in other system applications.

- Consider the other fluidic concepts presented in this effort for use in other system applications.

APPENDIX A

SYMBOLS AND NOMENCLATURE

A	Fluidic amplifier. Differentiated by subscripts
A_L	Cross-sectional area of load orifice
A_S	Cross-sectional area of supply nozzle
Bias	$\frac{\overline{P}_c - P_{TV}}{P_s - P_{TV}}$
d	Valve diameter
d_b	Bellows' effective diameter
FCPU	Flight Control Power Unit
K	Gain
$\dot{M}$	Mass flow rate
ΔP_a	Differential control pressure to proportional amplifier in concept B
P_c	Pressure associated with secondary and lesser flow path in a device
$\Delta P_c = P_{c1} - P_{c2}$	Differential control pressure
P_{c1}	Proportional amplifier control pressure
P_{c2}	Proportional amplifier control pressure
P_{CL1}	Left control pressure in a proportional amplifier
P_{CL2}	Left control pressure in a proportional amplifier
P_{CR1}	Right control pressure in a proportional amplifier
P_{CR2}	Right control pressure in a proportional amplifier
P_f	Reference pressure
P_{in}	Gas pressure upstream of the flow controller
P_o	Pressure in the vortex chamber
$\Delta P_0 = P_{01} - P_{02}$	Differential output pressure
P_{OL}	Left output pressure in a proportional amplifier

P_{OR}	Right output pressure in a proportional amplifier
P_R	Regulated pressure required at inlet to thrust chamber
P'_R	Pressure upstream of venturi section in concept C
$P_R(T)$	Regulated pressure as a function of temperature
P_S	Pressure associated with the primary flow path through the controller and generally is also the input pressure (P_{IN})
P'_s	Supply pressure to vortex amplifier in concept A
$P(T)$	Pressure as a function of temperature
P_{TV}	Pressure at the throat of the venturi
P_x	Diaphragm pressure
P_{x1}	Pressure acting on one side of double bellows
P_{x2}	Pressure acting on one side of double bellows
PCA	Propellant conditioning assembly
Q_R	Volume flow rate
R	Fluidic resistor (orifice, restrictor). Differentiated by subscripts
T	Temperature
T_r	Temperature of the regulated gas
V	Vent. Differentiated by subscripts
V_L	Volume associated with the laminar restrictor
V_R	Volume in the lines between the controller and the thrust chamber
V_T	Volume associated with the turbulent orifices in the sensing bridge of concept C
W	Controller output flow for experimental test
W_c	Control flow
W_R	Controller output flow
$\dot{W}_R$	Controller output flow
W_S	Radial flow in a vortex amplifier
$\dot{W}_v$	Controller valve flow rate

APPENDIX B

FLUERIC* APPROACHES

The initial effort of the program was to derive and evaluate feasible concepts for the flow controller. Evaluation of various approaches led to the conclusion that a flueric flow control system was not feasible for this application. As a result several hybrid fluidic approaches were evolved and subsequently evaluated. However, it is worth reviewing the various flueric approaches that were eliminated earlier in the program. Although these approaches are not suitable for this particular application, they are described briefly here for potential consideration in a subsequent system application.

The all-flueric concepts are:

- Diverter System
- Single-Source Vortex
  - Control by a Single Orifice
  - Control by an Amplifier System
- Dual-Source Vortex

DIVERTER SYSTEM

This system has the primary fluidic component sized to provide the required output flow at the lowest supply pressure and highest temperature; it dumps excess flow at the higher supply pressures and lower gas temperatures. The schematic for this system is shown in Figure 44.

This approach was eliminated because of the weight penalty that would be necessary for the extra fuel that would be dumped to vent.

SINGLE-SOURCE VORTEX VALVE

This approach would use a single-pressure-source vortex valve. A single pressure source and orifices would be used to obtain the required control-to-supply pressure difference in order for the vortex valve to throttle the flow. Two types of implementation for this approach are shown in Figures 45 and 46.

Single-Source Vortex Control by a Single Orifice

The method is shown in Figure 45. The inlet pressure (P_{in}) also acts as the control pressure (P_C). The vortex supply pressure (P_S), which must be lower than the control pressure in order to have throttling capabilities, is obtained by a series orifice in the input line.

---

*No moving parts.

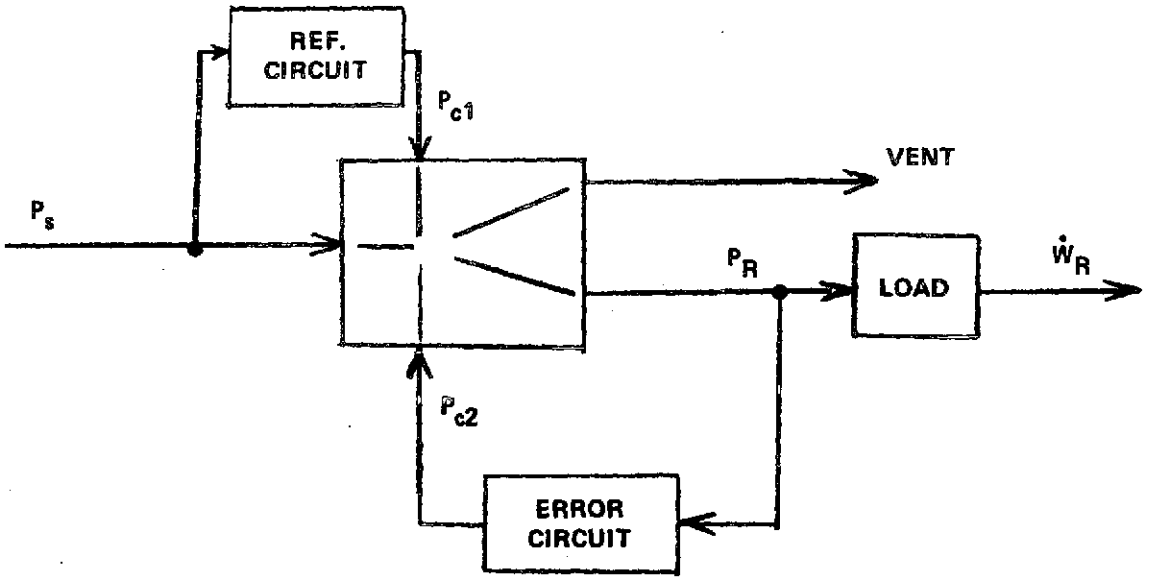

Figure 44 - Schematic Diagram of Diverter System

The net effect of such a circuit can be shown to have only about a 1.2 to 1 (W_{max}/W_{min}) throttling capability. This concept was eliminated, then, since it does not provide sufficient throttling capability for the desired flow controller.

Single-Source Vortex Control by an Amplifier System

This is another pure fluidic approach to obtain flow regulating capabilities This circuit schematic is shown in Figure 46 and the detailed circuit is shown in Figure 47. The circuit consists of four main parts. They are:

(a) Vortex valve for throttling

(b) A gain block to drive the vortex valve

(c) A pressure error and temperature compensating circuit

(d) A choked venturi combination to establish a lower pressure reference.

Although the circuit offers the advantage of no moving parts, this concept was eliminated for several reasons:

(a) It has not been demonstrated whether a flow throttling capability of better than 2-to-1 can be accomplished. This is based on limited testing of a vortex valve driven by a proportional amplifier.

(b) The number of fluidic elements required to implement each part of the circuit is large enough to raise serious questions about system accuracy and stability, caused by complex interactions of fluidic parts, and about potential fluid noise.

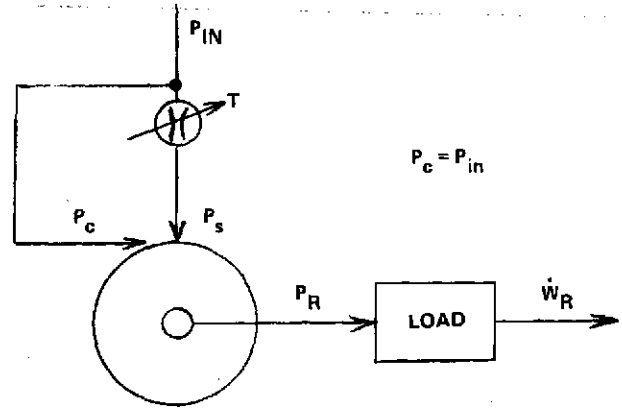

Figure 45 - Control of Single-Source Vortex Valve by a Single Orifice

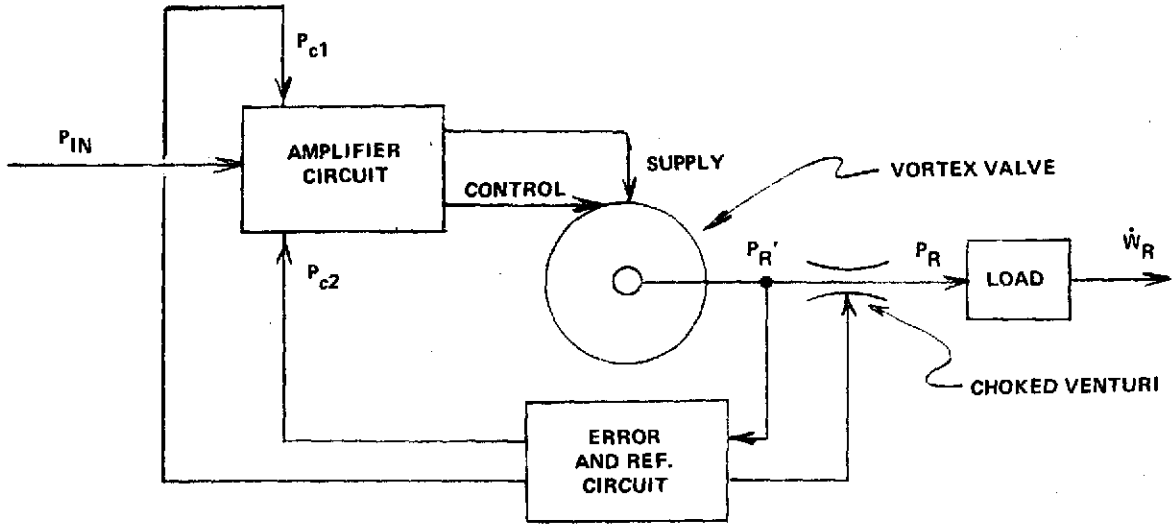

Figure 46 - Control of a Single-Source Vortex Valve by an Amplifier Circuit

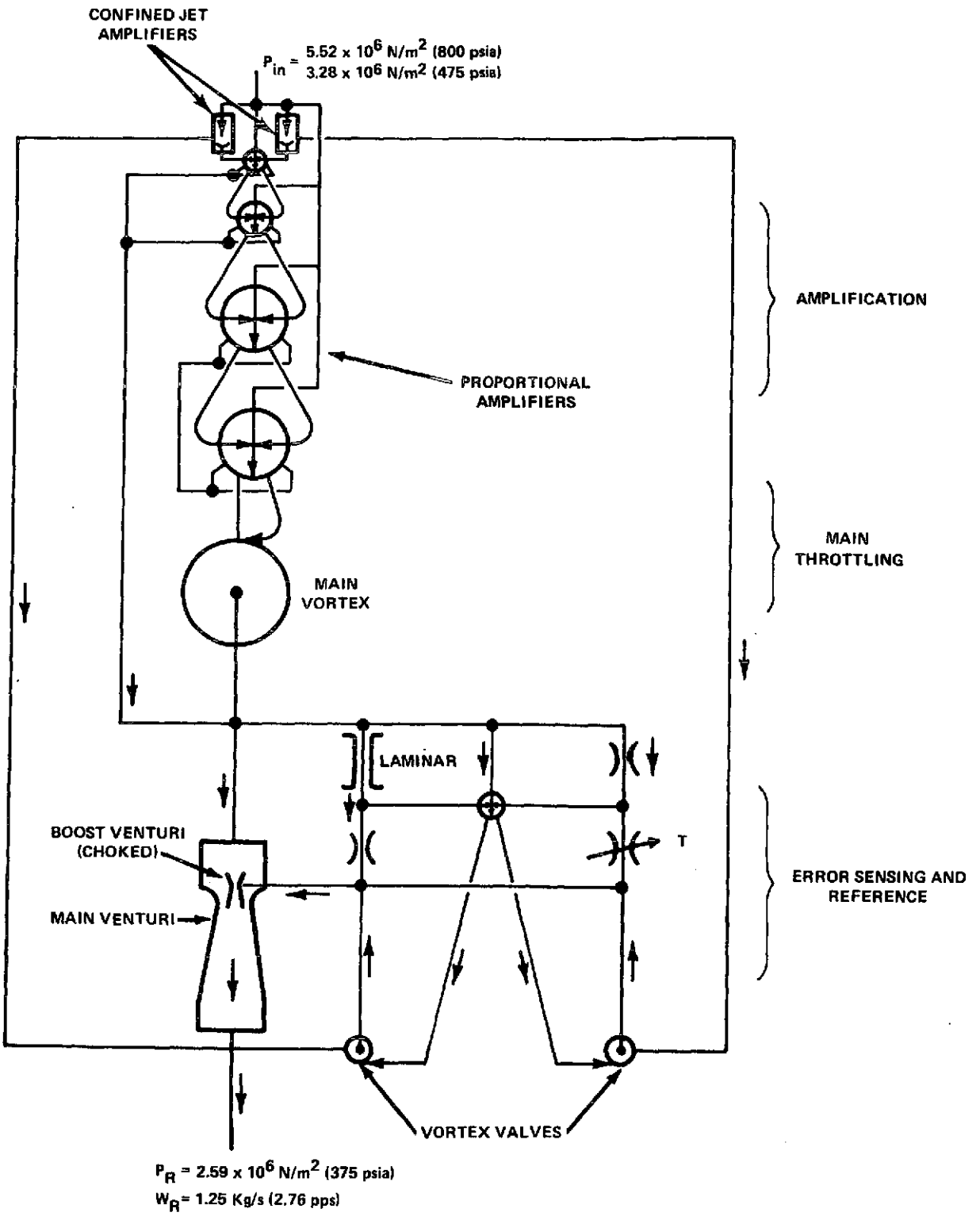

Figure 47 - Fluidic O_2 Regulating System

(c) The required operating characteristics of a number of the fluidic elements have not been demonstrated.

(d) Because of the number of elements that would be required, past experience has shown that much increased development time and cost would be necessary for the test evaluation portion of this concept.

For the above reasons, the potential development success and accuracy of the proposed approach was rated poor and therefore eliminated from further consideration.

DUAL-SOURCE VORTEX VALVE

The dual-source vortex valve requires a separate control and supply pressure source. One possible configuration is shown in Figure 48. The pressure difference between supply and control pressure for the regulating vortex valve is developed by a common, coarse, fluidic regulator located at the propellant accumulators. However, it is not clear of what elements the coarse fluidic regulator would consist. Three other important aspects are that system response would be coupled to that of the coarse regulator, double lines to the final regulator would be needed, and additional valving would probably be necessary for start-up and shut-down operation. For these reasons, this approach was eliminated.

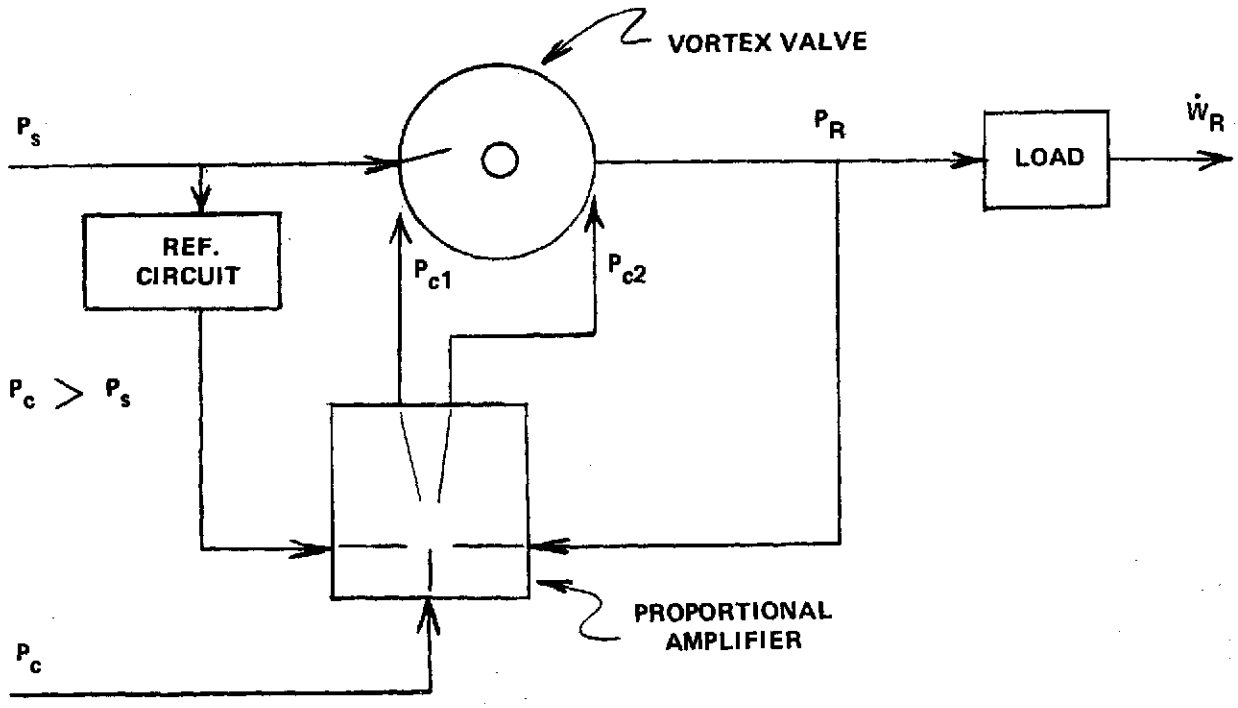

Figure 48 - Dual-Source Vortex

APPENDIX C

OTHER HYBRID FLUIDIC APPROACHES

During the concept derivation and evaluation period, several hybrid fluidic concepts evolved which had more potential than any of the flueric approaches. One concept was known at the beginning of the effort from similar work conducted for the U.S. Navy. A second concept evolved from the first during the initial effort of this program. Two more concepts were derived during the concept evaluation phase. One concept was subsequently rated the most potential fluidic concept and was therefore discussed in the main body of this report. The other hybrid fluidic concepts are briefly reviewed in this appendix.

A brief summary of the control elements for each of these three concepts is listed in Table VI. It can be seen that the primary flow modulation is by a mechanical metering element while the error sensing and control are handled by the fluidic elements.

TABLE VI - SUMMARY OF CONTROL ELEMENTS FOR HYBRID CONCEPTS

Hybrid Concept	Primary Flow Area Modulation	Pressure Error Sensing	Amplification	P(T) Reference
A	Mechanical Metering Element	Confined-Jet Amplifier	Vortex Amplifier	Temperature-Sensitive Orifices With By-Pass Flow
B	Mechanical Metering Element	Orifice-Amplifier Bridge	Vortex Amplifier	Temperature-Sensitive Orifices With By-Pass Flow
D	Mechanical Metering Element	Vortex Amplifier	Vortex Amplifier	Temperature-Sensitive Orifices With Feedback Flow

Although these concepts were eventually eliminated from further development, some other system application or a revision in the specifications for this application could warrant a renewed evaluation of these hybrid concepts.

HYBRID FLUIDIC CONTROLLER - A

The functional block diagram is shown in Figure 49 and the system schematic is shown in Figure 50. Mechanical moving parts perform the primary flow area

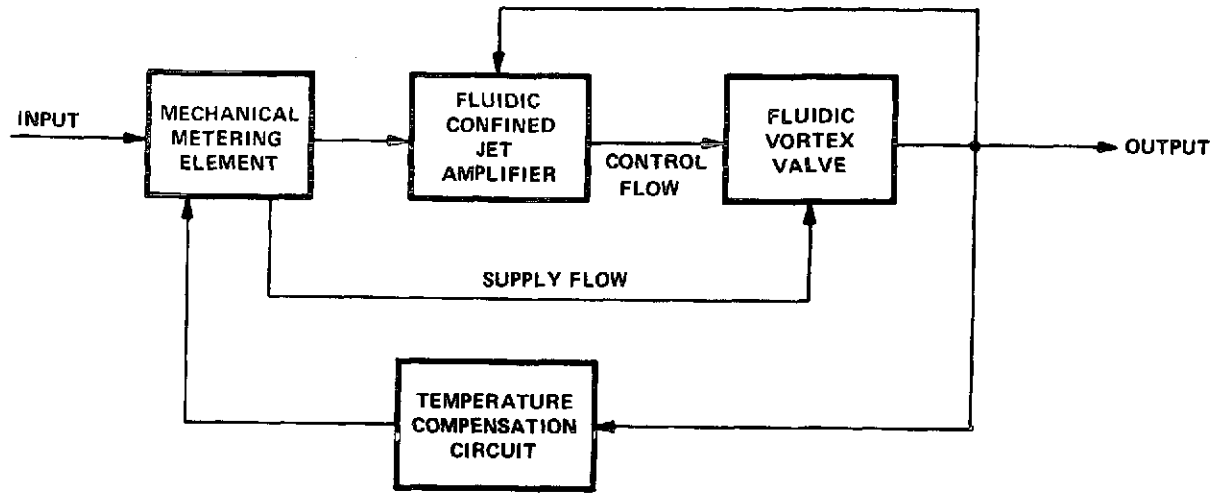

Figure 49 - Functional Block Diagram of Hybrid Fluidic Concept A

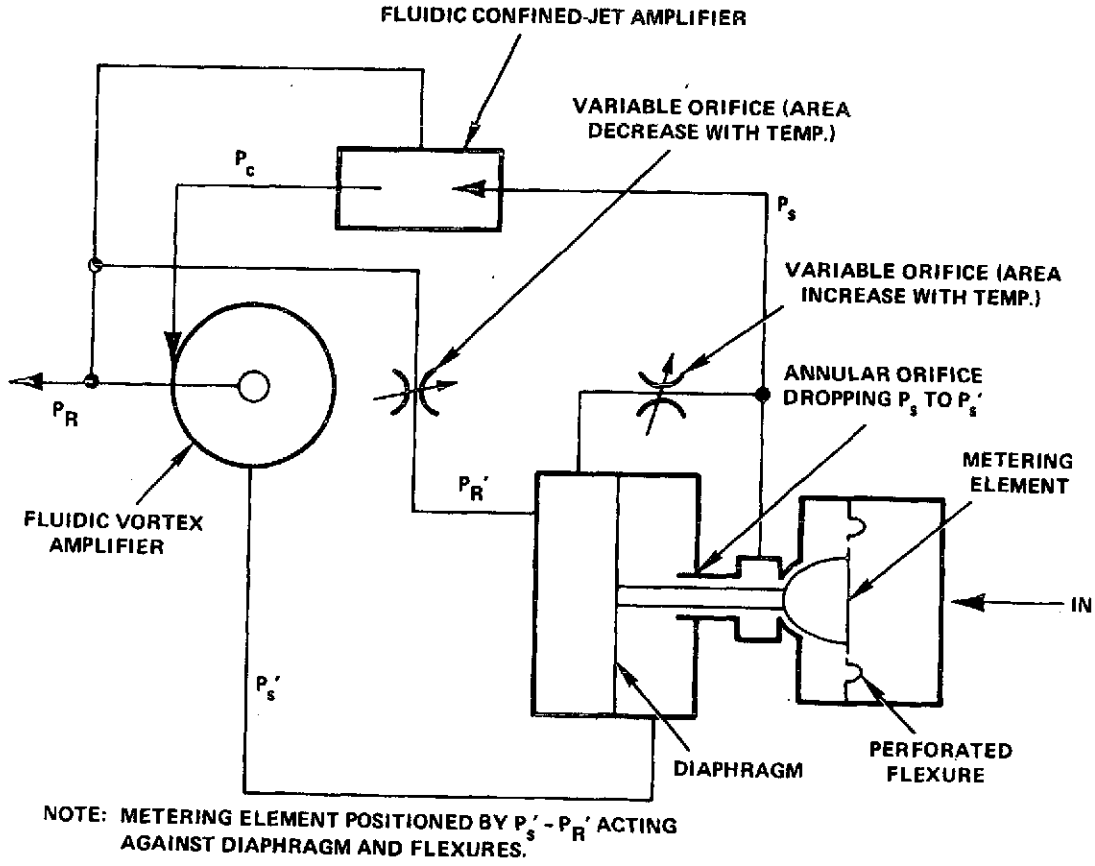

Figure 50 - Schematic Diagram of Hybrid Fluidic Concept A

modulation with fluidic elements providing position reference to the primary metering area and final throttling of the flow.

The confined-jet amplifier was considered the critical component in the circuit for operation with low pressure drop. To examine this element, a variable model confined-jet amplifier was built and tested. Test results (shown in Figure 51) revealed that a minimum input pressure of about 5.34×10^6 N/m^2 (775 psia) would be necessary for possible operation with the confined-jet amplifier as a control element.

An option to the confined jet that had potential was a proportional amplifier used in line with error sensing orifices. A closed-vent proportional amplifier was built and tested for its potential in the circuit (see Figure 52). Results of the tests at low pressure ratios showed that gain was too low for feedback control, a high supply pressure would be required, and fluid noise was a problem. It might have been possible to improve the noise conditions in the design of the amplifier, but the other factors of low gain and high pressure drop led to the elimination of this concept.

HYBRID FLUIDIC CONTROLLER - B

This approach is similar to that discussed in the previous section except that implementation of the fluidic elements is quite different. The functional block diagram is shown in Figure 53 and the system schematic is shown in Figure 54. The proportional amplifier is used in line with laminar and turbulent error sensing orifices. The vortex valve in this case has two opposing control pressures and a third control is brought in to obtain some initial swirl for bias. The initial swirl places the steady-state operating point down on the throttling curve.

An important element in this design is the proportional amplifier. Tests were conducted to consider proportional amplifier operation in this type of circuit. Results (see Figure 52) showed that low gain, large pressure drop, and fluid noise made this concept less desirable than the type C controller. In addition, the multiple input type of vortex would require its own development since most prior work on vortex devices have been for a single signal input. Therefore, this concept was eliminated from further consideration.

HYBRID FLUIDIC CONTROLLER - D

The hybrid concept D was considered to have more potential than either concepts A or B and was therefore evaluated in greater detail. The functional block diagram for the type D controller is shown in Figure 55 and the schematic is shown in Figure 56. The major control elements are:

- poppet
- diaphragm
- spring
- vortex chamber

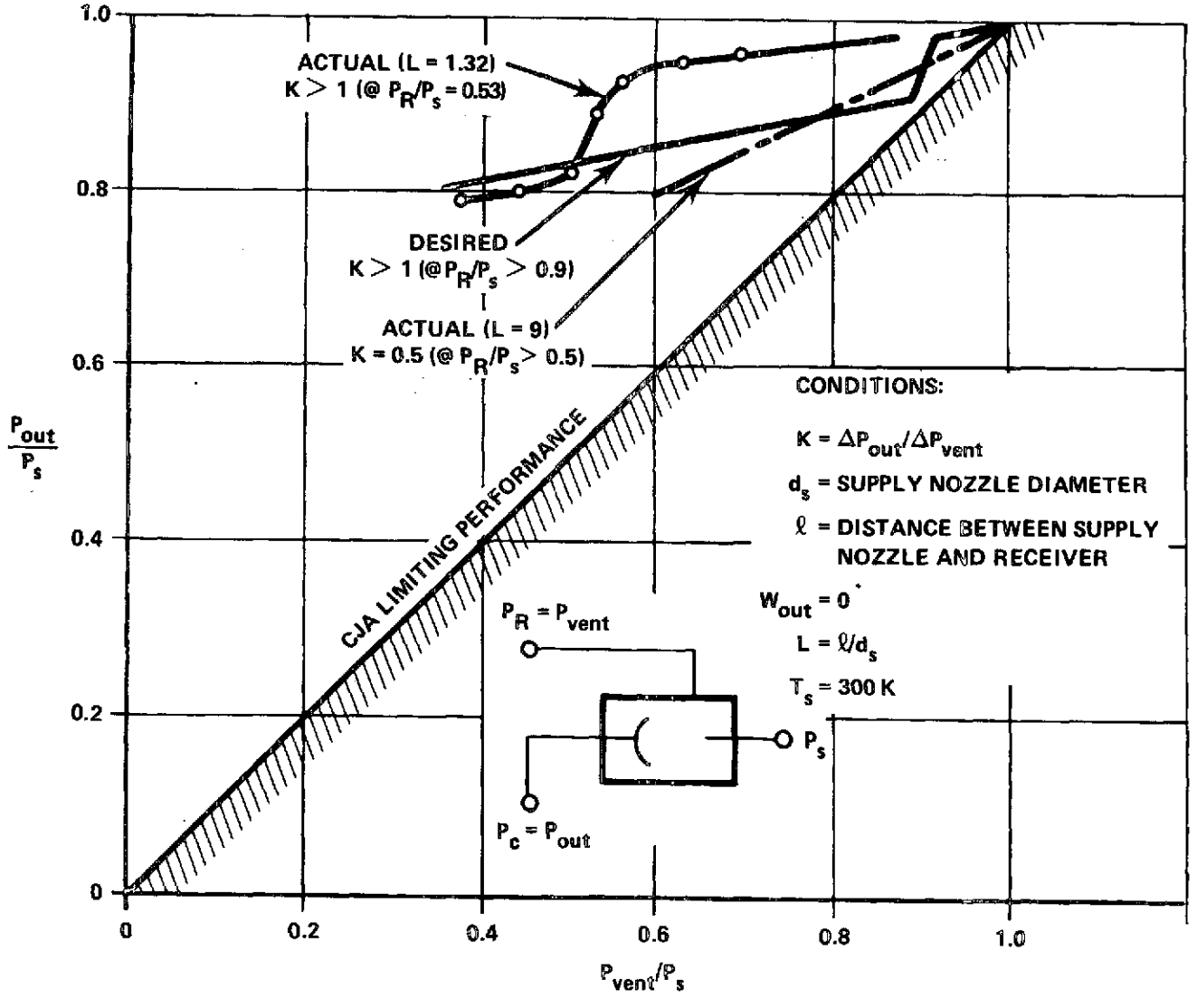

Figure 51 - Confined-Jet Amplifier Performance

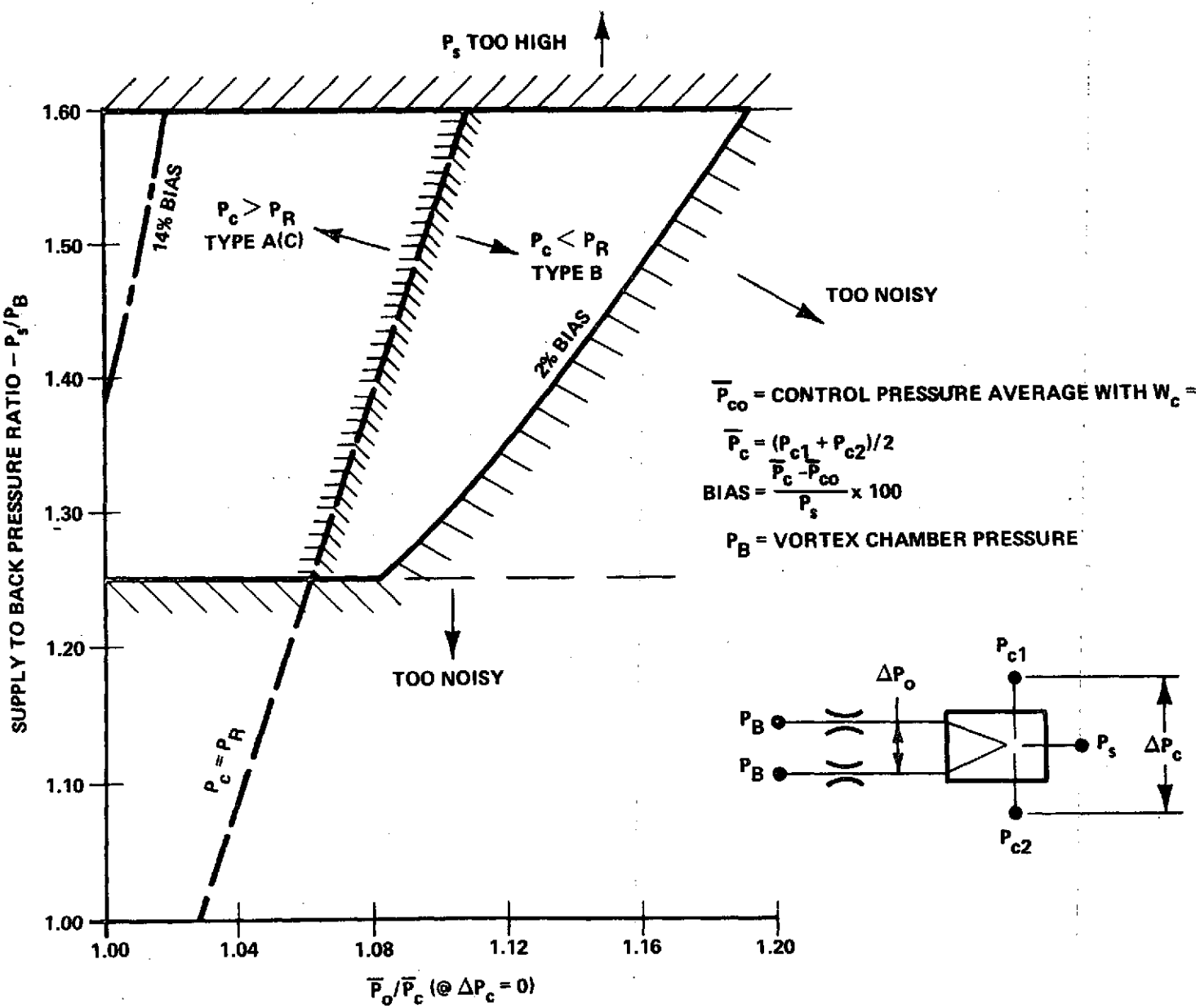

Figure 52 - 15PA36 Proportional-Amplifier Results

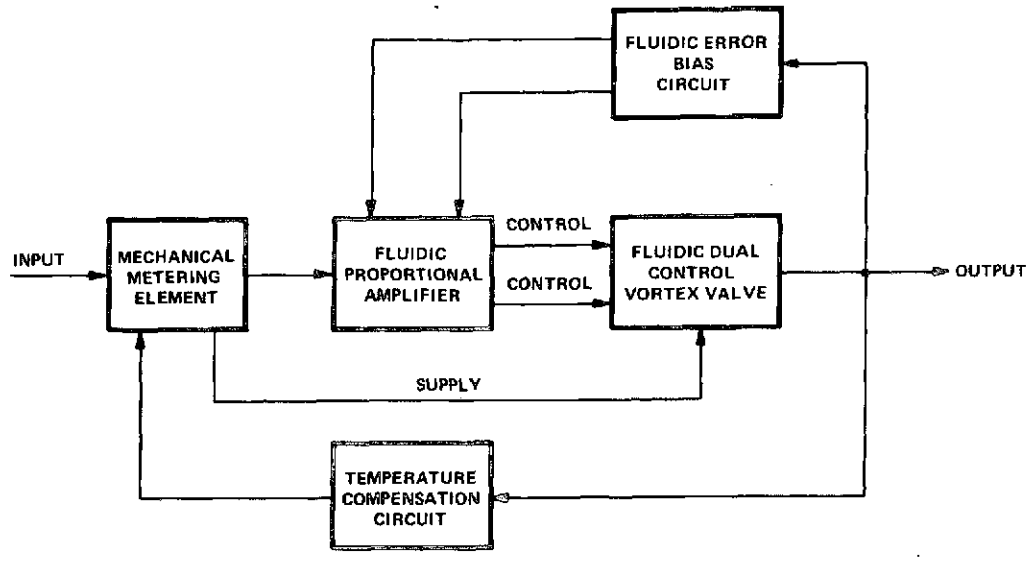

Figure 53 - Functional Block Diagram of Hybrid Fluidic Concept B

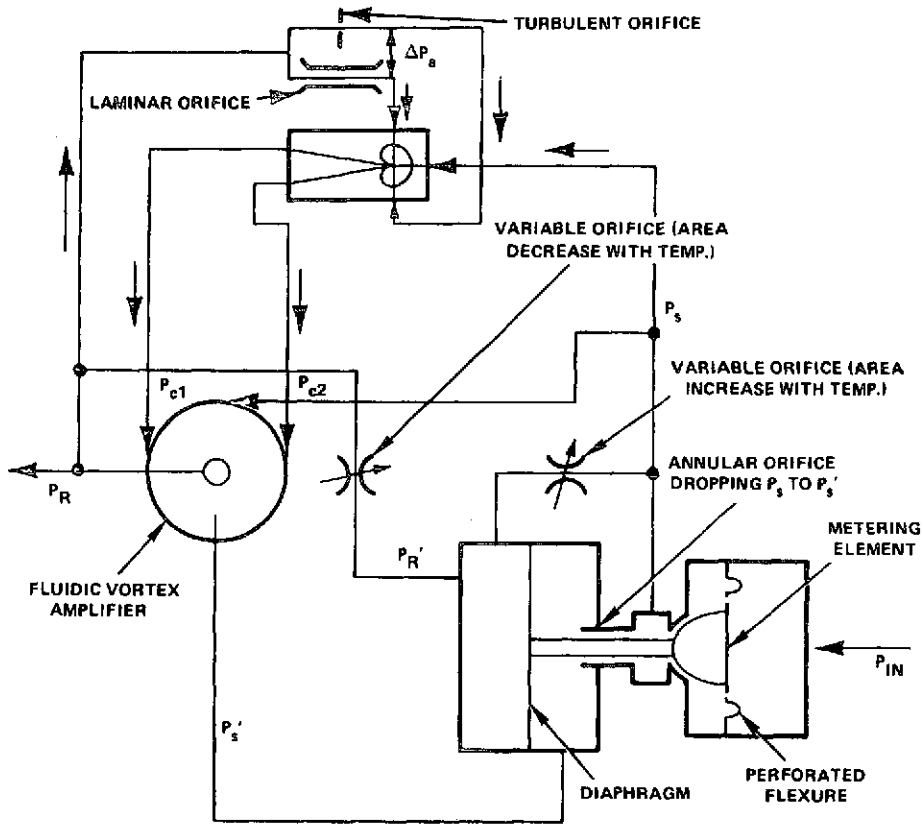

Figure 54 - Schematic Diagram of Hybrid Fluidic Concept B

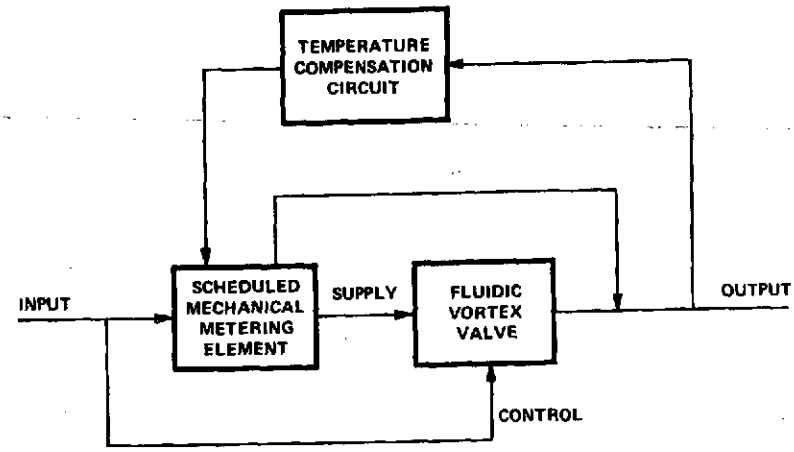

Figure 55 - Functional Block Diagram of Hybrid Fluidic Concept D

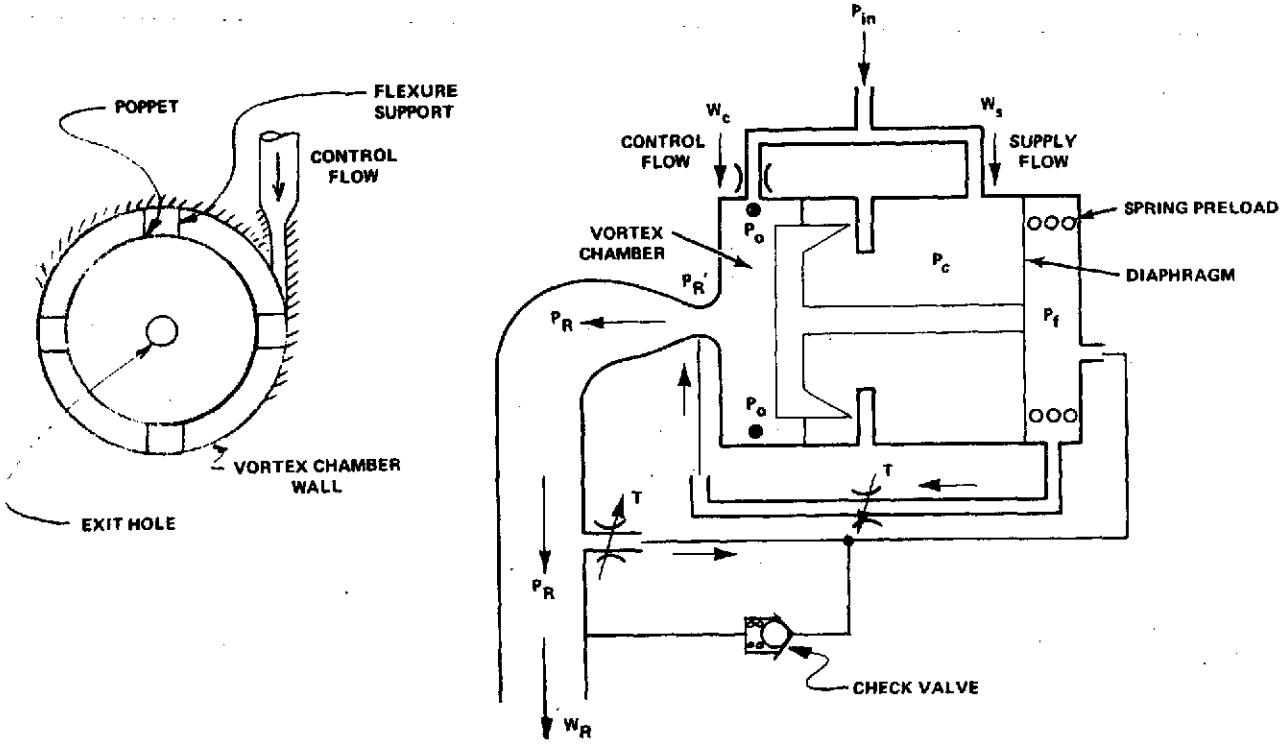

Figure 56 - Schematic Diagram of Hybrid Fluidic Concept D

- venturi
- temperature compensator (2)
- check valve
- manifolding

The inlet pressure is used both as a source of radial flow through the vortex and as control, or swirl, flow. Therefore, the inlet pressure is equal to the control pressure, $P_{in} = P_c$. The radial flow, W_s, into the vortex chamber is governed by the pressure drop, $P_c - P_o$, into the vortex chamber and the poppet area, πdx. The force balance on the poppet governs the gap x. The design is constructed so that P_c internally balances itself, thereby producing no unbalance force component on the poppet. This is accomplished by making the poppet surface area equal to the effective diaphragm area.

The requirement is to maintain the output flow, W_R, constant. Therefore,

$$W_c + W_s = W_R = \text{constant} \qquad \text{(C-1)}$$

This relationship between W_c and W_s can be held by having the proper gap, x, for every value of input pressure, P_c. Once the required gap is known for a particular vortex with various input pressures, that gap versus chamber pressure determines what the spring force must be to balance the poppet.

The requirements for a vortex valve to operate in this concept are typified in Figure 57. As shown, the desired characteristics are vertical turndown curves (P_c = CONST) over the pressure range. Vertical curves allow for reliable characteristics that the area scheduler can match. In addition the vertical characteristics can then be manipulated mathematically to scale up or down in flow or size to optimize performance.

In summary, the vortex chamber pressure is used directly to control the area, dropping P_c to P_o. P_o is the radial component of flow in the vortex chamber. The inlet pressure acts directly as a control source to obtain swirl and thereby provide the required flow throttling. For Figure 56, P_R is shown fed back as a reference to the back-side of the diaphragm. Temperature compensation would be achieved by the use of a venturi and a set of temperature compensating orifices. The reference line to the venturi throat would use a small percentage of total flow.

Breadboard Tests

To study the potential of this concept, the metering element and the vortex valve were built separately for testing. The test schematic is shown in Figure 58.

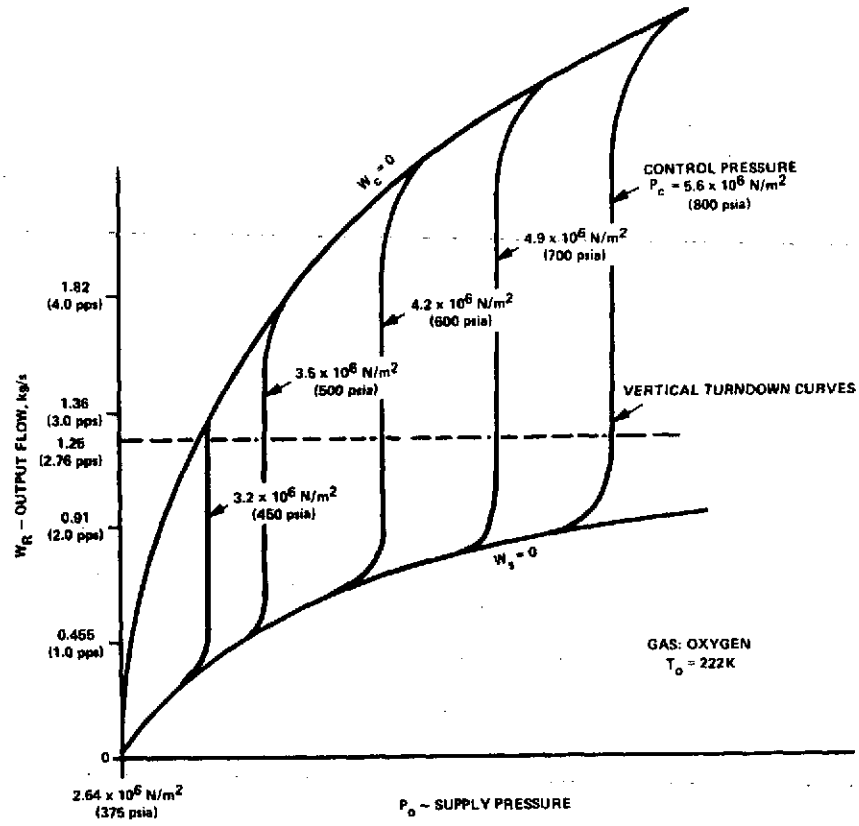

Figure 57 - Typical Vortex Characteristics of Hybrid Fluidic Concept D

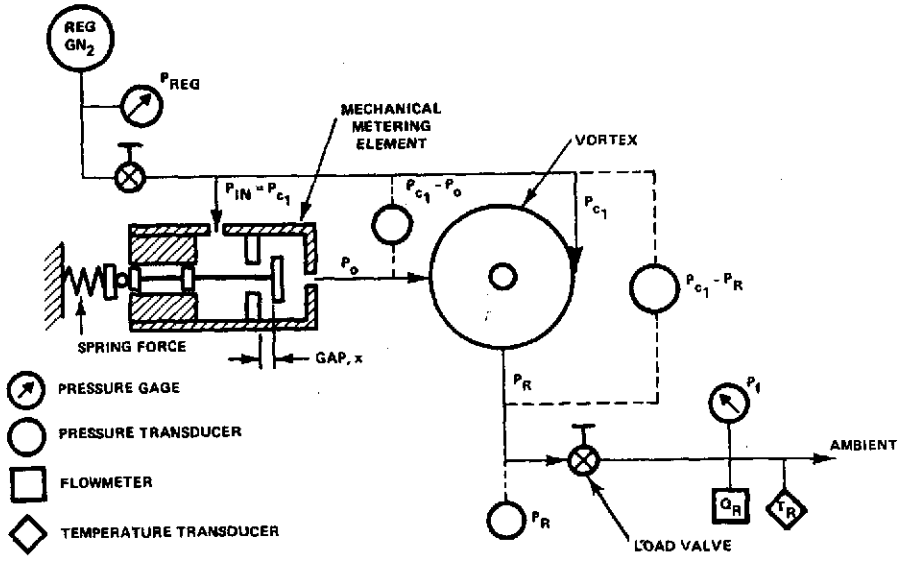

Figure 58 - Schematic Diagram for Breadboard Test

A nonlinear spring force was used to control the gap for radial flow into the vortex chamber rather than using a tapered gap area. Proper preload was also accomplished by spring force rather than using the reference pressure P_f to act on a diaphragm.

Characteristics of the vortex at scaled-down flow rates are shown in Figure 59. Fourteen points were taken with increasing input pressures to define the relationship between P_c and P_o to provide constant flow output of about 0.018 Kg/s (0.04 pps). Data for the points are also listed in Table VII. Equation (C-1) is then used to define the required spring force at every poppet gap. This relationship is shown in Figure 60. The point numbers correspond to those in Figure 59. Springs were then used to curve-fit this function.

TABLE VII - VORTEX REQUIREMENTS FOR W = 0.018 Kg/s (0.04 pps)

Point	$P_{cl} - P_s$		P_s	
	N/m^2	psi	N/m^2	psia
1	0.003×10^6	0.4	2.986×10^6	433
2	0.014	2.0	3.179	461
3	0.018	2.6	3.289	477
4	0.022	3.2	3.420	496
5	0.028	4.0	3.592	521
6	0.033	4.8	3.778	548
7	0.045	6.5	4.192	608
8	0.051	7.4	4.454	646
9	0.051	7.4	4.689	680
10	0.055	8.0	4.840	702
11	0.058	8.4	4.958	719
12	0.061	8.8	5.089	738
13	0.069	10.0	5.295	768
14	0.080	11.2	5.495	797

Reference: Figure 59.

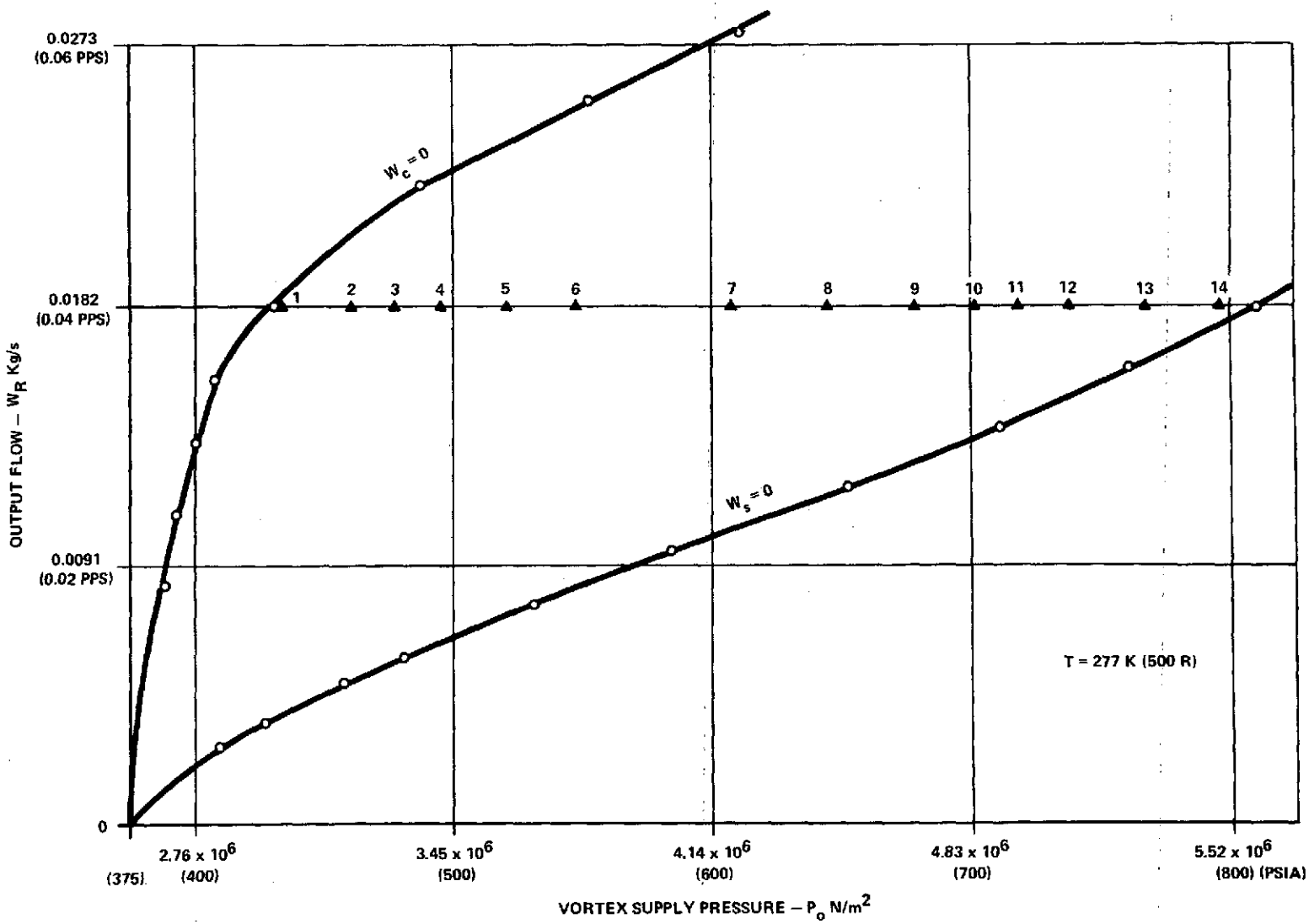

Figure 59 - Vortex Characteristics for Scaled-Down Flow

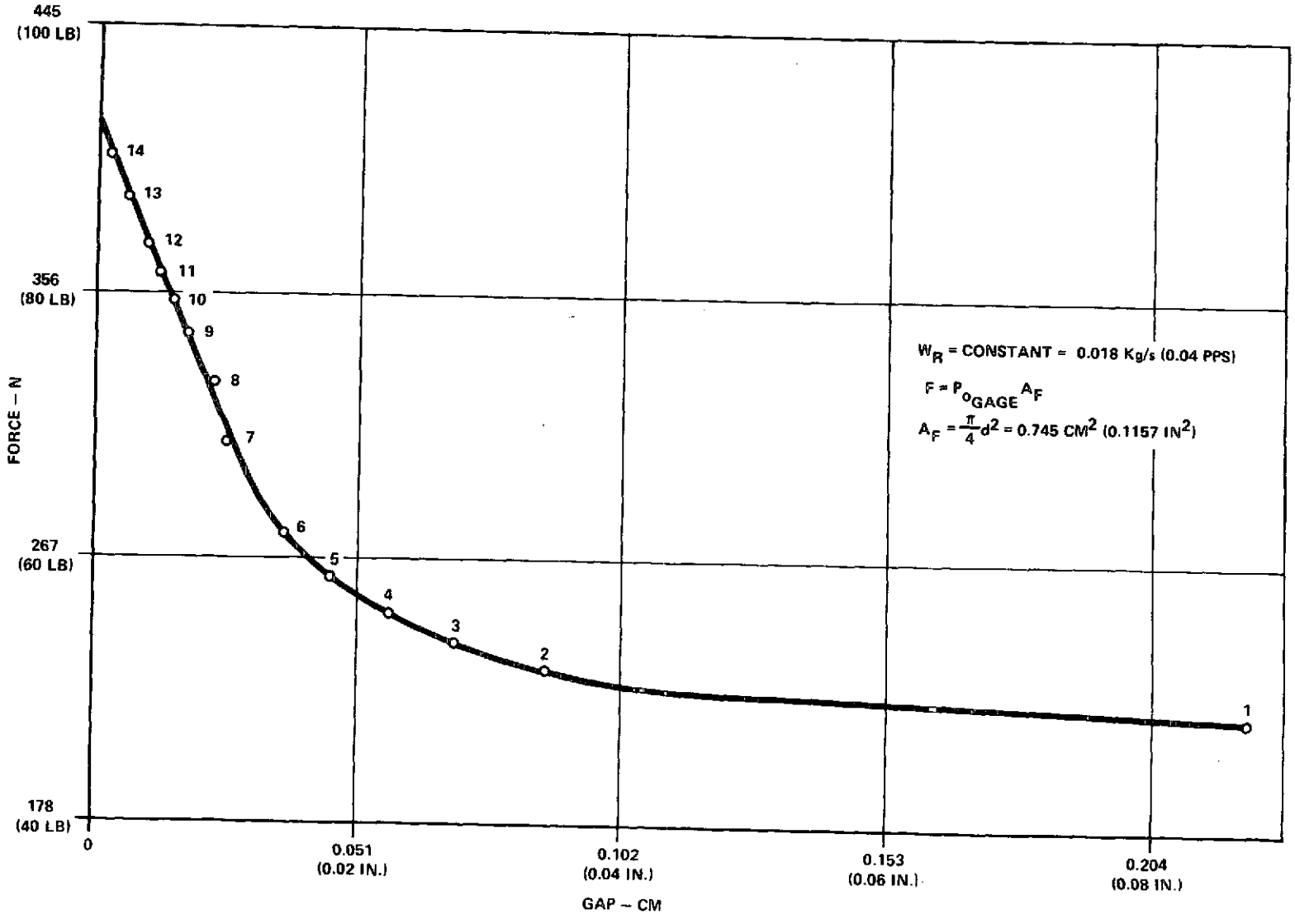

Figure 60 - Required Force versus Gap for Mechanical Metering Element

Results of a steady-state test run are shown in Figure 61. Sources of inaccuracies for this run are variations in spring force from the desired value, some friction in the breadboard version of the poppet because of the guided sleeve and possibly measurement errors. Inaccuracies in the spring force correlate directly with inaccuracies in flow in a ratio of about 1:1 (i.e., 1 percent spring force error produces about 1 percent flow error). This becomes very significant since temperature effects on the spring force must be taken into account.

The prime items that were investigated by the tests were: vortex characteristics with subsonic exit flow; minimum pressure drop for operation; sensitivity to spring force and other potential anomalies. Test results indicated sufficient vortex strength at subsonic flow conditions, sensitivity to spring force setting, and a larger minimum pressure drop than needed in the type C controller.

Temperature Compensation

To consider the effects of temperature on the operating characteristics, a computer program using prior vortex data was utilized. Although absolute values could not be compared to the breadboard tests discussed above, the trends of operation with temperature were assumed to be quite representative. Figure 62 shows the required metered area for vortex supply flow over the pressure drop range and for different temperatures to maintain constant flow rate. The nonlinear characteristic is, of course, undesirable. If the supply flow area were to be adjusted by a steady-state adjustment of P_f by way of the temperature compensating orifices, a representative compensation curve of the vortex supply area would be as shown in Figure 63. However, even if this curve were monitored exactly by the compensating elements, the accuracy over the temperature range would be only within about ± 4 percent.

Summary of Controller - D

In summary of the hybrid fluidic concept D, the following advantages and disadvantages can be enumerated. The controller has few moving parts, potentially good response, and general design simplicity. However, the required nonlinear spring force function, high pressure drop, sensitivity to downstream oscillations and large package volume are decided disadvantages.

In conclusion, then, for the desired specifications, the concept D controller must be rated as no better than a coarse controller for the current application. The inaccuracy figure results from the following sources of error:

Inaccuracy caused by upstream pressure

Inaccuracy caused by temperature effects on vortex-poppet operation

Inaccuracy caused by temperature effects on spring force

Inaccuracy in temperature compensation orifices

Inaccuracy caused by downstream fluctuations

Inaccuracy caused by spring force setting

Hysteresis, fluid noise, shock and vibration

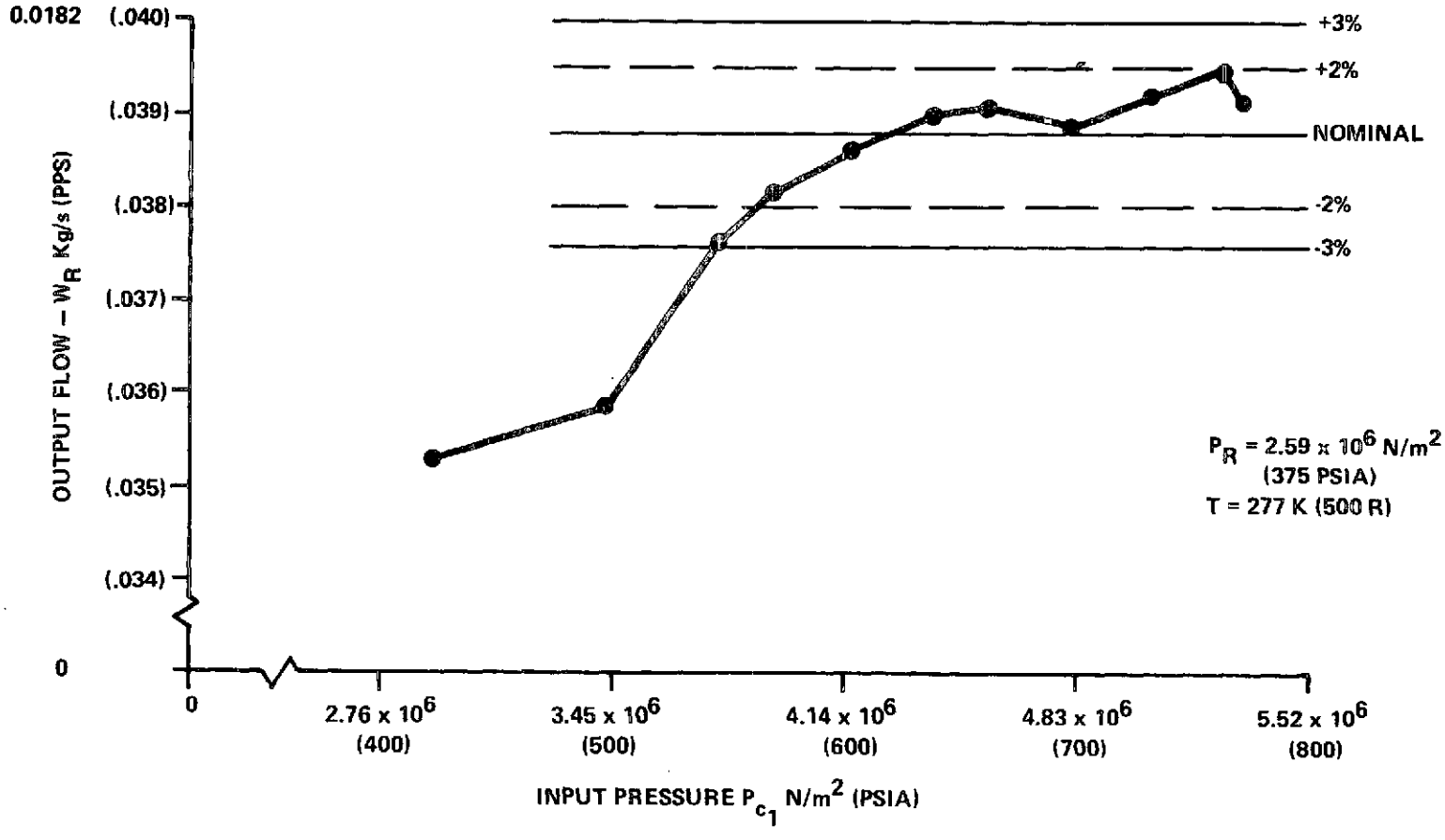

Figure 61 - Steady-State Flow Control for Hybrid Fluidic Concept D

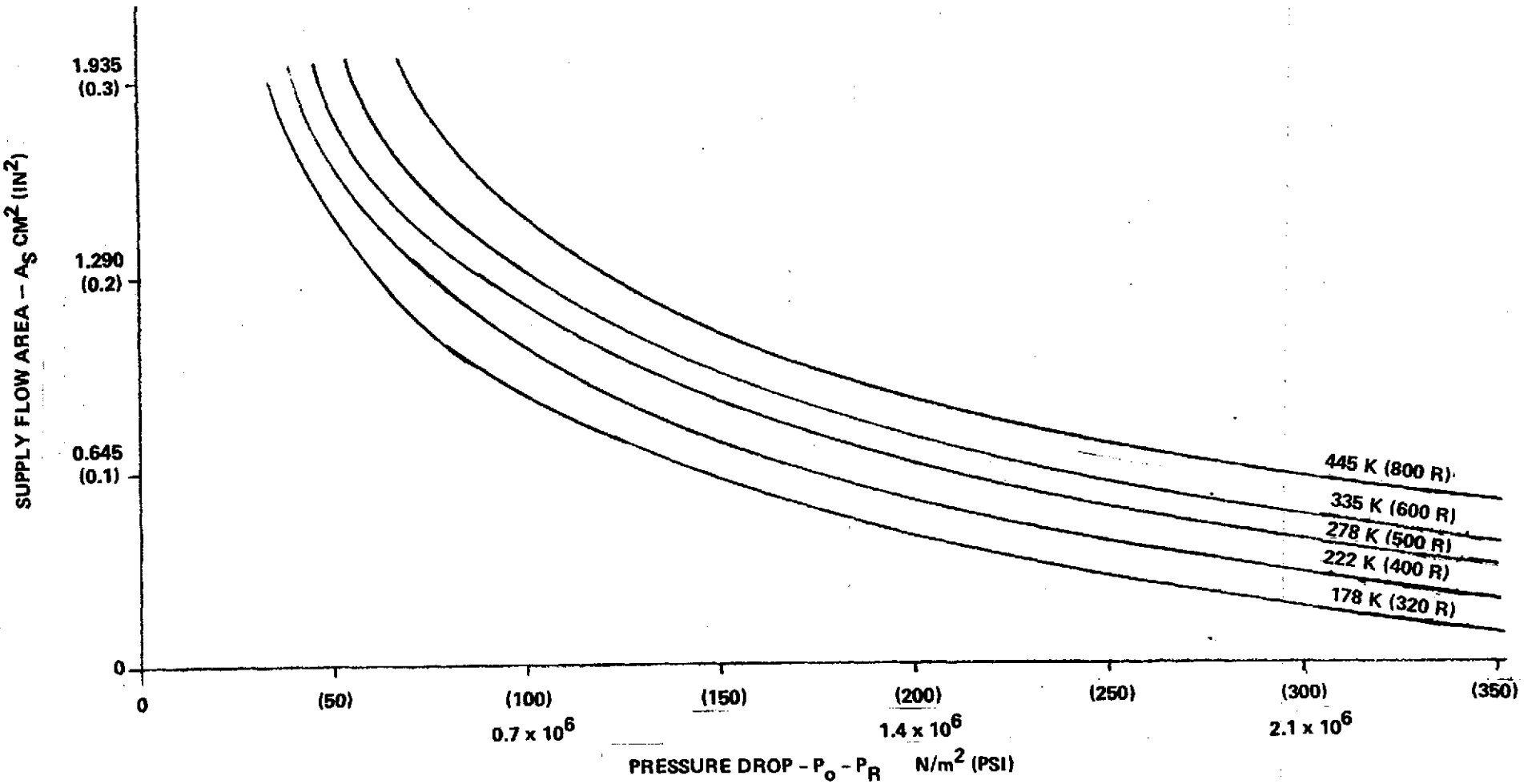

Figure 62 - Required Metered Area for Vortex Supply Flow

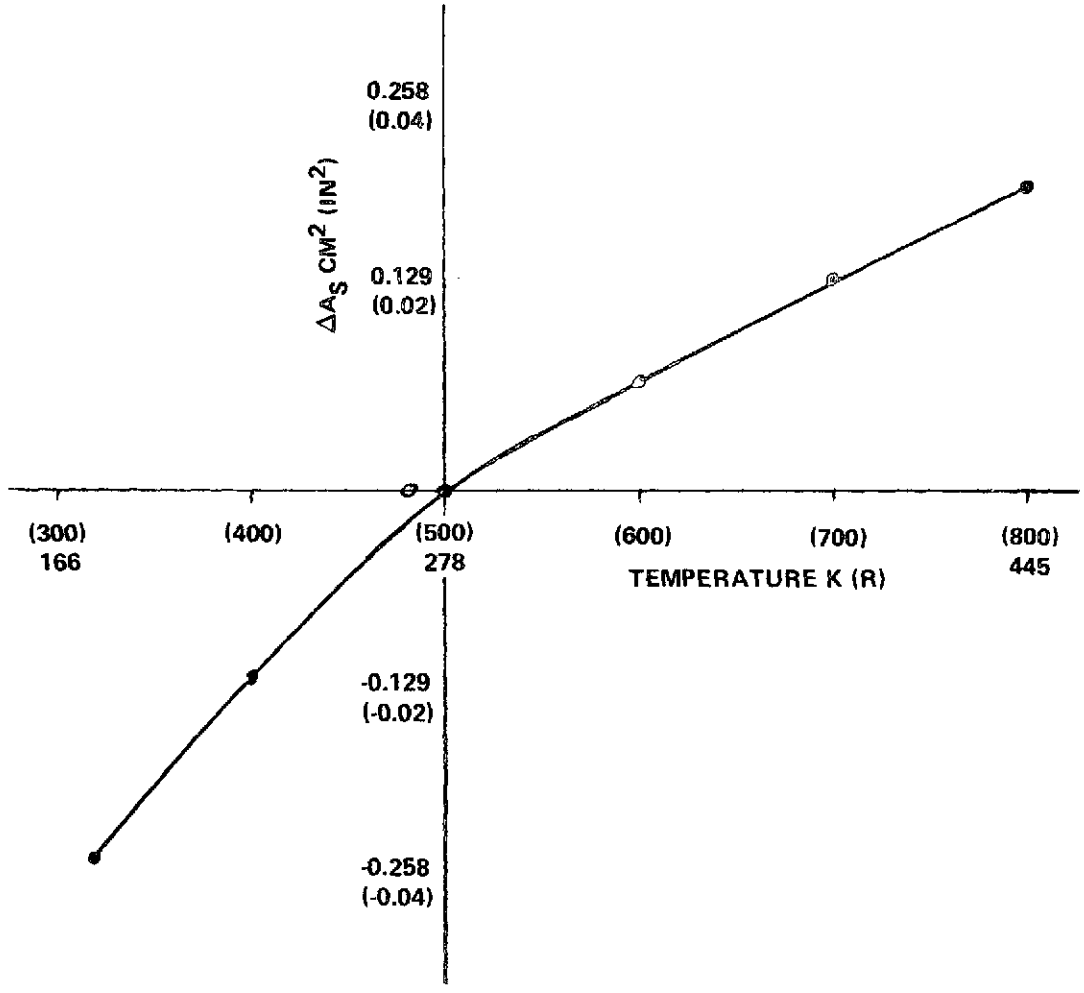

Figure 63 - Compensation Area versus Temperature

DISTRIBUTION LIST FOR FINAL REPORT

NAS3-14390 Rocketdyne CR-134510

National Aeronautics & Space Administration
Lewis Research Center
21000 Brookpark Road
Cleveland, Ohio 44135

1	Attn: Contracting Officer, MS 500-313
5	E. A. Bourke, MS 500-205
1	Technical Utilization Office, MS 3-16
1	Technical Report Control Office, MS 5-5
2	AFSC Liaison Office, MS 501-3
2	Library MS 60-3
1	Office of Reliability & Quality Assurance, MS 500-211
1	N. T. Musial, MS 500-113
4	P. N. Herr, Project Manager, MS 500-203

1 Director, Manned Space Technology, RS
Office of Aeronautics & Space Technology
NASA Headquarters
Washington, D. C. 20546

2 Director Space Prop. and Power, RP
Office of Aeronautics & Space Technology
NASA Headquarters
Washington, D. C. 20546

1 Director, Launch Vehicles & Propulsion, SV
Office of Space Science
NASA Headquarters
Washington, D. C. 20546

1 Director, Materials & Structures Div., RW
Office of Aeronautics & Space Technology
NASA Headquarters
Washington, D. C. 20546

1 Director, Advanced Missions, MT
Office of Manned Space Flight
NASA Headquarters
Washington, D. C. 20546

1 Director, Physics and Astronomy Programs, S G
Office of Space Science
NASA, Headquarters
Washington, D. C. 20546

1 Director, Planetary Programs, S L
Office of Space Science
NASA, Headquarters
Washington, D. C. 20546

1 Office of Aeronautics & Space Technology, R
NASA, Headquarters
Washington, D. C. 20546

1 Minnesota Mining & Manufacturing Company
900 Bush Avenue
St. Paul, Minnesota 55106
Attn: Library

1 National Aeronautics & Space Administration
Ames Research Center
Moffett Field, California 94035
Attn: Library

1 National Aeronautics & Space Administration
Flight Research Center
P. O. Box 273
Edwards, California 93523
Attn: Library

1 Director, Technology Utilization Division
Office of Technology Utilization
NASA Headquarters
Washington, D. C. 20546

1 Office of the Director of Defense
Research & Engineering
Washington, D. C. 20301
Attn: Office of Asst. Dir. (Chem Technology)

10 NASA Scientific and Technical Information Facility
P. O. Box 33
College Park, Maryland 20740
Attn: NASA Representative

1 Nation Aeronautics & Space Administration
Goddard Space Flight Center
Greenbelt, Maryland 20771
Attn: Library

1 National Aeronautics & Space Administration
John F. Kennedy Space Center
Cocoa Beach, Florida 32931
Attn: Library

1 National Aeronautics & Space Administration
Langley Research Center
Langley Station
Hampton, Virginia 23365
Attn: Library

1 National Aeronautics & Space Administration
Manned Spacecraft Center
Houston, Texas 77001
Attn: Library
1 J. G. Thibodaux, Jr.

1 National Aeronautics & Space Administration
George C. Marshall Space Flight Center
Huntsville, Alabama 35912
Attn: Library
1 Hans G. Paul

1 Jet Propulsion Laboratory
4800 Oak Grove Drive
Pasadena, California 91103
Attn: Library

1 Defense Documentation Center
Cameron Station
Building 5
5010 Duke Street
Alexandria, Virginia 22314
Attn: TISIA

1 Arnold Engineering Development Center
Air Force Systems Command
Tullahoma, Tennessee 37389
Attn: Library

1 Advanced Research Projects Agency
Washington, D. C. 20525
Attn: Library

1 Air Force Missile Test Center
Patrick Air Force Base, Florida
Attn: Library
1 L. J. Ullian

1 Air Force Rocket Propulsion Laboratory (RPR)
Edwards, California 93523
Attn: Library

1 Air Force Rocket Propulsion Laboratory (RPM)
Edwards, California 93523
Attn: Library

1 Air Force Office of Scientific Research
Washington, D. C. 20333
Attn: Library

1 Space & Missile Systems Organization
Air Force Unit Post Office
Los Angeles, California 90045
Attn: Technical Data Center

1 Office of Research Analyses (OAR)
Holloman Air Force Base, New Mexico 88330
Attn: Library
RRRD

1 U. S. Air Force
Washington, D. C.
Attn: Library

1 Commanding Officer
U. S. Army Research Office (Durham)
Box CM, Duke Station
Durham, North Carolina 27706
Attn: Library

1 U. S. Army Missile Command
Redstone Scientific Information Center
Redstone Arsenal, Alabama 35808
Attn: Document Section

1 Bureau of Naval Weapons
Department of the Navy
Washington, D. C.
Attn: Library
1 J. Kay

1 Commander
U. S. Naval Weapons Center
China Lake, California 93557
Attn: Library

1 Director (Code 6180)
U. S. Naval Research Laboratory
Washington, D. C. 20390
Attn: Library

1 Picatinny Arsenal
Dover, New Jersey 07801
Attn: Library

1 Air Force Aero Propulsion Laboratory
Research & Technology Division
Air Force Systems Command
United States Air Force
Wright-Patterson AFB, Ohio 45433
Attn: APRP (Library)

1 Aerojet Liquid Rocket Company
P. Os Box 15847
Sacramento, California 95813
Attn: Technical Library 2484-2015A
1 R. Stiff

1 Aerospace Corporation
2400 E. El Segundo Blvd.
Los Angeles, California 90045
Attn: Library-Documents
1 J. G. Wilder

1 Battelle Memorial Institute
505 King Avenue
Columbus, Ohio 43201
Attn: Report Library, Room 6A

1 Bell Aerosystems, Inc.
Box 1
Buffalo, New York 14240
Attn: Library
1 T. Reinhardt
1 W. M. Smith

1 Boeing Company
Space Division
P. O. Box 868
Seattle, Washington 98124
Attn: Library

1 Boeing Company
P. O. Box 1680
Huntsville, Alabama 35801

1 Chemical Propulsion Information Agency
Applied Physics Laboratory
8621 Georgia Avenue
Silver Spring, Maryland 20910

1 Chrysler Corporation
Missile Division
P. O. Box 2628
Detroit, Michigan
Attn: Library

1 Chrysler Corporation
Space Division
P. O. Box 29200
New Orleans, Louisiana 70129
Attn: Librarian

1 Curtiss-Wright Corporation
Wright Aeronautical Division
Woodridge, New Jersey
Attn: Library

1 Fairchild Stratos Corporation
Aircraft Missiles Division
Hagerstown, Maryland
Attention: Library

1 Research Center
Fairchild Hiller Corporation
Germantown, Maryland
Attn: Library

1 Republic Aviation
Fairchild Hiller Corporation
Farmington, Long Island
New York

1 Convair Aerospace Division
Research Laboratory
P. O. Box 80986
San Diego, California 92138
Attn: Library

1 Missiles and Space Systems Center
General Electric Company
Valley Forge Space Technology Center
P. O. Box 8555
Philadelphia, Pa. 19101
Attn: Library

1 General Electric Company
Flight Propulsion Lab. Department
Cincinnati, Ohio
Attn: Library

1 Grumman Aircraft Engineering Corporation
Bethpage, Long Island, New York
Attn: Library
1 J. Gavin

1 Ling-Temco-Vought Corporation
P. O. Box 5907
Dallas, Texas 75222
Attn: Library

1 Lockheed Missiles and Space Company
P. O. Box 504
Sunnyvale, California 94087
Attn: Library

1 Marquardt Corporation
16555 Saticoy Street
Box 2013 - South Annex
Van Nuys, California 91409
1 T. Hudson

1 Denver Division
Martin-Marietta Corporation
P. O. Box 179
Denver, Colorado 80201
Attn: Library

1 Western Division
McDonnell Douglas Astronautics
5301 Bolsa Ave
Huntington Beach, California 92647
Attention: Library

1 McDonnell Douglas Aircraft Corporation
P. O. Box 516
Lambert Field, Missouri 63166
Attn: Library
L. Kohrs

1 Rocketdyne Division
Rockwell International
6633 Canoga Avenue
Canoga Park, California 91304
Attn: Library, Department 596-306
1 S. Domokos

1 Space & Information Systems Division
North American Rockwell
12214 Lakewood Blvd.
Downey, California
Attn: Library
1 R. Fields

1 Northrop Space Laboratories
3401 West Broadway
Hawthorne, California
Attn: Library

1 Rocket Research Corporation
Willow Road at 116th Street
Redmond, Washington 98052
Attn: Library

1 Thiokol Chemical Corporation
Redstone Division
Huntsville, Alabama
Attn: Library

1 TRW Systems Inc.
1 Space Park
Redondo Beach, California 90278
Attn: Tech. Lib. Doc. Acquisitions
1 D. H. Lee

1 United Aircraft Corporation
Pratt & Whitney Division
Florida Research & Development Center
P. O. Box 2691
West Palm Beach, Florida 33402
Attn: Library

MATERIAL INSPECTION AND RECEIVING REPORT

1. PROC. INSTRUMENT IDEN (CONTRACT)	(ORDER) NO.	6. INVOICE NO. / DATE	7. PAGE / OF	8. ACCEPTANCE POINT
NAS3-14390			1 / 1	D

2. SHIPMENT NO.	3. DATE SHIPPED	4. B/L	5. DISCOUNT TERMS
ERC0052Z	74SEP04	TCN Not Assigned Z	

9. PRIME CONTRACTOR CODE 02602	10. ADMINISTERED BY CODE
Rocketdyne Division Rockwell International Corporation 6633 Canoga Avenue Canoga Park, Calif. 91304	NASA/Lewis Research Center 21000 Brookpark Road Cleveland, Ohio
11. SHIPPED FROM (IF OTHER THAN 9) CODE FOB: D	**12. PAYMENT WILL BE MADE BY CODE**
See Block 9	Finance Division/Audit Branch 21000 Brookpark Road Cleveland, Ohio 44135
13. SHIPPED TO CODE	**14. MARKED FOR CODE**
NASA/Lewis Research Center 21000 Brookpark Road Cleveland, Ohio 44135	Contracting Officer Rocket & Spacecraft Procurement Section M/S 500-313

15. ITEM NO.	16. STOCK / PART NO. — DESCRIPTION (X INDICATES NUMBER OF SHIPPING CONTAINERS - TYPE OF CONTAINER - CONTAINER NO.)	17. QUANTITY SHIP'D / REC'D.	18. UNIT	19. UNIT PRICE	20. AMOUNT
*See Below	Final Report NASA CR-134510 R-9395 "Investigation of Propellant Flow Control System" Additional distribution made in accordance with the contract	107 (1) + 3 Glossy Photographs			

21. PROCUREMENT QUALITY ASSURANCE

A. ORIGIN

☐ POA ☐ ACCEPTANCE OF LISTED ITEMS HAS BEEN MADE BY ME OR UNDER MY SUPERVISION AND THEY CONFORM TO CONTRACT, EXCEPT AS NOTED HEREIN OR ON SUPPORTING DOCUMENTS.

DATE _____ SIGNATURE OF AUTH GOVT REP _____

TYPED NAME AND OFFICE

B. DESTINATION

☐ POA ☐ ACCEPTANCE OF LISTED ITEMS HAS BEEN MADE BY ME OR UNDER MY SUPERVISION AND THEY CONFORM TO CONTRACT, EXCEPT AS NOTED HEREIN OR ON SUPPORTING DOCUMENTS.

DATE _____ SIGNATURE OF AUTH GOVT REP _____

TYPED NAME AND TITLE

22. RECEIVER'S USE

QUANTITIES SHOWN IN COLUMN 17 WERE RECEIVED IN APPARENT GOOD CONDITION EXCEPT AS NOTED.

DATE RECEIVED _____ SIGNATURE OF AUTH GOVT REP _____

TYPED NAME AND OFFICE

IF QUANTITY RECEIVED BY THE GOVERNMENT IS THE SAME AS QUANTITY SHIPPED, INDICATE BY (✓) MARK; IF DIFFERENT, ENTER ACTUAL QUANTITY RECEIVED BELOW QUANTITY SHIPPED AND ENCIRCLE.

23. CONTRACTOR USE ONLY

A. G.O.	B. SUB-ACCT	C.	D.
9363			

E. CONTROL NUMBERS

F.	G. GROSS WT.	H. CUBE

I. LENGTH	J. WIDTH	K. HEIGHT

OTHER CONTRACTOR INFORMATION:

P. *IN COMPLIANCE WITH TASK V, PARA. C OF THE CONTRACT

UNCLASSIFIED

L. CERTIFICATION - INSPECTION & CONTRACT PERFORMANCE	M. PACKAGING INFORMATION	N. PAID DATE	O. PACKING LIST NO.
74SEP04	GOLDENROD	74SEP04 bp	Z-74-7245

DD FORM 1 AUG 67 250 REPLACES EDITION OF 1 OCT. 1966 WHICH MAY BE USED